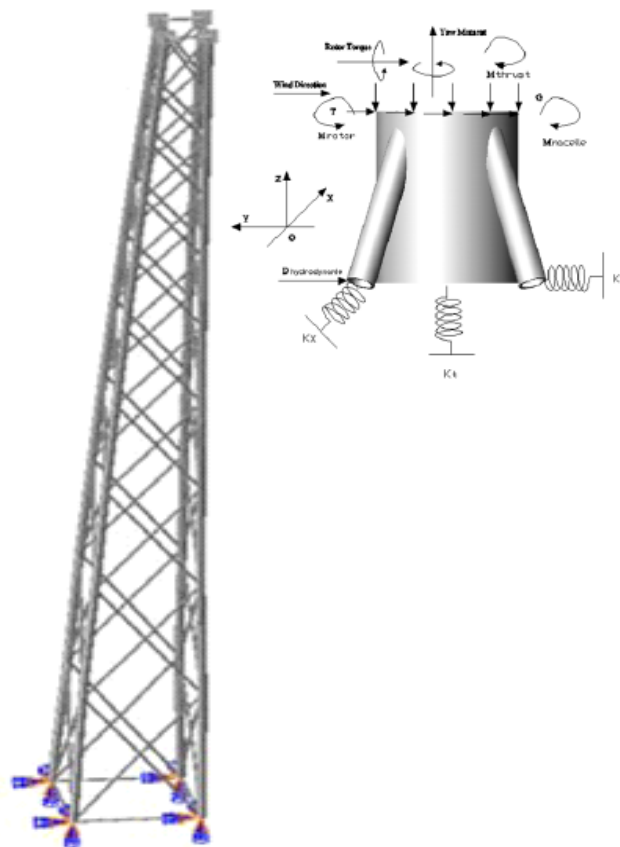


Wei Gong

Lattice Tower Design of Offshore Wind Turbine Support Structures

Trondheim, June/2011

NTNU
Norwegian University of
Science and Technology
Faculty of Engineering Science and Technology
Department of Civil and Transport Engineering





Report Title: Lattice Tower Design of Offshore Wind Turbine Support Structures	Date: 14/JUNE/2011
	Number of pages (incl. appendices):
	Master Thesis <input type="checkbox"/>
	Project Work <input checked="" type="checkbox"/>
Name: Wei Gong	
Professor in charge/supervisor: Geir Moe, Daniel Zwick	
Other external professional contacts/supervisors:	

Abstract:

Optimal design of support structure including foundation and turbine tower is among the most critical challenges for offshore wind turbine. With development of offshore wind industry heading for deeper ocean areas, new support structural concept such as a full lattice tower could be proven to be more advantageous than others when consideration of cost, safety and even environment aspects, etc are taken into.

This thesis first gave introduction of present industrial applications of hybrid support structural concept combing a lattice foundation and monotower in relatively deep water areas before the presenting and introduction of challenges with the transition piece component. Conceptual model of transition piece design for a full lattice tower support structure proposal was discussed extensively which included consideration of structural form, functional requirement, mechanical condition, etc. A mechanical model of transition piece with regards to boundary condition and load conditions was also provided. Design and analysis of two different types of transition piece models under various load conditions were performed during preliminary design and with conclusion drawn, a refined final design of transition piece model for the full lattice tower support structural concept which has also included more practical aspects was assessed through investigation of its performance under varying load conditions and different load cases. This refined final design was found to be the most optimal design fulfilling all relevant requirements at a comparable structural cost. Conclusion and recommendation was therefore given in the last part.

This thesis work is serving for a novel proposal of support structural concept for future offshore wind industry and relevant present experience is in fact nonexistent. The work applied present industrial information of hybrid support structure as basis along with consideration of offshore wind turbine structural and operational mechanism and their respective requirement. Structural analysis of transition piece design was conducted by means of finite element analysis technique and structural load conditions were simulated through up-to-date numerical modeling code for offshore wind turbine structure. Due to absence of relevant verification sources, advice and correction of the thesis content is much appreciated.

Keywords:

- | |
|-----------------------------------|
| 1. Offshore Wind Turbine |
| 2. Wind Turbine Support Structure |
| 3. Transition Piece |
| 4. Lattice Tower |

(signature)

MASTER THESIS

(TBA4920 Marin Byggeteknikk, master thesis)

Spring 2011

for

Wei Gong

Lattice Tower Design of Offshore Wind Turbine Support Structures

BACKGROUND

For offshore wind turbines to be installed in less than 70m water depth, bottom-fixed support structures will probably be used. Nearly all bottom fixed turbines have up to now been installed in moderate water depth, say 10-25m and then usually a monopile foundation has been preferred, but in a depth of 30-70m lattice tower geometry will probably turn out to be advantageous. A lattice topology could be used for the entire support structure between sea bottom and turbine nacelle or for the lower part of the tower only. So far, only the latter, so-called hybrid concepts have been installed offshore. These concept permits the use of a standard tubular tower for the upper part but a complicated transition piece is needed at the intersection to the lattice. The fully lattice tower concept is a relatively new proposal for support structures and one critical question in the design of such a structure is the design of the tower top and the interaction between it and the nacelle.

TASK DESCRIPTION

The student shall give a brief overview over existing support structure designs based on space frame/lattice tower topology and define the functional requirements for features installed or occurring at the intersection between the tower and nacelle, typically for transmission of electrical energy, structural loads and yaw control.

Then one or a few tower top designs should be analyzed in detail for the most critical cases to estimate stresses and deflections. Also attention should be paid to fatigue and if feasible some fatigue life estimates made. Abaqus might be a suitable computational tool for the job, but the student is free to make other choices.

GENERAL ABOUT CONTENT, WORK AND PRESENTATION

The task description for the master thesis is meant as a framework for the work of the candidate. Adjustments might be done as the work progresses. Tentative changes must be done in cooperation and agreement with the supervisor and professor in charge at the Department. (Also including external cooperative partners where this is applicable).

In the evaluation thoroughness in the work will be emphasized, as will be documentation of independence in assessments and conclusions. Furthermore the presentation (report) should be well organized and edited; providing clear, precise and orderly descriptions without being unnecessary voluminous.

The report shall include: (templates are found on <http://www.ntnu.no/bat/skjemabank>)

- Standard report front page.
- Title page with abstract and keywords (signed by the student).
- Summary and acknowledgement. Table of content including list of symbols, figures, tables and enclosures. If useful and applicable a list of important terms and abbreviations should be included.
- The main text.
- Clear and complete references to material used, both in text and figures/tables. This also applies for personal and/or oral communication and information.
- Text of the Thesis (these pages) signed by the professor in charge.
- The report must have a complete page numbering.
- The thesis may possibly be written as a scientific article. The report must come with report front and title pages and, if necessary, with appendices that document the work performed in the process of writing of the article.

Submission procedure

- The complete, original report (un-bounded).
- Two copies (bounded).
- If applicable: X additional copies if agreed upon for instance with external partner (to be paid for by the Department or the external partner)
- CD with the complete report (pdf-format) and all assisting or underlying material.
- A brief (one to two A4 pages including possible illustrations) popular science summary of the work, aiming at publication on the Department's web-site. Include a copy of this html document on the CD. Template is found on: <http://www.ntnu.no/bat/skjemabank>

The summary shall include the objectives of the work, explain how the work has been conducted, present the main results achieved and give the main conclusions of the work. Advice and guidelines for writing of the report is given in: "Writing Reports" by Øivind Arntsen. Additional information on report writing is found in "Råd og retningslinjer for rapportskrivning ved prosjekt og masteroppgave ved Institutt for bygg, anlegg og transport" (In Norwegian). Both are posted on <http://www.ntnu.no/bat/skjemabank>

Documentation collected during the work, with support from the Department, shall be handed in to the Department together with the report.

According to the current laws and regulations at NTNU, the report is the property of NTNU. The report and associated results can only be used following approval from NTNU (and external cooperation partner if applicable). The Department has the right to make use of the results from the work as if conducted by a Department employee, as long as other arrangements are not agreed upon beforehand.

Tentative agreement on external supervision, work outside NTNU, economic support etc

Separate description to be developed, if and when applicable.

Health, safety and environment (HSE)

The health, safety and environmental (HSE) work at NTNU shall constitute continuous and systematic efforts that are integrated into the primary activities. NTNU emphasizes the safety for the individual employee and student. The individual safety shall be in the forefront and no one shall take unnecessary chances in carrying out the work. Information in English on HSE is given on: <http://www.ntnu.no/hse>. In particular, if the student is to participate in field work, visits, field courses, excursions etc. during the Master Thesis work, he/she shall make himself/herself familiar with the *Fieldwork HSE Guidelines* <http://www.ntnu.no/hms/retningslinjer/HMSR07E.doc>. General HSE provisions that apply in all laboratories and workshops are given on: <http://www.ntnu.no/hse/labhandbook>.

The students do not have a full insurance coverage as a student at NTNU. If a student wants the same insurance coverage as the employees at the university, he/she must establish an individual travel and personal injury insurance. More information about students and insurance is found on the faculty HSE page on: <http://www.ntnu.no/ivt/adm/hms/>. (Documents are in Norwegian only, ask the supervisor to explain).

Start and submission deadlines

The work on the Master Thesis starts on **January 17, 2011**

The thesis report original (not bounded) and 2 bounded copies and the CD as described above shall be submitted at the latest on **June 14, 2010 at 1500 hrs.**

Professor in charge: Geir Moe

Other supervisors: Daniel Zwick

Department of Civil and Transport Engineering, NTNU

Date:

Signature

Professor in charge

DEDICATION

Upon completion of my master study of Coastal and Marine Engineering and Mangement (CoMEM) under Erasmus Mundus programme funded by European Parliament, this thesis is dedicated to all those who have helped, supported, shared joy and gone through difficulties with me during the last two-year period of study. It is also hoped that this thesis will be able to provide useful information to the exciting offshore wind industry of my great enthusiasm.

ACKNOWLEDGEMENT

This thesis work was completed within Marine Civil Engineering Group, Department of Civil and Transport Engineering, NTNU from where a lot of assistance and help is received. Professor Geir Moe's approval of this thesis task assignment to me as well as his guidance, explanation and clarification provided during the period of this work is very much appreciated. Mr. Daniel Zwick's fulfillment of supervision of this thesis has helped proceeding the thesis progress. In addition, Professor Øivind Asgeir Arntsen has provided much practical help without which the thesis could not be completed in a smooth progress. Support from the Marine Civil Engineering Group for my participation of OMAE2011, Rotterdam is also indeed thanked.

PREFACE

By the time being of this thesis work, offshore wind industry is undergoing prosperous development and advancement which comes out as a call of global energy strategy and environment issue. One of the most critical challenges for offshore wind turbine involves the optimal design of support structure including foundation and turbine tower. With development of offshore wind industry heading for deeper ocean areas, new support structural concept might be proven to be more advantageous than conventional types when consideration of cost, safety and even environment aspects, etc are taken into. This thesis is therefore aiming to support optimal novel support structural design of future deep water bottom fixed offshore wind turbine.

A full lattice support structure concept ranging from seabed to nacelle assembly has been proposed for relatively deep water areas, e.g. 30m-70m. This new concept might be able to provide a better solution for deep water fixed offshore wind turbine but a critical component connecting this full lattice structure and the upper nacelle assembly, namely transition piece, has become another critical challenge which has not been studied so far. This thesis first gave introduction of present industrial applications of hybrid support structural concept combing a lattice foundation and monotower before the presenting and introduction of challenges with the transition piece component. Conceptual model of transition piece design for a full lattice support structure proposal was discussed extensively later. A mechanical model of transition piece with regards to boundary condition and load conditions was provided for structural analysis and numerical modeling purpose. Based on experience from hybrid support structural concept, design and analysis of two different types of transition piece models under various load conditions were performed during preliminary design and with conclusion drawn from this preliminary design phase, a refined final design of transition piece model for the full lattice support structural concept which has also included more practical aspects was assessed through investigation of its performance under varying load conditions and different load cases. This refined final design was found to be the most optimal design fulfilling all relevant requirements at a comparable structural cost. Conclusion and recommendation was therefore given in the last part.

TABLE OF CONTENT

1 INTRODUCTION.....	1
1.1 Introduction of offshore wind turbine.....	1
1.1.1 Offshore wind development and wind turbine system.....	1
1.1.2 Wind turbine support structure.....	1
1.1.3 Wind turbine control system.....	2
1.2 Background and content of this work.....	2
1.2.1 Background.....	2
1.2.2 Content.....	3
1.3 Scope and limitation.....	3
2 LATTICE SUPPORT STRUCTURE FOR OFFSHORE WIND TURBINE.....	5
2.1 Introduction of lattice structure.....	5
2.2 History of lattice tower for onshore wind turbine.....	5
2.3 Current application of lattice support structure for offshore wind turbine.....	6
2.3.1 OWEC jacket quattropod for Beatrice demo wind farm.....	6
2.3.2 OWEC jacket quattropod for Alpha Ventus offshore wind farm.....	7
2.3.3 RAMBØLL jacket for the Upwind project.....	8
2.3.4 RAMBØLL jacket for the OC4 project.....	8
2.3.5 REpower jacket.....	8
2.4 Summary of lattice as support structure for offshore wind turbine.....	9
2.5 Introduction of transition piece.....	9
2.6 Transition piece for early onshore wind turbine supported by lattice tower.....	10
2.7 Transition piece for hybrid offshore wind turbine support structures.....	10
2.7.1 Transition piece for Beatrice demo wind farm.....	10
2.7.2 Transition piece for Alpha Ventus offshore wind farm.....	11
2.7.3 Transition piece for the Upwind and OC4 project.....	11
2.7.4 Transition piece for REpower jacket in Bremerhaven.....	11
2.8 Summary of transition piece designs.....	12
3 CONCEPTUAL MODEL OF TRANSITION PIECE.....	15
3.1 Geometrical requirement.....	15
3.2 Functional requirement.....	16
3.2.1 Power transmission equipment.....	16
3.2.2 Yaw system.....	19
3.3 Mechanical requirement.....	23
3.3.1 Connection with the lattice support structure.....	23
3.3.2 Connection with the nacelle assembly.....	23
3.4 Mechanical model of transition piece.....	24
3.4.1 Boundary condition.....	25
3.4.2 Analysis of a full lattice support structure concept.....	25
3.4.3 Load condition.....	31
4 PRELIMINARY DESIGN OF TRANSITION PIECE.....	39
4.1 Proposed model.....	39
4.1.1 Frame-cylinder model.....	40
4.1.2 Cone-strut model.....	41
4.2 Finite element model.....	41
4.2.1 Model introduction.....	41

4.2.2 Boundary condition	42
4.2.3 Loading.....	42
4.3 Finite element analysis result	43
4.3.1 Modal analysis.....	43
4.3.2 RNA weight.....	44
4.3.3 Rotor thrust.....	46
4.3.4 Hydrodynamic load	55
4.3.5 Drive train vibration	59
4.3.6 Rotor torque.....	59
4.3.7 Yaw moment.....	62
4.4 Conclusion	66
5 FINAL DESIGN OF TRANSITION PIECE.....	69
5.1 Model geometry	69
5.2 Structural dimension	70
5.3 Model selection.....	72
5.4 Functional fulfillment	73
5.5 Load analysis.....	73
5.5.1 RNA load.....	74
5.5.2 Operation under aero load.....	76
5.5.3 Operation under aero load with yaw motion.....	81
5.5.4 Operation under aero & hydro load at identical wind wave direction	86
5.5.5 Operation under aero & hydro load with unidentical wind wave direction	90
5.6 Investigation on more compact design.....	95
5.7 Fatigue.....	96
5.8 Manufacturing.....	98
5.9 Conclusion	98
6 CONCLUSION AND RECOMMENDATION.....	99
6.1 Conclusion	99
6.2 Recommendation	100
REFERENCE.....	101
APPENDIX I.....	103
APPENDIX II	105
APPENDIX III	107
APPENDIX IV	108
APPENDIX V	109
APPENDIX VI.....	113
APPENDIX VII.....	116

LIST OF FIGURES

Figure 1.1 Components of a Horizontal Axis Wind Turbine.....	2
Figure 2.1 Example of Lattice Tower for Onshore Wind Turbines.....	5
Figure 2.2 Hybrid Support Structure for Offshore Wind Turbine.....	6
Figure 2.3 OWEC Jacket Quattropod on Offshore Wind Turbine.....	7
Figure 2.4 RAMBØLL Jacket Substructure Configuration for Upwind Project.....	8
Figure 2.5 REpower 5MW Wind Turbine on a Jacket Substructure.....	9
Figure 2.6 Transition Piece of REpower Jacket.....	12
Figure 3.1 Geometrical Profile for Transition Piece.....	15
Figure 3.2 Various Geometrical Models for Transition Piece.....	16
Figure 3.3 Equipment Arrangement in an Onshore Monotower Wind Turbine.....	17
Figure 3.4 Application of J-tube for Power Cable Protection for Offshore Wind Turbine.....	18
Figure 3.5 Power Transmission Cable for Offshore Wind Farm.....	18
Figure 3.6 Power Transmission Cable Layout in Transition Piece.....	18
Figure 3.7 Different Yawing Concepts.....	19
Figure 3.8 Configuration of a Roller Bearing System.....	20
Figure 3.9 Various Types of Roller Bearing.....	20
Figure 3.10 Configuration of Gliding Bearing System.....	21
Figure 3.11 Location of Yaw Drive in REpower 5MW Turbine System.....	22
Figure 3.12 Transition Piece Connection with Yaw Bearing inside the Nacelle Assembly.....	24
Figure 3.13 Bolting Connection of Yaw Bearing and Cylinder Flange.....	24
Figure 3.14 Boundary Condition of Transition Piece Using Spring System.....	25
Figure 3.15 Support Structure Bending Frequency Range.....	27
Figure 3.16 Configuration of a Lattice Support Structure for a 5MW Reference Offshore Wind Turbine.....	28
Figure 3.17 Rotor Nacelle Assembly Weight on Transition Piece.....	31
Figure 3.18 Stream Tube of Rotor Disk Theory.....	32
Figure 3.19 Rotor Thrust Force on Transition Piece.....	33
Figure 3.20 Hydrodynamic Load (Acceleration or Displacement) on Transition Piece.....	33
Figure 3.21 Rotor Torque on Transition Piece.....	34
Figure 3.22 Misalignment of Incoming Wind with Rotor Axis.....	36
Figure 3.23 Yaw Moment on Transition Piece.....	36
Figure 3.24 Mechanical Model of Transition Piece Including Boundary Condition and Various Loads.....	37
Figure 4.1 Methodology for Transition Piece Modeling and Analysis.....	39
Figure 4.2 Geometrical Configuration Requirement for Transition Piece.....	39
Figure 4.3 Frame-cylinder Transition Piece Model.....	40
Figure 4.4 Cone-strut Transition Piece Model.....	40
Figure 4.5 Finite Element Models of Transition Piece.....	41
Figure 4.6 Coordination System Illustration.....	42
Figure 4.7 Transition Piece Stress Condition under RNA Weight.....	44
Figure 4.8 Oscillation of Vertical Load on Support Structure Top due to RNA Weight with Consideration of Rotor Aerodynamics.....	45
Figure 4.9 Misalignment of Yaw Axis and Mass Centers of Rotor and Nacelle.....	45
Figure 4.10 Transition Piece Response under RNA Weight and Its Induced Moment.....	46
Figure 4.11 Thrust Coefficient in Relation to Wind Speed.....	47
Figure 4.12 Response of Transition Piece under Theoretical Static Thrust Load.....	48
Figure 4.13 Transition Piece Response under Static Thrust and RNA Load.....	49
Figure 4.14 Time Series of Normal Turbulent Wind with Mean Wind Speed 24m/s and Turbulence Intensity 15.7%.....	50
Figure 4.15 Theoretical Thrust Load on Rotor Disk.....	50
Figure 4.16 Simulated Thrust Load from HAWC2.....	50
Figure 4.17 Structural Response of Frame-cylinder TP under Dynamic Thrust Load.....	51
Figure 4.18 Frame-cylinder TP Response under Thrust Load at Max. Negative and Positive Deflection Time Points.....	52
Figure 4.19 Structural Response of Cone-strut TP under Dynamic Thrust.....	53
Figure 4.20 Cone-strut TP Response under Thrust Load at Max. Negative and Positive Deflection Time Points.....	54
Figure 4.21 Power Spectral Density of Simulated Dynamic Thrust Load Time Series.....	55

Figure 4.22 Origin and Coordination for Hydrodynamic Load Computation	55
Figure 4.23 Water Surface for a Simulated 4.0m Wave Condition	56
Figure 4.24 4.0m Wave Load on Lattice Leg from HAWC2 Simulation.....	56
Figure 4.25 Applying Simulated Wave Load on Lattice Support Structure	57
Figure 4.26 Top Displacement of Lattice Support Structure under 4.0m Wave.....	57
Figure 4.27 Water Surface for a Simulated 10m Wave Condition	57
Figure 4.28 10.0m Wave Load on Lattice Leg from HAWC2 Simulation.....	58
Figure 4.29 Top Displacement of Lattice Support Structure under 10m Wave.....	58
Figure 4.30 Buckling of Trusses below Water Surface of Lattice Support Structure under 10m Wave	59
Figure 4.31 Rotor Torque under a Normal Turbulent Wind Condition.....	60
Figure 4.32 Deformation of Frame-cylinder TP under Rotor Torque	60
Figure 4.33 Frame-cylinder TP Stress Condition at Time Point of Max. Stress under Rotor Torque	61
Figure 4.34 Deformation of Cone-strut TP under Rotor Torque	61
Figure 4.35 Z-displacement of Cone-strut TP under Rotor Torque.....	61
Figure 4.36 Cone-strut TP Stress Condition at Time Point of Max. Stress under Rotor Torque.....	62
Figure 4.37 Rotor Torque between 250 and 300s.....	62
Figure 4.38 Wind Speed Time Series of a Normal Turbulent Wind Model with +20° Yaw Angle	63
Figure 4.39 Yaw Moment around Yaw Axis under a Normal Turbulent Wind Model with +20° Yaw Angle	63
Figure 4.40 Torsional Structural Deformation of Frame-cylinder TP under Yaw Moment at a Time Point	64
Figure 4.41 Rotational Displacement along Yaw-axis of Frame-cylinder TP under Yaw Moment at Time Point of Maximum.....	64
Figure 4.42 Stress Condition of Frame-cylinder TP under Yaw Moment at Time Point of Maximum	64
Figure 4.43 Torsional Structural Deformation of Cone-strut TP under Yaw Moment at a Time Point	65
Figure 4.44 Rotational Displacement along Yaw-axis of Cone-strut TP under Yaw Moment at Time Point of Maximum.....	65
Figure 4.45 Stress Condition of Cone-strut TP under Yaw Moment at Time Point of Maximum	65
Figure 4.46 Yaw Moment at Time Interval of Maximum Values	65
Figure 5.1 Geometrical Configuration of Transition Piece	69
Figure 5.2 Joint of Truss Components.....	70
Figure 5.3 Connection with Lattice Support Structure	70
Figure 5.4 Overall View of Transition Piece.....	70
Figure 5.5 Transition Piece Weight with Varying Heights and Cone Thicknesses	71
Figure 5.6 Power Transmission Cable inside the Transition Piece	73
Figure 5.7 Stress Condition under RNA Load.....	75
Figure 5.8 Rotor and Nacelle Mass along Yaw Axis	75
Figure 5.9 Illustration of Incoming Wind Direction under Aero Load Case	76
Figure 5.10 Structural Stress Condition at Time Point of Max. Stress under Thrust & Torque Loads	76
Figure 5.11 Time Series of Stress at Critical Region under Thrust & Torque Loads.....	77
Figure 5.12 Time Series of Transition Piece Response under Rotor Thrust and Torque Loads.....	77
Figure 5.13 Illustration of Incoming Wind Direction under Angled Aero Load Case	78
Figure 5.14 Transition Piece Stress Condition at Time Point of Max. Stress under Angled Thrust & Torque Loads.....	78
Figure 5.15 Time Series of Stress at Critical Region under Angled Thrust & Torque Loads	79
Figure 5.16 Transition Piece Vibration under Angled Thrust & Torque Loads	79
Figure 5.17 Time Series of Transition Piece Response under Angled Rotor Thrust and Torque Loads	80
Figure 5.18 Thrust Load Applied on Top of Lattice Support Structure	81
Figure 5.19 Lattice Structural Response to Thrust Load	81
Figure 5.20 Illustration of Rotor Axis Direction	82
Figure 5.21 Transition Piece Stress Condition at Time Point of Max. under Aero Load with Yaw Motion	82
Figure 5.22 Time Series of Stress at Critical Truss Joint under Aero Load with Yaw Motion	83
Figure 5.23 Transition Piece Deformation under Aero Load with Yaw Motion	83
Figure 5.24 Torsional Vibration along Yaw Axis at Critical Node under Aero Load with Yaw Motion... 83	83
Figure 5.25 Translational Displacement at A Joint Node on Upper Edge under Aero Load with Yaw Motion	84
Figure 5.26 Transition Piece Stress Condition at Time Point of Max. under Aero Load with Yaw Motion at Varied Direction	84

Figure 5.27 Time Series of Stress at Critical Truss Joint under Aero Load with Yaw Motion at Angled Direction.....	84
Figure 5.28 Transition Piece Deformation under Aero Load with Yaw Motion at Angled Direction.....	85
Figure 5.29 Torsional Vibration along Yaw Axis at Critical Node under Aero Load with Yaw Motion at Angled Direction	85
Figure 5.30 Time Series of Transition Piece Response under Aero Load with Yaw Motion at Angled Direction.....	85
Figure 5.31 Water Surface Elevation and Hydro Load of a 10m Irregular Airy Wave on Lattice Leg.....	86
Figure 5.32 Lattice Support Structure Response to 10m Wave Load.....	87
Figure 5.33 Illustration of Identical Incoming Wind & Wave Direction.....	88
Figure 5.34 Transition Piece Stress Condition at Time Point of Max. under Aero & Hydro Load from Identical Direction.....	88
Figure 5.35 Displacement in X & Y Direction of Transition Piece under Combined Aero & Hydro Load at Identical Wind-Wave Direction.....	89
Figure 5.36 Transition Piece Stress Condition at Time Point of Max. under Aero-Hydro Load & Yaw Moment at Identical Wind-Wave Direction	89
Figure 5.37 Time Series of Stress at Critical Top Edge and Base Joint under Aero-Hydro Load with Yaw Moment at Identical Wind-Wave Direction	90
Figure 5.38 Torsional Vibration along Yaw Axis at Critical Node under Aero-Hydro Load with Yaw Moment at Identical Wind-Wave Direction	90
Figure 5.39 Illustration of Perpendicular Incoming Wind & Wave Directions.....	90
Figure 5.40 Transition Piece Stress Condition at Time Point of Max. under Aero & Hydro Load with Perpendicular Wind-Wave Direction	91
Figure 5.41 Time Series of Stress at Critical Location under Aero & Hydro Load with Perpendicular Wind-Wave Direction	91
Figure 5.42 Transition Piece Stress Condition at Time Point of Max. under Aero & Hydro Load with Yaw Moment with Perpendicular Wind-Wave Direction.....	92
Figure 5.43 Time Series of Stress at Critical Location under Aero & Hydro Load with Yaw Moment with Perpendicular Wind-Wave Direction	92
Figure 5.44 Transition Piece Response under Aero & Hydro Load with Yaw Moment with Perpendicular Wind-Wave Direction	93
Figure 5.45 Torsional Vibration along Yaw Axis at Critical Node under Aero-Hydro Load with Yaw Moment with Perpendicular Wind-Wave Direction.....	93
Figure 5.46 Response of Compact Transition Piece Design under Combined Aero & Hydro Loads	95
Figure 5.47 Response of Compact Transition Piece Design under Combined Aero & Hydro Loads with Yaw Motion.....	96
Figure 5.48 Rainflow Counting of Cycle Number against Load Range for Aerodynamic Loads within Simulation Period of 600s	97
Figure 5.49 Material S-N Curve	97
Figure II.1 Modal Shapes of Numerical Lattice Model 12L	106
Figure III.1 Eigen Models of Transition Piece	107
Figure IV.1 Exceedance Probability for Largest Out-of-plane Blade Bending Load in 10-minute	108
Figure V.1 Flow Velocities and Accelerations at Varying Water Depths for a 4.0m Wave Condition....	110
Figure V.2 Flow Velocities and Accelerations at Varying Water Depths for a 10m Wave Condition....	112
Figure VI.1 Deflection of Cylinder Top Edge Points of the Frame-cylinder TP under Rotor Torque	114
Figure VI.2 Deflection of Cone Top Edge Points in the Cone-strut TP under Rotor Torque.....	115
Figure VII.1 First 12 Eigen Modes of Transition Piece of 3m-high and 0.2m-thick.....	117

LIST OF TABLES

Table 2.1 Weight Break-down for OJQ Jacket at Alpha Ventus Project.....	7
Table 2.2 Design Parameters of RAMBØLL Jacket Substructure for Upwind Project.....	8
Table 2.3 Properties of Jacket Members for OC4 Project.....	8
Table 2.4 Wind Turbine Size Trend.....	10
Table 3.1 Comparison of Different Types of Yaw Bearings.....	21
Table 3.2 Gross Properties of a 5 MW Reference Wind Turbine.....	26
Table 3.3 Material Properties for Lattice Support Structure.....	28
Table 3.4 Comparison of Lattice Structural Properties Based on Varying Design Concepts.....	29
Table 3.5 Properties of Two Concepts for a Lattice Support Structure Design Proposal.....	30
Table 3.6 Rotor Nacelle Assembly Weight of a 5MW Wind Turbine.....	31
Table 4.1 Material Properties for Transition Piece.....	40
Table 4.2 Structural Dimension of Frame-cylinder TP.....	40
Table 4.3 Structural Dimension of Cone-strut TP.....	40
Table 4.4 Meshing of the Finite Element Models.....	41
Table 4.5 Stiffness of Lattice Support Structure as Boundary Condition.....	42
Table 4.6 Load Conditions on Transition Piece.....	43
Table 4.7 Eigen Frequencies of Transition Piece.....	43
Table 4.8 Rotor Thrust Load under Characteristic Wind Velocities.....	47
Table 4.9 Mass Proportions of Dynamic Drive Train Components.....	59
Table 4.10 Summary of Transition Piece Behaviour under Various Load Cases.....	67
Table 5.1 Dimension & Weight of Varying Transition Piece Designs.....	71
Table 5.2 Weight Breakdown of a 3.0m High, 0.20m Thick Transition Piece.....	71
Table 5.3 Modal Analysis of Varying Transition Piece Designs.....	72
Table 5.4 Structural Response of Varying Transition Piece Designs under Yaw Moment.....	72
Table 5.5 Load Conditions on Final Transition Piece Design.....	74
Table 5.6 Load Cases for Final Transition Piece Analysis.....	74
Table 5.7 Transition Piece Response under Various Load Cases.....	94
Table 5.8 Fatigue Life Prediction under Various Load Cases at Critical Structural Stress Region.....	98
Table 6.1 Comparison of Various Transition Piece Concepts.....	100

LIST OF SYMBOLS

a	Axial induction factor [1]
a'	Angular induction factor [1]
A	Cross section area of cylinder [m ²]
A_r	Rotor disk area [m ²]
c	Airfoil chord length [m]
C_D	Drag coefficient [1]
C_L	Lift coefficient [1]
C_M	Inertia coefficient [1]
C_T	Thrust coefficient [1]
D	Diameter of cylinder [m]
f	Wave force in line of structure [N/m]
ΔF_D	Blade element drag force [N/m]
ΔF_L	Blade element lift force [N/m]
ΔF_t	Blade element tangential wind force [N/m]
K_t	Torsional spring coefficient [N·m/rad]
$K_{x/y}$	Bending spring coefficient [N/m]
L_n	Nacelle gravity moment arm to yaw axis [m]
L_r	Rotor gravity moment arm to yaw axis [m]
$M_{nacelle}$	Nacelle assembly mass [kg]
M_{rotor}	Rotor mass [kg]
N_b	Number of blades [1]
P	Turbine rotor rotational frequency [Hz]
ΔQ	Blade element torque [N·m/m]
r_b	Rotor blade radius [m]
Δr_b	Length of blade element [m]
T	Rotor thrust load [N]
u	Flow (wave/wind) velocity [m/s]
u_t	Tangential wind velocity on blade element [m/s]
U_{hub}	Wind velocity at rotor hub [m/s]
U_r	Wind speed at rotor disk plane [m/s]

U_w	Downstream wake speed [m/s]
U_∞	Upstream free wind speed [m/s]
$\overline{\omega}$	Angular wind velocity increase [m/s]
ρ_{air}	Air density [kg/m ³]
ρ_{water}	Sea water density [kg/m ³]
ϕ	Angle of inflow [°]
Ω	Original wind angular velocity [m/s]

SUMMARY

The thesis is composed of six chapters:

Chapter 1 provides a brief introduction of offshore wind turbine in terms of its support structure and control system, etc. Background, scope and limitation of this thesis work is also described.

In Chapter 2 lattice structure employed as support structure for wind turbine is introduced from its past application on early small-scale onshore wind turbine to its current application on hybrid offshore wind turbine. Transition piece of lattice support structure on early onshore wind turbine and recent hybrid offshore wind turbine is introduced afterwards with description and analysis of several up-to-date industrial project examples.

Conceptual design model of transition piece for a full lattice support structure proposal is extensively discussed in Chapter 3. The conceptual model takes into consideration of transition piece's geometrical requirement, functional requirement and its mechanical requirement. Various aspects including transition piece interference with lattice support structure, yaw bearing and layout of power transmission equipment are discussed. A schematized mechanical model of transition piece including its boundary condition and load condition is provided for structural analysis and numerical modeling purpose.

In Chapter 4, two transition piece design concepts, namely, frame-cylinder type and cone-strut type are analyzed in a parallel manner by means of structural finite element analysis technique. The preliminary analysis of these two concepts is mainly based on information and experience of transition piece applied on recent hybrid offshore wind turbine projects and comparison of performance of these two concepts under varying load conditions is given.

Based on conclusion drawn from preliminary analysis and consideration of more practical aspects, a final transition piece model designed for a full lattice support structure is proposed and analyzed extensively in Chapter 5. Analysis of this transition piece model performance under different load cases considering aerodynamic and hydrodynamic loads is conducted and this new model is found to have the best preferred performance under the investigated load cases, at a comparable structural cost with other models analyzed in the preliminary design phase. Fatigue issue and investigation of cost reduction feasibility is also provided for this final design.

Conclusion and recommendation are provided in Chapter 6.

Cited reference and relevant appendices are also attached.

1 INTRODUCTION

1.1 Introduction of offshore wind turbine

1.1.1 Offshore wind development and wind turbine system

Since the completion of the first offshore wind farm Vindeby in 1991 by Denmark [1], offshore wind industry has seen tremendous progress and the development is still increasingly going on with a number of projects under construction and many new projects being proposed. In 2009, the demo project of Hywind [2] was initiated in Norway which is the world's first full-scale deep water floating offshore wind turbine. Numerous new growths are taking place in the development of offshore wind industry, which comes out as a call of global energy demands and a cleaner future environment.

An offshore wind farm is usually composed of a number of offshore wind turbine units located in the offshore area. The number of offshore wind turbines and the location of the site depend on the specific geotechnical environment and the topographical, meteorological and hydrological conditions, etc. Offshore wind turbines are units forming the offshore wind farm and generating electrical power from the wind kinetic motion. Conventionally offshore wind turbines are bottom founded with the structures connected to sea bed via varying types of foundation. Research and development is undergoing study of floating offshore wind turbine with the structure moored via a number of mooring lines fastened to sea bed or supported by a tension leg structure, etc. The content of this thesis will however concentrate on the conventional bottom founded offshore wind turbine because of its wide application and its importance in fundamental practice.

For conventional bottom founded offshore wind turbine, the whole system is composed of several components with each serving its own function. Generally, for onshore wind turbine, there are two types of concepts: horizontal axis wind turbine and vertical axis wind turbine. The large commercial vertical axis wind turbine concept is hindered due to its dynamic and stability problems, which makes most of the production of wind turbines nowadays horizontal axis type (Figure 1.1). A typical horizontal axis wind turbine is usually composed of the following components: rotor (including blades and hub), drive train, electrical system, nacelle, power control system, tower, foundation, etc. The rotor is generating wind kinetic motion to kinetic motion of the drive train through the rotation of rotor blades. Drive train, electrical system, power control system etc are responsible for the production and control of power generated through the kinetic motion of the blades. Tower and foundation are support structures connecting the turbine with the ground for onshore wind turbine or sea bed for offshore wind turbine.

1.1.2 Wind turbine support structure

In this thesis, support structure of wind turbine includes the tower and the foundation (Some author may only refer support structure to the tower). For the support structure, various structural forms exist. Tower could be a tubular structure or lattice (also called truss or jacket) structure or a hybrid type combining both the previous while foundation could be a monopile or a tripod pile or even a gravity base structure. The behavior of support structure of a wind turbine under dynamic external loading in the offshore environment is important for the performance of the wind turbine itself including the

power production output. On the other hand, proper design of the support structure is also a solution to the issue of structural safety and reduction of input cost.

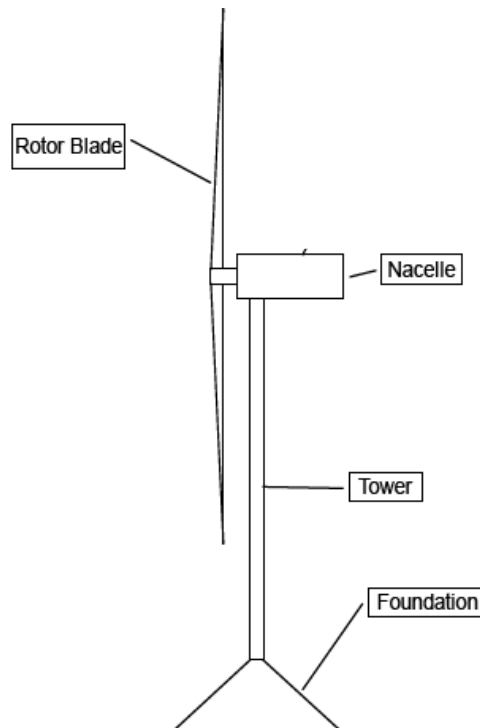


Figure 1.1 Components of a Horizontal Axis Wind Turbine

1.1.3 Wind turbine control system

In addition to the proper structural design, the control system is also an important aspect for the sound operation of a wind turbine. The aim of creating a wind turbine is to generate electrical power at a reasonable amount of input and with lower negative impacts on the environment. However, under the stochastic and dynamic wind environment and the complex wave impacts offshore, control system is demanded in order to reduce the external loads, lengthen the structure's life span and optimize the power production. For instance, two types of power regulation concepts are usually applicable to a horizontal axis bottom founded wind turbine: the active power control method (pitch control) regulating the power by pitching the blades and the passive power control method (stall control) uses the stall effect to reduce the lift forces. Yaw control is employed to make sure the rotor is able to capture the maximum wind kinetic motion in order to optimize the power production. The connection between the power generated by a wind turbine and the grid receiving the electrical power should also be under the regulation of the control system in order to smooth the operation of the wind turbine. In all, control system is employed for offshore wind turbine in order to enhance the safety, optimize the production and lower the cost.

1.2 Background and content of this work

1.2.1 Background

This thesis work is majorly focusing on offshore wind turbine support structure and in particular, a crucial component that connects the support structure and the nacelle assembly (called transition piece in this thesis). For offshore wind turbines to be installed in water depth shallower than 70m, conventional bottom founded support

structures will probably continue to be used. Nearly all bottom founded offshore wind turbines have up to the time being been installed in moderate water depth (10-25m) and usually a monopile foundation has been preferred. In a depth of 30-70m, however, lattice tower geometry will probably turn out to be advantageous. A lattice topology could be used for the entire support structure between sea bottom and turbine nacelle (foundation and tower) or only for the part beneath the tower. So far, only the latter hybrid concept has been installed in practice. This concept permits the use of a standard tubular tower for the upper part but a complicated transition piece is needed at the intersection to the lattice. The full lattice support structure concept is a relatively new proposal for offshore wind turbine and one critical challenge in the design of such a structure is the design of the lattice top and the connection between it and the nacelle. The thesis is therefore based on proposal of a full lattice support structure concept connecting the sea bed and up to the turbine nacelle assembly with consideration of designing a proper transition piece between the lattice structure and the nacelle assembly.

1.2.2 Content

Under such background, the thesis will thus cover the following aspects:

- (1) A brief overview of existing support structure designs based on space frame or lattice topology as well as existing designs of transition piece on hybrid offshore wind turbine support structure;
- (2) Conceptual model of the transition piece including its geometrical configuration limitation, functional requirement such as layout of power transmission equipment and connection with the yaw system, and a mechanical model understanding the boundary condition from the lattice support structure and all the external loads the transition piece is subjected to;
- (3) Numerical analysis of proposed transition piece models under different load conditions and various load cases in order to compare the performance of different designs and to select the best optimal model for practice;
- (4) Conclusion of the thesis work and recommendations for relevant future applications.

1.3 Scope and limitation

As research and development of offshore wind industry is further strengthened and deepened, the trend of offshore wind farm development is heading for a maximum production capacity in future and the size of future offshore wind farm will become more and more significant. Challenges remain and will even grow where questions related to structural safety, high commercial cost and impact on surrounding environment are all arising.

This thesis is endeavoring to solve one of the greatest challenges for a novel type of support structure for offshore wind turbine and the purpose is to achieve a balance point between the safety, cost and the overall performance. Limitations exist because there is no existing experience to learn from for this thesis topic and many resources in the offshore wind industry are still not accessible to public. The whole thesis work is majorly based on conceptual studies and numerical analysis whereas there is a lack of verification from either physical modeling or industrial experience. The thesis is

Introduction

Lattice Tower Design of Offshore Wind Turbine Support Structures

therefore trying to produce a work within its scope that could be useful or applied as reference when future relevant projects are to be planned.

2 LATTICE SUPPORT STRUCTURE FOR OFFSHORE WIND TURBINE

2.1 Introduction of lattice structure

At current stage of offshore wind development, reducing the amount of input cost is still a big challenge. Wind energy is positive in the way that the wind resource is renewable and it does not produce harmful impact like green house gas from conventional power source. However, one of the shortcomings with offshore wind is that the amount of input makes it not as much commercially competitive as other conventional power generation sources for the time being.

The tower accounts for approximately 20% of the total manufacturing cost for a wind turbine [3]. For turbines with higher rated power capacity, the percentage could be even increasing. Reduction of cost could be made through various methods: optimization of structural form can save material cost if sufficient structural strength is maintained or manufacturing cost can be lowered by means of mass production. The latter is in fact the reason why large scale wind farm development is becoming the interests of many. As for optimization of structural form, the 20% or even higher cost of the tower could be possibly reduced if for instance lattice structure is applied as support structure for wind turbine. Lattice structure possesses advantages in that it generally requires less material; the wave load impact in the offshore environment is also reduced due to the reduced impacted area compared with monopile structure. On the other hand, transportation of lattice structure is also much more convenient when road transportation capacity of 4-6m is limited if a larger dimension of monopile is required for a larger scale wind turbine.

2.2 History of lattice tower for onshore wind turbine

Lattice tower applied as wind turbine support structure does not come until recently. In fact, during the earliest period of onshore wind turbine development, lattice tower was already adopted. This type of structure is simple to construct and stiff in function. A lot of such structures can be seen on the early onshore wind turbines (Figure 2.1).



(a) Lattice Tower for Small Wind Turbine

(b) Lattice Tower for Large Wind Turbine

Figure 2.1 Example of Lattice Tower for Onshore Wind Turbines

Lattice Support Structure for Offshore Wind Turbine ***Lattice Tower Design of Offshore Wind Turbine Support Structures***

As the size of wind turbine increased, lattice tower was gradually displaced by tubular tower. In the early experimental stage of wind energy and especially when the size of wind turbine was still moderate, the emphasis was not placed on cost reduction of the tower, which is why the tubular tower was very widely and popularly used. However, as commercialization of wind energy is urged and the size of wind turbine grows, after cost reduction measurements on mechanical components like the gearbox and generator are achieved, cost minimization associated with the turbine support structure is again attracting interests and this is why these years the lattice structure is receiving more and more attentions, especially on large scale offshore wind turbines.

2.3 Current application of lattice support structure for offshore wind turbine

Going offshore, there is an even more urgent demand for cost reduction compared with onshore situation. If onshore lattice tower was abandoned because of a particular preference on aesthetics, the offshore sees no such problem since offshore wind turbine is located at a distance from the coast, far from public eyes. Using lattice structure in offshore has also a positive effect when considering the wave and current load on the structure because the flow impacting area on a lattice structure is much smaller than that on a tubular structure. Another big advantage for the lattice support structure is the significant reduction of material cost compared with the tubular structure. With a given height and stiffness, the expenditure of material for a lattice support structure is less than the case of tubular tower by up to 40% [4]. This therefore results in a very considerable cost advantage.

For current applications, hybrid concept composed of a lattice structure at the lower part and a tubular tower structure at the upper part already exists for many projects (Figure 2.2). The application of such concept is usually in deep water depth ranging from 20m to 50m. A full lattice support structure design for offshore wind turbine in deep water region is yet found in practice. The following paragraphs introduce several projects of hybrid design existing in sea:



Figure 2.2 Hybrid Support Structure for Offshore Wind Turbine [5]

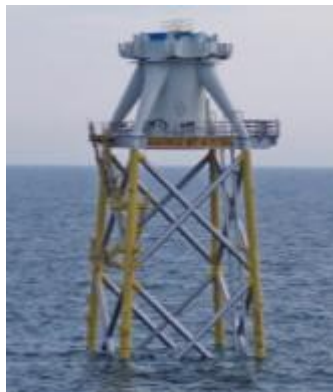
2.3.1 OWEC jacket quattropod for Beatrice demo wind farm [6]

This demo project is composed of two 5MW wind turbines installed adjacent to the Beatrice oil field, 25 km off the east coast of Scotland. The two units are located in

Lattice Support Structure for Offshore Wind Turbine
Lattice Tower Design of Offshore Wind Turbine Support Structures

water depth up to 45m and each has a turbine weighing about 410 tons, fitted with three blades each 63m long. The turbine is mounted on a tall tower which then sits above a substructure fixed to sea bed. Hub height of the wind turbine is about 88m above sea surface.

For the substructure supporting the tower, which is a tapered steel monopile weighing about 210 tons, there are two design concepts. One of the designs is the OWEC Jacket Quattropod (OJQ) (Figure 2.3(a)) which weighs about 750 tons plus the piling arrangements. This design meets the required stiffness and fatigue life. The square base of the OJQ has sides 20m long, thus covering about 400m² of seabed. There is an alternative tripod structure concept which has a slightly larger base area (about 600m²). Both types of substructure can be fixed to the seabed either by suction piles or by driven steel piles.



(a)OJQ for Beatrice Wind Farm



(b)OJQ for Alpha Ventus Wind Farm

Figure 2.3 OWEC Jacket Quattropod on Offshore Wind Turbine [5]

2.3.2 OWEC jacket quattropod for Alpha Ventus offshore wind farm [7]

This wind farm is situated about 45 km north of the island of Borkum, Germany, in water depth of 30 meters. The wind farm is composed of 12 wind turbines acting as the first offshore wind farm for Germany. 6 of these 12 wind turbines employ the OWEC Jacket Quattropod as substructure supporting the tower and the above turbine (Figure 2.3(b)). Each of the OJQ wind turbine is designed for a 5MW turbine. Weight of the nacelle with rotor and hub is about 410 tons and the OJQ weighs about 500 tons (Table 2.1) while the tower above it weighs about 210 tons. The jacket structure has a height of 56 meters.

Table 2.1 Weight Break-down for OJQ Jacket at Alpha Ventus Project [8]

Jacket Frame (Legs & Bracings)	Primary Structure: $\Sigma=425\text{tons}$	Jacket Subtotal: $\Sigma=510\text{tons}$	Total Weight per Installation $\Sigma=825\text{tons}$
Pile Sleeves Transition Piece including Platform			
Boat Landings (2 units) Miscellaneous (e.g. J-tubes) Anodes	Secondary Structure: $\Sigma=85\text{tons}$		
Piles	315tons (8 piles, D=1067mm, L=50m, t=30mm)		

2.3.3 RAMBØLL jacket for the Upwind project [9]

In this project, the jacket support structure is designed for a 5MW baseline turbine (weighing about 350 tons including nacelle and rotor) in 50m water depth. The four legged jacket has four levels of X-braces and four central piles with a penetration depth of 48m grouted to the jacket legs. The total height of the jacket from mud line including the transition piece and excluding the tower is 70.15m. The upper conical tower has a total height of 68m resulting in a hub height of 90.55m above the mean sea surface. The bottom tower section has a diameter of 5.6m. The complete support structure configuration is shown in Figure 2.4. Design parameters of this jacket substructure concept are shown in Table 2.2.

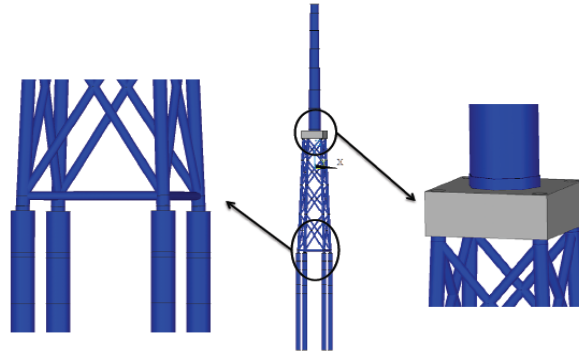


Figure 2.4 RAMBØLL Jacket Substructure Configuration for Upwind Project [9]

Table 2.2 Design Parameters of RAMBØLL Jacket Substructure for Upwind Project [9]

Base Width		Pile Diameter	Pile Penetration	Jacket Weight	All 4 Piles	Total Jacket Weight (incl. Piles)
Bottom	Top					
12m	8m	2082mm	48m	545tons	438tons	983tons

2.3.4 RAMBØLL jacket for the OC4 project [10]

In this design, the substructure is similar to the RAMBØLL design concept described above for the Upwind project. Properties of the tubular members for the jacket substructure are shown in Table 2.3. The height of this jacket substructure ranges from water depth -45m to 20.15m above mean sea level. The base area is 12m×12m and the jacket top area is 8m×8m.

Table 2.3 Properties of Jacket Members for OC4 Project [10]

Component	Outer Diameter (m)	Thickness (mm)
X- and Mud Braces	0.8	20
Leg at Lowest Level	1.2	50
Leg at 2 nd to 4 th Level	1.2	35
Leg Crossing Transition Piece	1.2	40
Pile	2.082	60

2.3.5 REpower jacket [11]

WeserWind Offshore Construction Georgsmarienhütte in 2008 built a jacket substructure for offshore wind turbine for the purpose of testing on land (Figure 2.5). A REpower 5MW offshore turbine was installed on this jacket structure. The jacket structure is approximately 57 meters in height and has a total weight of around 320 tons. Standard steel pipes from the pipeline construction industry are used for the jacket. The base of the foundation has a total area of nearly 300 m² with the width of 17 meters.

Lattice Support Structure for Offshore Wind Turbine

Lattice Tower Design of Offshore Wind Turbine Support Structures



Figure 2.5 REpower 5MW Wind Turbine on a Jacket Substructure [11]

2.4 Summary of lattice as support structure for offshore wind turbine

While lattice tower used for onshore wind turbine has a long history, though it was replaced later by monotower, the application of lattice as support structure for offshore wind turbine has started recently. Current applications of such lattice structure are usually taking place in deep water depth of 30-50m, used as substructure supporting monotower and designed for 5MW turbine weighing around 350-410 tons including nacelle and rotor. The dimension of these lattice substructure designs vary from case to case. While the OJQ design weighs around 510 tons (piles exclusive) supporting tower of 210 tons and turbine of 410 tons, the RAMBØLL jacket concept weighs about 550 tons supporting turbine of 350 tons. In all of the previous designs, there is a critical connection between the lattice substructure and the upper tower – the transition piece (TP). The design of this transition piece has a significant variation ranging from a concrete design (Upwind) to a steel design (Beatrice and Alpha Ventus) and from a gravity base design to a steel conical design or even a steel bracing design. Detailed introduction and these designs will be following.

Unlike for early onshore wind turbines where lattice structure is applied as full tower (Figure 2.1), for offshore wind turbine the lattice structure is only used as a substructure supporting the monotower above it (Figure 2.2). A full lattice design as support structure for offshore wind turbine has yet been implemented. Application of such concept will unavoidably induce another problem: the connection between the lattice support structure and the turbine nacelle assembly, especially when aspects as the yaw system, power transmission cable layout, etc are considered. The next chapter will provide detailed description of this transition piece component including a case study of lattice as full support structure proposed for a 5MW offshore wind turbine.

2.5 Introduction of transition piece

For the concept of a full lattice structure supporting offshore wind turbine, an important issue is the appropriate connection of the lattice structure and the rotor nacelle assembly. Early onshore wind turbine with turbine and rotor of small dimension has set up previous experience, however, when the offshore wind farms go to regions of much deeper water depth, the desired power capacity is becoming higher and higher and the dimension as well as weight of the turbine nacelle assembly increases significantly (Table 2.4), the role this transition piece plays will no doubt become a critical issue for

the design of the whole wind turbine unit. In March 2011, Vestas published its new product of V164-7.0MW designed for offshore purpose [12]. The new turbine has a rotor diameter of 164m and the weight of the rotor nacelle assembly reaches almost 500 tons. Under this industrial background with full of challenges, problems related to transition piece connection with the yaw system, arrangement and layout of the power transmission cables, ultimate and fatigue load transferring from the rotor nacelle assembly to the support structure, etc all arise.

Table 2.4 Wind Turbine Size Trend

Year	1980	1985	1990	1995	2000	2005	2011	2015	2020
Rotor Diameter(m)	15	20	40	50	112	126	150	175	252-300
Rated Power(MW)			<5.0			5.0	7.0-7.5	10	20

2.6 Transition piece for early onshore wind turbine supported by lattice tower

Early development of onshore wind turbines has set up experience of how to deal with this transition piece. However, the dimension of the early turbines and their weight cannot be compared with the multi megawatt requirement of present needs and even larger turbine units in future, not to mention whether complex functional requirements including the yaw control was taken into consideration or not in those early designs. A frame-cylinder system composed of an external steel frame of supports and an internal steel moncolumn in the core is adopted in the small wind turbine of Figure 2.1(a). A single steel moncolumn structure sitting on top of the lattice support structure and supporting the nacelle assembly is employed in the larger turbine of Figure 2.1(b). These concepts are somehow early prototypes for the transition piece design of the more recent hybrid offshore wind turbine support structures.

2.7 Transition piece for hybrid offshore wind turbine support structures

2.7.1 Transition piece for Beatrice demo wind farm

This design employs a frame-cylinder system (Figure 2.3(a)). The four legs of the bracing sit on top of the four legs of the lattice substructure respectively and linearly enlarge in diameter to connect with a cylinder structure inside the frame of bracings. The four legs of this transition piece have uniform structural dimension but the diameter of each leg varies from the connecting end with the lattice substructure leg to the other end with the internal cylinder. At the connecting points with the lattice legs, the diameter of the four bracing legs is at the same magnitude with the lattice legs. At the other end, the diameter of the bracing legs is increased significantly by almost 2-3 times which strengthens the connection with the cylinder structure in the core. There is a ring plate sitting above the four connecting ends between the bracing legs and the cylinder. On top of the cylinder a complex system exists which should be able to allow convenient and robust connection between the upper tower and this transition piece. At the surface right above the lattice substructure locates the platform of this offshore wind turbine. According to M. Seidel [8], this design is relatively heavy but it enables a wide jacket tip and flexible batter angels.

2.7.2 Transition piece for Alpha Ventus offshore wind farm

In the Alpha Ventus offshore wind farm, the same jacket substructure design OJQ is used on half of the total number of wind turbines. The transition piece design is however altered from its older brother for the Beatrice wind farm.

In this more recent design (Figure 2.3(b)), the transition piece is designed obviously lighter than the previous design for the Beatrice wind farm. The structural form stays the same, which consists of a steel cylinder in the core, four legs of bracing connecting the lattice legs and the internal cylinder, a ring plate sitting on top of the upper bracing leg joints and other miscellaneous components. Compared with the Beatrice design, the dimension of the bracing legs and the core cylinder are all reduced. Diameter of each bracing leg still shows variation from the lower connection joint to the upper one, but the degree of this variation is shrunk much more than the previous design resulting in a more or less uniform diameter that is nearly the same as that of the lattice substructure legs. Geometric comparison between this Alpha Ventus design and the previous Beatrice design shows a trend of lighter design and hence lower material cost. Reasons for this design alternation could include the different load conditions in each specific site. Nevertheless, the lattice substructure design is generally the same and the installed turbine units in these two projects are also the same (REpower 5MW). An improvement made after the experience from the older brother design could be another reason for the alternation in this more recent design.

2.7.3 Transition piece for the Upwind and OC4 project

By the time of this thesis work, the RAMBØLL jacket concept has not been put into practice yet. In this design concept, however, RAMBØLL proposes a different configuration of lattice substructure from the OJQ design, i.e., the bottom width of RAMBØLL jacket is designed as 12m whereas the OJQ has a bottom width of around 20m. The transition piece employed here is also significantly different, being a rigid massive concrete block weighing 666 tons with a dimension of 4m×9.6m×9.6m (Figure 2.4). Connection with the lattice substructure is made via grouting of the upper part of the four lattice legs into the concrete block.

The material for the transition piece has been chosen as reinforced concrete rather than the other steel concept, which is based on a cost benefit evaluation. The concrete transition piece has the weight as a disadvantage. However, it is neither as susceptible to fatigue damage nor as labour intensive compared to a steel transition piece [9].

2.7.4 Transition piece for REpower jacket in Bremerhaven

For this solution developed by REpower (Figure 2.6), the structure is lighter compared with the first OJQ Beatrice transition piece. The structure has a truncated cone shape with four external struts connected to the cone surface. These four struts sit on the four jacket legs respectively and extend upwards before the flange connection with the upper tower. The height of the steel cone is about 7 meters and the structure weighs about 50 tons. The structure has so far only been tested for a relatively steep batter angle and a narrow jacket top [8].



Figure 2.6 Transition Piece of REpower Jacket [8]

2.8 Summary of transition piece designs

Although designs of the transition piece vary according to specific and individual project requirements including the loading condition, connecting structural dimension, the rotor nacelle assembly weight, etc, there are some general types of the transition piece design for selection and consideration:

(1) Frame-cylinder. This design is composed of a steel frame of bracings in the outside and a steel cylinder structure in the core. Both early onshore lattice tower supported wind turbine (Figure 2.1(a)) and recent hybrid offshore wind turbine (Figure 2.3) have applied this design concept. From a structural characteristics point of view, this combination of an external frame system and an internal cylinder structure will increase the strength and the robustness of the transition piece. The bracing legs are designed to allow for convenient connection with the lattice substructure and the internal cylinder structure is employed for connection with the upper tower, through the application of a specific flange connection. The more recent design of such a transition piece concept for the OJQ in Alpha Ventus project (Figure 2.3(b)) has a shrunk design and reduced weight than the earlier design for the same OJQ in Beatrice wind farm (Figure 2.3(a)).

(2) Steel Cone. This design has a simpler geometry profile compared with the previous frame-cylinder structure. Reduction of material cost might be achieved through the elimination of the bracing legs but the larger dimension of the cone structure will in the same time require a higher demand of material cost. Connection with the lattice legs requires the addition of a number of struts (Figure 2.6). This type of transition piece has only been tested for the REpower jacket on land. For onshore wind turbine a cylinder structure with uniform diameter rather than the truncated cone shaped can be found (Figure 2.1(b)).

(3) Concrete block. This design has only been proposed in the research stage and not been seen in real practice yet. The advantage of such a design is its cost benefit. A heavy concrete block weighing several hundred tons will have a big influence on the dynamic behavior of the whole support structure system. The decision to adopt this heavy transition piece design concept should be specifically made in combination with the analysis of support structure's dynamic properties.

All the above design concepts are either actually employed or only studied for onshore lattice tower supported wind turbines and hybrid offshore wind turbines. Since there is no existing experience of a full lattice structure supported offshore wind turbine, there is

Lattice Support Structure for Offshore Wind Turbine
Lattice Tower Design of Offshore Wind Turbine Support Structures

no design prototype to learn from for a transition piece design between a full lattice support structure and directly the turbine nacelle assembly. However, the previously introduced concepts of the frame-cylinder structure and the steel cone structure could be possibly applied as connection for the lattice support structure and the nacelle assembly due to the light weight characteristic. The heavy design like the concrete block might be possible for the hybrid support structure concept but should be avoided for a full lattice supported offshore wind turbine because an addition of this heavy component from the transition piece which is almost at the same or even bigger magnitude of the rotor nacelle assembly weight will force the support structure to bear an extremely large mass of over twice as much as a normal turbine nacelle assembly at the structure top. An inclination of the structural vertical axis will thus induce a significantly larger bending moment at the base of the support structure as well as a much larger deflection of the structure itself. Detailed analysis of the previously mentioned design concepts will be introduced in the following chapters.

Lattice Support Structure for Offshore Wind Turbine
Lattice Tower Design of Offshore Wind Turbine Support Structures

3 CONCEPTUAL MODEL OF TRANSITION PIECE

Design of transition piece can only be possible after understanding all the requirements that this component should meet. Previous experience and existing design models can be referred to but a good design should always be able to look into the specific characteristics of each individual project. After the outcome of a conceptual design model, further analysis and adjustment can be made in order to ensure every detailed requirement. A suitable conceptual model should take into consideration the following aspects.

3.1 Geometrical requirement

The transition piece is employed as a connection between the lattice support structure and the turbine nacelle assembly. Normally, the top area of the lattice structure will be a square plane with equal width. Considering the yaw rotation mechanism, the connection with the upper nacelle assembly is usually through the yaw bearing which will be introduced later. Yaw bearing ring normally has a circular profile which allows the rotation of the nacelle around the yaw axis. Therefore, these lower and upper geometrical characteristics call for a transition piece with a square base profile and a circular top profile (Figure 3.1).

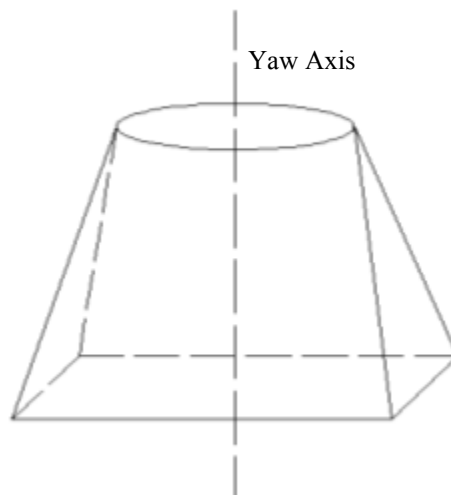


Figure 3.1 Geometrical Profile for Transition Piece

A simple solid structure with complex external profile could be able to meet this geometrical requirement; however, such type of structure increases the complexity of manufacturing and limits the possibility of out-of-factory assembling. Another solution is composed of a cylinder structure in the middle which meets the upper geometrical profile requirement and a frame of supporting legs outside which forms the base geometry of a square shape (Figure 3.2(a)). This is the geometrical model adopted by the frame-cylinder type of transition piece that has been applied on both onshore wind turbines and offshore hybrid wind turbines. In addition, a cone (strictly speaking, truncated cone) shaped cylinder with a number of struts connected on the cone surface at the four corners also satisfies the geometry requirement (Figure 3.2(b)). This model is used on the REpower 5MW wind turbine for test purpose (Figure 2.6). Even for the concrete block concept of RAMBØLL jacket (Figure 2.4), the transition piece suits the lattice substructure top surface and the upper tower can be grouted into the concrete

block. Various structural profiles which can meet the above mentioned geometry characteristics suffice but for simplicity, with consideration of manufacturing, transportation, assembly and structural cost, the existing frame-cylinder concept and the cone-strut concept seem to have more advantages than the others.

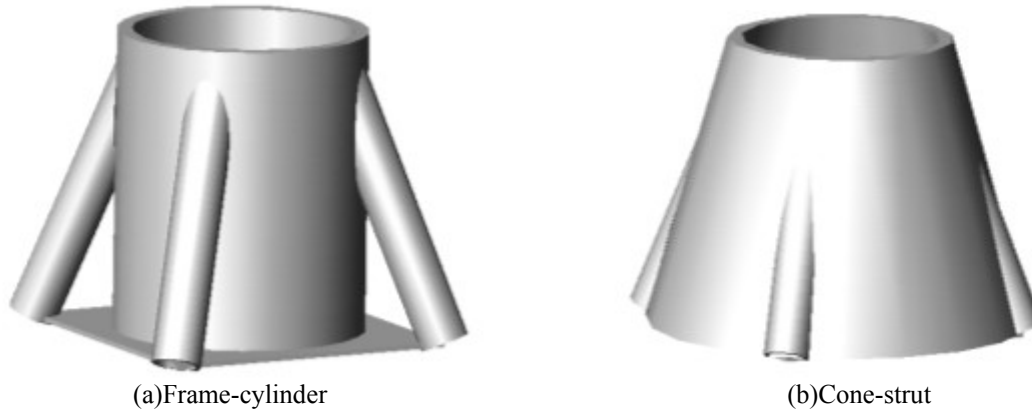


Figure 3.2 Various Geometrical Models for Transition Piece

3.2 Functional requirement

In addition to the geometrical challenge, the transition piece should also be able to meet a number of functional requirements. Transition piece is a critical design component which needs careful detailing. Several authors have previously shown lattice support structure design proposals, but this transition structure was often only sketched and not realistically designed. There is a large uncertainty for those proposals because the transition piece is the greatest design challenge (M. Seidal [8]). Functional requirement need to be observed regarding the following aspects:

3.2.1 Power transmission equipment

For conventional monotower support structure, all the electrical equipment including power transmission cable, switchgear and even the transformer can be located inside the support structure (Figure 3.3). For a lattice support structure, location of large size equipment can be a challenge because there is no external coverage for protection of the equipment. This problem appears especially in the harsh offshore environment where corrosion and other environmental eroding sources are present.

Particularly, for the power transmission cable, one of the challenges is the twisting of the cables (e.g. the cable loop for twisting in Figure 3.3). For offshore wind turbine, an additional consideration of lay out of the cables in the sea water is required. When the lattice structure is applied as support structure, the challenge of cable arrangement is no doubt increased. Current solution for protection of power transmission cables in offshore employs external equipment like the J-tube (Figure 3.4). The J-tubes provide solution for cable placement in the sea water, however, these additional equipment also add cost to the amount of input. Elimination of the J-tube will reduce the cost, if alternative solutions for cable placement are possible. For lattice support structure, since the diameter of the lattice leg of existing designs is usually around 1.0m, there is thus a requirement on the maximum diameter of the power transmission cable to be used if the solution can be made by means of locating the power transmission cable inside one of the four lattice legs. Alternatively, if there are a multiple number of cables transmitting

Conceptual Model of Transition Piece
Lattice Tower Design of Offshore Wind Turbine Support Structures

the power from the turbine, these cables can be separated into each of the four legs respectively, which however can be avoided because the present industry is able to provide power transmission cable at convenient dimension. ABB [14] has experience of utilizing various types of cables, including HVDC Light (High Voltage Direct Current) for DC transmission (Figure 3.5(a)) and XLPE (Cross-linked Polyethylene) for AC transmission (Figure 3.5(b)). Both types have been applied in existing offshore wind farms already (Appendix I). The properties of the HVDL Light cable and the XLPE cable are referring to [16] & [17].

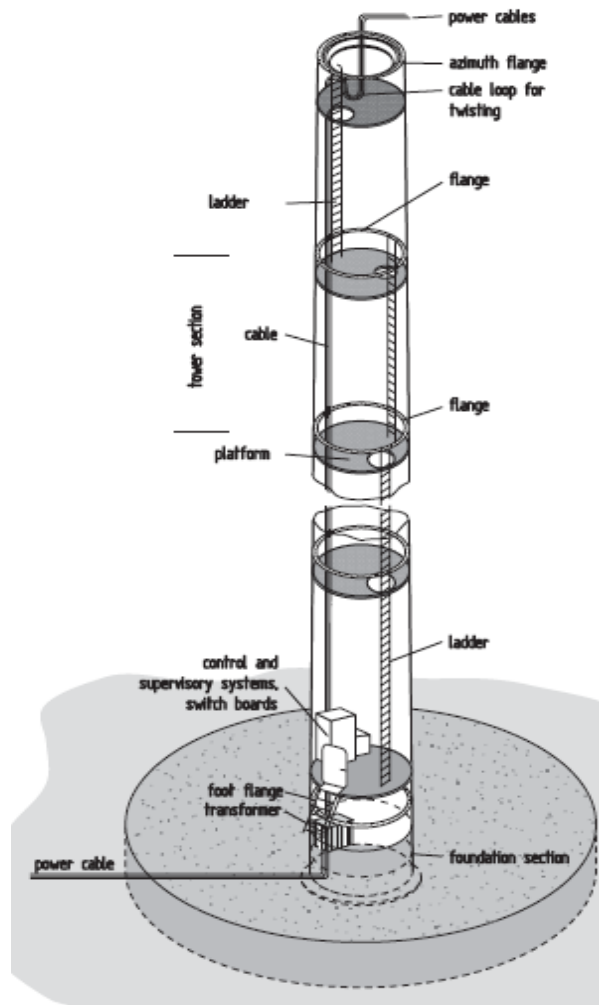
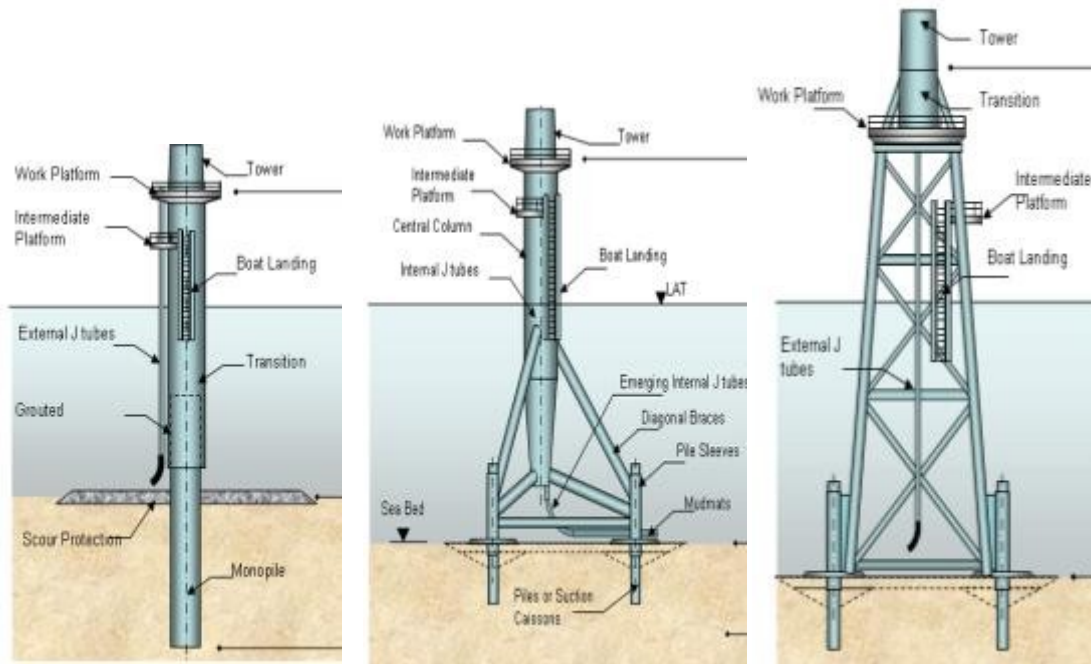


Figure 3.3 Equipment Arrangement in an Onshore Monotower Wind Turbine [3]

For HVDC Light of 300kV cable bipole, cable diameter reaches up to 155mm for the submarine use and 131mm for land use. Diameter of single-core XLPE cable reaches up to 141mm for 400kV nominal voltage while diameter of three-core XLPE cable reaches up to 247mm for 275kV nominal voltage. The lattice support structure leg could thus be able to accommodate the power cable for a wind turbine with rated power of multi megawatt. Layout of the cable through the transition piece could be made inside the cylinder for the frame-cylinder type transition piece or inside the cone for the cone-strut type (Figure 3.6). As for large-size electrical equipment like switchboard and transformer, onshore lattice supported wind turbines can find an easy solution of building an accommodating house and locating these components on the base ground inside the lattice or just beside the lattice structure (Figure 2.1). For offshore wind farms, usually a specific platform accommodating the relevant equipment will be required [18].

Conceptual Model of Transition Piece
Lattice Tower Design of Offshore Wind Turbine Support Structures



(a) Monopile Foundation (b) Tripod Foundation (c) Lattice Foundation
 Figure 3.4 Application of J-tube for Power Cable Protection for Offshore Wind Turbine [13]

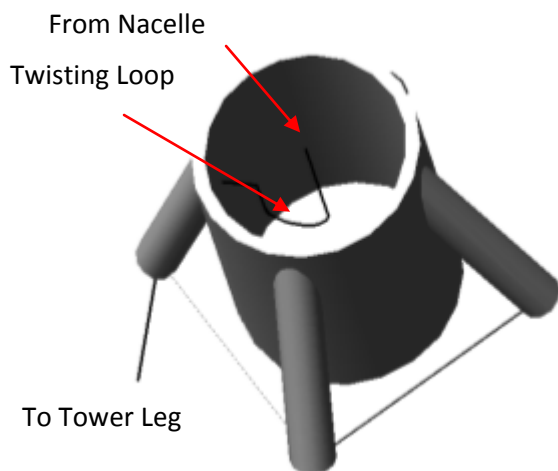


(a) HVDC Light for DC

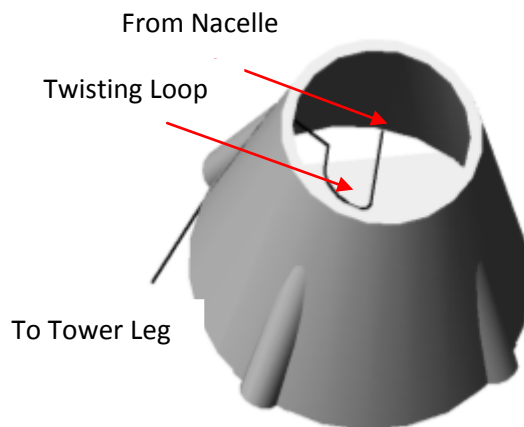


(b) Single-core and 3-cores XLPE for AC

Figure 3.5 Power Transmission Cable for Offshore Wind Farm [15]



(a) Cable Arrangement in Frame-cylinder TP



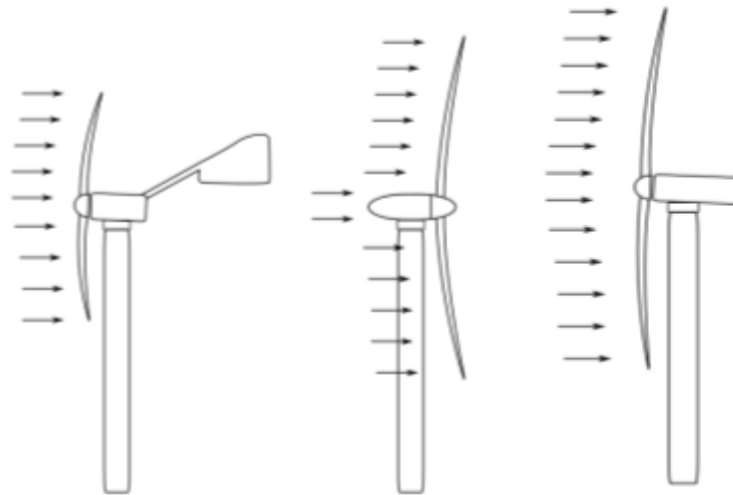
(b) Cable Arrangement in Cone-strut TP

Figure 3.6 Power Transmission Cable Layout in Transition Piece

3.2.2 Yaw system

If the rotor is to fully capture the power from wind, it should be oriented correctly with respect to the incoming wind direction. A yaw angle, i. e. an angle deviation between rotor axis and mean wind direction, causes a loss of power production. In general the rotor can be oriented into the wind by three types of yawing concepts (Figure 3.7):

- (1) Aerodynamic yawing via wind vanes or fan-tail wheels;
- (2) Free yawing of downwind rotor;
- (3) Active yawing by motorized yaw drive.



(a)Aerodynamic Yawing (b)Passive/Free Yawing (c)Active/Motorized Yawing
Figure 3.7 Different Yawing Concepts [19]

The first concept is not found in present large turbines any more. For modern wind turbines of multi-megawatt rated power with rotor nacelle assembly mass of over 300 tons and rotor diameter of over 120m, this yawing method is far outdated. As for the idea to exploit free yawing of a downwind rotor, if this is successful, manufacturing cost can be saved. However, attempts to introduce free yawing to large turbines have not been successful so far. Motorized yawing had not been intended originally but initial tests with the prototype showed that correct and stable free yawing of the rotor was not possible so that a motorized yaw drive had to be subsequently installed. Extensive test programs were carried out on the experimental American MOD-0 turbine to investigate free rotor yawing [20] and these tests confirmed that accurate free yawing could not to be achieved. The presently exclusively employed motorized yaw system or active yaw system has the task of automatically orienting the rotor and the nacelle into the wind. Some of the components of this active yaw system are integrated into the nacelle and some should be connected with the transition piece. The entire system consists of the following components:

Yaw bearing

Yaw bearing is subject to contradictory requirements. On one hand it should ensure easy-running yawing and a long service life and on the other hand yaw damping is desirable, even during the yawing, in order to avoid unwanted yawing oscillation. These requirements can be met both by a conventional roller bearing and by a gliding bearing. The traditional design consists of a large roller bearing whereas a four-point ball bearing is used often in more recent designs. The alternative is a gliding bearing in which the nacelle moves on sliding elements made of synthetic material. One advantage of the

gliding bearing consists in that no elaborate brakes and braking rings as in roller bearing are required.

(1) Roller yaw bearing

The roller yaw bearing is a common technical yaw bearing solution followed by many wind turbine manufacturers because it offers low turning friction and smooth rotation of the nacelle. The low turning friction permits the implementation of slightly smaller yaw drives compared to the gliding bearing solution, but on the other hand requires a yaw braking system (Figure 3.8). Various types of roller bearings are available (Figure 3.9) and for more recent wind turbine yaw bearing, the ball bearing still has a dominating position.

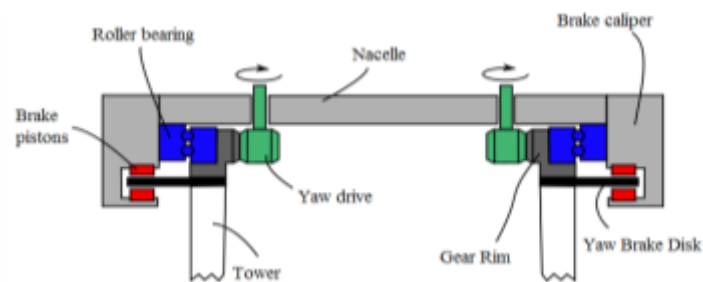
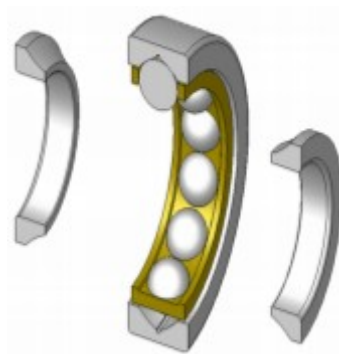


Figure 3.8 Configuration of a Roller Bearing System [19]



(a) Four-point-contact Radial Ball Bearing



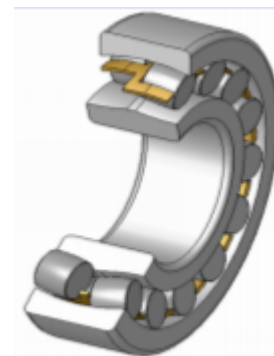
(b) Single-row Angular-contact Ball Bearing



(c) Cylindrical Roller Bearing



(d) Tapered Roller Bearing



(e) Double-row Spherical Roller Bearing

Figure 3.9 Various Types of Roller Bearing [19]

(2) Gliding yaw bearing

The gliding yaw bearing is a combined axial and radial bearing. The modern yaw bearings can restrain the nacelle from being rotated by the moments induced by the upper half of the rotor sweep disk and the torque of the drive train. Principally, the simplest way to accomplish the yaw bearing task with gliding elements is with two gliding planes for the axial loads (top and bottom) and a radial gliding surface for the radial loads. Consequently, the gliding yaw bearing comprises three surfaces covered with multiple gliding pads. These gliding pads come in sliding contact with a steel disk, which is usually equipped with gear teeth to form a gliding-disk/gear-rim (Figure 3.10).

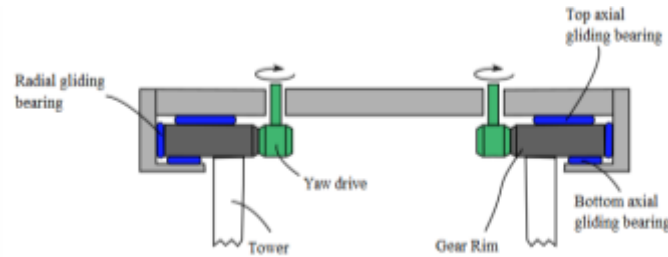


Figure 3.10 Configuration of Gliding Bearing System [19]

(3) Comparison of yaw bearings

For the purpose of designing an optimal transition piece, it is essential to study the differences of various types of yaw bearings so as to understand the pros and cons of each type for the selection for a multi megawatt offshore wind turbine. Generally, selection of the yaw bearing type should include considerations of the loads, the yawing rate, required life time and available space within the nacelle assembly. Differences between the roller yaw bearing and the gliding yaw bearing are shown below in Table 3.1.

Table 3.1 Comparison of Different Types of Yaw Bearings

Category	Roller	Gliding
Segmentation	Non-segmented	Segmented or Non-segmented
Friction	Small	Normal
Yaw Drive	Small	Normal
Elaborate Bracking	Needed	Not necessary
Lubrication		Central lubrication or Self lubricated elements
Repair	Disassembly needed	Reparability via individual segment for segmented system; External crane or mechanical or hydraulic jack needed for non-segmented system
Products	REpower 5M (4-point ball bearing) REpower 6M (4-point ball bearing)	Vestas V90-3.0MW (Friction gliding bearing)

As previously mentioned, for present large size wind turbines, roller bearing especially the four-point ball bearing is widely used. The gliding bearing on the other hand has successful applications on small size and medium size (Vestas V90-3MW) turbines.

Yaw drive

The two choices for the yaw drive are hydraulic and electrical components. Promoters of the hydraulic system name lower cost, smaller size and also higher torque as

advantages. Another advantage of hydraulic yaw drive is that it is easy to control compared with electric drive. The power of the drive motor depends on the rate of adjustment required. Electric motor is being increasingly used in more recent yaw drives. The hydraulic drive is being replaced by the controllable electric drive motor. Some manufacturers are using electric yaw drive with integrated brakes so that separate yaw brakes are no longer required.

The number of the yaw drives and their location with regards to the yaw bearing vary from design to design. The yaw drives may be located at the outer surface of the yaw bearing ring (Figure 3.11) or they may be located at the inner surface of the yaw bearing ring (Figure 3.8 & Figure 3.10). The REpower 5MW wind turbine, for instance, has yaw drives connecting with the outer surface of the yaw bearing ring.

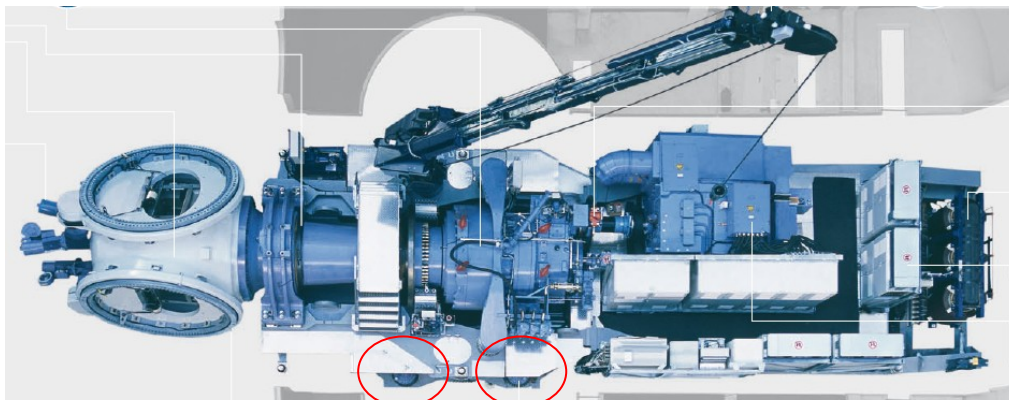


Figure 3.11 Location of Yaw Drive in REpower 5MW Turbine System

Yaw brakes

In order to avoid the drive motors from having to absorb the yawing moment after a completed yawing operation, a yaw brake is required unless special electrical yaw drives with integrated braking function are used.

Locking system

In larger turbines, the yaw drive is positively locked in position for extended standstill period, for example for maintenance. This job is handled by one or several locking bolts.

Yaw control system

Yawing the nacelle into the wind direction requires a special control and operating logic. The yaw control mechanism is basically a function of the yaw angle. For instance, the wind measuring system of the turbine provides a mean value of the wind direction over a period of ten seconds. This value is compared with the instantaneous position of the rotor axis every two seconds. If the deviation remains below 3 degrees, the yaw control system will not be activated. If the yaw angle is small, for example 10 degrees, yawing is carried out within 60 seconds, if it is greater, e.g. 20 degrees, the yaw is accomplished within the subsequent 20 seconds. If the yaw angle determined exceeds a value of 50 degrees, the rotor is yawed immediately. On the other hand, yawing starts at rotor standstill at a low wind speed, e. g. 1 m/s below cut-in speed. If the wind speed exceeds cut-out value, the rotor will not be yawed. If extreme yaw angles occur at the non-rotating turbine with such extreme wind speed, the yaw brakes can slip so that the aerodynamic forces can passively yaw the leeward rotor, which provides a protection for the yaw system under extreme wind speed in combination with extreme yaw angle [21]. Apart from trying to keep the mean yaw angle as small as possible, the yawing

rate of the rotor is also determined by taking into consideration the rotational moments. The yawing rate is normally about 0.3-0.5 %/s. Failure statistics of wind turbines display a conspicuous accumulation in the “yaw system” component. It is, therefore, absolutely imperative that the dynamic load situation and the vibrational behaviour of the yaw drive be analyzed.

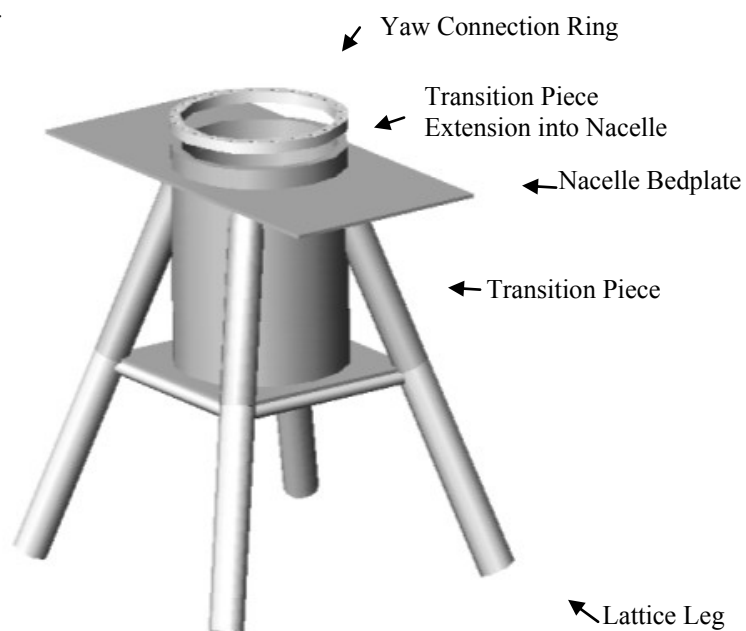
3.3 Mechanical requirement

3.3.1 Connection with the lattice support structure

Connection between the lower lattice support structure and the transition piece can normally be made through the welding of the lattice legs and the respective bracing legs of the frame-cylinder system or the external struts of the cone-strut system. Welding should ensure a sufficient strength which is able to transfer the loads from the rotor and nacelle to the lattice support structure. On the other hand, sufficient fatigue strength of the connections is also a big challenge. As for previously introduced hybrid design of OWEC jacket transition piece (Figure 2.3), a plane plate is employed covering the lattice top and can also be used as the service platform. The transition piece connecting the full lattice support structure and the turbine nacelle will however not necessarily require this plane plate acting as the service platform. However, the placement of a plane plate on top of lattice support structure will be able to connect the structural components of the lattice top bracings and the four legs, which helps increasing the plane stiffness of the whole support structure. Furthermore, this plane plate also provides foundation for the sitting of the cylinder and cone base for both types of the transition piece.

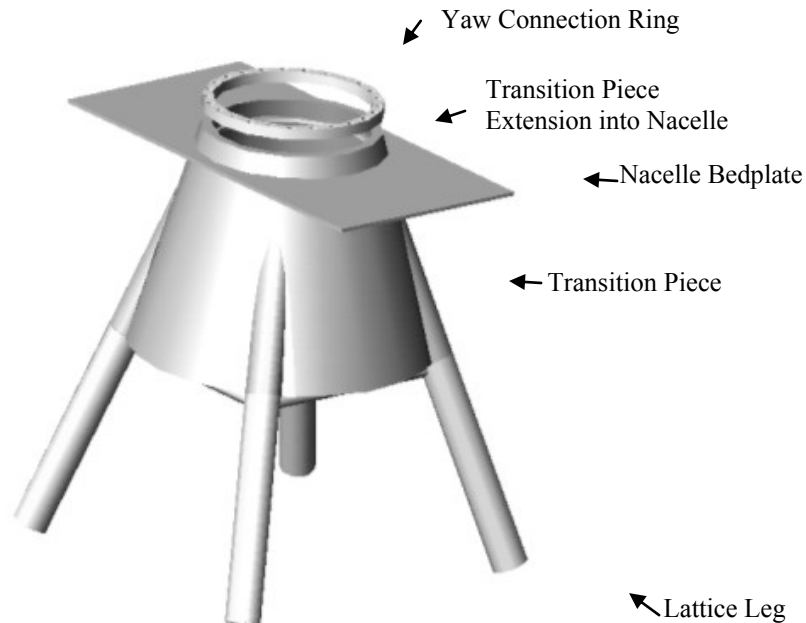
3.3.2 Connection with the nacelle assembly

Connection between the transition piece and the upper turbine nacelle assembly is usually made through the connection of the yaw bearing ring and the cylinder component of the transition piece (Figure 3.12). This connection method firstly requires a match of the geometrical dimension of the transition piece cylinder and that of the yaw bearing outer ring. Connection of these two components is usually made by means of bolting (Figure 3.13).



(a) Transition Piece (Frame-cylinder) Connection with Yaw Bearing Ring

Conceptual Model of Transition Piece
Lattice Tower Design of Offshore Wind Turbine Support Structures



(b) Transition Piece (Cone-strut) Connection with Yaw Bearing Ring
Figure 3.12 Transition Piece Connection with Yaw Bearing inside the Nacelle Assembly



Figure 3.13 Bolting Connection of Yaw Bearing and Cylinder Flange [22]

The bolting should ensure a sufficient level of strength due to the existence of the highly complex loading conditions to be transferred at this crucial conjunction. An inner flange in the transition piece cylinder might be needed for the convenience of sufficient connection with the yaw bearing ring. No matter what type of transition piece concept is to be applied, an extension of the cylinder core or the upper part of the cone concept should be designed in order to allow for connection with the yaw bearing inside the nacelle's protection. In offshore environment, exposure of the yaw bearing outside the turbine nacelle will no doubt increase the probability of damage due to the harsh environmental eroding factors present.

3.4 Mechanical model of transition piece

Based on previous description of conceptual design requirements for the transition piece in terms of the geometry, power utilities layout and especially the yaw bearing connection aspects, mechanical model of the transition piece can be simplified as following for engineering modeling and structural analysis.

3.4.1 Boundary condition

The lower boundary condition of the transition piece is basically depending on the structural characteristics of the lattice support structure. A spring system of three degrees of freedom should be sufficient to satisfy the need:

- (1) Fixed constraint in the Z direction (vertical, Figure 3.14) due to connection with the lattice support structure and a spring system in the X and Y direction (horizontal) concerning the bending stiffness of the lattice support structure in the respective direction. The spring coefficients are thus K_x & K_y which are based on the static bending stiffness of the lattice support structure.
- (2) A torsional spring system depending on the torsional stiffness of the support structure in the X-O-Y plane. The spring coefficient is thus K_t which is the static torsional stiffness of the lattice support structure.

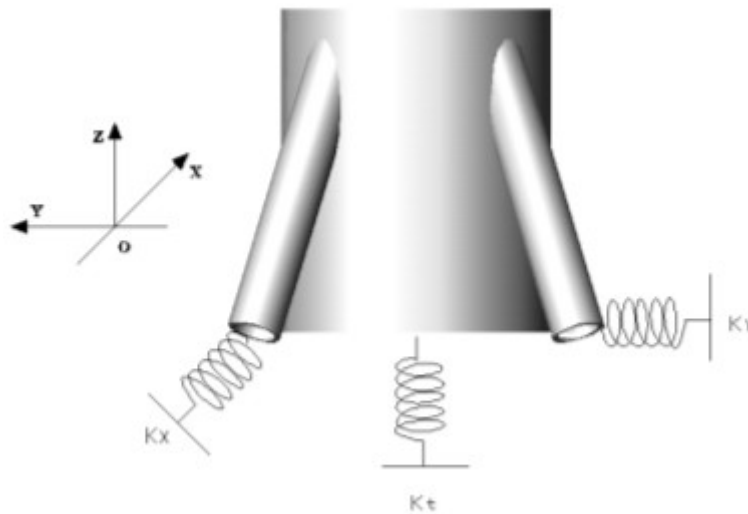


Figure 3.14 Boundary Condition of Transition Piece Using Spring System

3.4.2 Analysis of a full lattice support structure concept

In order to provide reliable parameters to serve as boundary condition for the transition piece, proposal of a full lattice structure acting as support structure (including tower and substructure) for a reference offshore wind turbine is made. Due to the absence of design experience in this field, the design here will be partly based on previous hybrid concepts introduced in Chapter 2. Physical properties of such a design including the total mass distribution, overall dimension, structural member parameters, etc are given. Modal analysis regarding the structural dynamic characteristics is also performed. Detailed load analysis of such a structure is however not the main focus of this thesis. Linear bending and torsional stiffness will be finally provided to give basis on assessment of the structural strength and also to provide parameters for transition piece boundary.

Design requirement

The background of this lattice support structure design is at water depth of 30m supporting a 5MW reference wind turbine (Table 3.2). Hub height of this offshore wind turbine is set at 90m which makes the total height of the lattice structure 120m. Total mass of the nacelle and rotor (rotor nacelle assembly, RNA) is 350 tons.

Conceptual Model of Transition Piece
Lattice Tower Design of Offshore Wind Turbine Support Structures

Table 3.2 Gross Properties of a 5 MW Reference Wind Turbine [23]

Rated Power	5MW
Rotor Position & Configuration	Upwind, 3 Blades
Rotor & Hub Diameter	126m, 3m
Hub Height	90m
Cut-in, Rated, Cut-out Wind Speed	3m/s, 11.4m/s, 25m/s
Cut-in, Rated Rotor Speed	6.9rpm, 12.1rpm
Overhang, Shaft Tilt, Precone	5m, 5°, 2.5°
Rotor Mass	110tons
Nacelle Mass	240tons

For wind turbine dynamic analysis, one of the most important requirements for keeping the vibration behavior of the turbine as a whole under control is to prevent the exciting rotor forces from resonating with the support structure's bending frequencies. The exciting forces of the rotor can be assigned to two categories [3]:

- (1) Exciting forces occurring with the rotor's rotational frequency. These are primarily forces from mass imbalances;
- (2) Exciting forces occurring with the rotor's rotational frequency multiplied by the number of rotor blades. Among these are the "aerodynamic imbalances", i.e. forces developing as a result of an asymmetrical air flow against the rotor (tower shadow effect, vertical wind shear).

In the above mentioned 5MW reference turbine with a three-bladed rotor, the aerodynamic frequency of excitation occurs at three times of the rotational frequency of the rotor (3P). The support structure's first natural bending frequency must not under any circumstance coincide with these aerodynamic exciting forces. Moreover, care must be taken to ensure a certain margin from the multiples of the rotor frequency. Experience from existing turbines indicates that a safety distance of 0.25P from the dominant frequency of excitation (3P) and of 0.15-0.20P from the less critical ones (1P) is a good guide value [3]. In addition, for offshore wind turbines, another important task is to avoid the resonance of the support structure and the sea state. Typically, wave periods in the sea may range from 5s to 20s. This therefore requires that the natural frequencies of the support structure should have a certain margin from the range of 0.05Hz to 0.2Hz. Accordingly, the Campbell diagram for the support structure's bending frequency supporting the above mentioned 5MW reference turbine is shown in Figure 3.15. The speed range of rotor is 6.9rpm (Cut-in) to 12.1rpm (Rated). Several design concepts are available:

- (1) A stiff support structure concept requiring the support structure's first bending frequency above the maximum 3P frequency of 0.6554Hz at the rated rotor speed.
- (2) A soft or very soft concept resulting in a support structure's first bending frequency between 0.2420 and 0.3162 Hz which is in the range of frequencies between 1P and 3P. This concept is adopted by the previous mentioned RAMBØLL jacket substructure for the Upwind project.
- (3) An extremely soft concept placing the support structure's first bending frequency below the 1P frequency, i.e. 0.09Hz. However, this concept has an overlap region with the wave frequency range.

For a support structure of stiff design, the first natural frequency is not encountered during the start up or shut-down procedures, thus eliminating resonance hazard. On the

other hand, this problem with a risk of resonance does exist in the soft, very soft or extremely soft designs. In the course of wind turbine development, almost all manufactures changed to increasingly more flexible designs, for reason of economy. For the three-bladed rotor wind turbines, a soft design concept with the support structure's first natural bending frequency located between 1P and 3P is thus commonly adopted. However, if a lattice structure is used as support structure for offshore wind turbine, due to the already mentioned cost-effective aspect of such a structure, even a stiff concept of support structure design could still be advantageous with regards to the material saved, compared with a conventional monotower support structure.

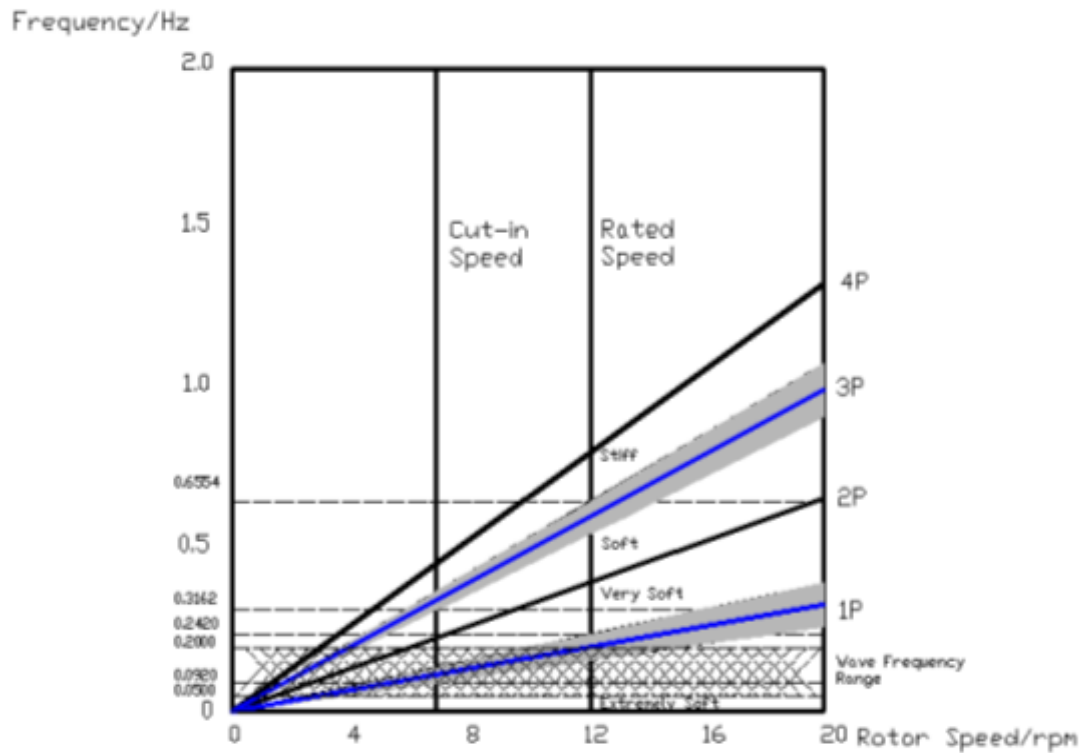


Figure 3.15 Support Structure Bending Frequency Range

Geometry

Considering the simplicity for design and manufacturing, four legs and ten levels of X bracings are suggested for the lattice structural design. Layout of the bracings is regulated in a way that the angel between each bracing and the respective leg is kept constant, leading to a constant K-joint angle for the whole structure. At the top of this structure there are four horizontal bracings connecting the four legs; at the bottom four mud bracings are placed connecting the four legs. The area at the top of the lattice structure is designed as 4m×4m, with consideration of transition piece connection to the turbine nacelle. Bottom width of this structure is a decisive factor for the stiffness and natural frequencies of this structure. In order to achieve a proper final design, studies of structural performance based on varying base width levels are performed in the following section. Nevertheless, this structure has a linear straight line configuration with the four legs tapered from bottom to top. The general configuration of this lattice structure is shown in Figure 3.16.

Conceptual Model of Transition Piece
Lattice Tower Design of Offshore Wind Turbine Support Structures

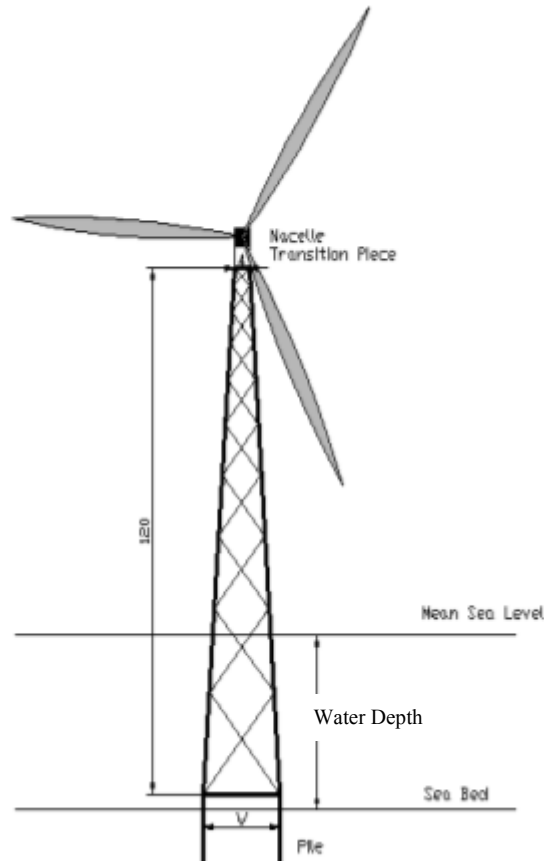


Figure 3.16 Configuration of a Lattice Support Structure for a 5MW Reference Offshore Wind Turbine

Numerical Modeling

By means of finite element analysis, numerical models of several different designs are set up. These different designs mainly consider two control factors, i.e. the base width and the structural member dimensions. Three levels of base width are studied and two types of structural member dimensions are analyzed: namely, one heavy concept and the other light concept. Steel is used as the material for the whole lattice structure. Material properties including density, Young’s modulus, Poisson’s ratio and damping are shown below. Comparison of these different design concepts is shown in Table 3.4. Eigen modes of model 12L in Table 3.4 are illustrated in Appendix II.

Table 3.3 Material Properties for Lattice Support Structure

Density	7850 kg/m ³
Young’s Modulus	2.1E+11 N/m ²
Poisson ratio	0.3
Structural damping	1%

Selection of design model

Selection of a suitable design of lattice support structure for offshore wind turbine shall take various factors into consideration:

(1) Cost

For the proposal of a full lattice support structure, cost efficient aspect has to be maintained at the maximum effort since this is one of the greatest advantages for a lattice structure design, providing it a bigger potential than the other structural types.

Conceptual Model of Transition Piece
Lattice Tower Design of Offshore Wind Turbine Support Structures

Table 3.4 Comparison of Lattice Structural Properties Based on Varying Design Concepts

Structural Overall Height (m)	120					
Base Area Width (m)	21		12		8	
Top Area Width (m)	4		4		4	
Median Overall Height/Width Ratio	9.6		15		20	
Structural Member Dimension Concept	H ⁽¹⁾	L ⁽²⁾	H	L	H	L
Model Index	21H	21L	12H	12L	8H	8L
Rotor Nacelle Assembly Weight (tons)	350	350	350	350	350	350
Estimated Transition Piece Weight ⁽³⁾ (tons)	50	50	50	50	50	50
Support Structure Weight (tons)	1075	523	1008	501	978	492
Linear Bending Stiffness (10 ³ kN/m)	12.327	7.764	4.904	3.052	2.597	1.584
Linear Torsional Stiffness (10 ⁵ kN-m/rad)	39.448	7.955	18.716	4.294	10.563	2.729
1 st fore-aft frequency (Hz)	0.7140	0.6250	0.4508	0.3913	0.3265	0.2807
1 st side-side frequency (Hz)	0.7140	0.6250	0.4508	0.3913	0.3265	0.2807
2 nd fore-aft frequency (Hz)	3.3938	>4	2.5595	2.4142	2.0470	1.9376
2 nd side-side frequency (Hz)	3.3938	>4	2.5595	2.4142	2.0470	1.9376
3 rd fore-aft frequency (Hz)	>7	>4	5.9886	5.1185	5.0745	4.4936
3 rd side-side frequency (Hz)	>7	>4	5.9886	5.1185	5.0745	4.4936
1 st torsional frequency (Hz)	4.0149	2.7172	2.9098	1.8590	2.1729	1.3575
2 nd torsional frequency (Hz)	4.9086	2.9192	5.6359	2.3789	5.3357	2.3167

Note:

(1)The H (for “heavy”) design applies member dimensions according to the RAMBØLL jacket substructure design, i.e. leg diameter 1.2m, leg thickness 0.04m; bracing diameter 0.8m, bracing thickness 0.02m.

(2)The L (for “light”) design is considered as reduced member dimensions, i.e. leg diameter 0.9m, leg thickness 0.035m and bracing diameter 0.36m, bracing thickness 0.014m.

(3)The design of the transition piece is a decisive factor for the vibrational behavior of the support structure. Generally a heavy design, e.g. concrete block (Para. 2.3.3) would reduce the overall natural frequencies and a light design, e.g. steel cone and/or bracing (Para. 2.3.1, 2.3.2 & 2.3.5) would result in a larger level of natural frequencies. The assumed weight value of 50 tons is based on assumption of a light design. Adjustment can be made if a heavier design is desirable.

From this sense, all the heavy design concepts in Table 3.4 shall be dealt with carefully because these designs seem to have lost the cost efficient characteristic of lattice support structure, requiring the amount of steel material weight of around 1,000 tons while previous hybrid designs only level up to a substructure cost of about 700 tons steel. Light design concepts weighing in the order of 500 tons could thus reflect the advantage of lattice support structure, which reduces the material weight of about 30% compared with the hybrid designs and even more if other concepts are considered.

(2) Vibration behavior

As previously described, the support structure’s first natural bending frequency should be avoided to encounter with the frequencies of the “mass imbalances” and “aerodynamic imbalance”. Serving the 5MW reference wind turbine (Table 3.2), the resulted first natural bending frequency should thus be either above 0.6554Hz for a stiff concept design or between 0.2460Hz and 0.3162Hz for a soft concept design or even below 0.0920Hz for an extremely soft concept. Models of 21L (0.6250Hz), 12L (0.3913Hz) and 8L(0.2807Hz) could be possibly adjusted to fall in this allowable range with help of minor dimension adjustment or redesign of the transition piece concept.

(3) Stiffness

The support structure’s stiffness is also a very crucial factor in terms of sufficient structural strength to the severe wind, wave, etc loads in the offshore environment. Comparison of linear bending and torsional stiffness without consideration of dynamic effects shows that a higher height/width ratio leads to a rapid decrease of the structural stiffness while the saving of the material cost is almost insignificant at all (e.g. from 21L to 8L, the stiffness is decreased by 80% but only 6% material is saved). Based on

Conceptual Model of Transition Piece
Lattice Tower Design of Offshore Wind Turbine Support Structures

this consideration, 21L is a probable design model as a stiff design concept and 12L is a probable model as a soft design concept. Either a stiff concept or soft concept should be adopted has to depend on various factors and each has its own characteristics. A balance of material cost and structural stiffness should be compromised to achieve the optimum overall benefits for the final decision.

Properties of an adjusted 21L design model in comparison with the redesigned 12L model which meets the above requirements with regards to cost efficient, dynamic vibration behavior and stiffness, etc are shown below:

Table 3.5 Properties of Two Concepts for a Lattice Support Structure Design Proposal

Design Concept	Stiff	Soft
Allowable First Bending Frequency (Hz)	> 0.6554	0.2460 - 0.3162
Base Area Width (m)	21	12
Median Overall Height-Width Ratio	9.6	15
Dimension of the 4 Legs	0.9m diameter, 0.04m thickness	0.9m diameter, 0.03m thickness
Dimension of X Bracings	0.36m diameter, 0.014m thickness	
Dimension of Mud and Top Bracing	0.36m diameter, 0.014m thickness	
Rotor Nacelle Assembly Weight (tons)	350	
Support Structure Weight (tons)	572	452
Transition Piece Concept	Light weight	Heavy weight
Estimated Transition Piece Weight ⁽³⁾ (tons)	50	350
Linear Bending Stiffness (10 ³ kN/m)	8.764	2.649
Linear Torsional Stiffness(10 ⁵ kN·m/rad)	8.143	4.175
1 st fore-aft frequency (Hz)	0.6574	0.2908
1 st side-side frequency (Hz)	0.6574	0.2908
1 st torsional frequency (Hz)	2.6521	1.5276
2 nd torsional frequency (Hz)	2.8740	1.8304

Conclusion

Existing industrial practice only sees hybrid design composed of a lattice substructure and a monotower for offshore wind turbine support structure (Beatrice demo project and Alpha Ventus). While site of offshore wind farm is going deeper and deeper, lattice structure acting as substructure for offshore wind turbine is expected to increase or even dominant in future market due to its various benefits inclusive of cost efficiency. A full lattice structure for offshore wind turbine (including tower and substructure) is not yet seen in industry. This concept makes use of the cost efficiency characteristic to a further step. Both a stiff concept and a soft concept design can be possible with regards to the specific requirement of the turbine to be supported and the site conditions. Design method will be an optimum compromise of cost, structural dynamics, structural strength and other functional requirements.

Transition piece connecting the lattice support structure and the rotor nacelle assembly plays an important role in the conceptual design of the support structure. Both light weight concept of transition piece design (Alpha Ventus) and heavy weight concept design (RAMBØLL proposal) could be possible. What should be born in mind and dealt with carefully is that the design of the transition piece influences to a large extent the vibrational behavior of the overall support structure where a heavy transition piece will lower the structural natural frequencies and a light transition piece will play the opposite effect. For instance, a light transition piece is easier to be combined with a stiff support

structure design while a heavy transition piece will possibly work well with a soft support structure design (Table 3.5).

3.4.3 Load condition

Loading condition of the transition piece is involving a number of forces and moments which are developing with time due to the stochastic environmental conditions. Basically the following loads should be considered for the analysis of the transition piece.

Rotor nacelle assembly weight

The rotor nacelle assembly weight is an important consideration for the design of wind turbine support structure. As the size of the turbine increases, the weight of this massive assembly also goes heavier, though technology for weight reduction has also achieved much progress. For a 5MW wind turbine, example of the typical weight of the rotor nacelle assembly is shown in Table 3.6. This massive weight is constantly acting on the transition piece (Figure 3.18) which is one of the challenges for the transition piece design.

Table 3.6 Rotor Nacelle Assembly Weight of a 5MW Wind Turbine

Component	Sub-component	Weight (kg)
Rotor	Blade	17740
	Hub	56780
Nacelle		240000
Total		350000

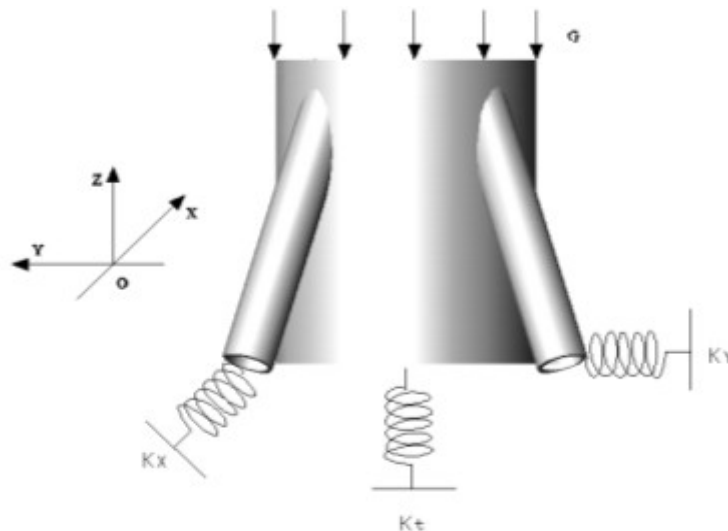


Figure 3.17 Rotor Nacelle Assembly Weight on Transition Piece

Rotor thrust

The thrust is the axial force applied by the wind on the rotor of a wind turbine. Based on Blade Momentum Theory (or Rankine-Froude Actuator-disk Theory) [24], if the wind turbine is simplified as in a stream tube (Figure 3.18) and considering the region with equal distance upstream and downstream of the rotor disk plane, the thrust force on the rotor will be:

$$T = \frac{1}{2} \rho_{air} A_r (U_{\infty}^2 - U_w^2) \quad (3-1)$$

Conceptual Model of Transition Piece
Lattice Tower Design of Offshore Wind Turbine Support Structures

with ρ_{air} the air density, A_r the rotor disk area, U_∞ the upstream free wind speed and U_w the downstream wake speed.

An axial induction factor is defined as the fractional decrease in wind velocity from the free upstream to the rotor disk

$$a = \frac{U_\infty - U_r}{U_\infty} \quad (3-2)$$

with U_r wind speed at the rotor disk plane which is equal to $\frac{U_\infty + U_w}{2}$.

Combing the above equations, the rotor thrust force will thus be:

$$T = 2\rho_{air}A_rU_\infty^2a(1-a) \quad (3-3)$$

or

$$T = \frac{1}{2}C_T\rho_{air}A_rU_\infty^2 \quad (3-4)$$

where C_T is the thrust coefficient which equals to $4a(1-a)$.

For high induction factor value ($a > 0.4$), Glauert's correction is applied:

$$C_T = \frac{(a - 0.143)^2 + 0.55106}{0.6427} \quad (3-5)$$

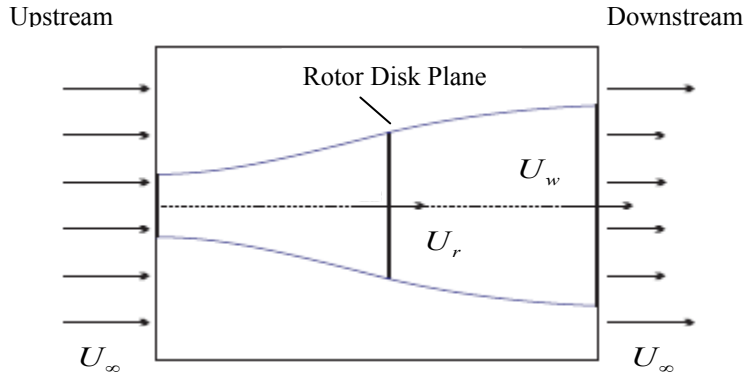


Figure 3.18 Stream Tube of Rotor Disk Theory

Because of the instantaneous change of the wind condition in magnitude and direction, the thrust force is also impacting on the wind turbine at rapidly changing pattern. The direct result is the changing bending moment at the base of the support structure. For consideration of the transition piece, this force is acting on the rotor, transferred to the nacelle and supported by the yaw bearing. The force on the yaw bearing is thus balanced by the reactive force of the transition piece. The force is modeled as acting in the plane parallel to the yaw bearing plane (Figure 3.19). For quasi-static analysis, at every time point, the force is acting from the direction of the mean wind speed. However, due to the change of the wind direction and thus the rotation of the rotor nacelle assembly because of yaw motion, the direction of this force is also changing instantaneously.

Conceptual Model of Transition Piece
Lattice Tower Design of Offshore Wind Turbine Support Structures

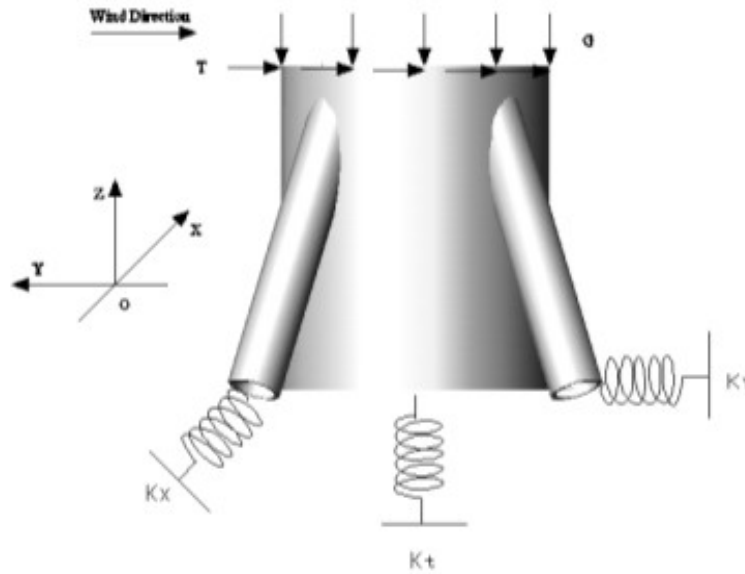


Figure 3.19 Rotor Thrust Force on Transition Piece

Hydrodynamic load

Due to the wave impact, the top of the lattice support structure is forced to vibrate with the wave magnitude and direction. This vibration gives acceleration to the transition piece in a similar way as a building is impacted by the ground seismic load. For slender cylinder structure, Morison model is one of the most frequently used models for predicting the wave load [25]. Morison recommended that forces exerted by unbroken surface waves on a vertical pile that extended from the sea bottom through the free surface consisted of two main components, i.e. the inertia and drag forces. The force in line of the structure is thus:

$$f = \frac{1}{2} \rho_{water} C_D D u |u| + \rho_{water} C_M A \frac{du}{dt} \quad (3-6)$$

where ρ_{water} is the sea water density, C_D and C_M are drag and inertia coefficients, D is the diameter of the cylinder, A is the cross section area of the cylinder and u is the horizontal flow velocity.

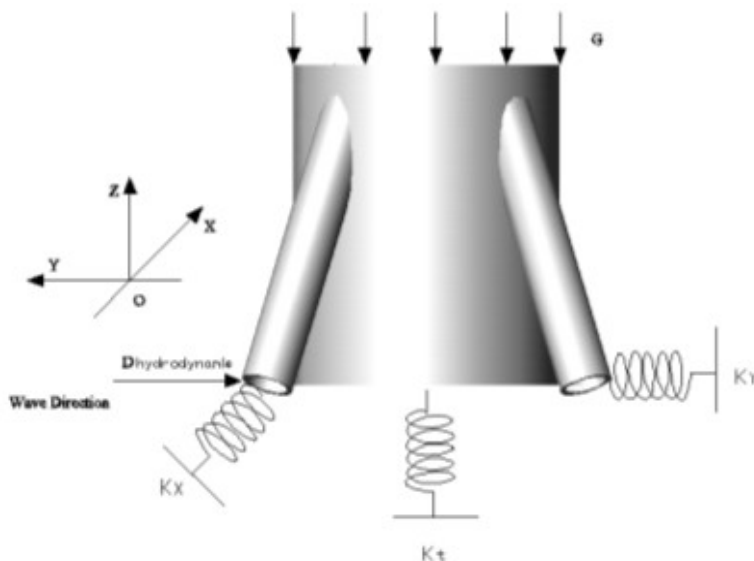


Figure 3.20 Hydrodynamic Load (Acceleration or Displacement) on Transition Piece

Drive train vibration

Torsional vibration of the drive train deserves consideration for the design of a proper transition piece. The series-connected components of the drive train such as rotor hub, rotor shaft, gearbox, high-speed shaft, brake and clutches have such diverging dimensions, mass distributions and material properties that an accurate analysis of vibrations can only be carried out to a limited extent. The major task of drive train vibration is to avoid resonance within the drive train system and with other components, e.g. the transition piece. According to Peeters, J. et al in his study of a wind turbine, the first three modes of the drive train vibration have natural frequencies of 2.03Hz, 4.42Hz and 8.71Hz respectively [26]. Nevertheless, varying designs of drive train could produce different results.

Rotor torque

In addition to the drive train vibration, rotor torque is also acting constantly on the nacelle assembly and thus has to be balanced by the transition piece along with the lattice structure. Rotor torque is transmitted through, for instance, the low speed shaft, the gearbox and the high speed shaft to the generator. The generator is therefore subjected to a torque and this must be carried by the transition piece. The vertical forces (along the yaw axis direction) on the transition piece will therefore have increased compression on one side and decreased compression on the opposite side, so that a moment about a horizontal axis roughly parallel with the rotor shaft but running through the symmetry axis of the yaw bearing ring is resulted due to the rotor torque. Although the presence of the gearbox and other components in the drive train system alter the torque from its original magnitude on the rotor blades, on a static equilibrium point of view, it can be assumed that the moment acting on the transition piece is equal to the magnitude of rotor torque.

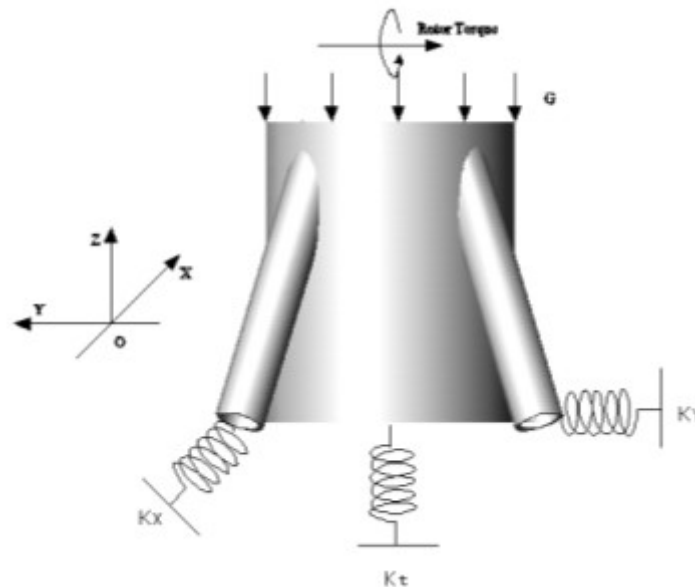


Figure 3.21 Rotor Torque on Transition Piece

The blade element theory [25] describes the aerodynamic forces, lift F_L and drag F_D , on a blade element. A full blade consists of various types of airfoils with different characteristics. The lift and drag forces on a blade element depend on the type of airfoil, the air density, the resultant wind velocity and the surface of the blade element. The equations for the lift and drag forces on a blade element are

$$\Delta F_L = \frac{1}{2} \rho_{air} c u^2 C_L \Delta r_b \quad (3-7)$$

$$\Delta F_D = \frac{1}{2} \rho_{air} c u^2 C_D \Delta r_b \quad (3-8)$$

with ρ_{air} air density, c airfoil chord length, u the resultant wind velocity, C_L and C_D the lift and drag coefficients and Δr_b length of the blade element.

The aerodynamic wind velocity u is the vector sum of the perpendicular and tangential wind velocities on the blade element. The angle of inflow ϕ is the angle between u and u_t . The lift and drag coefficients of the airfoil are related to the angle of attack. The angle of attack is the angle between the chord line and the resultant wind velocity u , which differs at each blade radius due to the twist distribution.

The tangential force F_t is expressed as a function of the drag and lift forces:

$$\Delta F_t = N_b (\Delta F_L \sin \phi - \Delta F_D \cos \phi) = \frac{1}{2} \rho_{air} N_b c u^2 (C_L \sin \phi - C_D \cos \phi) \Delta r_b \quad (3-9)$$

with N_b the number of blades.

The torque is therefore,

$$\Delta Q = \Delta F_t r_b \quad (3-10)$$

with r_b the rotor blade radius.

The axial and tangential wind velocities are not identical to the free stream wind speed and the rotational speed, respectively. Due to the presence of the turbine, these wind velocities are induced. The fractional decrease or increase of the wind velocity is represented by induction factors (e.g. Eq. 3-2). When wake rotation is included, the induced velocity at the rotor consists of not only the axial component but also a component in the rotor plane. The generation of rotational kinetic energy in the wake results in less extraction by the rotor than would be expected without wake rotation. Across the flow disk, the angular velocity of the air relative to the blade increases. The angular induction factor a' , is defined as $a' = \varpi / \Omega$ where ϖ is the angular velocity increase and Ω is the original angular velocity.

Applying the conservation of angular momentum, an expression for the rotor torque can be derived. The torque exerted on the rotor must be equal to the change in angular momentum. Hence,

$$\Delta Q = 4 \rho_{air} \pi u_p \Omega r_b a' (1-a) r_b^2 \Delta r_b \quad (3-11)$$

Yaw moment

When the incoming wind direction is misaligned with the rotor axis, a component of the aerodynamic load on the rotor will force the rotor nacelle assembly to rotate along the yaw axis in order to achieve a smaller angle between the incoming wind direction and the rotor axis. For modern active yawing concept with motorized yaw drive, yawing of the rotor nacelle assembly is driven by the motion of the yaw drive, based on result of field measurement device of the real time wind condition. Nevertheless, before the yaw drive takes action, a yaw moment will still act on the rotor nacelle assembly which will have to be

Conceptual Model of Transition Piece
Lattice Tower Design of Offshore Wind Turbine Support Structures

balanced by the support structure through the transition piece. Therefore, the transition piece is playing an important role of supporting this yaw moment. On a static equilibrium point of view, the magnitude of the yaw moment load acting on the transition piece should be equal to the overall yaw moment which is acting on the rotor nacelle assembly.

Magnitude of the yaw moment depends on various factors. The wind condition especially the angle between the incoming wind direction and the rotor axis plays a very important role. Aerodynamic properties of the rotating rotor will surely affect the pattern of the yaw moment. In addition, the distance between the yaw axis and the rotor disk plane is also an important parameter which determines the length of the yaw moment arm. A short design of this distance will therefore have advantage of reducing the magnitude of yaw moment on the transition piece.

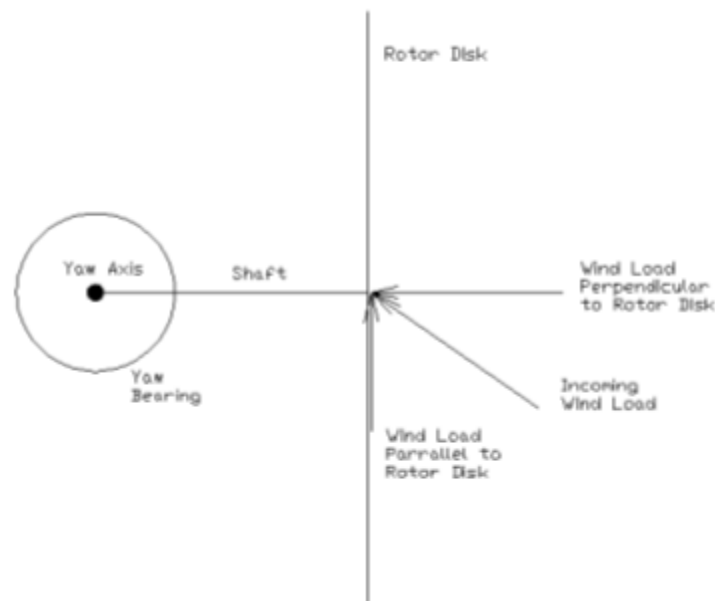


Figure 3.22 Misalignment of Incoming Wind with Rotor Axis

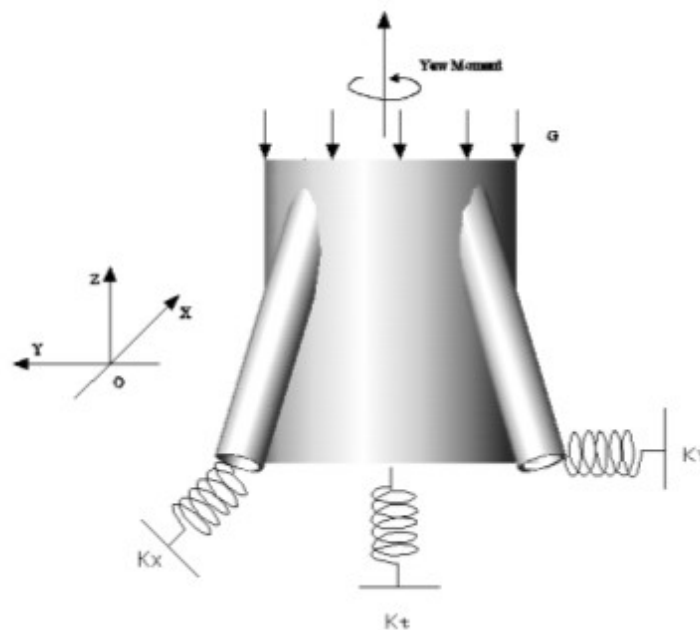


Figure 3.23 Yaw Moment on Transition Piece

Moment of forces

In addition to the above loads, due to the misalignment of the acting point or axis of the relevant forces and the position of the transition piece, some moments are resulted acting on the transition piece:

- 1) Moment of the nacelle weight. The moment arm is the horizontal distance between the nacelle mass centre and the yaw axis.
- 2) Moment of the rotor weight. The moment arm is the horizontal distance between the rotor hub and the yaw axis.
- 3) Moment of the thrust force. The moment arm is the vertical distance between the yaw bearing-transition piece interface and the rotor axis. Rotor tilt angle can be negligible.

Therefore, as a summary, the mechanical model of the transition piece taking into consideration of the boundary condition and various loads can be illustrated as below. This acts as the mechanical model for the numerical modeling in the following chapters.

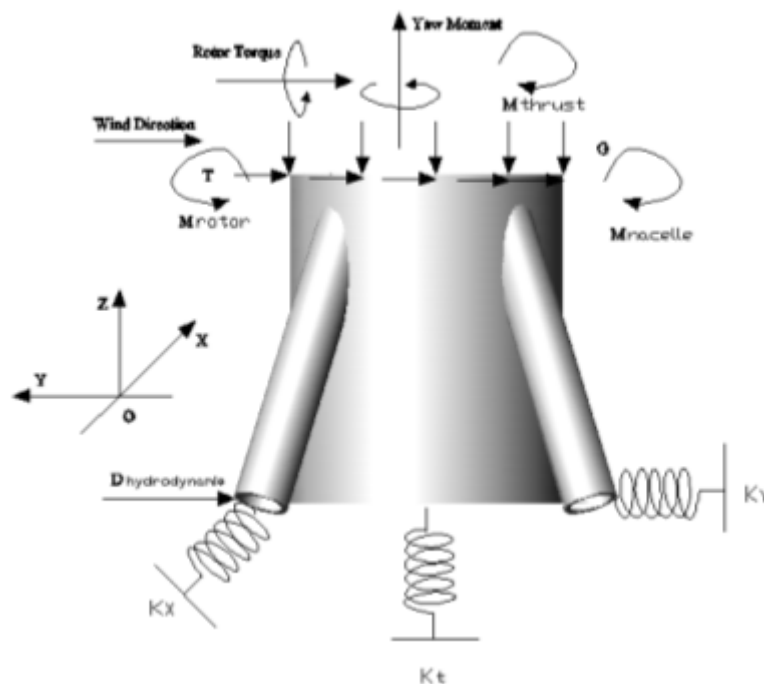


Figure 3.24 Mechanical Model of Transition Piece Including Boundary Condition and Various Loads

Conceptual Model of Transition Piece
Lattice Tower Design of Offshore Wind Turbine Support Structures

4 PRELIMINARY DESIGN OF TRANSITION PIECE

In this preliminary design procedure, two modeling cases are performed to study the structural behavior of two types of transition piece concepts under different loading conditions. Comparative results of the two model types are expected to further optimize the design of transition piece in the final design process. Structural analysis of transition piece is conducted on the respective finite element model created in Abaqus [28]. Aerodynamic and hydrodynamic loads are acquired from wind turbine simulation code HAWC2 [29] in addition to theoretical verification. The loads are then applied on the transition piece finite element models to study the structural behavior. Methodology is shown in the Chart below:

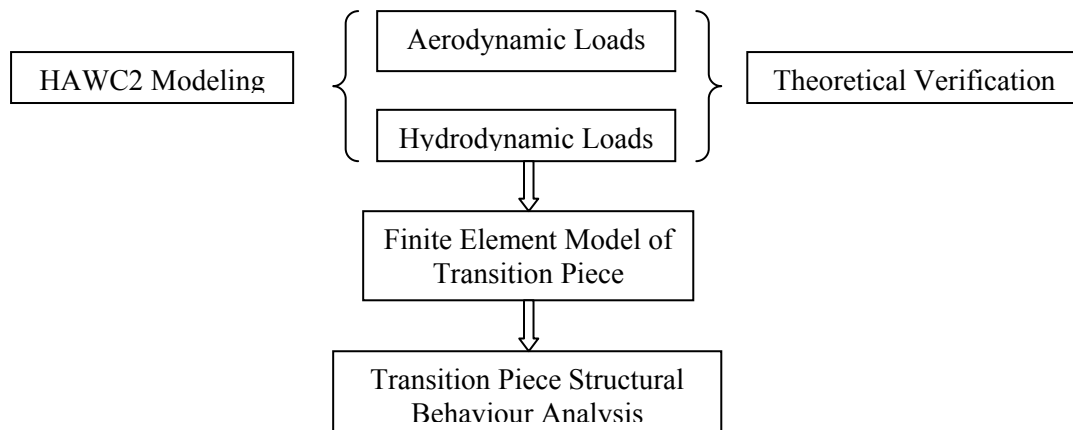


Figure 4.1 Methodology for Transition Piece Modeling and Analysis

4.1 Proposed model

Both models are subject to the same geometry configuration requirement, which includes 6.0m×6.0m area of lattice support structure top and a yaw connection bearing ring of 5.0m diameter. Diameter of the yaw bearing ring is based on present technology of the yaw bearing design for a 5MW wind turbine (a typical single-row 4-point contact ball bearing made from forged rings has a diameter up to 5.0-5.5m for a 5MW turbine [30]). The total height of the transition piece from the lattice top up to yaw bearing plane is set at 6.0m including 1.0m height of extension part inside the nacelle assembly for yaw connection purpose. The basic geometrical configuration is shown in Figure 4.2.

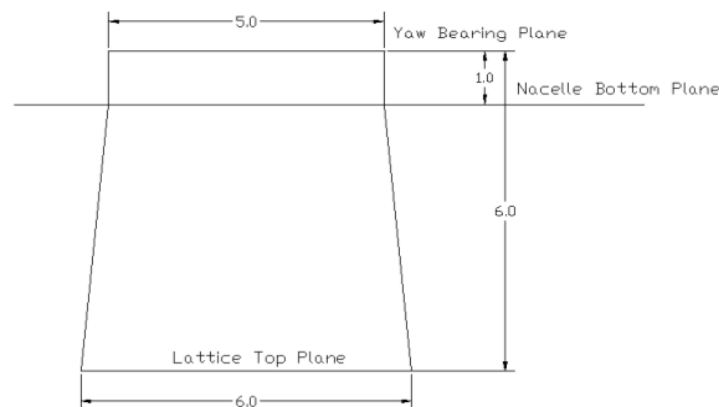


Figure 4.2 Geometrical Configuration Requirement for Transition Piece (Unit: m)

Preliminary Design of Transition Piece
Lattice Tower Design of Offshore Wind Turbine Support Structures

For both models, steel is used as the material for the whole transition piece. Steel properties are based on high strength alloy. Material properties including density, Young's modulus, Poisson ratio, structural damping, yield strength and ultimate strength are shown below in Table 4.1.

Table 4.1 Material Properties for Transition Piece

Property	Value
Density	7850 kg/ m ³
Young's Modulus	2.1E+11 N/m ²
Poisson Ratio	0.3
Structural Damping	1%
Yield Strength	6.9E+8N/ m ²
Ultimate Strength	7.6E+8 N/ m ²

4.1.1 Frame-cylinder model

As previously described, this model is composed of a cylinder in the middle, a plane in the bottom and four legs connecting the legs of the lattice support structure and the cylinder up to the nacelle bottom plane (Figure 4.3). Structural component dimensions of this model are listed in Table 4.2. The total structural mass is around 118 tons with mass centre at 2.21m above the base plane.

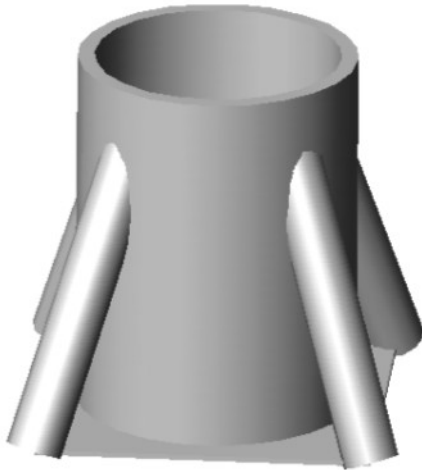


Figure 4.3 Frame-cylinder Transition Piece Model

Table 4.2 Structural Dimension of Frame-cylinder TP

Structural Component	Dimension
Cylinder	Outer Diameter 5.0m, Thickness 0.1m, Height 6.0m
Truss	Cross-section: Outer Diameter 0.9m, Thickness 0.035m; Axial Length: 5.3m
Bottom Plane	Area 6.0m×6.0m, Thickness 0.1m



Figure 4.4 Cone-strut Transition Piece Model

Table 4.3 Structural Dimension of Cone-strut TP

Structural Component	Dimension
Cone	Base Outer Diameter 6.0m, Top Outer Diameter 5.0m, Thickness 0.1m, Height 6.0m
Strut	Cross-section: Outer Diameter 0.9m, Thickness 0.035m; Axial Length: 3.0m
Bottom Plane	Area 6.0m×6.0m, Thickness 0.1m

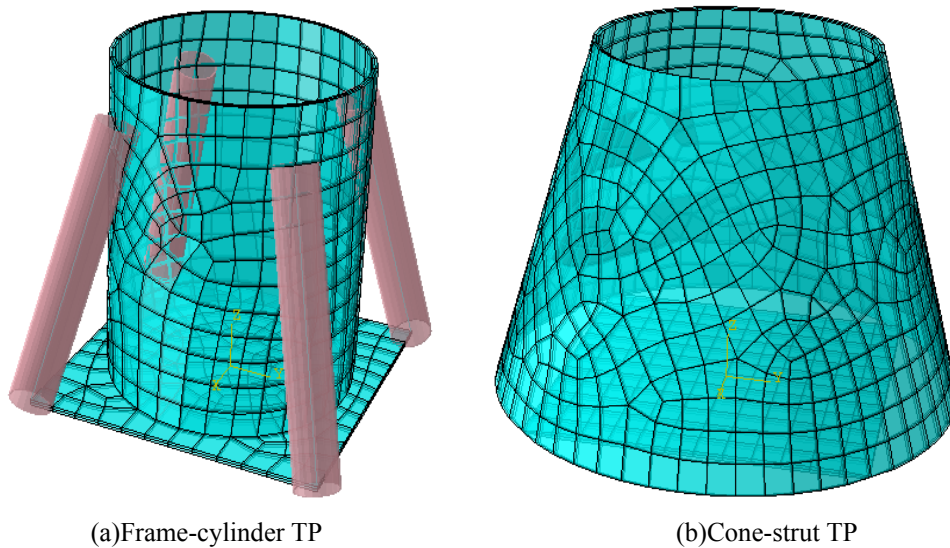
4.1.2 Cone-strut model

Alternatively, the cone-strut type model is also possible to serve as the transition piece. This model is composed of a truncated cone structure in the middle, a plane in the bottom covering and connecting the lattice support structure top and four short struts connecting the legs of the lattice support structure and the cone (Figure 4.4). The struts are designed in a way that they are connecting with the cone to the mid elevation of the cone (3.0m high from the bottom plane). Total mass of the structure is about 140 tons with mass centre at 2.15m above the bottom plane. Structural properties of the model are shown in Table 4.3.

4.2 Finite element model

4.2.1 Model introduction

For purpose of structural analysis, finite element models of the above two designs are built (Figure 4.5). Model of the frame-cylinder design remains the same with its geometrical shape whereas model of the cone-strut design takes off the four short struts since they are considered to mainly be used for connection between the transition piece cone and the lattice support structure and to have insignificant contribution to the strength of the total structure. Meshing information of the two finite element models is listed in Table 4.4.



(a)Frame-cylinder TP (b)Cone-strut TP
 Figure 4.5 Finite Element Models of Transition Piece

Table 4.4 Meshing of the Finite Element Models

Model Type	Frame-cylinder TP	Cone-strut TP	Criteria for Quadrilateral Elements: 10° smaller face corner angle, 160° larger face corner angle, 10 aspect ratio
Number of Nodes	630	867	Criteria for Triangular Elements: 0.01 shape factor, 5° smaller face corner angle, 170° larger face corner angle, 10 aspect ratio
Number of Elements	618	812	
Line Elements	44# B31	0	
Quadrilateral Elements	556# S4R	796# S4R	
Triangular Elements	18# S3	16 #S3	

Meshing size is based on the compromise of computational cost and sufficiency of result accuracy. Verification of meshing type and size could be based on assessment of elements in terms of shape factor, face corner angle, aspect ratio, geometric deviation factor, edge dimension, stable time increment, etc [31]. A denser meshing of the model

will in general help increasing the computation accuracy but meanwhile the time cost will also be amplified. The above two models are found to fulfill the criteria limits specified and are within a suitable limit of acceptable computational time.

4.2.2 Boundary condition

Boundary condition is dependent on lattice structural stiffness. Based on results in Para. 3.4.1 & 3.4.2, elastic foundation with the following spring coefficients is applied on the finite element models. Boundary condition is applied at the nodes of the four corners of the base plane for both models because these nodes are the connection joints with the lower lattice support structure. All movements in other directions than the ones listed in Table 4.5 are constrained. The coordination system is referred to Figure 4.6. All coordination systems in the following paragraphs refer to the same as in Figure 4.6, if not particularly specified.

Table 4.5 Stiffness of Lattice Support Structure as Boundary Condition

Type	Direction	Magnitude
Bending	X	8.0E+6 N/m
Bending	Y	8.0E+6 N/m
Torsion	Z	8.0E+8 N·m/rad

4.2.3 Loading

Description of the relevant loads the transition piece is subjected to and thus to be applied on the finite element models is given in Para. 3.4.3. Here the detailed loading conditions with regards to magnitude and direction are shown in Table 4.6. Direction of the load is according to coordination system in Figure 4.6. Moment direction is based on right hand coordination system. For load incurred by the drive train vibration, because the mass of the drive train is included in the rotor nacelle assembly (RNA) weight, only dynamic analysis of the drive train vibration problem will be considered in order to assess the probability of resonance between the transition piece and the drive train vibration.

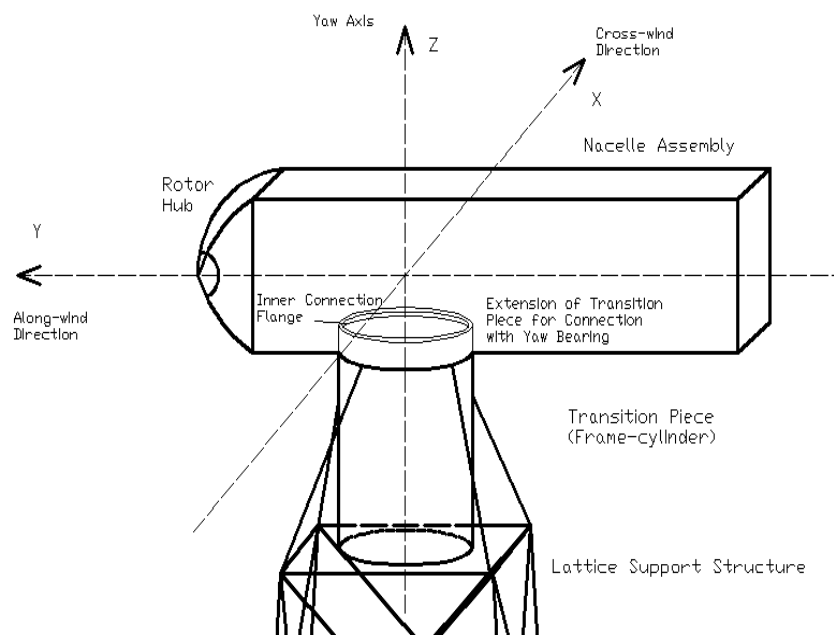


Figure 4.6 Coordination System Illustration

Preliminary Design of Transition Piece
Lattice Tower Design of Offshore Wind Turbine Support Structures

Table 4.6 Load Conditions on Transition Piece

Load	Magnitude	Direction	Comment
Rotor Nacelle Assembly Weight	350×9.8 kN	-Z	Act on top of transition piece.
Rotor Thrust	$T = \frac{1}{2} C_T \rho_{air} A U_{\infty}^2$ (Eq. 3-4)	mean wind direction	Magnitude and direction of thrust is constantly changing with the wind condition. Time series of thrust force at different directions are applied on the transition piece.
Hydrodynamic Load	$f = \frac{1}{2} \rho_{water} C_D D u u $ $+ \rho_{water} C_M A \frac{du}{dt}$ (Eq. 3-6)	mean wave direction	Magnitude and direction of hydrodynamic load is constantly changing with the wave condition. Time series of wave induced vibration on the lattice support structure is employed to assess the influence on the transition piece.
Drive Train Vibration			Dynamic analysis with regards to resonance is considered.
Rotor Torque	$\Delta Q = 4 \rho_{air} \pi u_p \Omega r_b a' (1-a) r_b^2 \Delta r_b$ (Eq. 3-11)	mean wind direction	Simulation result from HAWC2 is employed to be applied on the transition piece model.
Yaw Moment	Depending on wind condition and rotor dynamics, especially cross-wind conditions.	+Z	Simulation result from HAWC2 is employed to be applied on the transition piece model.
Nacelle Weight Moment to Yaw Axis	240×9.8×1.9kN·m	varied with rotor axis direction	Nacelle mass centre is assumed at 1.9m downwind from the yaw axis [23].
Rotor Weight Moment to Yaw Axis	110×9.8×5.0 kN·m	varied with rotor axis direction	Rotor (hub and blades) mass centre is assumed at 5.0m upwind from the yaw axis [23].
Thrust Moment	$T \times 1.0$ kN·m	mean wind direction	Vertical distance from the rotor center to the yaw bearing is assumed to be 1.0m. The moment is ignored in this study.

4.3 Finite element analysis result

4.3.1 Modal analysis

Table 4.7 Eigen Frequencies of Transition Piece

Mode	Frame-cylinder TP		Cone-strut TP	
	Frequency(Hz)	Comment	Frequency(Hz)	Comment
1 st	1.3099	X-Y translational	1.2380	X-Y translational
2 nd	1.3099	Y-X translational	1.2380	Y-X translational
3 rd	3.9157	1 st torsional	2.2372	1 st torsional
4 th	13.844	cylinder buckling	6.2691	base buckling
5 th	27.059	cylinder buckling	9.6551	cone buckling
6 th	27.137	cylinder buckling	12.838	base buckling
7 th	31.166	base buckling	12.838	base buckling
8 th	41.435	base buckling	15.605	base buckling
9 th	41.532	cylinder buckling	19.114	cone buckling

Modal analysis of the two finite element models is performed to assess the dynamic properties of the two types of transition piece. For the frame-cylinder type, the first three eigen modes refer to the translational and torsional vibration and higher eigen modes include the buckling of the cylinder and the base plane. For the cone-strut type, the same characteristics apply. Based on results of Table 4.7, generally the cone-strut transition piece has slightly lower natural frequencies than the frame-cylinder type. First

eigen modes of the two types of transition piece are shown in Appendix III. Modal analysis here only considers the selfweight of the transition piece without added mass of the RNA on top.

4.3.2 RNA weight

RNA weight constitutes a constant component of the total loads that the transition piece is subjected to endure. In this design, a total RNA mass of 350 tons is used based on experience of a 5MW wind turbine [23]. The static load is applied on top edge of the two models and the element stress condition is shown below. Maximum von Mises stress [32] is 22.37MPa which occurs close to the connection points of the trusses and the cylinder in the frame-cylinder model whereas maximum von Mises stress in the other model occurs at the connection points at the base of the cone, which is about 16.31MPa. Stress condition at the connecting points with the base in the frame-cylinder model is reduced, at the sacrifice of a high local stress condition in the region of the connecting points on the cylinder. Nevertheless, it can be seen that the cone-strut transition piece has a better performance, e.g., lower maximum stress, under the static load of the RNA weight. Stress accumulation at the connection joints of the trusses and the cylinder in the frame-cylinder type is not unexpected and the maximum stress in this type of design is over 37% higher than that in the other design.

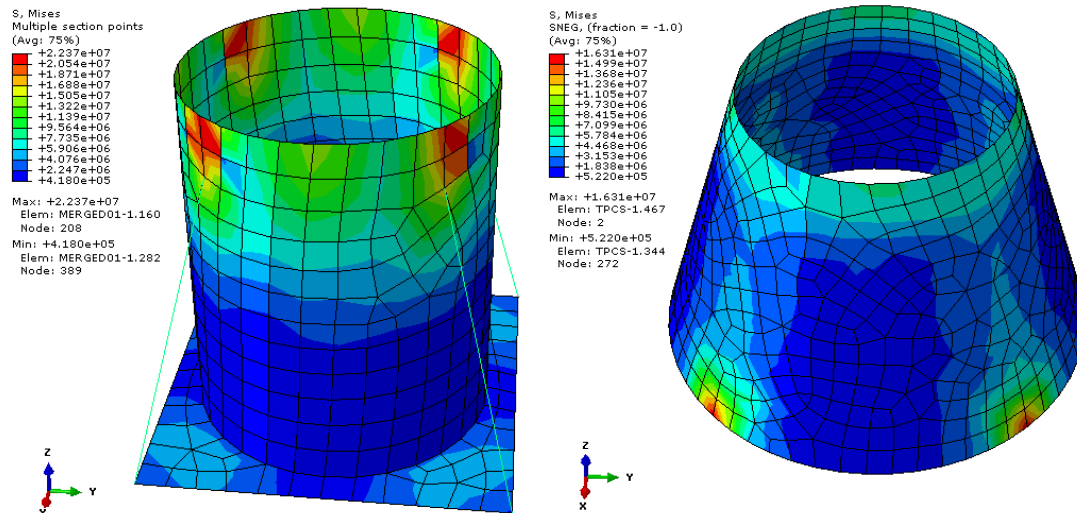


Figure 4.7 Transition Piece Stress Condition under RNA Weight

In the above analysis, the total weight of the nacelle assembly and the rotor is applied as constant with time. During the operation period of the turbine, however, due to the rotating of the rotor blades, the mass of the rotor will have variation with time (Figure 4.8). The frequency of this variation depends on the wind condition and rotor aerodynamics. The range of oscillation is within $\pm 7\%$ off the mean value. Consideration of this time variation of the RNA weight due to the rotation of the rotor is not included in the above analysis.

Because of the misalignment of the yaw axis and the mass centers of the rotor and the nacelle (Figure 4.9), an eccentric moment is resulted acting on the transition piece. Ideally the mass centre of the nacelle and the rotor hub can be designed in a way that the resulted moments will cancel each other at the yaw axis. However, for more realistic and practical situation, a certain moment will always exit. According to Table 4.6, due

Preliminary Design of Transition Piece
Lattice Tower Design of Offshore Wind Turbine Support Structures

to the distance of the rotor and nacelle center of gravity to the yaw axis, a moment of 921.2 kN·m is resulted. Structural performance under the combined RNA weight and its moment is shown below in Figure 4.10. Comparing Figure 4.7 and Figure 4.10, it can be seen that the moment acting on the transition piece has significant effect on the structural behavior of the transition piece. This moment increases the maximum stress in the frame-cylinder TP by 3.4 times while the stress condition of the cone-strut TP has increased over 6.0 times. The moment is applied on the top edge of both models.

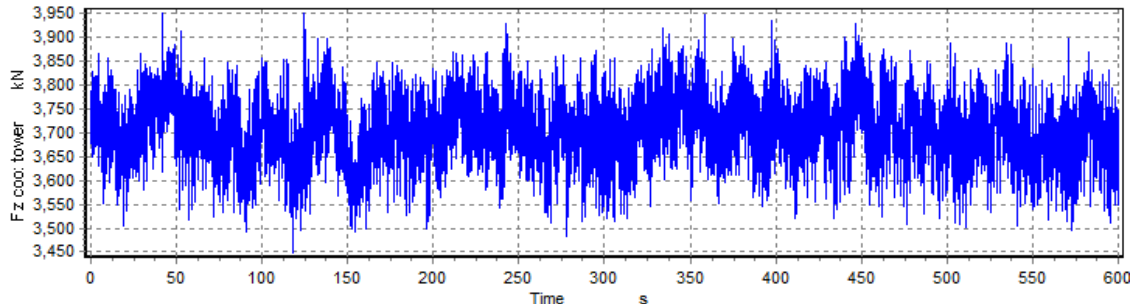


Figure 4.8 Oscillation of Vertical Load on Support Structure Top due to RNA Weight with Consideration of Rotor Aerodynamics

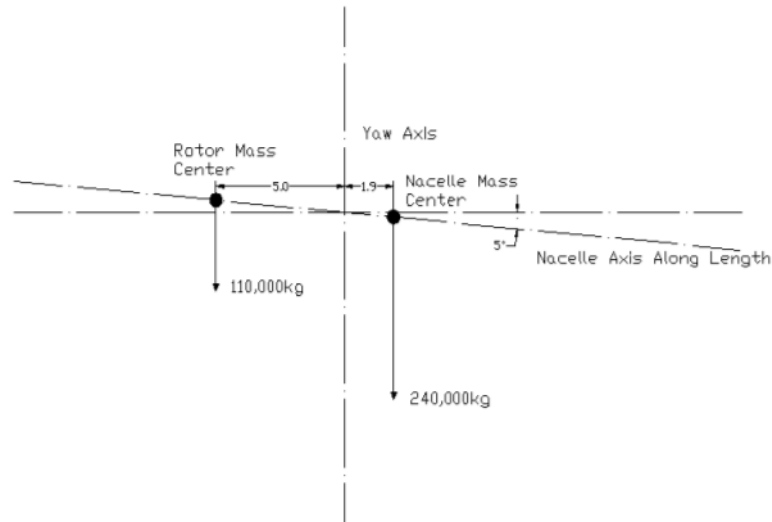
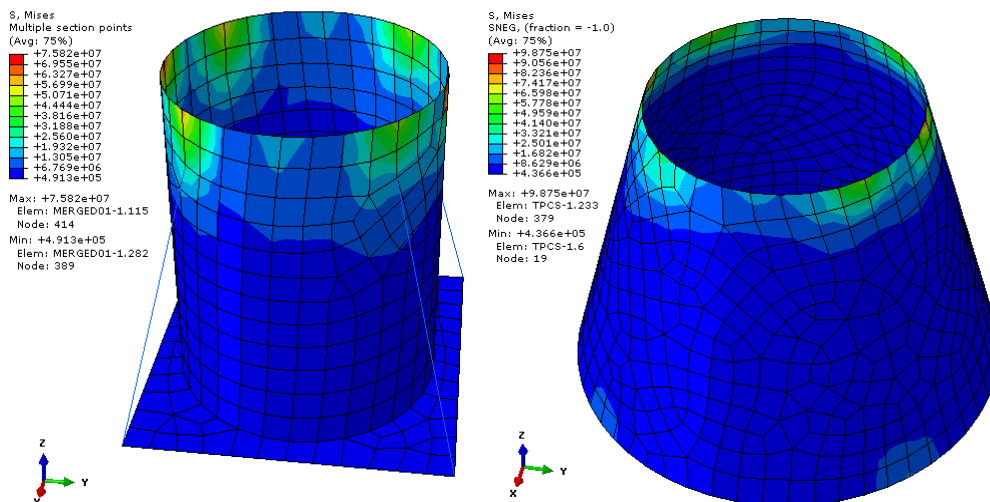
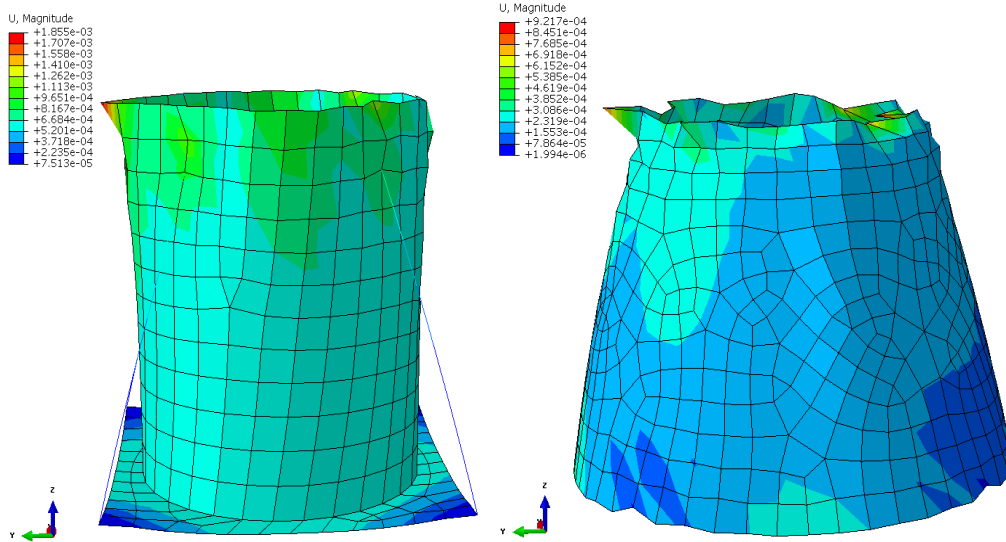


Figure 4.9 Misalignment of Yaw Axis and Mass Centers of Rotor and Nacelle



(a) Transition Piece Stress Condition under RNA Weight and Its Induced Moment



(b) Transition Piece Deformation under RNA Weight and Its Induced Moment
 Figure 4.10 Transition Piece Response under RNA Weight and Its Induced Moment

The reason for this sharp increase is mainly that the resulted moment of 921.1 kN·m in the above design (Figure 4.9) is too significant, accounting for about 17% of the moment induced by one load component, e.g. 5390 kN·m induced by the rotor gravity. Both the transition piece models are sensitive to this large amount of eccentric moment. A more reasonable design optimizing the arrangement of the rotor and nacelle center of gravity is no doubt beneficial for creating a zero moment along the yaw axis. In addition, stress condition and structural deformation under the RNA weight and moment load reveals an unsymmetrical pattern along the yaw axis (Z-axis).

4.3.3 Rotor thrust

According to the blade momentum theory [24], rotor thrust is dependent on the instantaneous wind condition and the rotor structural diameter (Eq. 3-4). In reality, as wind velocity has an instantaneously changing characteristic, the resulted rotor thrust load is a time series with varying magnitude and direction. On a first estimate, a static theoretical thrust force based on a specific wind velocity condition is applied on the transition piece. Dynamic analysis of transition piece structural response to the time series of a simulated real-time rotor thrust load is performed afterwards.

Static analysis

Wind speed, rotor diameter and thrust coefficient are depending parameters for prediction of thrust force. Based on the reference 5MW wind turbine, cut-in, rated and cut-out wind speeds are respectively 3.0m/s, 11.4m/s and 25.0m/s while the rotor diameter is designed as 123m with length of each blade 61.5m [23]. On the first order, thrust coefficient is based on formula $C_T = \frac{7m/s}{U_{hub}}$ (Figure 4.11) [33]. Resulted rotor thrust force at the three characteristic wind speeds is shown in Table 4.8.

Preliminary Design of Transition Piece
Lattice Tower Design of Offshore Wind Turbine Support Structures

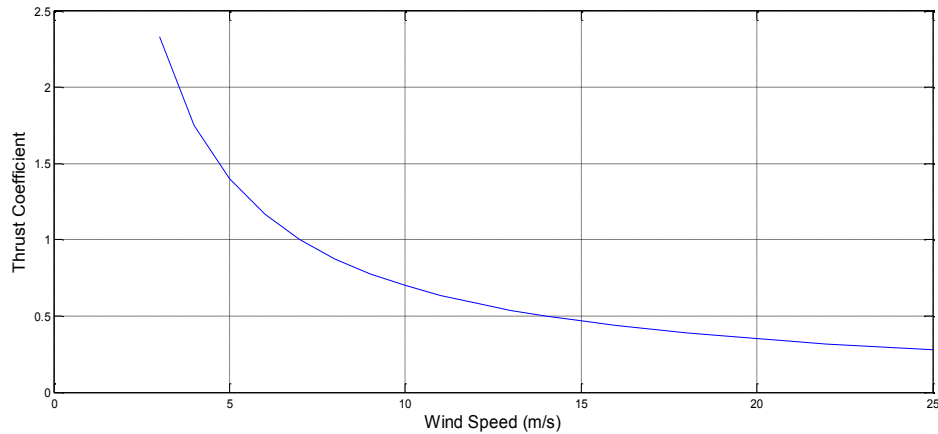
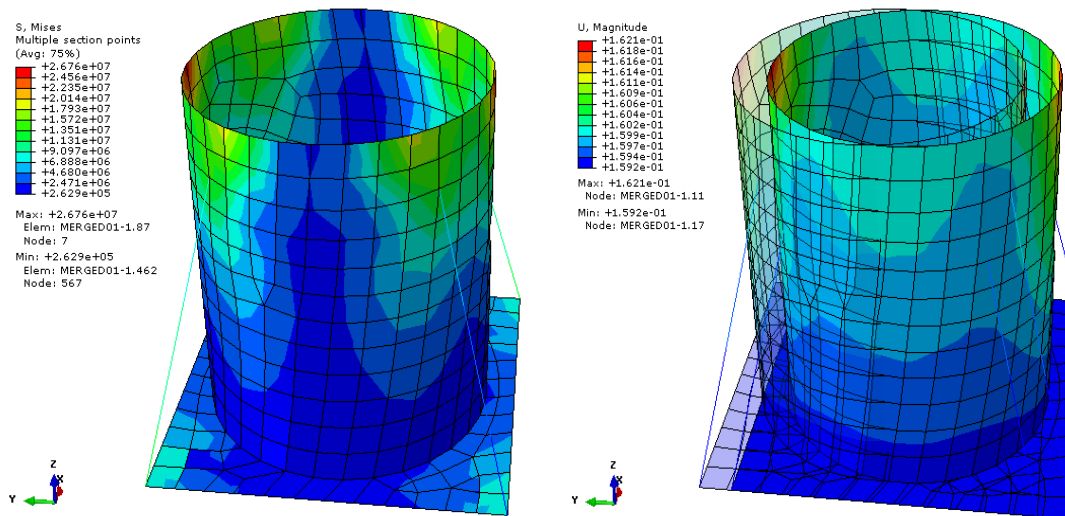


Figure 4.11 Thrust Coefficient in Relation to Wind Speed

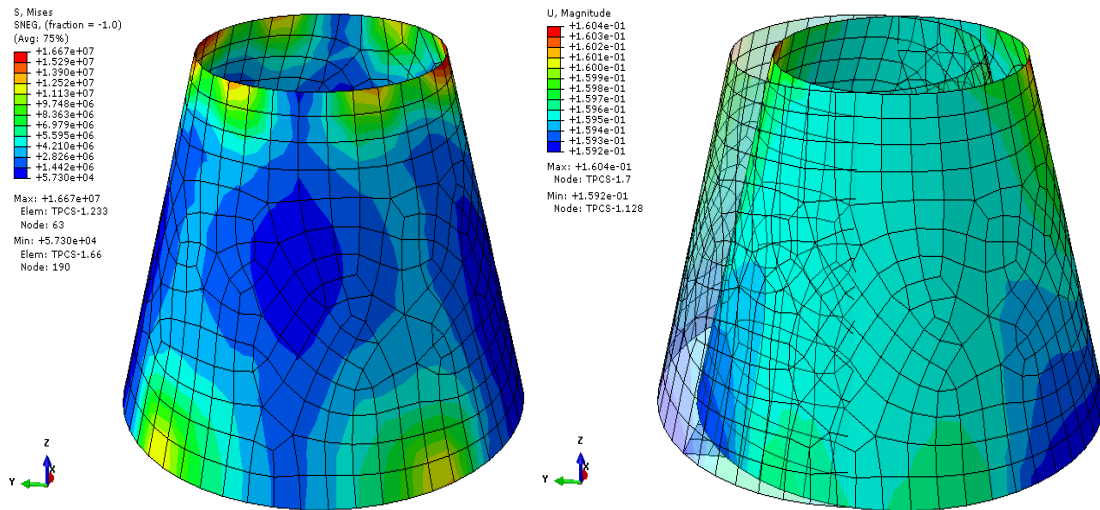
Table 4.8 Rotor Thrust Load under Characteristic Wind Velocities

Wind Velocity (m/s)	Rotor Diameter (m)	Thrust Coefficient	Theoretical Thrust Force on Rotor Disk (kN)
3.0 (cut-in)	123	2.333	290.93
11.4 (rated)	123	0.614	580.74
25.0 (cut-out)	123	0.280	1273.63

Applying the theoretical thrust force of 1273.63kN at 25.0m/s wind velocity on the models, results of the structural response of the transition piece are shown in Figure 4.12. For the frame-cylinder model, maximum stress of 26.76MPa occurs at the upper part of the cylinder along the incoming wind direction (Y axis in Figure 4.12) and the maximum displacement due to this thrust force is about 0.162m. However, because of the applied boundary condition based on the bending stiffness of the lattice structure, 0.159m displacement is considered to be induced by the bending of the lattice structure and the deflection of the transition piece itself is negligible. As for the cone-strut model, maximum stress is 16.67MPa, which is 37.7% lower than the maximum stress in the frame-cylinder model. Maximum stress occurs at the upper edge of the cone and structural deflection of the transition piece itself is also ignorable.



(a)Frame-cylinder Model Response under Theoretical Static Thrust Load



(b) Cone-strut Model Response under Theoretical Static Thrust Load
 Figure 4.12 Response of Transition Piece under Theoretical Static Thrust Load

Compared with the structural response of transition piece under RNA weight (Figure 4.6), the static rotor thrust force does induce a very comparable structural response of the transition piece, in terms of structural stress condition. Nevertheless, it is worthy to mention here that the cone-strut model seems to have an advantageous performance over the other under the static loads (RNA weight and static thrust force).

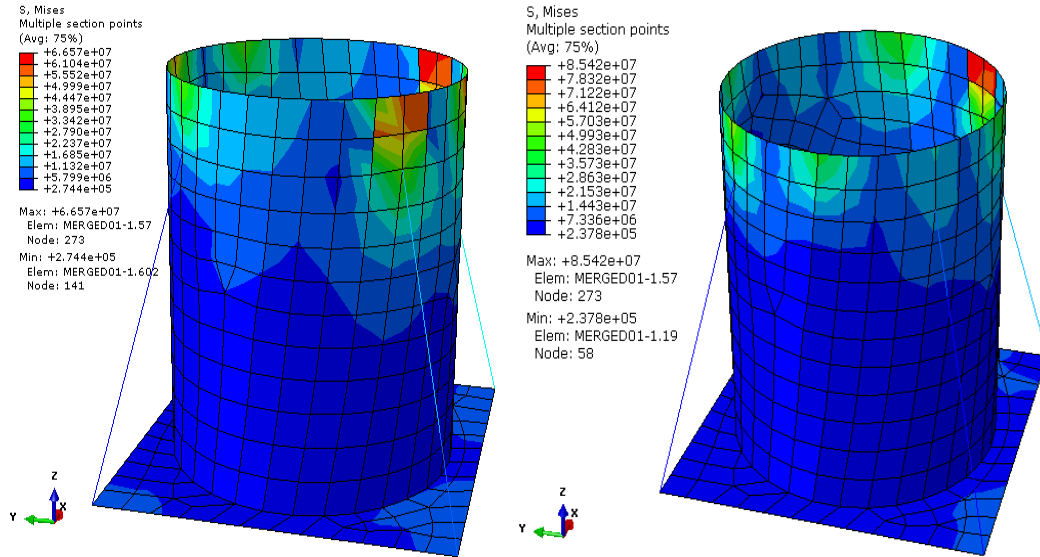
Static rotor thrust in combination with RNA weight & moment

After investigation of the structural response to the static theoretical rotor thrust alone, investigation of the transition piece performance under the combined static rotor thrust and the RNA weight and moment is done. The result is shown in Figure 4.13.

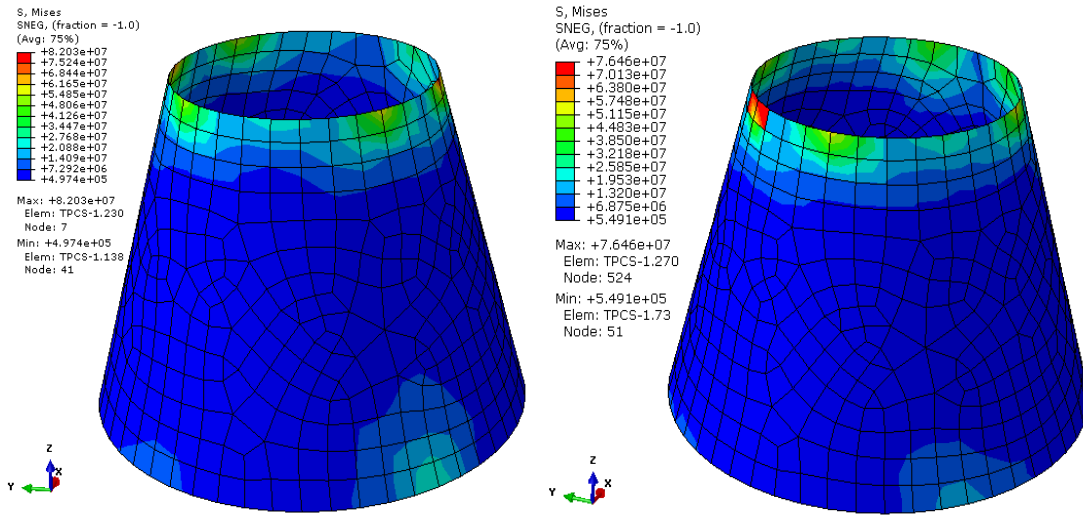
Two cases are considered in this analysis: the first case is without a yaw angle, i.e. the thrust force is applied to the $-Y$ direction and the second case is with a yaw angle of 45° , i.e. the thrust force is applied at 45° from $-Y$ direction, or vector $(1, -1, 0)$ direction in Figure 4.13. Based on the result below, it can be seen that with a yaw angle of 45° , maximum structural stress is increased by around 28% in the frame-cylinder model and decreased by 7.0% in the cone-strut model. The cone-strut model appears to be less sensitive to the direction of the thrust load which agrees well with its symmetric geometry profile.

Interestingly, however, comparing results of Figure 4.10(a) and Figure 4.13(a) & (c), it can be seen that thrust load seems to have eased the stress condition within the transition piece. The reason can be explained by the opposite trends between the effects from the RNA weight induced moment and the effects from the thrust force: the RNA weight induced moment has an effect of tilting the transition piece to the upwind side while the thrust force is pushing the transition piece to the downwind direction. It can be by this reason that maximum stress within the transition piece models is even lower with the addition of thrust load impacting, compared with the case of RNA load alone.

Preliminary Design of Transition Piece
Lattice Tower Design of Offshore Wind Turbine Support Structures



(a) Stress under Static Thrust & RNA Load (0° Yaw) (b) Stress under Static Thrust & RNA Load (45° Yaw)



(c) Stress under Static Thrust & RNA Load (0° Yaw) (d) Stress under Static Thrust & RNA Load (45° Yaw)

Figure 4.13 Transition Piece Response under Static Thrust and RNA Load

Dynamic analysis

Dynamic analysis of thrust load is performed to assess the structural response of the transition piece from a dynamic point of view. A 600-second time series of 24m/s mean wind speed with turbulence intensity of 15.73% is simulated (Figure 4.14). This 24m/s wind condition is employed to approximate a relatively extreme aerodynamic load condition for transition piece analysis. Appendix IV provides explanation of this approximation.

According to Eq. 3-4, theoretical thrust load on a static rotor disk under the above wind condition is computed as Figure 4.15. Considering the aerodynamic of the rotating rotor, the actual area of the rotor blades rather than a rotor disk, etc, simulation result of the rotor thrust load from HAWC2 code is given in Figure 4.16. By comparison of the theoretical value and the simulated value from HAWC2, it can be seen that the theoretical value is more conservative in magnitude and the simulated result takes into consideration the aerodynamics of the rotating blades. Power regulation control

Preliminary Design of Transition Piece
Lattice Tower Design of Offshore Wind Turbine Support Structures

mechanism is also influencing the simulated result. Here the analysis will be based on the less conservative HAWC2 simulation result. The magnitude of the rotor thrust load might not trigger a big issue for the transition piece analysis based on previous static analysis but the structural dynamic performance under the dynamic rotor thrust load with consideration of rotor aerodynamics is what to be explored.

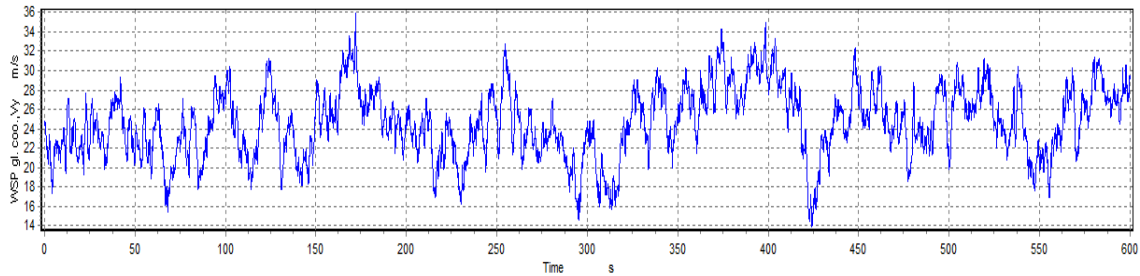


Figure 4.14 Time Series of Normal Turbulent Wind with Mean Wind Speed 24m/s and Turbulence Intensity 15.7%

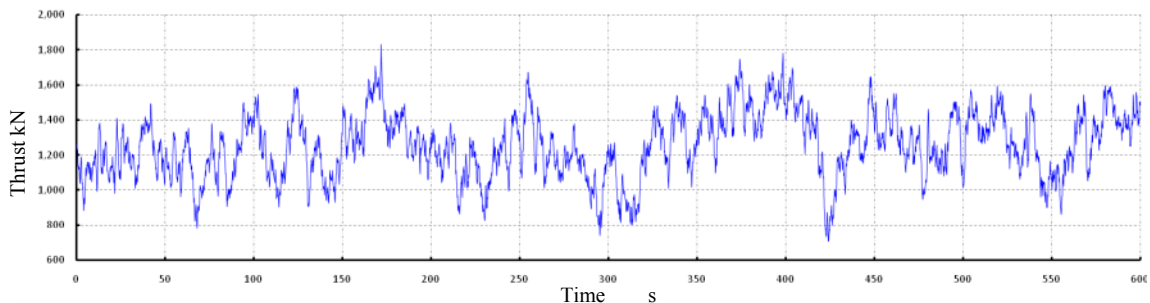


Figure 4.15 Theoretical Thrust Load on Rotor Disk

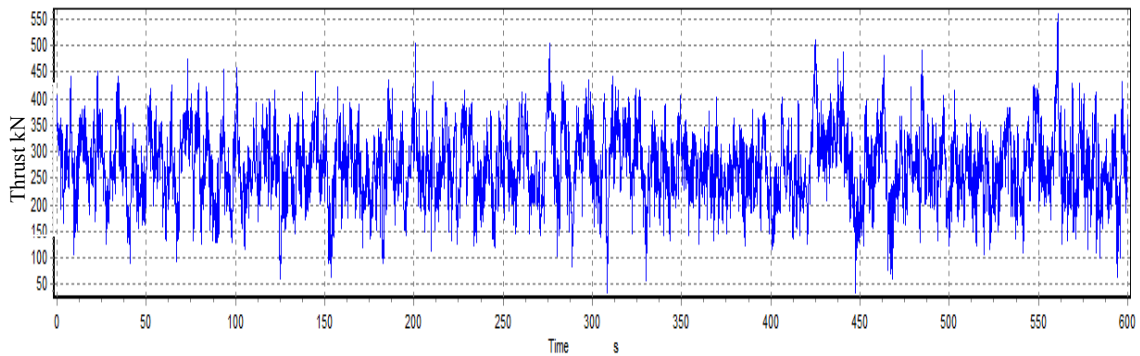
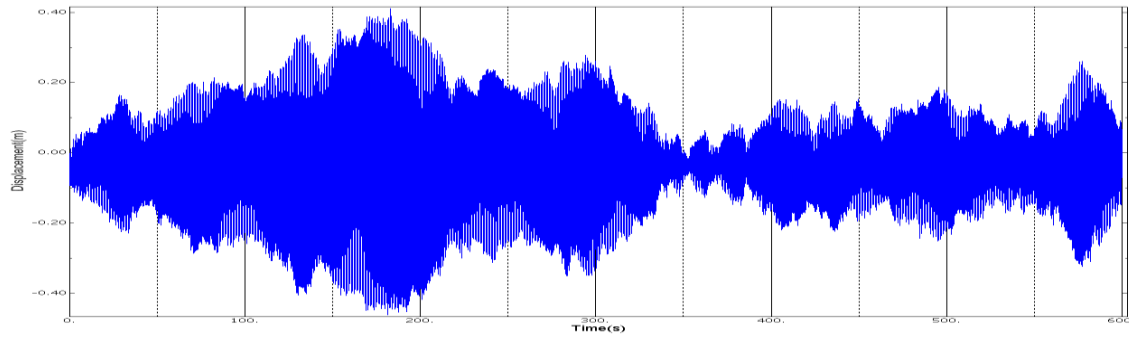


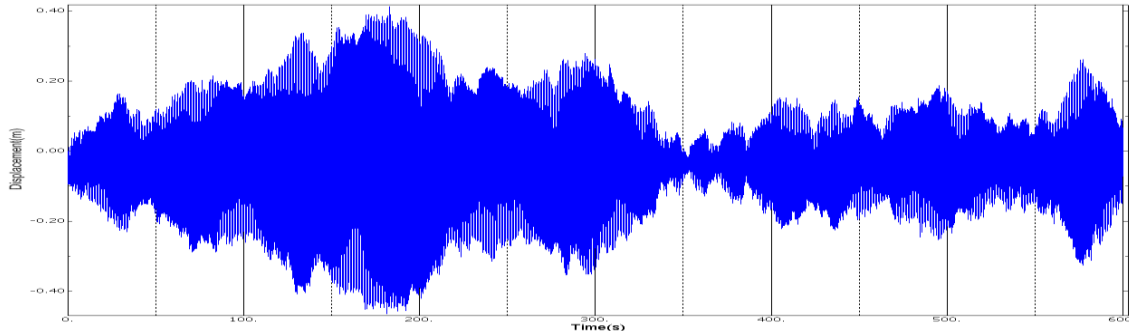
Figure 4.16 Simulated Thrust Load from HAWC2

Applying the dynamic time series of the rotor thrust load on the finite element model of the frame-cylinder transition piece, structural response at the base point and the top point in the thrust load direction is shown in Figure 4.17(a) & (b). Deflection pattern at the base and top points show almost identical characteristics, which reveals a quite insignificant deformation within the transition piece itself. Maximum oscillation of the structure reaches amplitude of over 0.4m both at the base and top points of the transition piece, which should be accounted for by the bending stiffness of the lattice support structure applied as boundary for the transition piece.

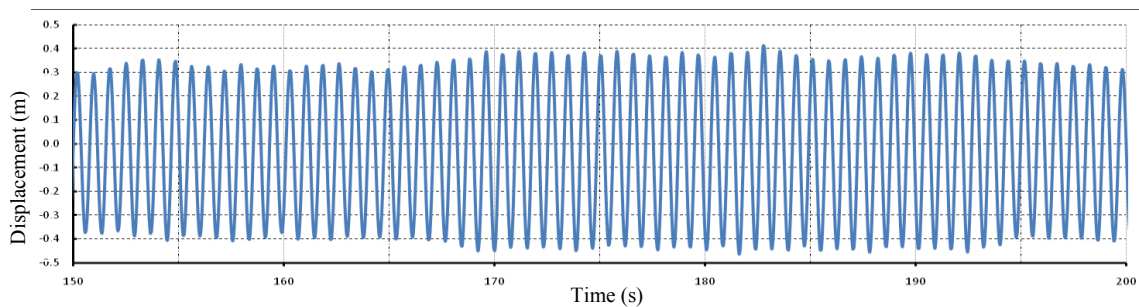
*Preliminary Design of Transition Piece
Lattice Tower Design of Offshore Wind Turbine Support Structures*



(a) Displacement at Base Point of Frame-cylinder TP



(b) Displacement at Top Point of Frame-cylinder TP



(c) Displacement at Top Point of Frame-cylinder TP between 150-200s

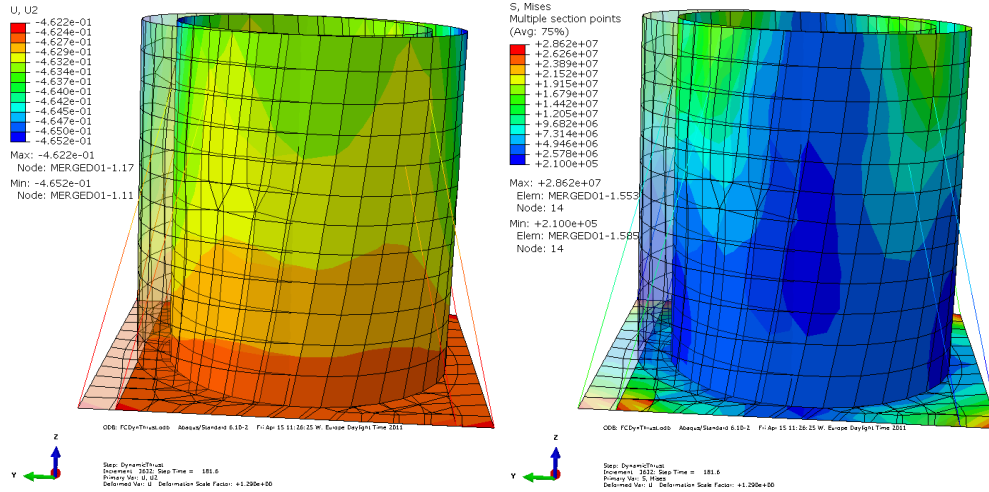
Figure 4.17 Structural Response of Frame-cylinder TP under Dynamic Thrust Load

Compared with the previous case under theoretical static rotor thrust (Figure 4.12), the simulated dynamic thrust load is reduced much in magnitude; however, the structural deformation under this dynamic load appears even more significant. The support structure applied as transition piece boundary is possible to have amplified vibrational magnitude under the dynamic thrust load. Nevertheless, transition piece itself shows negligible deflection within itself.

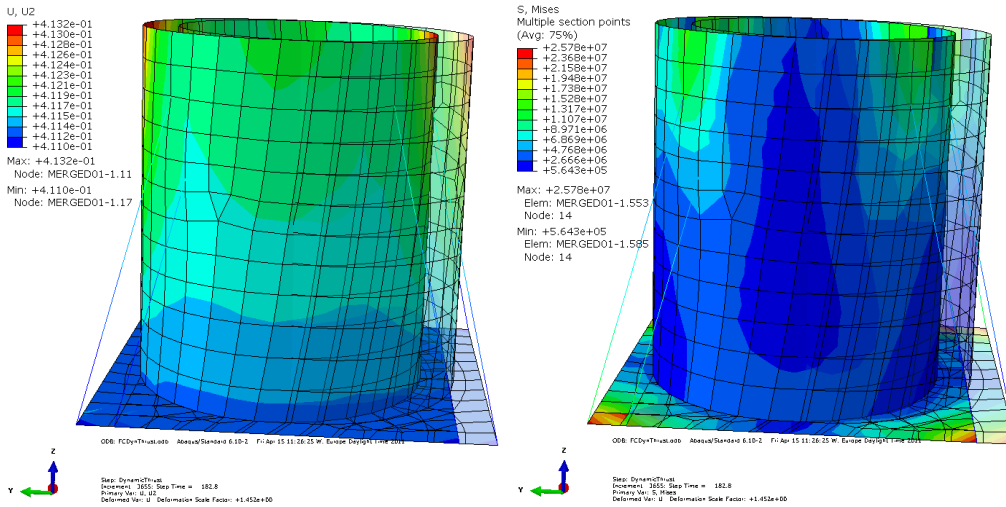
Under the above dynamic thrust load, the transition piece vibrates symmetrically around its original static position in the thrust and hence mean wind direction. At time point of 181.6s, the structure reaches maximum negative displacement (Figure 4.18(a)) and at a later time point of 182.8s, the positive displacement reaches its peak value (Figure 4.18(b)). Detailed thrust load during period of 150s to 200s is shown in Figure 4.19(c). In addition, the structural response possesses a vibration frequency of about 1.3Hz (Figure 4.17(c)) which corresponds to the first bending eigen frequency of the transition piece itself (Table 4.7). If a more complex model is employed taking into the consideration of the lattice support structure, the response of transition piece should then inherit both the characteristics of the eigen frequencies of the transition piece and also that of the lattice support structure. Connection points of the cylinder and the

Preliminary Design of Transition Piece Lattice Tower Design of Offshore Wind Turbine Support Structures

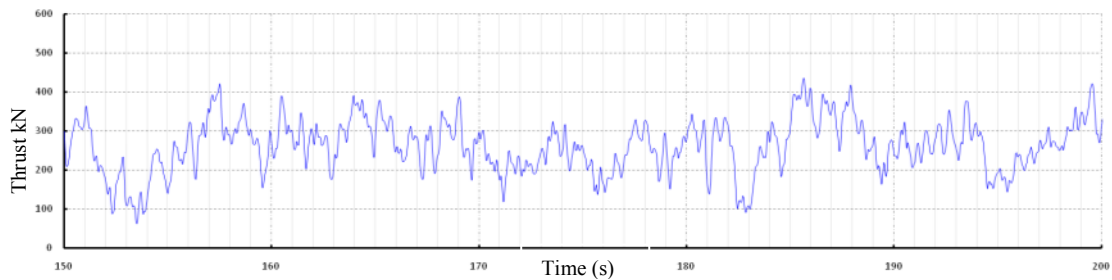
trusses are, due to the vibrational load, subjected to alternating cyclic stress condition. In addition, base connection points of transition piece and the lattice support structure are subjected to maximum stress condition. Fatigue failure of these connection points are very likely due to the complex load and stress condition and thus it is imperative to ensure the robustness and reliability of these connection points during design and manufacturing process.



(a) Displacement and Stress Condition at Time Point 181.6s (Max. Negative Deflection)



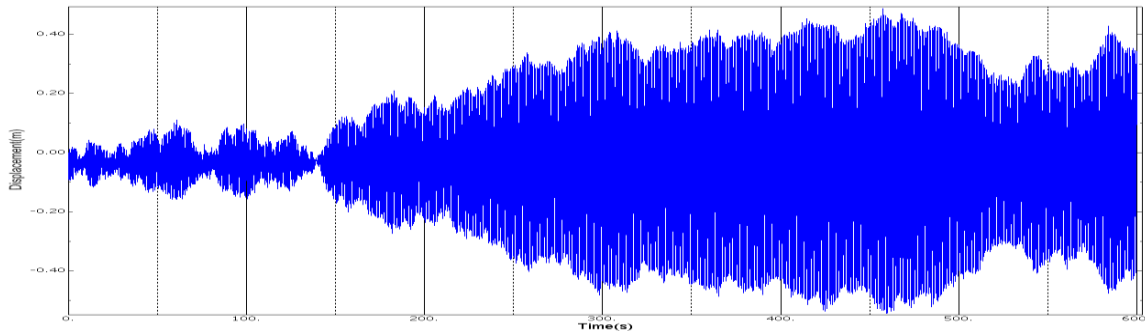
(b) Displacement and Stress Condition at Time Point 182.8s (Max. Positive Deflection)



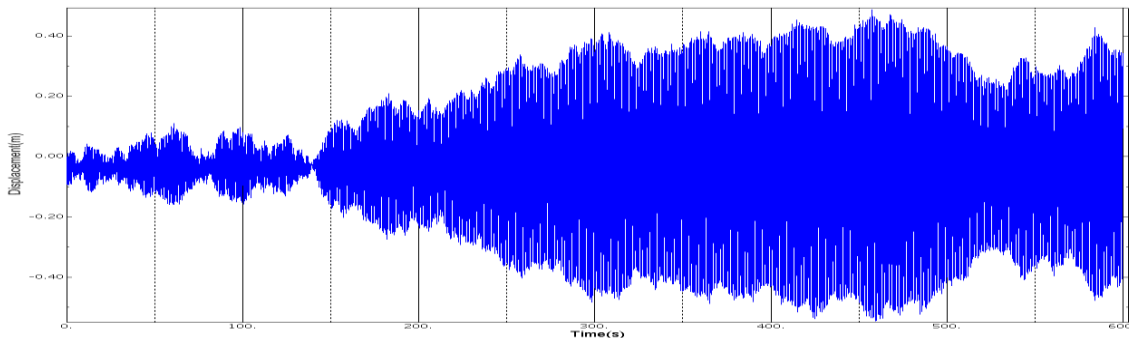
(c) Thrust Load between 150 and 200s

Figure 4.18 Frame-cylinder TP Response under Thrust Load at Max. Negative and Positive Deflection Time Points

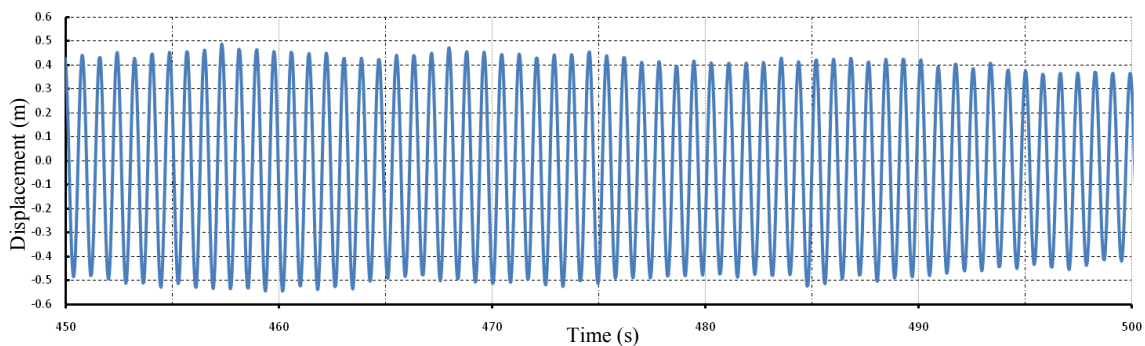
Applying the same dynamic thrust load on the cone-strut transition piece, structural response is resulted in Figure 4.19. Similar as the situation for the frame-cylinder TP in Figure 4.17, maximum vibration amplitude reaches about 0.5m under the dynamic thrust load, which is again associated with the applied bending stiffness of the lattice support structure. Structural deflection of the transition piece itself is insignificant. A significant difference between the responses of the two types of transition piece is the time point when the maximum structural response takes place. Comparing Figure 4.17(a) and Figure 4.19(a), it can be easily seen that for the frame-cylinder transition piece, maximum structural deformation occurs during the first half of the simulation period, i.e. 100s-250s whereas for the cone-strut transition piece, maximum response takes place during the later stage of the simulation period, i.e. 350s-500s. This difference can possibly be explained by the differences of the structural dynamics of the two transition pieces or may be associated with numerical simulation stability. A detailed investigation of the structural response of the cone-strut transition piece during time period of 450-500s reveals the structural eigen frequency of 1.2Hz (Figure 4.19(c)), which agrees well with the result computed in Table 4.7. Structural deflection and stress condition at time points of maximum displacement is shown in Figure 4.20.



(a) Displacement at Base Point of Cone-strut TP



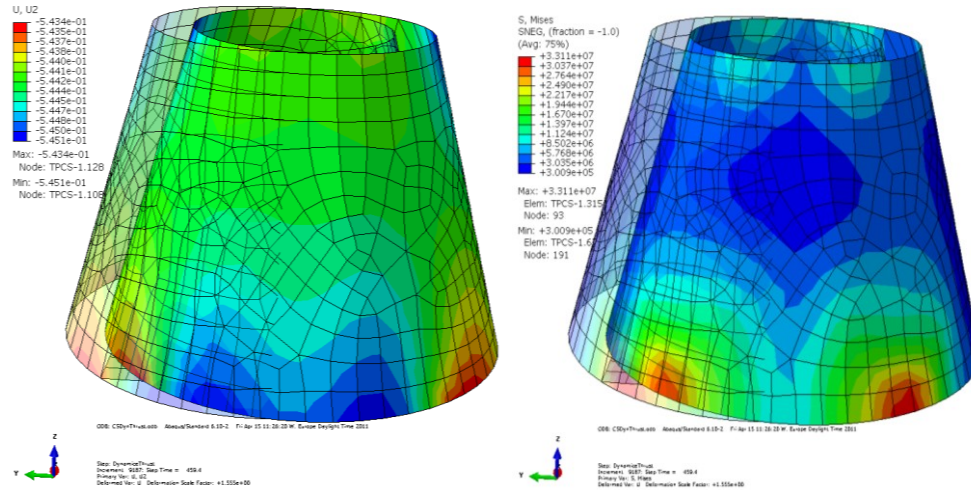
(b) Displacement at Top Point of Cone-strut TP



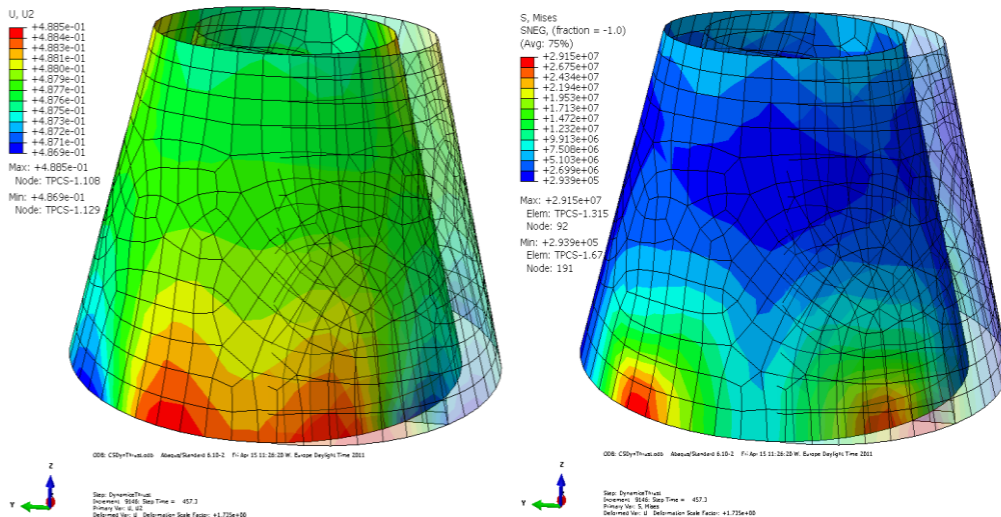
(c) Displacement at Top Point of Cone-strut TP between 450-500s

Figure 4.19 Structural Response of Cone-strut TP under Dynamic Thrust

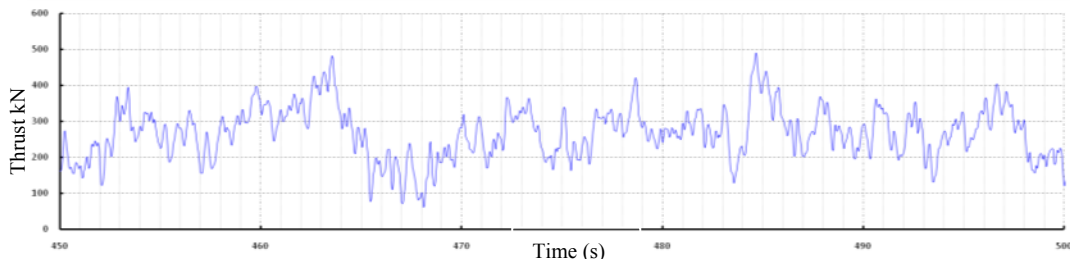
Preliminary Design of Transition Piece Lattice Tower Design of Offshore Wind Turbine Support Structures



(a) Displacement and Stress Condition at Time Point 459.4s (Max. Negative Deflection)



(b) Displacement and Stress Condition at Time Point 457.3s (Max. Positive Deflection)



(c) Thrust Load between 450 and 500s

Figure 4.20 Cone-strut TP Response under Thrust Load at Max. Negative and Positive Deflection Time Points

For the cone-strut transition piece, critical stress points are the connection points between the cone and the bottom base plane or rather, the lattice legs. Under the dynamic thrust load, the four connection points are subjected to alternating cyclic load with two of them at one side under the maximum stress condition during each cycle. Fatigue failure at these joints should undertake careful analysis in order to ensure the structural robustness.

Spectral analysis of the dynamic thrust load simulated from HAWC2 (Figure 4.16) is shown below. The load, which depends on the wind speed variation and the rotor dynamics, is majorly composed of low frequency components within the range of 1.0Hz. However, the frequency range of thrust load is not that likely to encounter with the natural frequencies of the lattice support structure, e.g., first bending modes at 0.6Hz for the hard design concept. Dynamic response of lattice support structure under dynamic rotor thrust load deserves further analysis in next chapter.

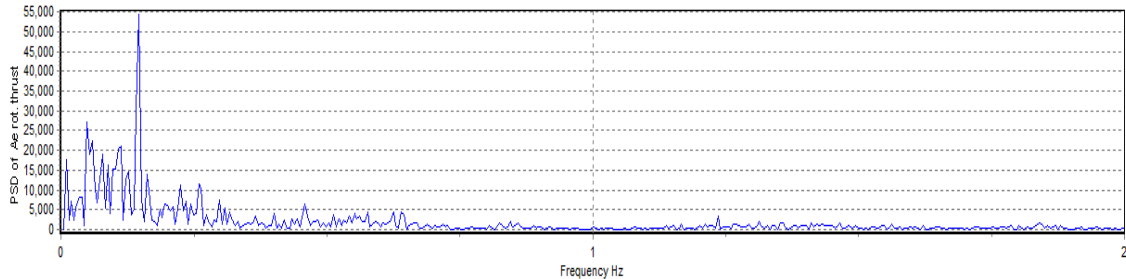


Figure 4.21 Power Spectral Density of Simulated Dynamic Thrust Load Time Series

4.3.4 Hydrodynamic load

Transition piece is not subjected to hydrodynamic load directly, however, the lattice support structure, on which the transition piece sits, is impacted constantly by wave load in the offshore environment. Two wave conditions are analyzed here where the first one corresponds to the moderate wave condition with significant wave height of 4.0m and the second condition corresponds to the more severe wave condition with significant wave height of 10.0m. Both wave conditions correspond to a wave period of 9.0s and time series of the irregular Airy waves [37] are generated using Jonswap spectrum [38]. The origin of the coordinate system for hydrodynamic load computation is set at seabed which makes the water surface at -30m (Figure 4.22). For the first condition of 4.0m wave, simulated sea surface elevation time series is shown in Figure 4.23. Flow velocities and accelerations in the incoming wave direction at different water depths refer to Appendix V.

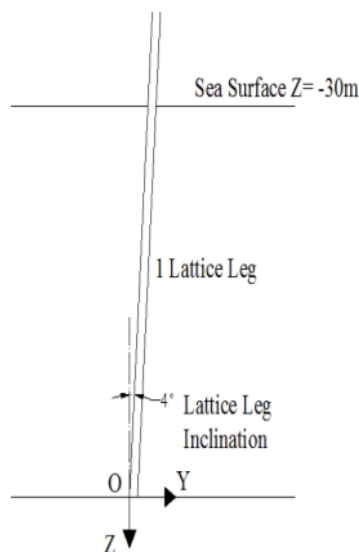


Figure 4.22 Origin and Coordination for Hydrodynamic Load Computation

Preliminary Design of Transition Piece
Lattice Tower Design of Offshore Wind Turbine Support Structures

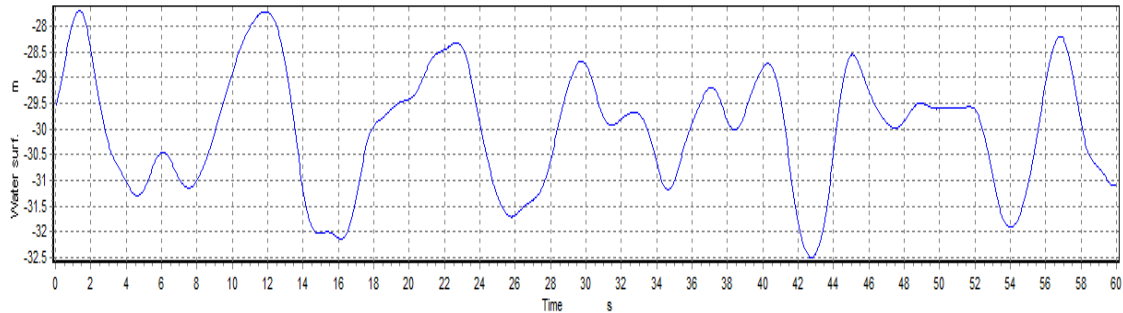
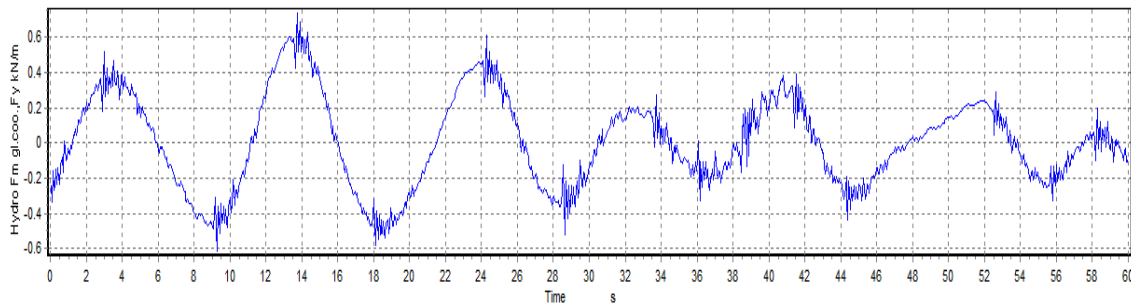
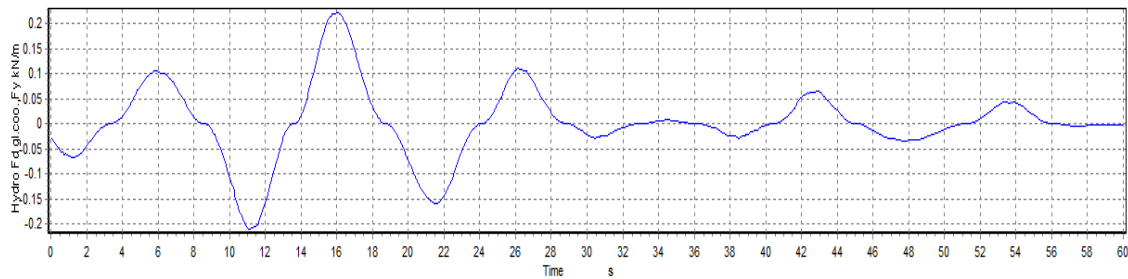


Figure 4.23 Water Surface for a Simulated 4.0m Wave Condition

Under this wave condition, the drag force and inertia force at characteristic location on the lattice leg are computed (Figure 4.24). The ripples in the simulated hydrodynamic forces on the lattice leg (Figure 4.24(a)) should be explained by the oscillation of the leg itself which has feedback on the load.



(a) Inertia Force on Lattice Leg



(b) Drag Force on Lattice Leg

Figure 4.24 4.0m Wave Load on Lattice Leg from HAWC2 Simulation

Based on previous study, the lattice leg is designed as a monopile with 0.9m diameter and 0.035m thickness. Inclination of the structure, which is about 4° in the vertical direction, does not cause significant difference in the resulted hydrodynamic load and is thus neglected. Considering the surface effect, the shallow water depth as well as a more conservative basis, the loads are uniformly applied on the finite element model of the lattice support structure (Figure 4.25). Top point response of the lattice support structure is shown in Figure 4.26.

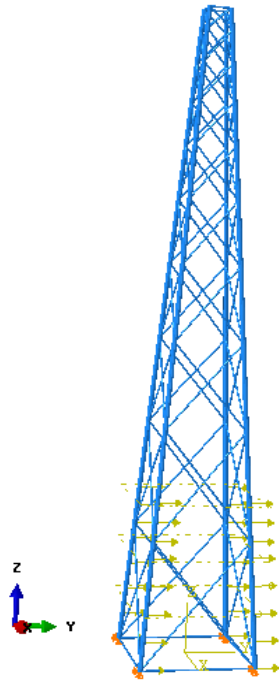


Figure 4.25 Applying Simulated Wave Load on Lattice Support Structure

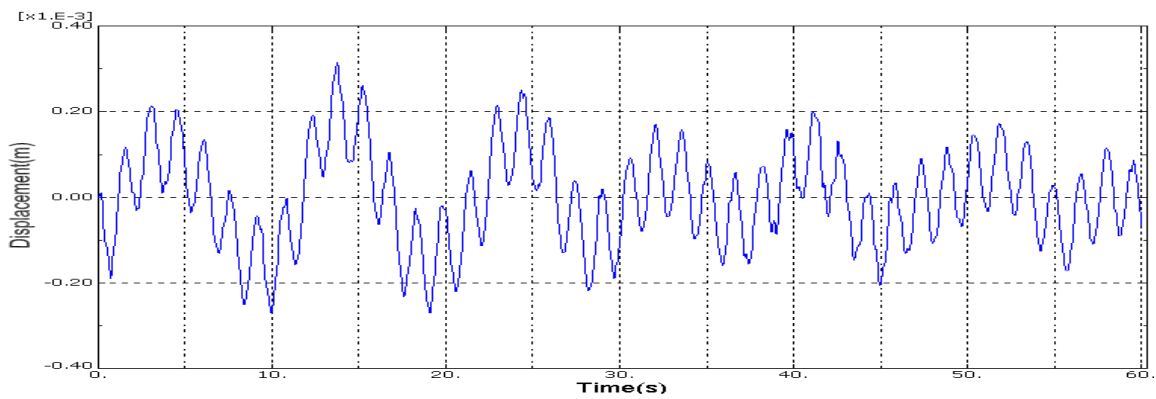


Figure 4.26 Top Displacement of Lattice Support Structure under 4.0m Wave

In the above result, maximum displacement at the lattice top under this 4.0m wave condition is negligible (0.3mm amplitude of vibration). A more severe condition of 10.0m wave is thus necessary for further investigation. For this more severe wave condition, time series of the water surface is shown below. Flow velocities and accelerations in the incoming wave direction at different water depths are referred to Appendix V.

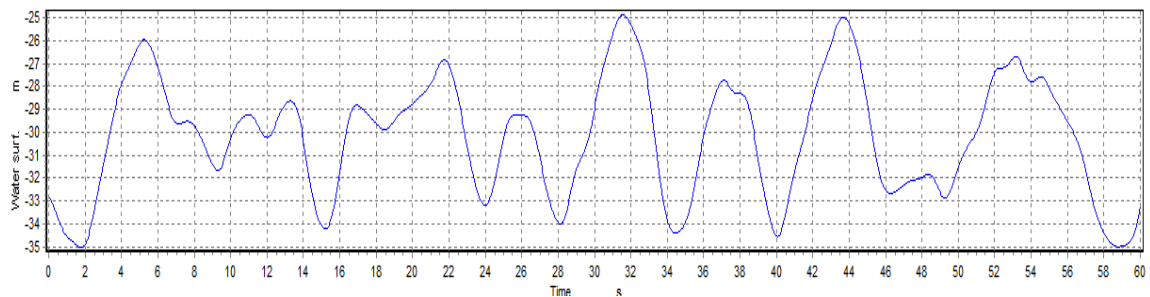
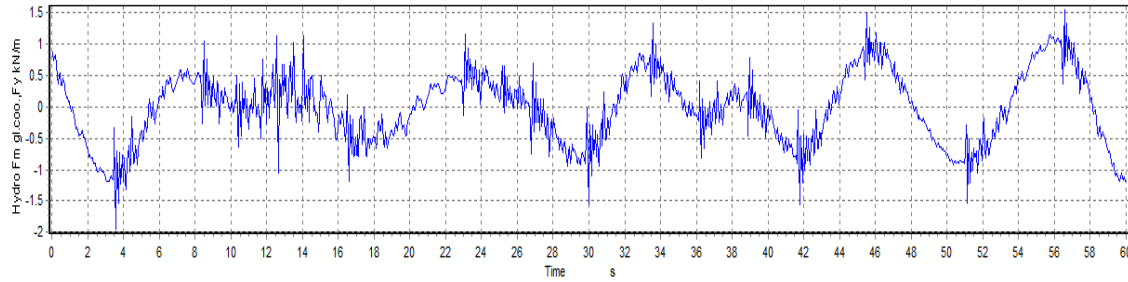


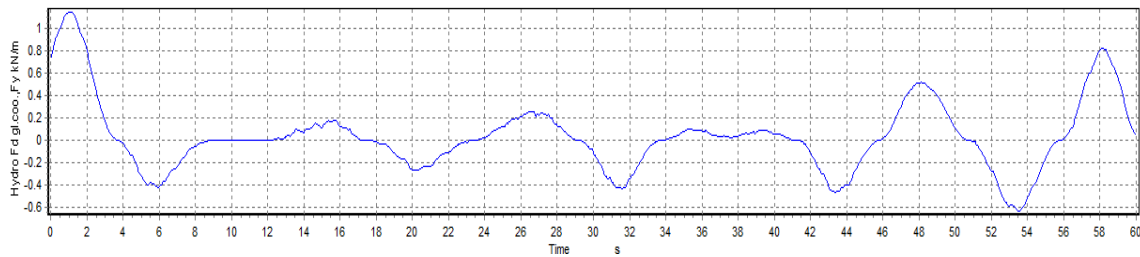
Figure 4.27 Water Surface for a Simulated 10m Wave Condition

Preliminary Design of Transition Piece
Lattice Tower Design of Offshore Wind Turbine Support Structures

The inertia force and drag force at representative location under this 10.0m wave condition on the same design of lattice leg are computed as below:



(a) Inertia Force on Lattice Leg



(b) Drag Force on Lattice Leg

Figure 4.28 10.0m Wave Load on Lattice Leg from HAWC2 Simulation

Applying the above loads on the lattice structure model, top displacement of the structure under this 10m wave condition is shown as in Figure 4.29. Even if the computed response is much more significant than that under the previous 4m wave condition, nevertheless, this magnitude of response is still within a reasonable and even negligible range with only 1.5mm amplitude of oscillation.

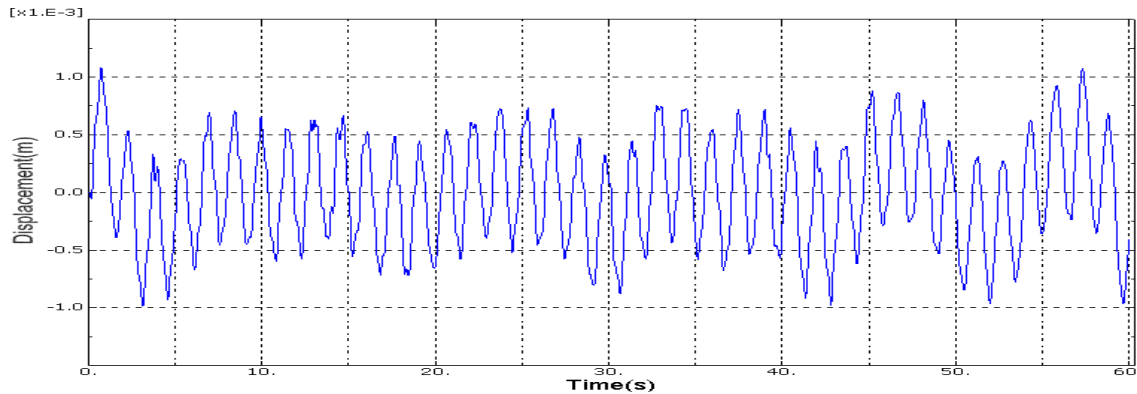


Figure 4.29 Top Displacement of Lattice Support Structure under 10m Wave

Based on previous analysis of the two wave conditions, the conclusion could be drawn that wave loads induce insignificant response on the top of the lattice support structure. However, buckling of the truss components below the sea surface under the hydrodynamic load could be a more important issue (Figure 4.30) which deserves future research. On the other hand, from the structural dynamics point of view, eigen frequency of the transition piece which is about 1.2-1.3Hz and the lattice support structure which is 0.3 or 0.6Hz depending on the type of design should be placed away from the frequency range of the wave motion, i.e. 0.05-0.2Hz (5s-20s wave period), in order to avoid structural resonance under the hydrodynamic load. This condition is thus satisfied here.

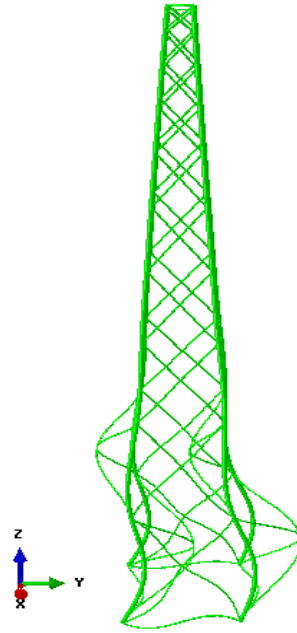


Figure 4.30 Buckling of Trusses below Water Surface of Lattice Support Structure under 10m Wave

4.3.5 Drive train vibration

During the entire operational life time of the wind turbine, drive train is undergoing rotational vibration. Electrical-mechanical drive train usually refers to the energy transmission chain without the rotor blades. However, for dynamic consideration, rotor blades are included here because they constitute the largest share in the rotating masses (Table 4.9) and play a decisive role in determining the dynamic behavior of the drive train system whose components have diverging dimensions and mass properties. The drive train system here is thus referred to the series connected components of rotor blades, rotor hub, rotor shaft, gearbox, high-speed shaft, etc.

Table 4.9 Mass Proportions of Dynamic Drive Train Components [3]

Wind Turbine	Aeroman	WKA-60	Growian
Blades	87%	91%	85%
Hub	2%	1%	8%
Generator	9%	7%	5%
Rest	2%	1%	2%

Vibration of the drive train system has its own dynamic characteristics and one of the major tasks should be to avoid resonance within the drive train system and with other components in the offshore wind turbine system. If, for instance, the first three modes of the drive train vibration possess natural frequencies of 2.03Hz, 4.42Hz and 8.71Hz respectively (Peeters, J. et al [26]), resonance between the vibration of the drive train and the transition piece torsional motion is likely to occur (Table 4.7). Optimization of either the drive train design or the transition piece design should be made in order to minimize the overlap of the eigen frequency range and thus reduce the likelihood of resonance.

4.3.6 Rotor torque

In addition to drive train torsional vibration, transition piece is subjected to rotor torque load. Because of the dominating proportion of the rotor (blades and hub), rotor torque

becomes one significant load. Rotor torque depends on the wind conditions, rotor blades properties etc (Eq. 3-11). Time series of rotor torque under a normal turbulent wind condition with mean wind speed 24m/s, turbulence intensity 15.7% and 20° yaw angle is shown in Figure 4.31. Yaw angle is defined as positive when it comes from the right hand side, seen from the rotor suction side to the incoming wind direction.

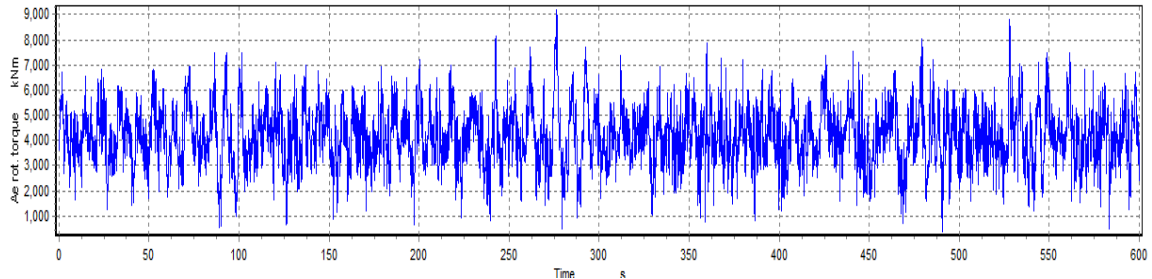


Figure 4.31 Rotor Torque under a Normal Turbulent Wind Condition

The above rotor torque is applied on the finite element models of the transition piece. The torque is applied at the incoming mean wind direction. For the frame-cylinder type, displacement in X, Y, Z directions of representative points on the cylinder top edge is shown in Figure VI.1 in Appendix VI.

Result shows that deflection of representative points at the two sides of the TP has similar trend in X and Y directions, which indicates a tilting deflection on the upper part of the TP (Figure 4.32). There is an uneven deflection in the vertical direction and this deformation is not in the same trend along the Z axis whose reason is because of the rotor torque, which makes a lifted deflection in the +X side and a pressed deflection in the -X side (comparing Figure VI.1(c) and VI.1(f)). Structural response is stably oscillating around a mean value within the period of simulation.

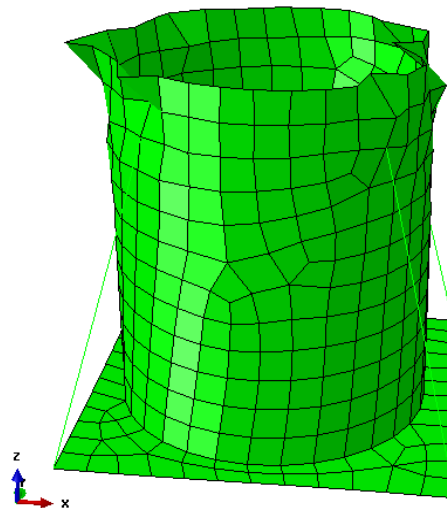


Figure 4.32 Deformation of Frame-cylinder TP under Rotor Torque (Scale Factor 284)

At a specific time point, Stress condition of the TP is shown in Figure 4.33. The unsymmetrical stress condition due to the rotor torque can be seen and maximum stress reaches 690.3MPa which is quite significant compared with all previous analysis results. Therefore, rotor torque has a significant effect on the stress condition of the frame-cylinder type transition piece and this effect should be very well considered during the design process.

Preliminary Design of Transition Piece
Lattice Tower Design of Offshore Wind Turbine Support Structures

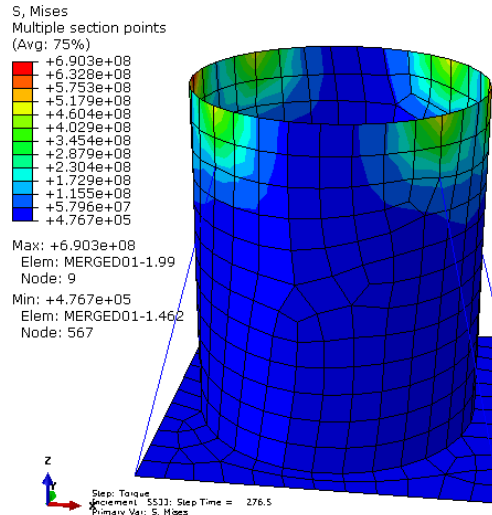


Figure 4.33 Frame-cylinder TP Stress Condition at Time Point of Max. Stress under Rotor Torque

For the cone-strut type of transition piece, displacement in the X, Y, Z directions of representative points on the cone top edge is shown in Figure VI.2. The deflection of the cone top edge shows similar type of structural deformation under the rotor torque as that of the frame-cylinder TP. The structure is tilted due to the rotor torque. The cone-strut TP structural deformation is shown below:

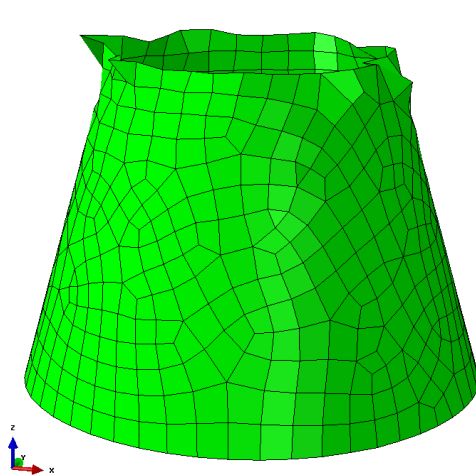


Figure 4.34 Deformation of Cone-strut TP under Rotor Torque

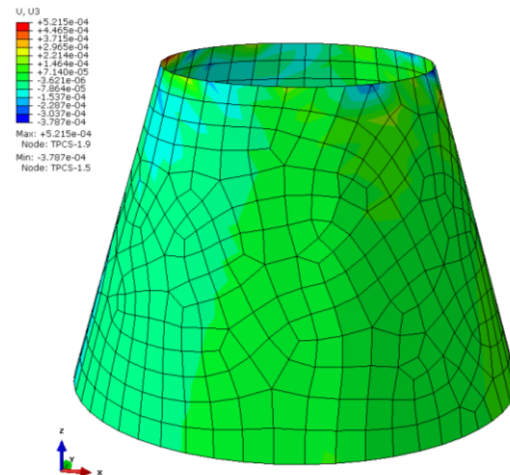


Figure 4.35 Z-displacement of Cone-strut TP under Rotor Torque

Z-displacement of representative nodes in Figure VI.2 does not fully reflect the deformation of the whole TP structure. Vertical displacement of the cone-strut TP at a given time point is shown in Figure 4.35. It can be easily seen that the magnitude of Z-displacement in the left side (-X) of the cone is larger than the magnitude of Z-displacement in the right side (+X), which corresponds to the effect of rotor torque load very well. Maximum stress condition of the cone-strut TP is shown in Figure 4.37. The unsymmetrical stress condition due to the rotor torque can also be seen and the maximum stress reaches 694.1MPa.

Preliminary Design of Transition Piece *Lattice Tower Design of Offshore Wind Turbine Support Structures*

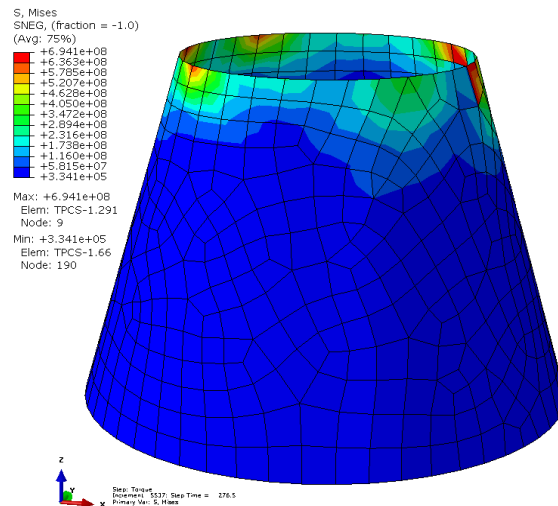


Figure 4.36 Cone-strut TP Stress Condition at Time Point of Max. Stress under Rotor Torque

Structural deflection of the cone-strut TP is comparable with that of the frame-cylinder TP. Maximum element stress of the cone-strut TP under the rotor torque load is also only slightly higher than the situation for the frame-cylinder TP. As the same situation for both types of the TP, rotor torque has a significant effect on the structural performance which induces unsymmetrical structural deflection along the axis approximately parallel to the rotor shaft and increases the maximum structural stress condition to a significant degree which should be given much attention. Maximum stress condition of both the frame-cylinder model and the cone-strut model occurs at time point of 276.5s. Detailed rotor torque load at time interval including this time point is shown in Figure 4.37. At this time point, the torque load reaches its maximum peak.

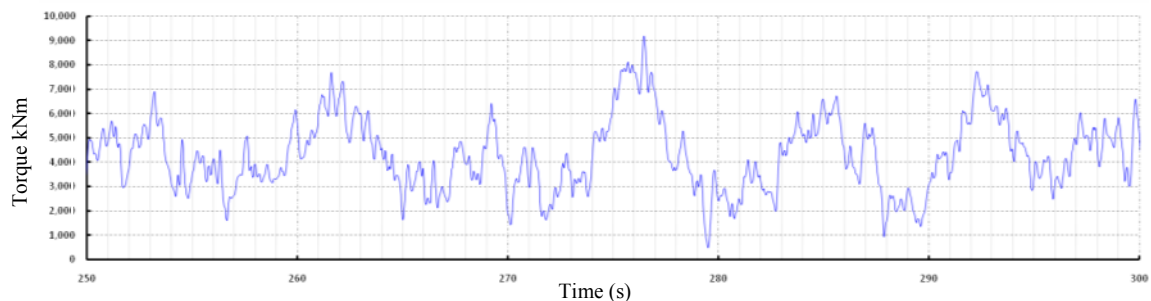
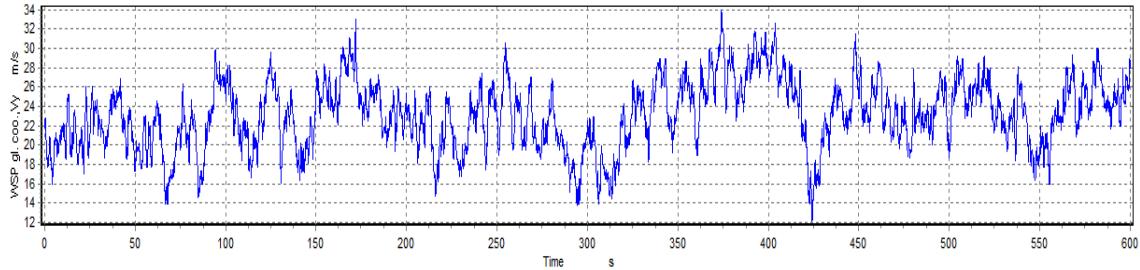


Figure 4.37 Rotor Torque between 250 and 300s

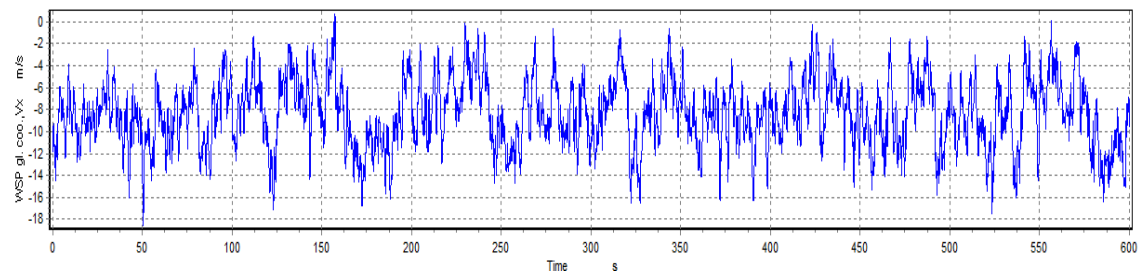
4.3.7 Yaw moment

Misalignment of the mean wind direction and the rotor hub axis induces the yawing motion of the rotor nacelle assembly and the yaw moment will thus have impact on the behavior of the transition piece. Time series of along-wind speed and cross-wind speed under a normal turbulent wind condition with mean wind speed 24m/s, turbulence intensity 15.7% and +20° yaw angle is shown in Figure 4.38. The two wind speed time series do not have identical trend within the simulation period due to the turbulence model used. Cross-wind mean speed is about 36% of the along-wind mean speed in magnitude for this case because of the significant simulated yaw angle of +20° applied. Due to the cross-wind load on the rotor nacelle assembly, the yaw moment around the yaw axis is shown in Figure 4.39. Magnitude of the yaw moment depends on the cross-

wind condition, the rotor aerodynamics and the rotor geometry in relation to the yaw axis. Simulated time series of the yaw moment under the above mentioned wind model is generally in phase with the cross-wind time series, with consideration of influence from the rotor aerodynamics, etc.



(a) Time Series of Along-wind Speed



(b) Time Series of Cross-wind Speed

Figure 4.38 Wind Speed Time Series of a Normal Turbulent Wind Model with +20° Yaw Angle

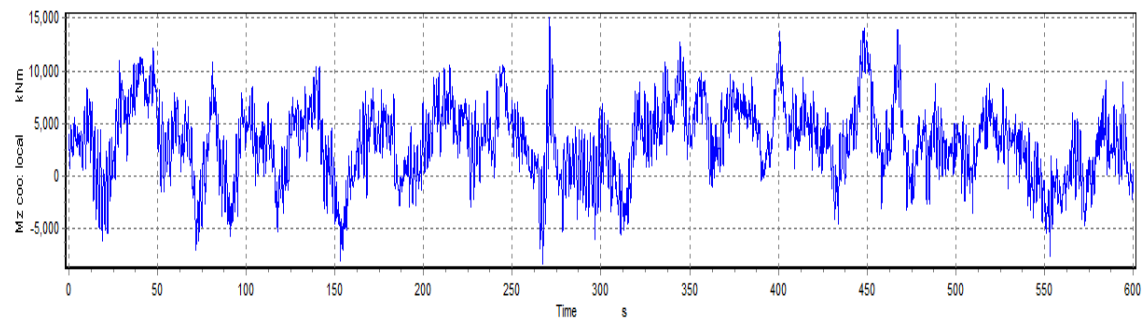
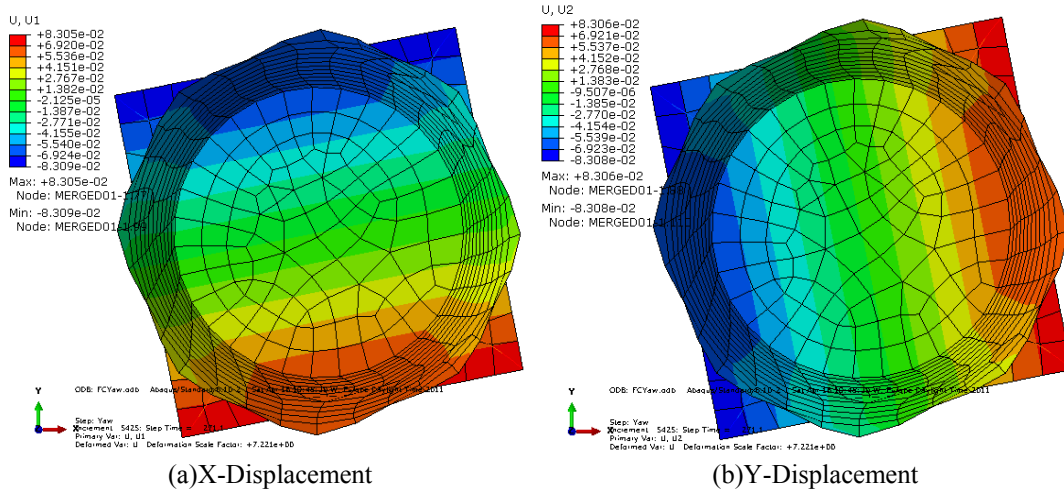


Figure 4.39 Yaw Moment around Yaw Axis under a Normal Turbulent Wind Model with +20° Yaw Angle

An important issue to mention is that due to the existence of the yaw bearing and the yaw drive system (Para. 3.2.2), the direct load on the transition piece should come from the yaw drive motion and be influenced by the type of yaw bearing. However, for simplification, the whole rotor nacelle assembly can be regarded as a single body and the cross-wind load on the rotor can thus be transferred as a yaw moment acting on the transition piece. In addition, any specifically designed control mechanism should in general be applied to reduce the load on the wind turbine system. Based on such thought with a more conservative consideration, the simulated yaw moment is applied on the finite element models of the transition piece to assess their structural performance under this loading condition. Similar as previous analysis, structural deformation and stress condition is the focus.

For the frame-cylinder TP, torsional deformation along the yaw axis under the applied yaw moment time series can be clearly seen (Figure 4.40 & 4.41). Maximum local stress reaches 708.6MPa at time point of 553.2s when the magnitude of the yaw

moment reaches one of its peak negative values (Figure 4.42). Deformation of the TP depends on the stiffness of the TP itself but in the meanwhile the applied torsional stiffness of the lattice structure as boundary condition has quite a significant influence. Maximum rotational displacement along the yaw axis occurs at time point 271.1s when the peak positive yaw moment is acting on the TP.



(a)X-Displacement (b)Y-Displacement
 Figure 4.40 Torsional Structural Deformation of Frame-cylinder TP under Yaw Moment at a Time Point

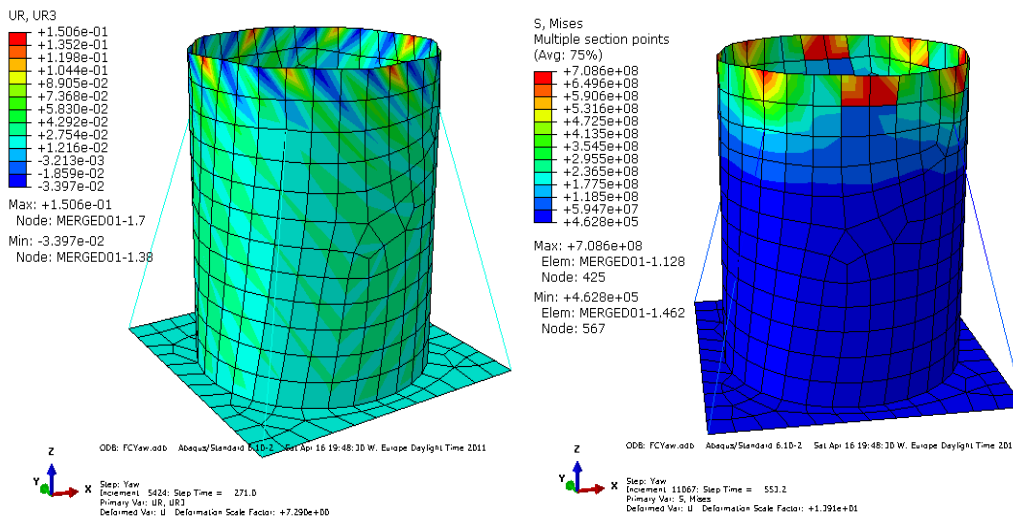


Figure 4.41 Rotational Displacement along Yaw-axis of Frame-cylinder TP under Yaw Moment at Time Point of Maximum

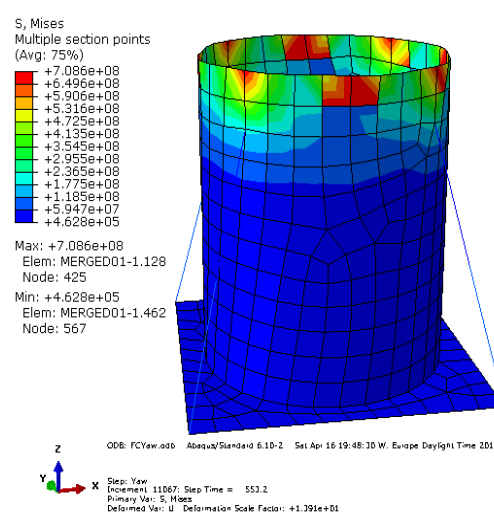


Figure 4.42 Stress Condition of Frame-cylinder TP under Yaw Moment at Time Point of Maximum

For the cone-strut TP model, the same yaw moment load is applied. The structure also shows torsional deformation along the yaw axis under the load and compared with the structural response of the frame-cylinder TP, the cone-strut TP has a larger torsional deformation (Figure 4.43). Maximum structural torsional response happens at time point of 271.2s when the yaw moment reaches the peak positive magnitude (Figure 4.44). Maximum element stress of the cone-strut TP reaches 743.4MP which is even higher than the maximum stress of the frame-cylinder TP under the same load condition (Figure 4.45). This extreme stress event happens also at time point of 553.2s when the yaw moment reaches its peak negative magnitude. Detailed yaw moment around time point of maximum negative peak and positive peak values is shown in Figure 4.46.

4.4 Conclusion

In the previous section, analysis of structural behaviour of two types of TP concepts under various loading conditions is performed. The loads analyzed include RNA weight, RNA weight induced moment, theoretical static rotor disk thrust, dynamic rotor thrust, drive train vibration, rotor torque and yaw moment. Hydrodynamic load's impact on the lattice support structure is also explored in order to assess the magnitude of influence on the transition piece. Time series of loads including dynamic rotor thrust, rotor torque, yaw moment and hydrodynamic load on lattice support structure are simulated from HAWC2 based on employment of wind and wave condition models. Summary of transition piece and lattice support structure response under various load conditions is shown in Table 4.10.

Rotor nacelle assembly weight constitutes a constant component on the stress condition of the transition piece. However, the load due to the weight alone does not trigger a big problem for the transition piece. Nevertheless, the induced moment due to the imbalance of the rotor gravity moment and nacelle gravity moment around the yaw axis leads to some significant increase of stress in both TP designs. It is thus highly suggested that an optimal design of the rotor and nacelle mass centers be made to avoid this gravity moment imbalance.

Rotor thrust load does not trigger big problem on the TP models, even if the relatively extreme wind load model is applied. Nevertheless, it is important to note that dynamic thrust load does induce an amplified vibration of the transition piece. The reason is associated with the boundary condition which is artificially applied based on previous numerical result of lattice support structure. Another issue is that due to the unsteady characteristics of the thrust load inherited with the instantaneous wind condition, maximum stress points on the TP will shift from side to side cyclically. Fatigue analysis at the connection joints of the models will thus be necessary to ensure sufficient connection robustness.

Magnitude of lattice support structure vibration under the hydrodynamic load depends on the severity of the wave environment and the lattice structural robustness, especially the bending stiffness. Simulation result in the above study shows extremely insignificant vibration of lattice structure top under the wave conditions, whereas buckling of the lower truss components below the sea surface could be a topic for future research. Natural frequencies of drive train torsional vibration should be avoided to overlap with the eigen frequencies of the transition piece, which can be taken care of during the design of either system.

For the above comparison of the two TP concepts, performance of the frame-cylinder TP slightly surpasses that of the cone-strut TP in terms of stress condition and structural deflection under loads of rotor thrust and yaw moment. The cone-strut TP seems only to possess advantages over the other type under static RNA weight load and theoretical rotor disk thrust. In this analysis the applied rotor torque and yaw moment could be over-standard in magnitude because of the applied wind model. However, this still shows the comparable differences of the structural behaviour of the two concepts under the rotor torque and the yaw moment.

Preliminary Design of Transition Piece
Lattice Tower Design of Offshore Wind Turbine Support Structures

Table 4.10 Summary of Transition Piece Behaviour under Various Load Cases

Load Condition		Frame-cylinder TP	Cone-strut TP	Comment
RNA Weight	Max. Stress	22.37MPa	16.31MPa	
	Max. Stress Location	Truss-cylinder connection points	Cone base connection points	
RNA Weight & Moment	Max. Stress	75.82MPa	98.75MPa	Significant stress increase due to RNA weight induced moment
	Max. Stress Location	Cylinder top edge & Truss-cylinder connection points	Cone top edge & Cone base connection points	
Theoretical Static Rotor Disk Thrust	Max. Stress	26.76MPa	16.67MPa	Lattice top displacement is depending on applied lattice stiffness
	Max. Stress Location	Cylinder top edge	Cone top edge	
	Structural Deflection	0.16m at lattice top, negligible for TP	0.16m at lattice top, negligible for TP	
Static Rotor Disk Thrust & RNA Load (0° Yaw)	Max. Stress	66.57MPa	82.03MPa	Increased stress condition due to thrust direction change for the frame-cylinder type and slightly decreased stress condition due to thrust direction change for the cone-strut type
	Max. Stress Location	Cylinder edge & Truss-cylinder connection points	Cone edge & Cone base connection points	
Static Rotor Disk Thrust & RNA Load (45° Yaw)	Max. Stress	85.42MPa	76.46MPa	
	Max. Stress Location	Cylinder edge & Truss-cylinder connection points	Cone edge & Cone base connection points	
Dynamic Thrust	Max. Stress	28.62MPa	33.11MPa	Vibration of lattice structure depends on lattice bending stiffness. Thrust load is based on normal turbulent wind with 24m/s speed and 15.7% turbulence intensity. Magnitude of vibration is seen as quite significant in this simulation study.
	Max. Stress Location	Base connection points	Base connection points	
	Structural Deflection	±0.46m vibration for lattice structure, negligible for TP	±0.55m vibration for lattice structure, negligible for TP	
Hydrodynamic Load (4.0m Wave Height)	Structural Deflection	±0.3mm vibration at lattice top		Irregular Airy wave model with T=9.0s and generated by Jonswap spectrum is applied. Buckling of lattice trusses deserve attention
Hydrodynamic Load (10.0m Wave Height)	Structural Deflection	±1.5mm vibration at lattice top		
Drive Train Vibration	Potential Resonance Mode	1 st torsional mode	1 st torsional mode	Depending on specific design of drive train system
Rotor Torque	Max. Stress	690.3MPa	694.1MPa	Torque load is based on normal turbulent wind with 24m/s speed, 15.7% turbulence intensity and 20° yaw angle.
	Max. Stress Location	Cylinder top edge & Truss-cylinder connection points	Cone top edge	
Yaw Moment	Max. Stress	708.6MPa	743.4MPa	Yaw moment is based on normal turbulent wind with 24m/s speed, 15.7% turbulence intensity and 20° yaw.
	Max. Stress Location	Cylinder top edge	Cone top edge	
	Structural Deflection	8.6° rotation around yaw axis	11.4° rotation around yaw axis	

Preliminary Design of Transition Piece
Lattice Tower Design of Offshore Wind Turbine Support Structures

5 FINAL DESIGN OF TRANSITION PIECE

Based on experience from preliminary analysis of the frame-cone transition piece and cone-strut transition piece concepts in the previous chapter, here a final design and analysis of transition piece model is proposed which combines structural strengths from the previous models and is aiming to meet more practical and functional requirements. In this final design, a model combining a cone component and a truss system is proposed which is expected to possess the advantageous characteristics of both types summarized in Table 4.10. The model here is also designed for a previously introduced lattice support structure model in Chapter 3 which makes this final design more practically useful.

5.1 Model geometry

In Para. 3.4.2, analysis of several lattice support structural models is performed (Table 3.5). Final transition piece model is designed for a lattice structure with $4\text{m}\times 4\text{m}$ top area as is used in all previous lattice designs. Diameter of the base of this transition piece is thus designed as 5.7m which equals to the diagonal length of the lattice top area, i.e., $4\sqrt{2}\text{m}$. As for the upper boundary of the transition piece, the major requirement is a proper connection with the yaw bearing ring which is introduced in Para. 3.3.2. For common practice, a yaw bearing of 5.0m diameter is used for 5MW wind turbines [30]. Therefore, the top diameter of the final transition piece is restricted as 5.0m . In addition, 1.0m extension of the transition piece is designed to be placed inside the nacelle assembly, which is able to allow for a more convenient connection between the nacelle assembly and the transition piece itself. Height of transition piece (designed as 6.0m in preliminary analysis) is not subject to specific functional or other requirement which thus deserves further investigation. The overall geometrical configuration of the transition piece is shown in Figure 5.1.

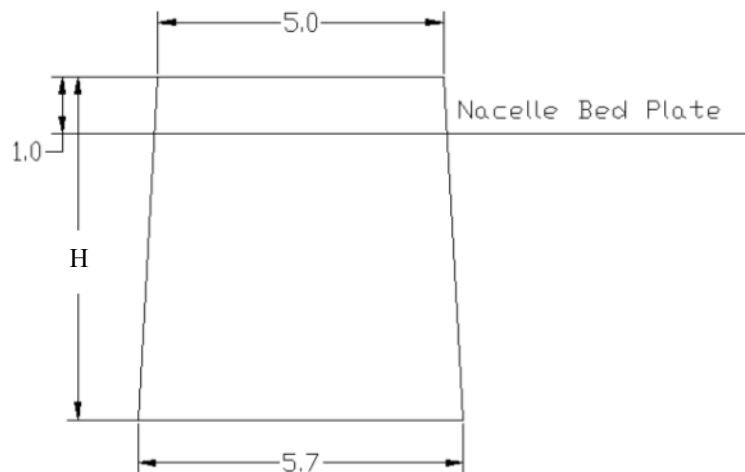


Figure 5.1 Geometrical Configuration of Transition Piece
(unit in meter; H to be determined)

Based on the above prerequisite, a truncated cone structure is suitable to meet these geometrical parameters. To strengthen the robustness of this cone structure, an inner truss system composed of four truss beams which connects the upper and lower boundary of the cone is designed. Truss components share a common joint in the center (Figure 5.2). Connection between this transition piece and the upper yaw bearing ring

is possible by means of bolting of the upper cone edge and the yaw bearing ring. A robust bolting connection at this location will thus require a sufficient cone shell thickness otherwise an additional connection flange should be created. On the other hand, connection of this transition piece to the lower lattice support structure triggers another challenge. Four short struts are placed at the lower edge of the cone which connect the four lattice legs and extend upwards on the cone surface (Figure 5.3). Sufficient welding strength is a crucial requirement for this type of connection. Overall view of the transition piece is illustrated in Figure 5.4.

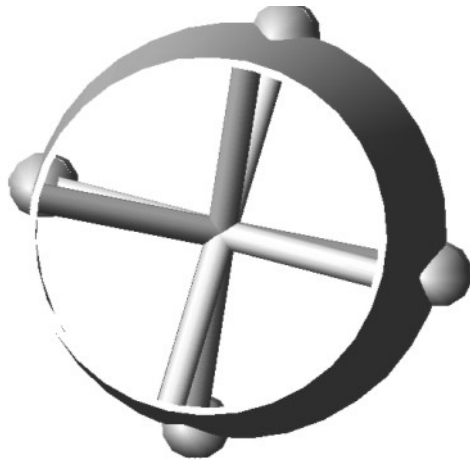


Figure 5.2 Joint of Truss Components

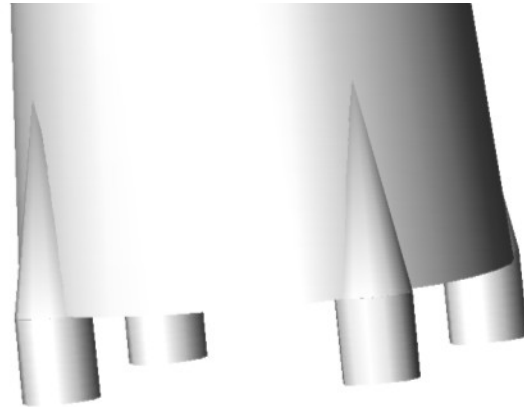


Figure 5.3 Connection with Lattice Support Structure

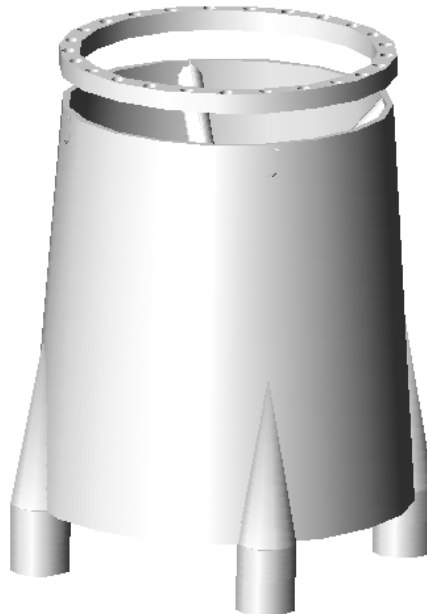


Figure 5.4 Overall View of Transition Piece (Scaled for H=6m)

5.2 Structural dimension

In addition to the geometrical configuration, dimension of the structural components has to be specified. As previously mentioned, transition piece height is a crucial parameter which influences the total weight, hence cost as well as the structural dynamic characteristic, e.g. structural eigen frequencies. On the other hand, cone thickness, truss components dimension, lattice connectors dimension all need to be specified. Figure 5.5

provides estimate of transition piece weight based on varying heights and cone thicknesses.

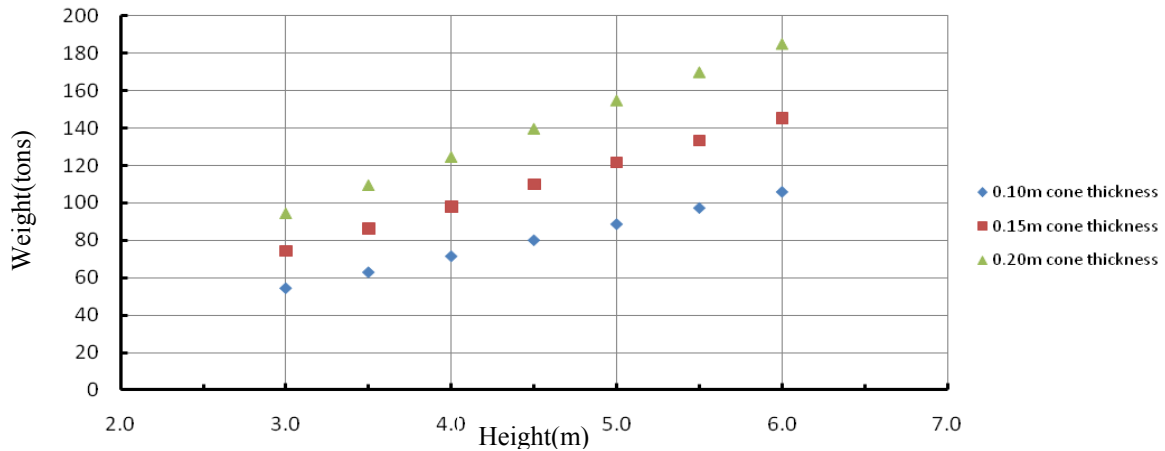


Figure 5.5 Transition Piece Weight with Varying Heights and Cone Thicknesses

Weight estimate in Figure 5.5 includes weight of the inner truss system and lower lattice connectors. Each truss component is designed as 0.4m diameter with 0.02m thickness and the connector is designed as 0.9m diameter with 0.04m thickness at the connecting surface with the lattice leg together with a solid cone connecting the transition piece cone surface up to half of the transition piece height below nacelle bed level. Weight restriction of overall 110tons is imposed on this final design and therefore the following models are filtered after this weight consideration. Table 5.2 shows weight breakdown of Model 3-20 in Table 5.1 as an example.

Table 5.1 Dimension & Weight of Varying Transition Piece Designs

Model Index	3-10	3-15	3-20	4-10	4-15	5-10	6-10
Height(m)	3.0	3.0	3.0	4.0	4.0	5.0	6.0
Cone Thickness (m)	0.10	0.15	0.20	0.10	0.15	0.10	0.10
Weight Excluding Lattice Connectors (tons)	44.4	64.2	84.0	58.0	84.4	71.8	85.5
Overall Weight (tons)	54.6	74.4	94.2	71.6	98.0	88.6	105.7

Table 5.2 Weight Breakdown of a 3.0m High, 0.20m Thick Transition Piece

Structural Component	Dimension	Weight
Cone	Base Outer Diameter 5.7m, Top Outer Diameter 5.0m, Thickness 0.2m, Height 3.0m	79.2tons
Truss	Cross-section: Outer Diameter 0.4m, Thickness 0.02m; Axial Length: 6.1m each	4.48tons
Lattice Connector	Cross-section at Connection: Outer Diameter 0.9m, Thickness 0.04m; Axial Length: 1.0m; Cone Connector: Base Diameter 0.9m, Height 1.0m.	10.2tons

5.3 Model selection

To select a suitable model among various designs, modal analysis and structural stress condition under simulated yaw moment load of these designs is computed to provide a first-order comparison among these different models. Selection of the yaw moment as a reference load among the others is based on result from previous analysis in Table 4.10 which shows the yaw moment appears to be one of the most critical loads for the transition piece. The same yaw moment is applied here as in the preliminary analysis stage where the magnitude and direction of the yaw load is referred to Figure 4.39 & Table 4.6.

Modal analysis indicates all the designs with varying heights and cone thicknesses have similar properties. Since the same boundary condition is applied for all the models (Table 4.5), a lighter design will normally render a model of larger natural frequencies. Among the designs in Table 5.3, the 1st translational frequency spans from 1.54Hz to 2.13Hz and the 1st torsional frequency ranges between 3.36Hz and 5.25Hz. On the other hand, all higher order modes of these models refer to cone buckling. The first 12 eigen modes of Model 3-20 are illustrated in Figure VII.1 in Appendix VII.

Table 5.3 Modal Analysis of Varying Transition Piece Designs

Model Index	3-10	3-15	3-20	4-10	4-15	5-10	6-10
1 st Translational Frequency (Hz)	2.13	1.77	1.55	1.87	1.55	1.58	1.54
1 st Torsional Frequency (Hz)	5.25	4.72	4.53	4.40	4.00	3.79	3.36
Higher Order Modes (Up to the 12 th Mode)	Cone Buckling						

Table 5.4 Structural Response of Varying Transition Piece Designs under Yaw Moment

Model Index	3-10	3-15	3-20	4-10	4-15	5-10	6-10
Weight Excluding Lattice Connectors (tons)	44.4	64.2	84.0	58.0	84.4	71.8	85.5
Maximum Stress (MPa)	1282	824.2	562.1	1331	748.1	1297	1261
Max. Stress Location	Cone Top Edge	Base Connection Points with Lattice Substructure	Base Connection Points with Lattice Substructure	Cone Top Edge	Base Connection Points with Lattice Substructure	Cone Top Edge	Cone Top Edge
Max. Structural Deflection (°)	7.5	3.9	2.6	8.0	4.0	8.4	7.5
Comment	For all the designs, maximum stress situation happens at time point of 271.1s when the yaw moment reaches its peak positive value (Figure 4.46).						

As for structural stress condition under the yaw moment load, analysis result shows a relatively wider range. First of all, it can be easily seen that the increase of the cone thickness has a significant beneficial effect on the stress condition under the yaw moment load. On the other hand, influence from the varying heights is not regarded as significant at all. For all the designs with cone thickness of 100mm, maximum stress happens at the cone top edge where the yaw moment is applied. However, for thicker designs of 150mm and 200mm, the most critical regions are shifted to the base connection points of the transition piece. It therefore proves that there is not much

specific demand to maintain a very high design whereas it is more meaningful to design a sufficiently thick model, though at the cost of more material input and perhaps a more difficult manufacturing process. Two 3m-high models are finally deserving further consideration based on compromise between the cost and the structural performance. The final one is focusing on the 3-20 model because of its significantly preferable structural performance under the yaw moment load, which is shown to be one of the most critical loads for transition piece from preliminary analysis

5.4 Functional fulfillment

As for functional requirements of transition piece, yaw bearing connection and the arrangement of the power transmission cable are among the major challenges. As described in Para. 3.2.1, theoretically, power transmission cable is possible to be directed from the nacelle assembly through the transition piece and then into one of the lattice legs (Figure 5.6), though many difficulties have to be solved for the realization of this ideal method. Practical experience still applies external equipment for the coverage and protection of power transmission cable (Figure 3.4). Whichever method is going to be used, the cable inside the transition piece will mostly require a loop for twisting. For the transition piece design here, there provides sufficient space to allow for the cable twisting loop. The sufficient space inside the transition piece also allows for arrangement of climbing stairs for personnel access.

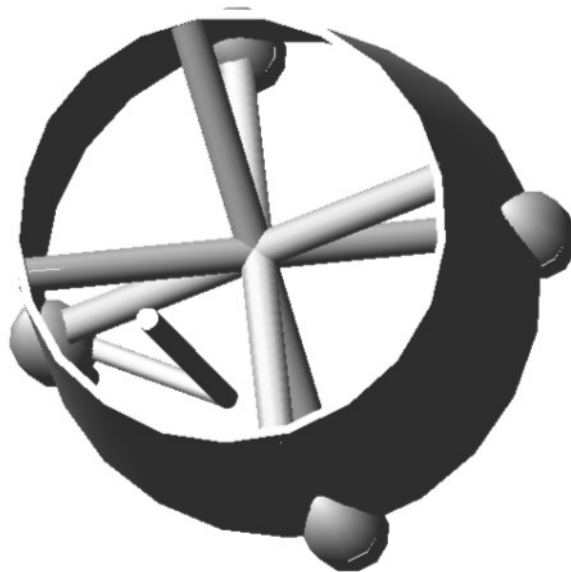


Figure 5.6 Power Transmission Cable inside the Transition Piece

As for connection with the yaw bearing, Figure 5.4 provides the principal method. Detailed connection method in terms of the type of bolting and whether or not an addition of specific connection flange will be required depends on the type of yaw bearing to be used, etc.

5.5 Load analysis

Load analysis of transition piece structural model is the main focus of this thesis. Based on load analysis results during the preliminary design stage, the type of loads to be applied on this final transition piece model will majorly stay the same. Table 5.5 includes description of loads to be analyzed for the final design of transition piece

Final Design of Transition Piece
Lattice Tower Design of Offshore Wind Turbine Support Structures

model 3-20. Various load cases in combination of the loads in Table 5.5 are described in Table 5.6.

Table 5.5 Load Conditions on Final Transition Piece Design (Coordination refer to Figure 4.6)

Load	Magnitude	Direction	Comment
Rotor Nacelle Assembly Weight	350×9.8 kN	-Z	Act on top edge of transition piece.
RNA Eccentric Moment	921.2 kN·m	Varying with rotor axis direction	Act on top edge of transition piece.
Rotor Thrust	$T = \frac{1}{2} C_T \rho_{air} A U_{\infty}^2$ (Eq. 3-4)	Refer to load case	Simulated time series of thrust load is applied at different directions on transition piece model.
Hydrodynamic Load	$f = \frac{1}{2} \rho_{water} C_D D u u $ $+ \rho_{water} C_M A \frac{du}{dt}$ (Eq. 3-6)	Refer to load case	Hydrodynamic load is applied in form of acceleration time series at transition piece base in various load cases.
Drive Train Vibration			Probability of resonance should be avoided during design and selection of the drive train system.
Rotor Torque	$\Delta Q = 4 \rho_{air} \pi u_p \Omega r_b a' (1-a) r_b^2 \Delta r_b$ (Eq. 3-11)	Refer to load case	Simulation result from HAWC2 is employed to be applied on transition piece model.
Yaw Moment	Depending on wind condition and rotor dynamics, especially cross wind conditions.	+Z	Simulation result from HAWC2 is employed to be applied on transition piece model.

Table 5.6 Load Cases for Final Transition Piece Analysis

Load Case	Description of Situation	Comment
RNA	At rest or out of operation	
RNA + Thrust + Torque	Operation under aero load	Two cases of varying wind directions
RNA + Thrust + Torque + Hydro	Operation under aero and hydro loads	Only 10m wave height is considered. Differing cases of varying directions of wind and wave loads
RNA + Thrust + Torque + Yaw	Operation under aero load with yaw motion	Two cases of varying wind directions
RNA + Thrust + Torque + Yaw + Hydro	Operation under aero and hydro loads with yaw motion	Only 10m wave height is considered. Differing cases of varying directions of wind and wave loads

5.5.1 RNA load

Under the RNA load, structural stress condition is shown in Figure 5.7. It can be seen that compared to the preliminary designs (Para. 4.3.2), stress condition of the final transition piece design has been improved much. Maximum von Mises stress is only 9.34MPa at the bottom connection joints between the transition piece and the lattice structure, if only the RNA weight is considered. When the rotor and nacelle weight induced moment is included, maximum stress reaches 20.2MPa which occurs at the

upper edge of the cone where this moment load is applied. Structural deformation under the RNA load is negligible.

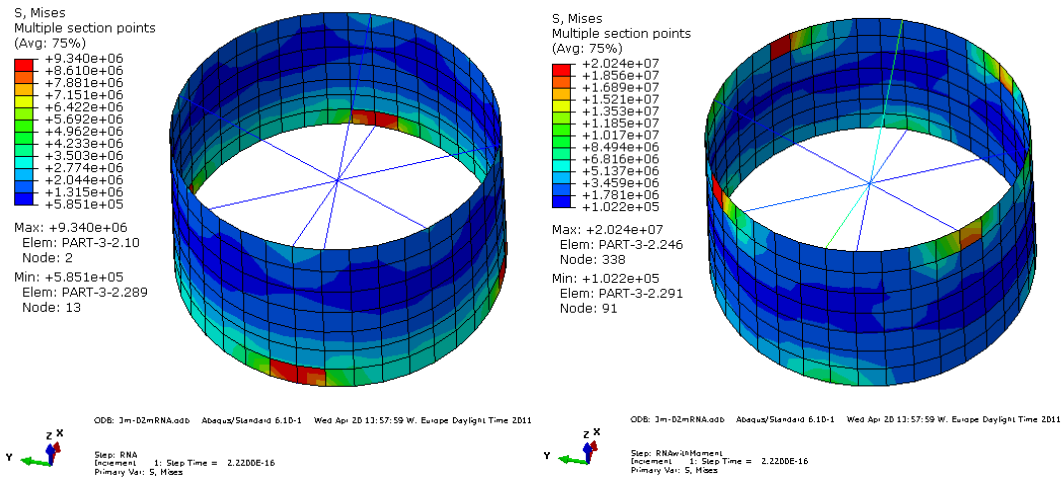


Figure 5.7 Stress Condition under RNA Load

Although maximum stress condition under the RNA load is moderate, it can be clearly seen that the induced moment by the imbalance of the mass center of the nacelle and rotor has an obvious negative effect on the stress condition of the transition piece. It is thus meaningful for this moment to be possibly eliminated through a proper design of the rotor and nacelle mass distribution. To solve this problem, if the below condition is met, there will be no eccentric moment acting along the yaw axis due to the rotor and nacelle gravity load. This issue can be taken care of during the design of the turbine.

$$M_{rotor} \times L_r = M_{nacelle} \times L_n \quad (5-1)$$

where M_{rotor} and $M_{nacelle}$ are the masses of the rotor and the nacelle assembly and L_r and L_n are the respective moment arms to the yaw axis.

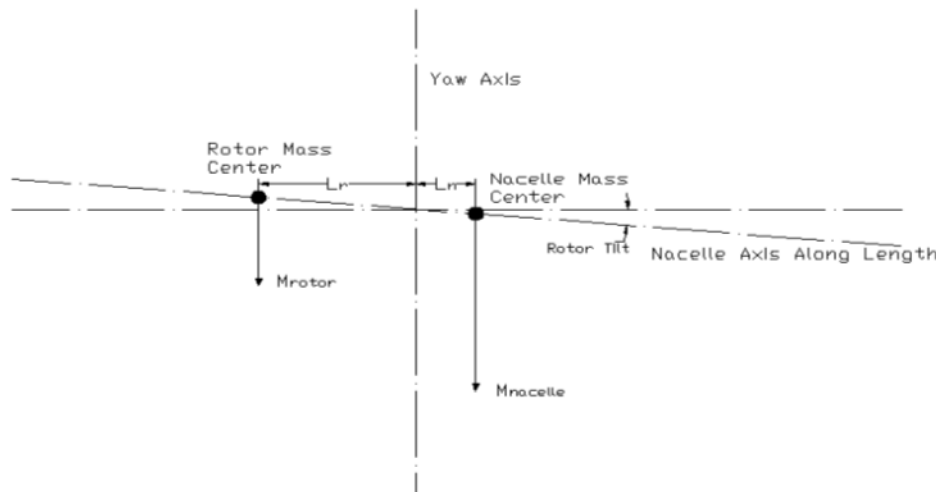


Figure 5.8 Rotor and Nacelle Mass along Yaw Axis

In the analysis here and the following section, the eccentric moment of RNA is still included to provide results on a more conservative basis.

5.5.2 Operation under aero load

For this case rotor thrust and torque loads are applied on the transition piece model to assess its performance under the aerodynamic load. Applied rotor thrust is under normal turbulent wind with 24m/s mean wind speed and 15.73% turbulence intensity (Figure 4.16) and rotor torque is based on the same wind model with 15.73% turbulence intensity but at a slightly lower mean wind speed (Figure 4.31). Identical wind model could be used to generate simulated rotor thrust and torque. However, the slightly different mean wind speed used here is regarded as negligible for the purpose of assessing transition piece dynamic performance.

In the first analysis, the incoming wind direction is from +Y direction (Figure 5.9) which shares axis with two truss components inside the transition piece. Maximum structural stress is found to occur at time point 276.5s when the rotor torque reaches its peak value (Figure 4.37). Critical stress regions are at the diagonal corners on the upper edge where there is no truss component supporting the cone edge. However, maximum stress of 201.8MPa is reduced much compared with preliminary design case. Time series of structural von Mises stress at critical element during the simulation period is shown in Figure 5.11. Stress condition is in general in phase with rotor torque load which shows the dominating effect from the torque load.

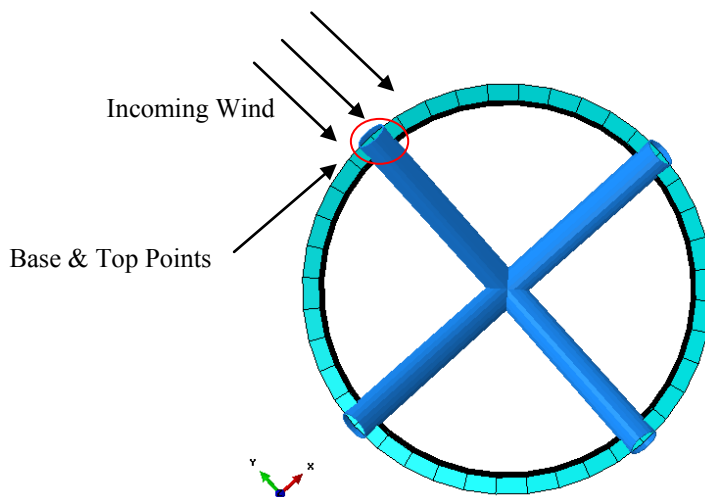


Figure 5.9 Illustration of Incoming Wind Direction under Aero Load Case

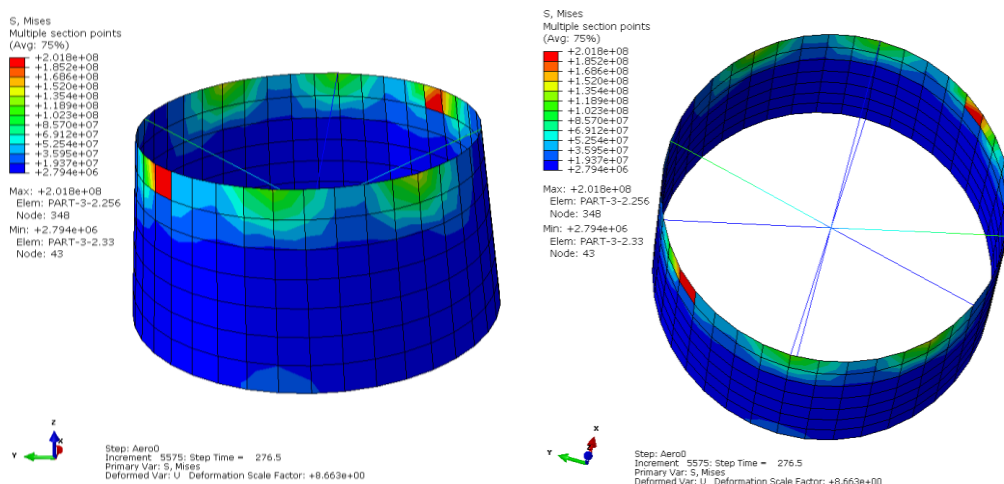


Figure 5.10 Structural Stress Condition at Time Point of Max. Stress under Thrust & Torque Loads

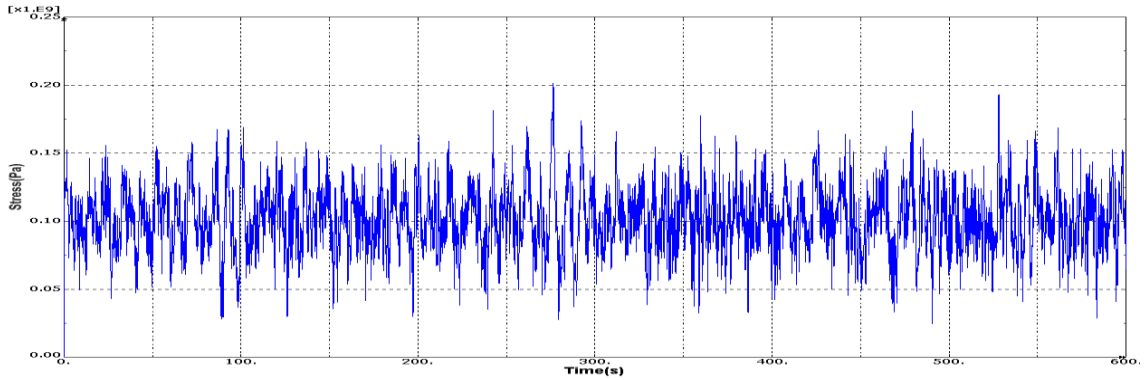
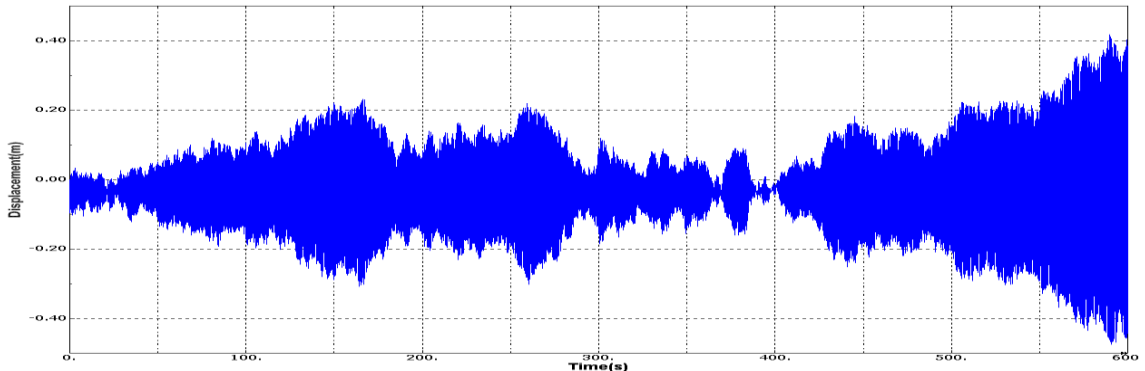
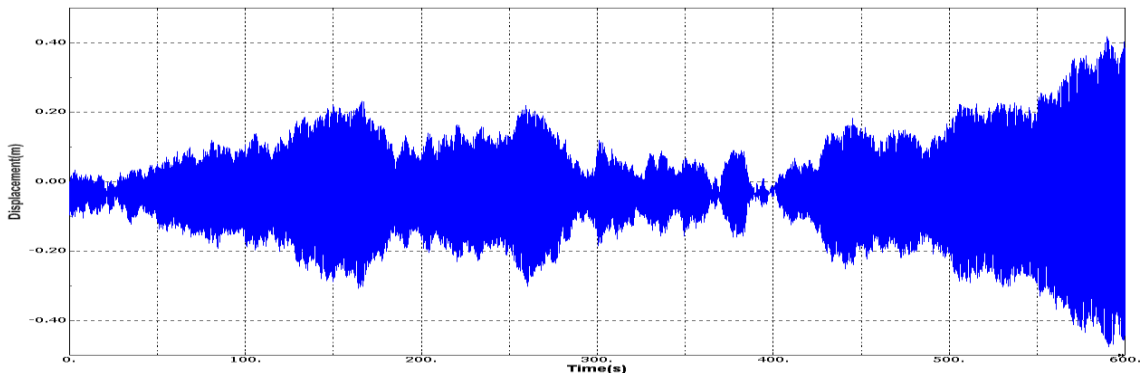


Figure 5.11 Time Series of Stress at Critical Region under Thrust & Torque Loads

As for structural deflection under this load case, vibration of the base point and top point in the incoming wind direction (Figure 5.9) is shown below. Maximum vibration amplitude reaches $\pm 0.5\text{m}$ whereas the structural deflection within the transition piece itself is negligible, because of its small size and its rigid body characteristics.



(a) Displacement at Transition Piece Base



(b) Displacement at Transition Piece Top

Figure 5.12 Time Series of Transition Piece Response under Rotor Thrust and Torque Loads

Compared with analysis in the preliminary designs, it can be explained here that the applied boundary condition which is based on analysis of lattice support structural stiffness has a decisive influence on the vibration magnitude of the transition piece whereas on the other hand, the trend of vibrational displacement time series is influenced more by the model of the transition piece itself (Figure 4.17, 4.19 & 5.12). $\pm 0.5\text{m}$ vibrational magnitude under the applied rotor thrust is regarded as significant and therefore the bending stiffness of the lattice support structure is preferred to be enhanced in order to reduce the magnitude of vibration under rotor thrust load.

Final Design of Transition Piece
Lattice Tower Design of Offshore Wind Turbine Support Structures

For the second analysis case, the incoming wind direction is changed to come from 45° between +Y & +X direction (Figure 5.13) whereas all the other load conditions are kept the same. This case is to explore the sensitivity of transition piece to varied load directions. Maximum structural stress is found to occur at time point 276.5s when the rotor torque reaches its peak value (Figure 4.37). Critical stress regions are again at the diagonal corners on the upper edge where there is no truss component supporting the cone edge. However, for this angled case, maximum stress reaches 239.4MPa which is 19% higher than the previous unangled case. Therefore, the transition piece model shows a certain degree of sensitivity to the aero load direction, which is mostly because of the nonuniform alignment of the inner truss system. Time series of structural von Mises stress at critical element during the simulation period is shown in Figure 5.15. Stress condition is also in general in phase with rotor torque but the magnitude of the stress is increased comparing Figure 5.11 & 5.15.

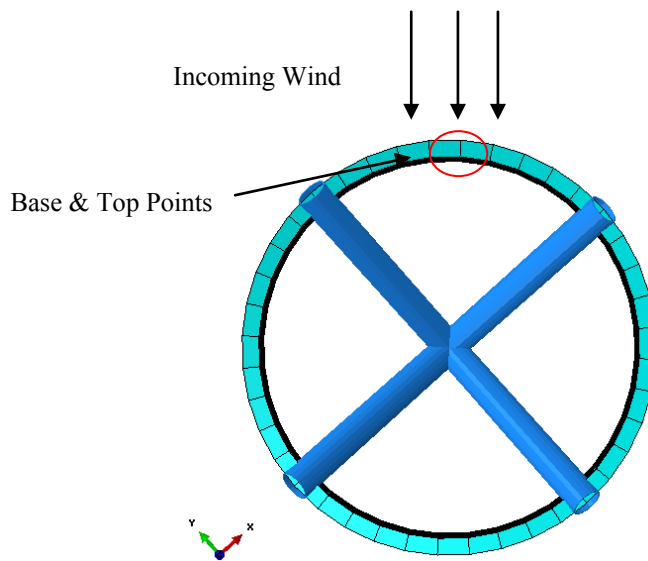


Figure 5.13 Illustration of Incoming Wind Direction under Angled Aero Load Case

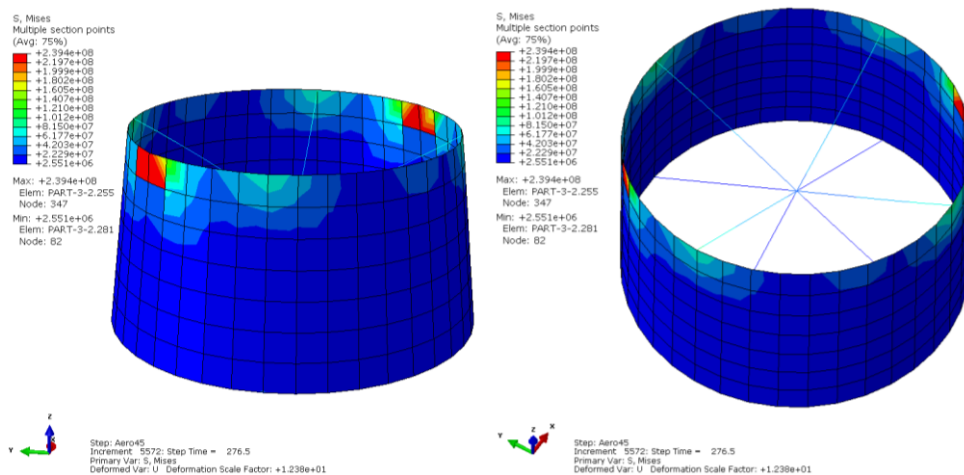


Figure 5.14 Transition Piece Stress Condition at Time Point of Max. Stress under Angled Thrust & Torque Loads

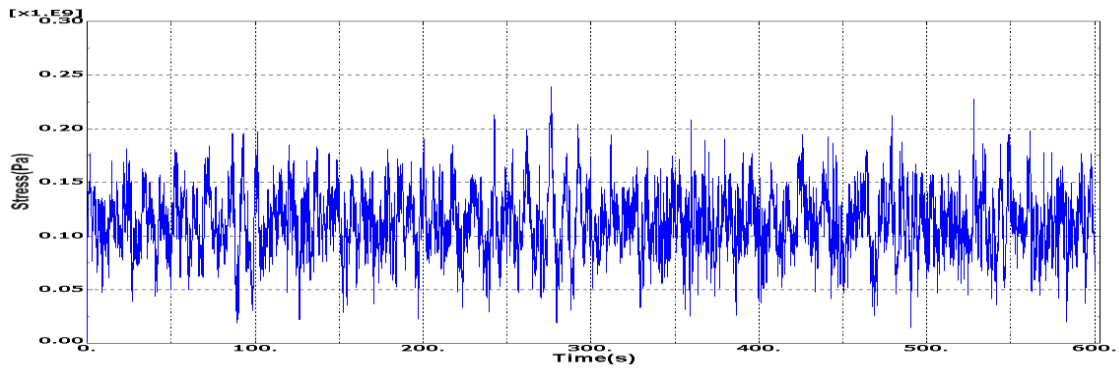


Figure 5.15 Time Series of Stress at Critical Region under Angled Thrust & Torque Loads

As for structural deflection under this load case, transition piece vibrates along the incoming wind direction Figure 5.16. Maximum vibration amplitude reaches $\pm 0.4\text{m}$ which is slightly reduced compared to the previous case. The reason for this reduction is that the overall bending stiffness at this angled direction is increased to $\sqrt{2}$ times of the original value. The trend of the vibrational displacement time series is in general the same as the unangled case (Figure 5.12 & 5.17). Due to the existence of rotor torque, vibrations at X and Y directions are not exactly identical both in phase and in magnitude.

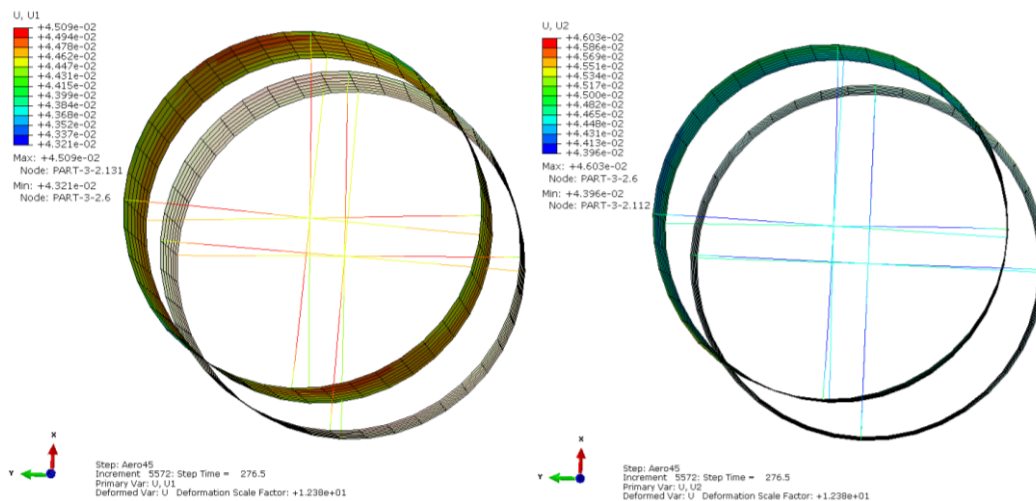


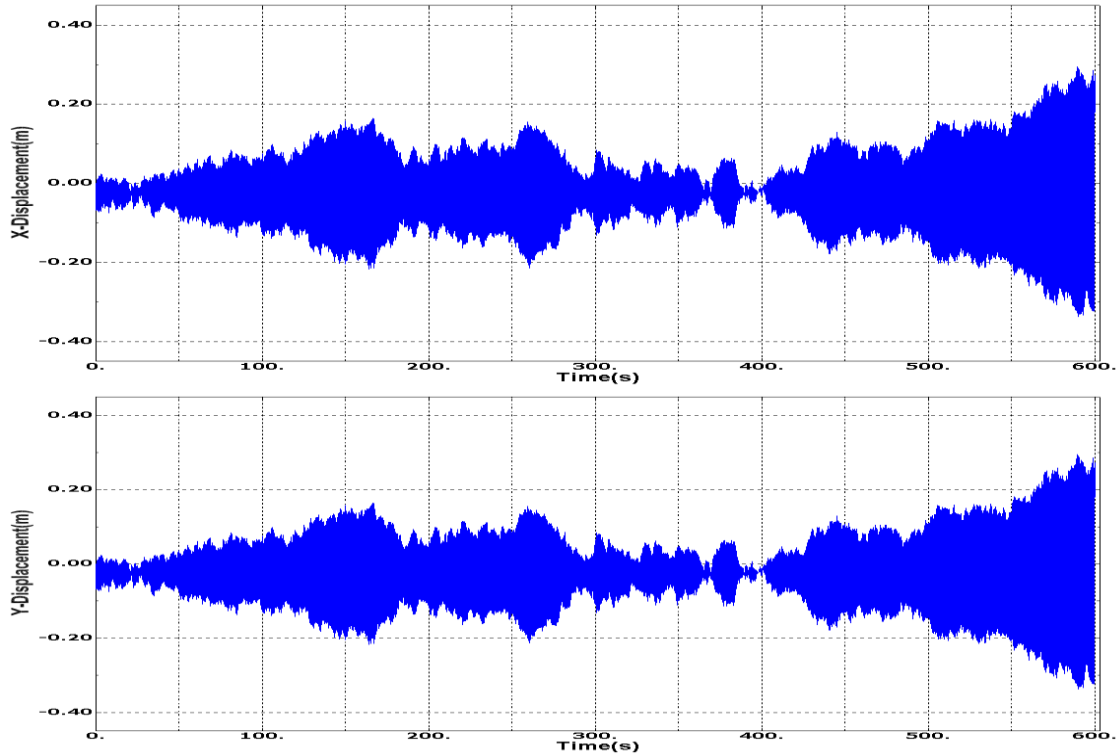
Figure 5.16 Transition Piece Vibration under Angled Thrust & Torque Loads

As previously stated, vibration of the transition piece under the applied thrust load reaches a magnitude that is regarded as too significant for normal operation. Resulted magnitude of vibration has to be influenced by the applied boundary condition. Parameters for the applied boundary condition are based on analysis of various lattice support structure models in Chapter 3 (Table 3.4). In order to further explore the influence from this applied boundary, the same thrust load is applied on a lattice support structure model (Table 3.5 stiff). Time series of displacement and acceleration at the lattice top is shown in Figure 5.19.

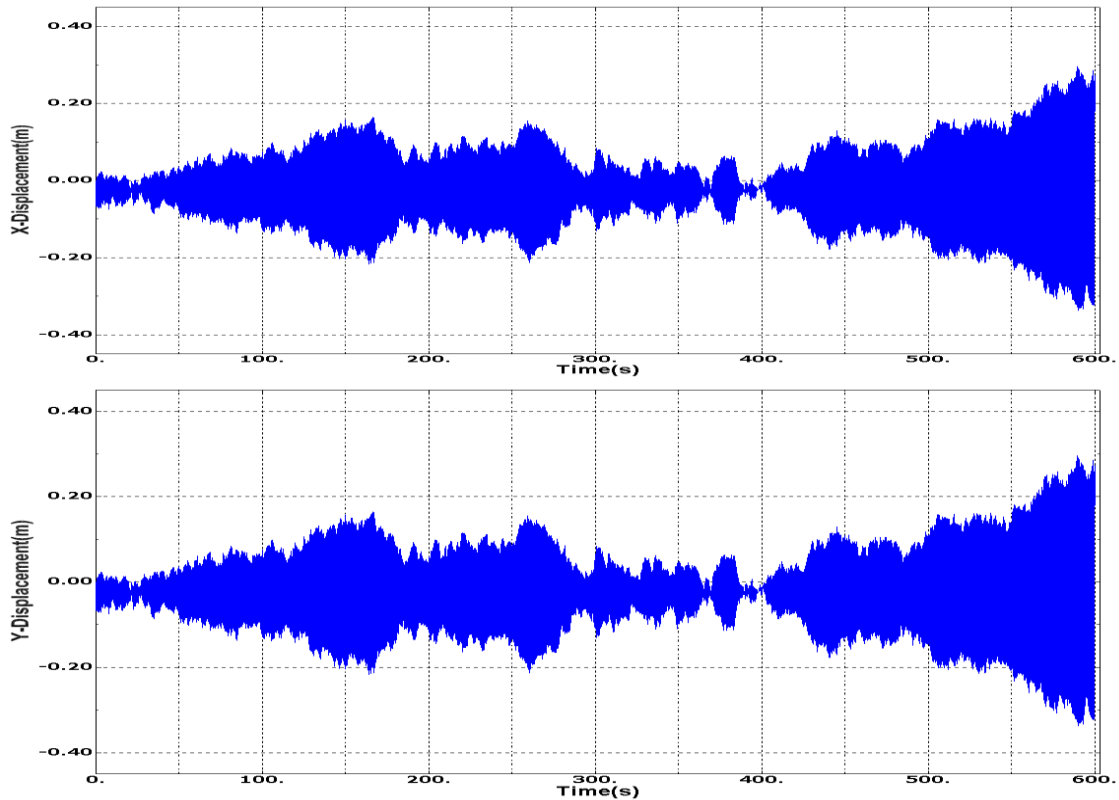
Comparing response of transition piece and that of the lattice support structure under the same thrust load, it can be seen that vibration of the transition piece is influenced by the applied boundary condition. However, vibration of transition piece includes higher frequency components which should come from the eigen frequency of the transition piece itself. Vibration magnitude of lattice structure ($\pm 0.3\text{m}$) is found to be less than that of transition piece ($\pm 0.5\text{m}$). One reason for this could be the less conservative value of

Final Design of Transition Piece
Lattice Tower Design of Offshore Wind Turbine Support Structures

bending stiffness used ($8.0E+6$ N/m) compared to the actual bending stiffness of the lattice structure ($8.76E+6$ N/m). In addition, the simplified spring boundary condition which only takes the first mode of the lattice support structure and thus loses its higher modes strength might account for another reason.



(a) Displacement in X & Y Direction at Transition Piece Base



(b) Displacement in X & Y Direction at Transition Piece Top

Figure 5.17 Time Series of Transition Piece Response under Angled Rotor Thrust and Torque Loads

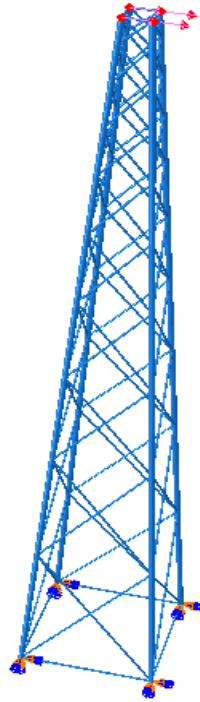
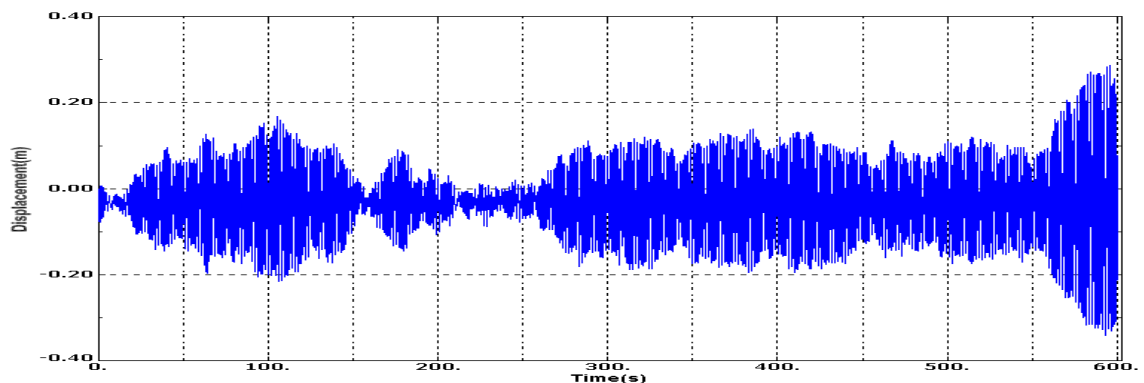
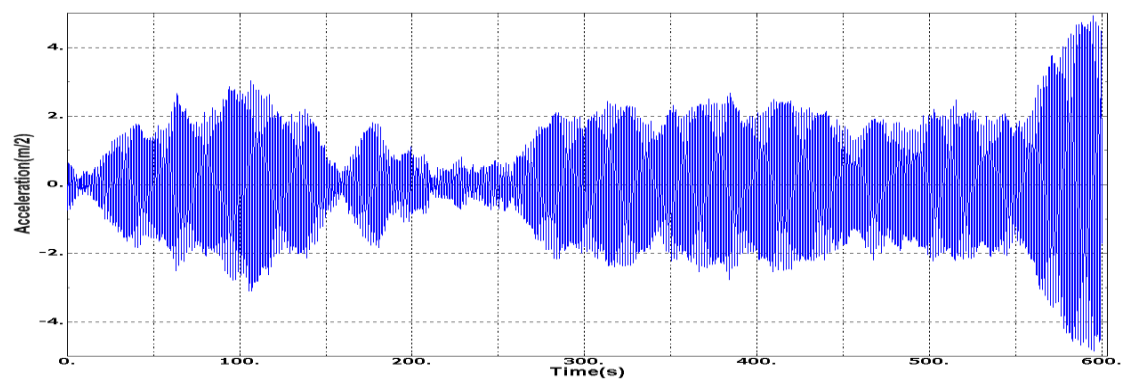


Figure 5.18 Thrust Load Applied on Top of Lattice Support Structure



(a) Displacement at Lattice Top under Thrust Load



(b) Acceleration at Lattice Top under Thrust Load

Figure 5.19 Lattice Structural Response to Thrust Load

5.5.3 Operation under aero load with yaw motion

In this load case, yaw moment load is acting on transition piece along with the previously described rotor thrust and rotor torque. Thrust and torque loads remain the

same as employed in the previous analysis and the applied yaw moment is referred to Figure 4.39. This yaw moment is simulated based on the same normal turbulent wind model with 24m/s mean wind speed, 15.73% turbulence intensity and 20° yaw angle. For the first case, rotor axis is aligned with +Y direction while for the second case rotor axis is aligned at 45° between +Y & +X direction (Figure 5.20).

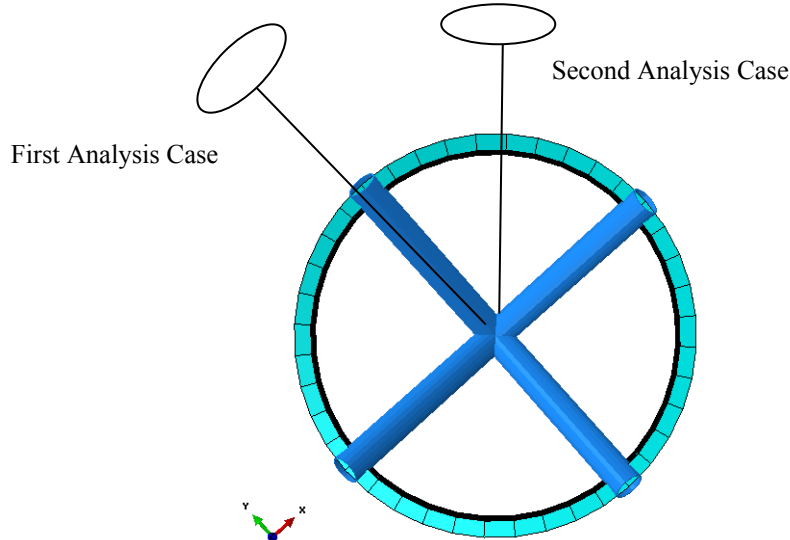


Figure 5.20 Illustration of Rotor Axis Direction

Under the first case, maximum structural stress occurs at time point 271.1s when the yaw moment reaches its peak value (Figure 4.46). Maximum stress of 565.3MPa occurs at the four base connection points. Time series of von Mises stress at the most critical joint is shown in Figure 5.22. It can be seen that stress condition at the joint has a significant vibration in stress magnitude which deserves fatigue analysis. The trend of stress time series is in general in phase with the yaw moment load (Figure 4.39). An enhanced design of the truss system could be expected to possibly reduce the stress condition under the yaw load. Structural deformation under this load case is composed of translational vibration due to rotor thrust and torsional vibrational due to yaw moment (Figure 5.23).

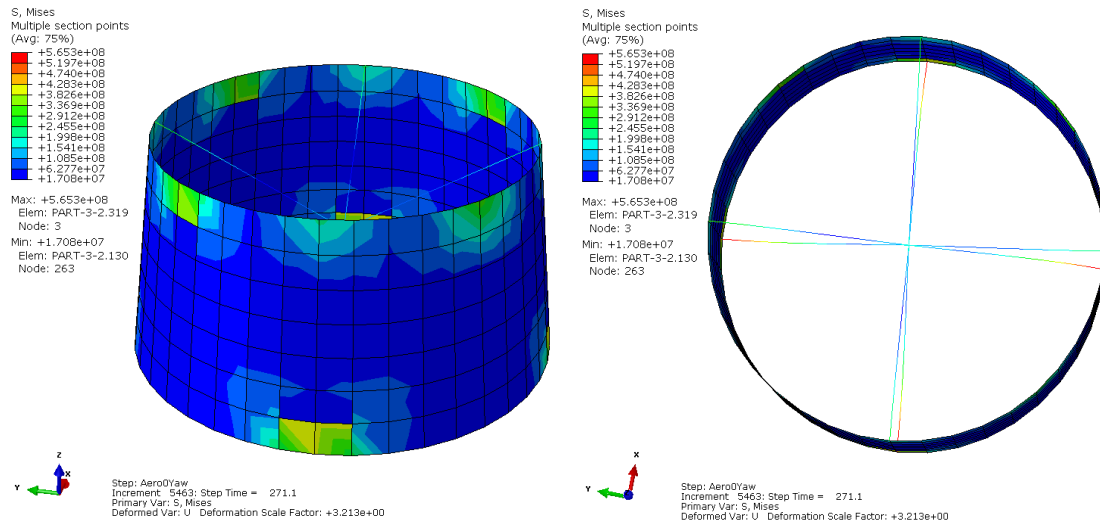


Figure 5.21 Transition Piece Stress Condition at Time Point of Max. under Aero Load with Yaw Motion

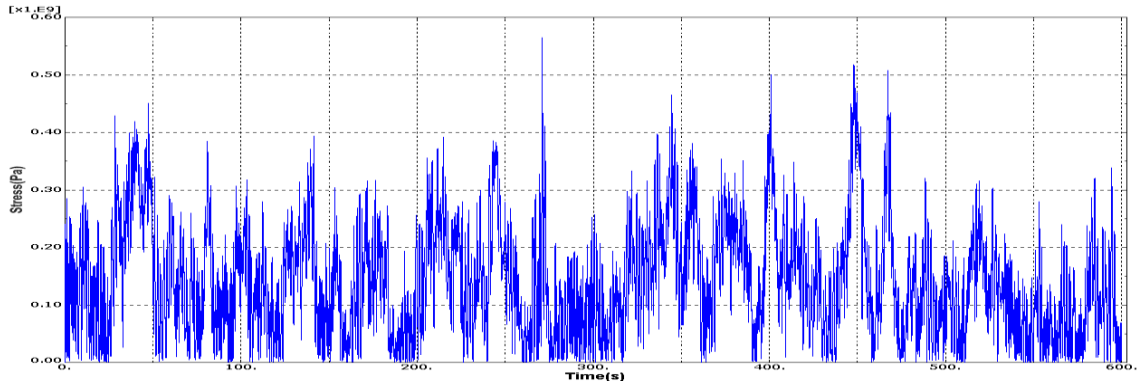


Figure 5.22 Time Series of Stress at Critical Truss Joint under Aero Load with Yaw Motion

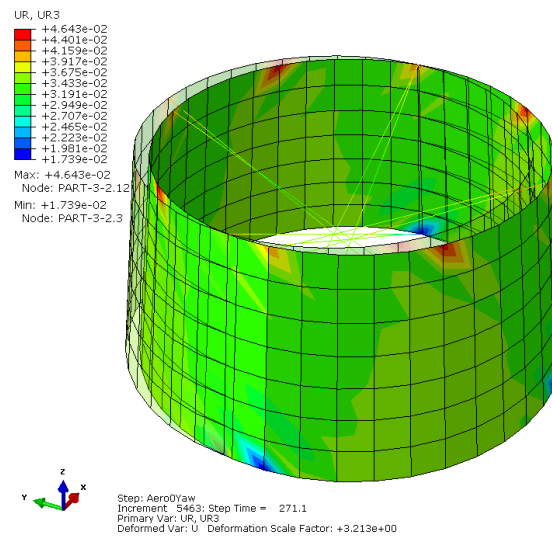


Figure 5.23 Transition Piece Deformation under Aero Load with Yaw Motion

For the torsional vibration due to yaw moment, critical region happens at cone upper edge. Time series of torsional vibration along the yaw axis at critical node is shown in Figure 5.24. Magnitude of vibration ranges from -1.4° to 2.7° whereas the phase of vibrational motion keeps with that of the yaw moment load. As for translational vibration under the thrust load, Figure 5.25 shows displacement time series at X(U1, green line) and Y(U2, blue line) directions. X displacement is caused by the yaw rotational motion which also keeps in phase with the yaw moment load. Y displacement follows the rotor thrust load.

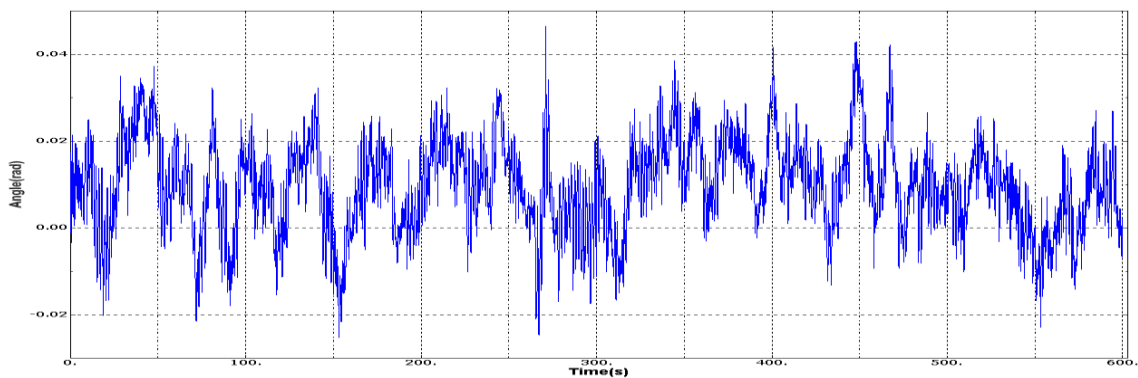


Figure 5.24 Torsional Vibration along Yaw Axis at Critical Node under Aero Load with Yaw Motion

Final Design of Transition Piece
Lattice Tower Design of Offshore Wind Turbine Support Structures

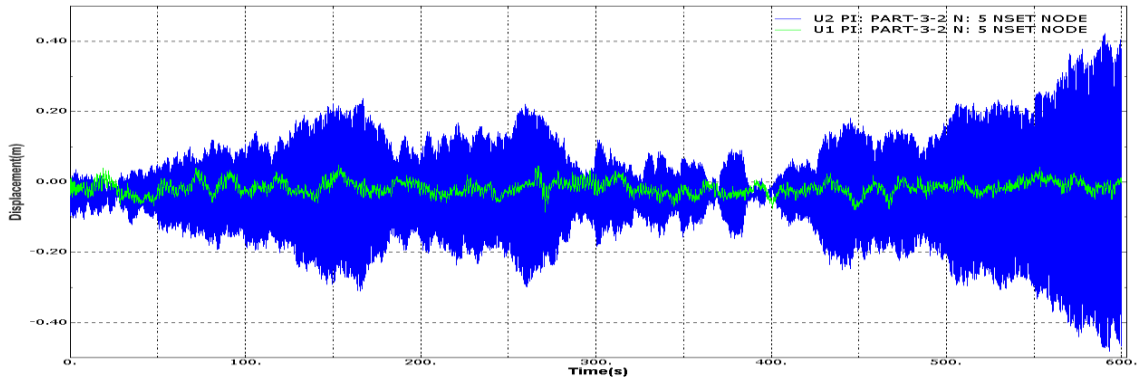


Figure 5.25 Translational Displacement at A Joint Node on Upper Edge under Aero Load with Yaw Motion

The second case will now explore sensitivity of transition piece to aero load direction with yaw motion coupled. For this case, rotor axis is assumed to located at 45° between +Y & +X direction (Figure 5.20). During the entire simulation period, maximum stress condition occurs also at time point 271.1s when the yaw moment load reaches its peak value. Maximum stress reaches 554.5MPa which is almost at the same level with the previous unangled situation. This critical stress condition occurs at the same base connection joint of the cone and the truss component. Time series of stress condition at this joint is shown in Figure 5.27.

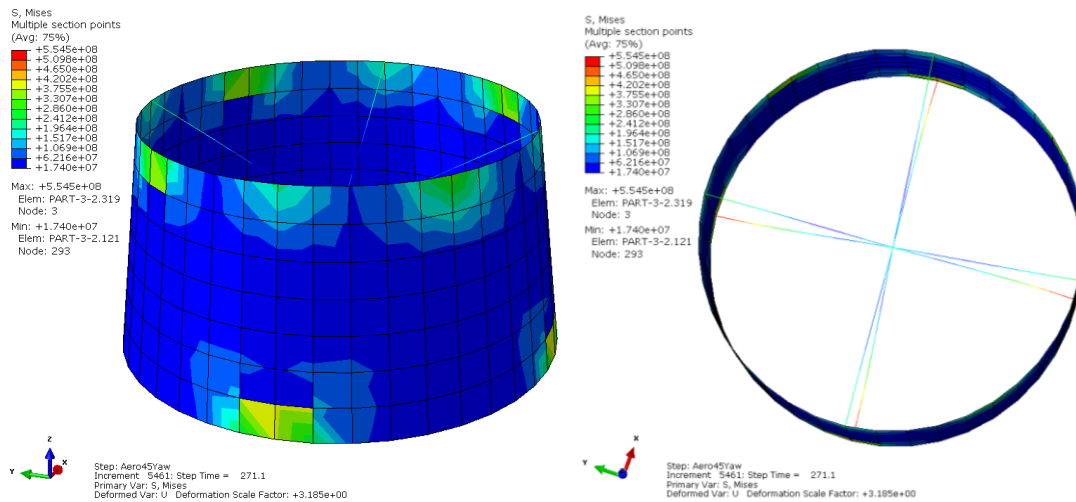


Figure 5.26 Transition Piece Stress Condition at Time Point of Max. under Aero Load with Yaw Motion at Varied Direction

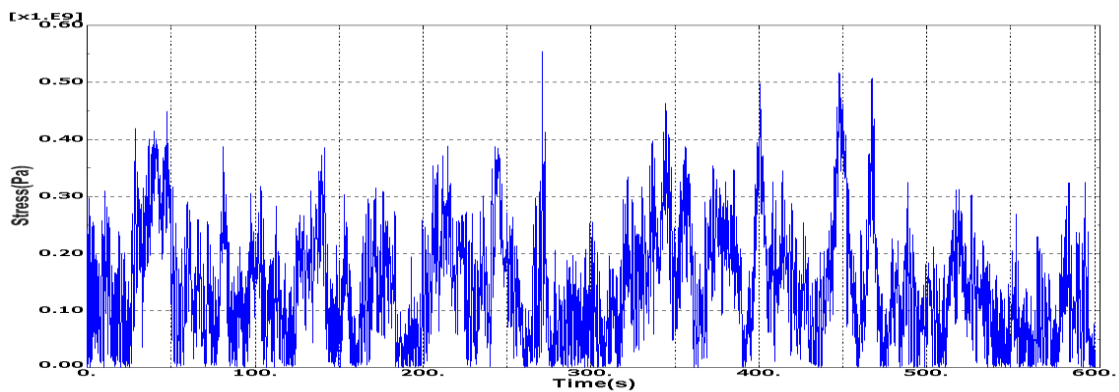


Figure 5.27 Time Series of Stress at Critical Truss Joint under Aero Load with Yaw Motion at Angled Direction

Under this load case, deformation of the transition piece is composed of torsional vibration under yaw moment load and translational vibration at 45° between +Y & +X direction under rotor thrust (Figure 5.28). Torsional vibration time series at critical element is shown in Figure 5.29 which is very close to previous analysis result in Figure 5.24.

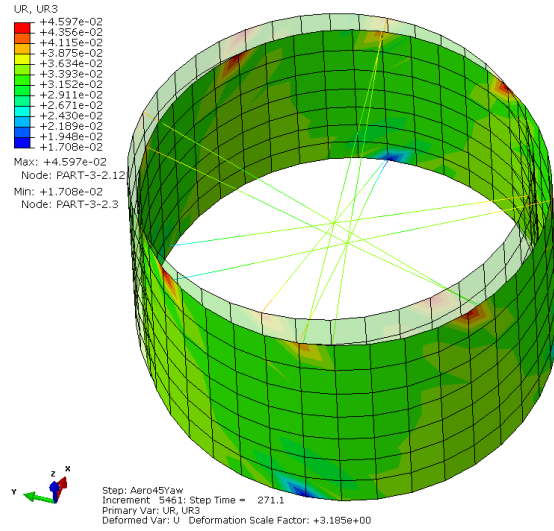


Figure 5.28 Transition Piece Deformation under Aero Load with Yaw Motion at Angled Direction

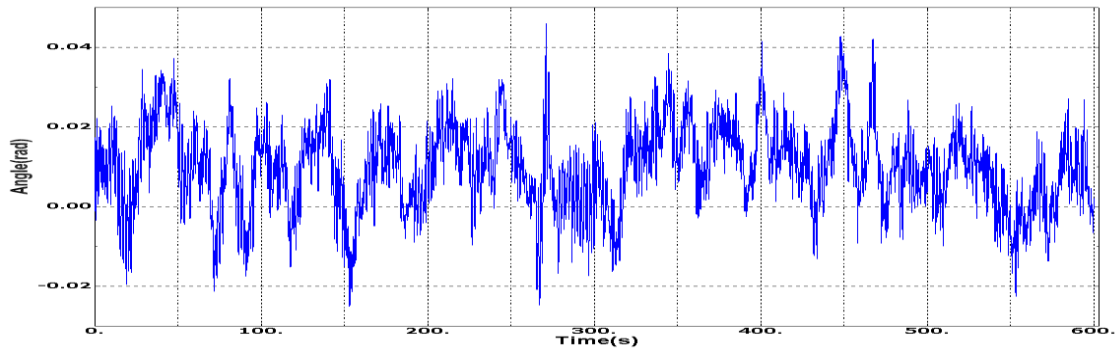


Figure 5.29 Torsional Vibration along Yaw Axis at Critical Node under Aero Load with Yaw Motion at Angled Direction

As for translational vibration under the thrust load component, motion of a node at the thrust load direction on upper cone edge is shown below. Vibration in both X(U1, green line) and Y(U2, blue line) directions are generally identical both in magnitude and phase. The difference should be accounted by the influence from rotor torque and yaw moment's twisting effect.

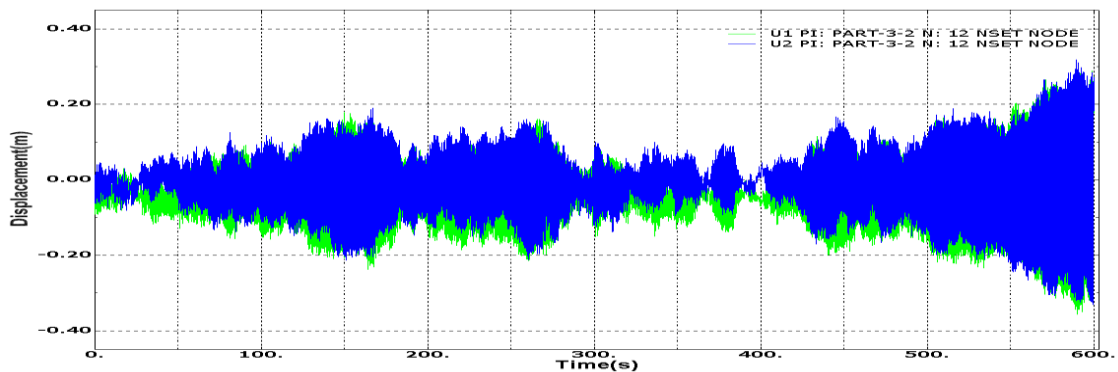
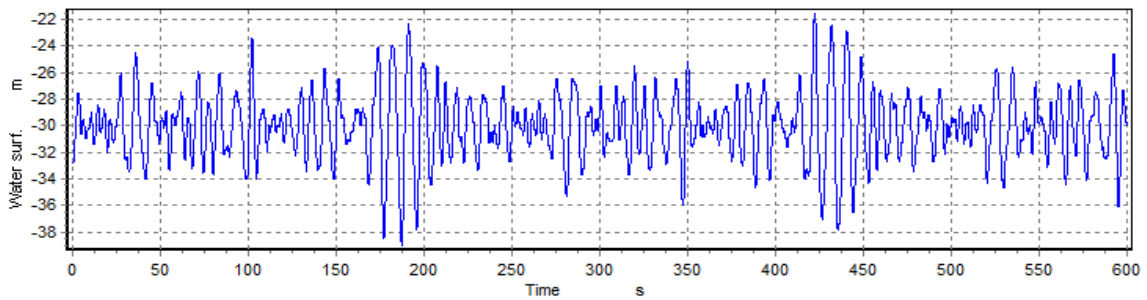


Figure 5.30 Time Series of Transition Piece Response under Aero Load with Yaw Motion at Angled Direction

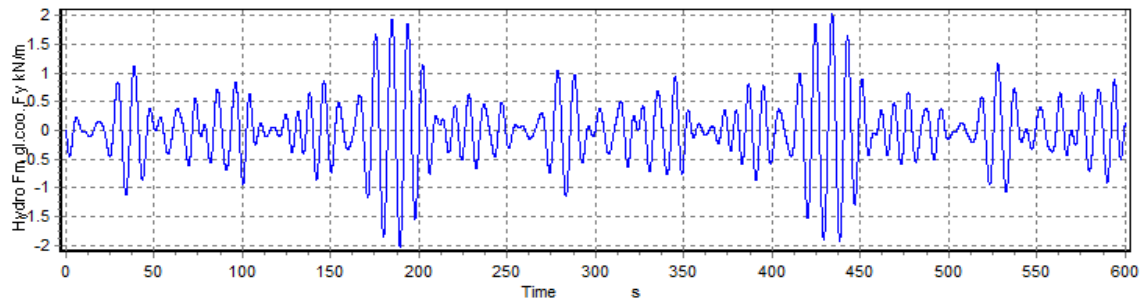
By far transition piece response to aerodynamic loads are investigated. Yaw moment load appears to be the most critical one among all the other loads under various load cases. Transition piece deformation to yaw moment load is not significant; however, its response to rotor thrust reaches a vibration magnitude that deserves much attention for practical purpose. Response of transition piece shows a certain degree of sensitivity to varied load directions, nevertheless, the difference is not beyond expectation. In the following, influence from the hydrodynamic load on the lattice support structure is explored in combination with the above aerodynamic loads.

5.5.4 Operation under aero & hydro load at identical wind wave direction

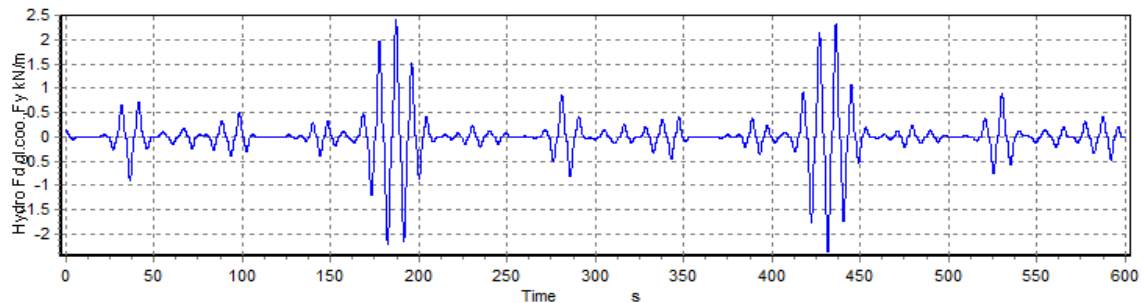
In order to explore transition piece response to coupled aero and hydro loads, 600s time series of hydro load properties is simulated to match the entire aero load simulation period. By experience in the preliminary analysis, 10m high irregular Airy wave with 9s period is generated to compute the hydro load on the lattice support structure and its response. Water surface elevation and the inertia and drag loads at representative point on the submerged part of the lattice support structure are shown respectively in figure below.



(a) Water Surface Elevation for a 10m Irregular Airy Wave (Sea Surface at -30m (Figure 4.22))



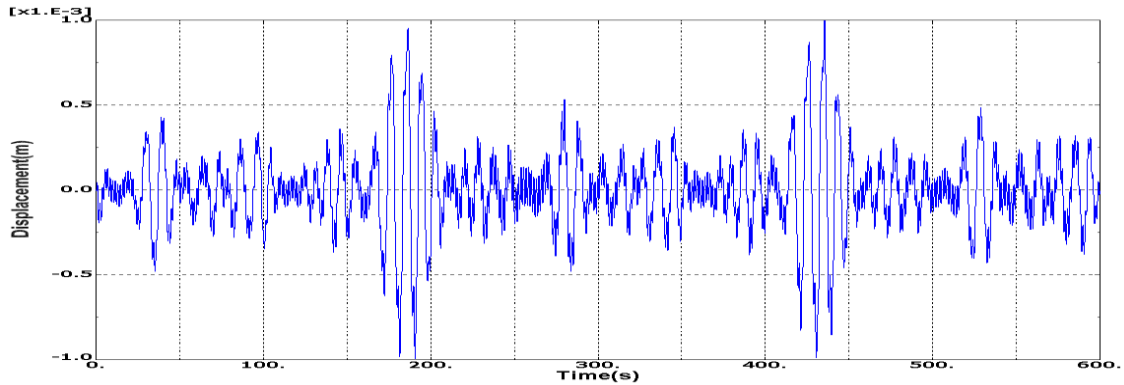
(b) Inertia Force on Lattice Leg



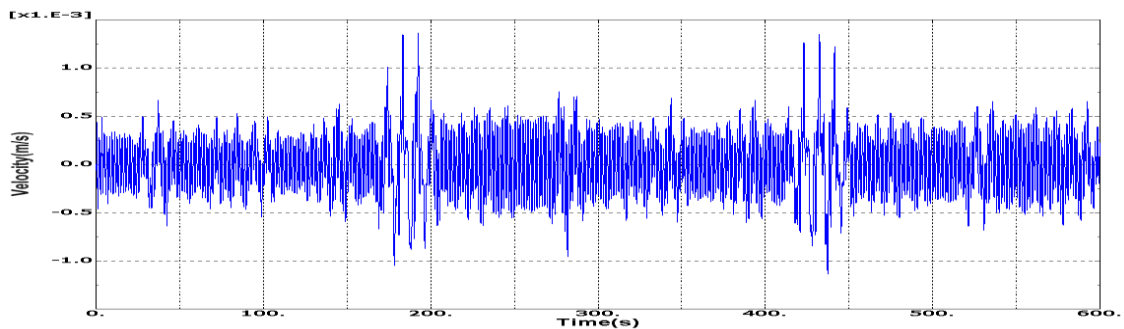
(c) Drag Force on Lattice Leg

Figure 5.31 Water Surface Elevation and Hydro Load of a 10m Irregular Airy Wave on Lattice Leg

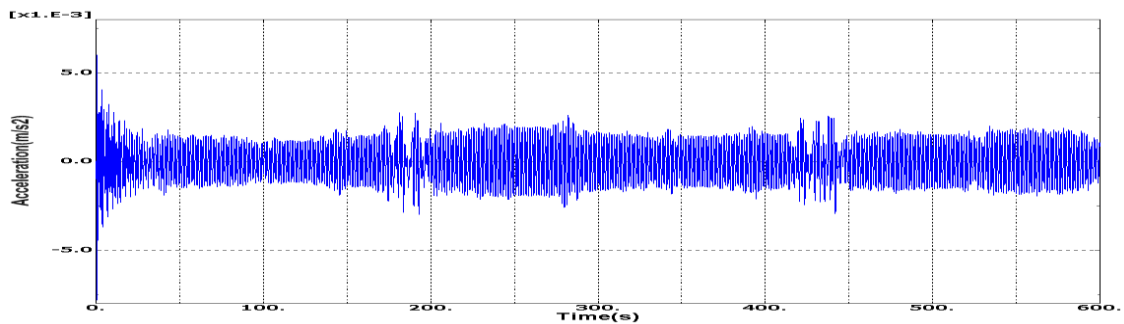
The above hydro load is applied on the lattice support structure and the response of lattice structure top point in form of displacement, velocity and acceleration time series is shown in Figure 5.32. Magnitude of vibration reaches $\pm 1.0\text{mm}$ which generally agrees with the 60s simulation result in previous preliminary analysis (Figure 4.29). Acceleration time series are then applied on transition piece base as a boundary load in combination with the relevant aero loads to investigate transition piece response under combined aero and hydro loads.



(a) Displacement Time Series at Lattice Top under Hydro Load



(b) Velocity Time Series at Lattice Top under Hydro Load



(c) Acceleration Time Series at Lattice Top under Hydro Load

Figure 5.32 Lattice Support Structure Response to 10m Wave Load

In the first case, time series of acceleration at lattice top (Figure 5.32(c)) and time series of dynamic thrust load (Figure 5.19(b)) are applied at the same direction at 45° between +Y & +X direction (Figure 5.33) on transition piece base and top edge respectively, in addition to rotor torque moment on transition piece top edge, to explore the combined effects of hydro load, thrust load and rotor torque on the transition piece structural model. In this case the direction of the incoming wind and wave is thus assumed identical.

Final Design of Transition Piece
Lattice Tower Design of Offshore Wind Turbine Support Structures

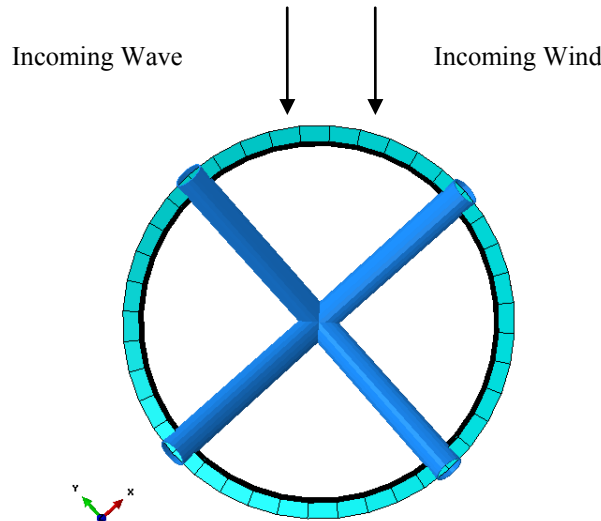


Figure 5.33 Illustration of Identical Incoming Wind & Wave Direction

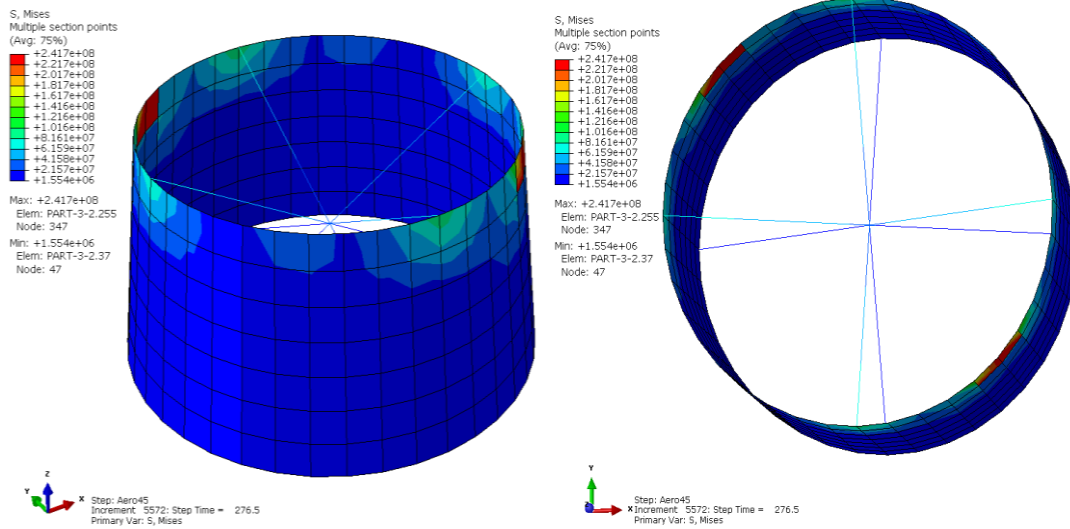
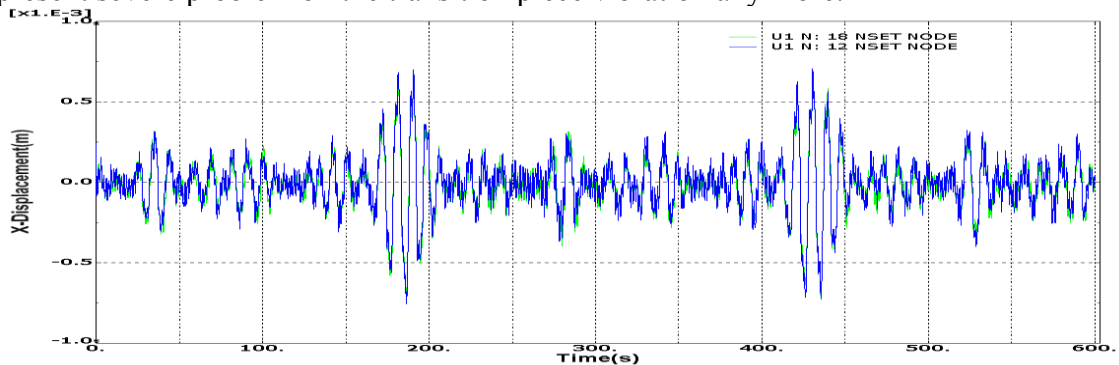
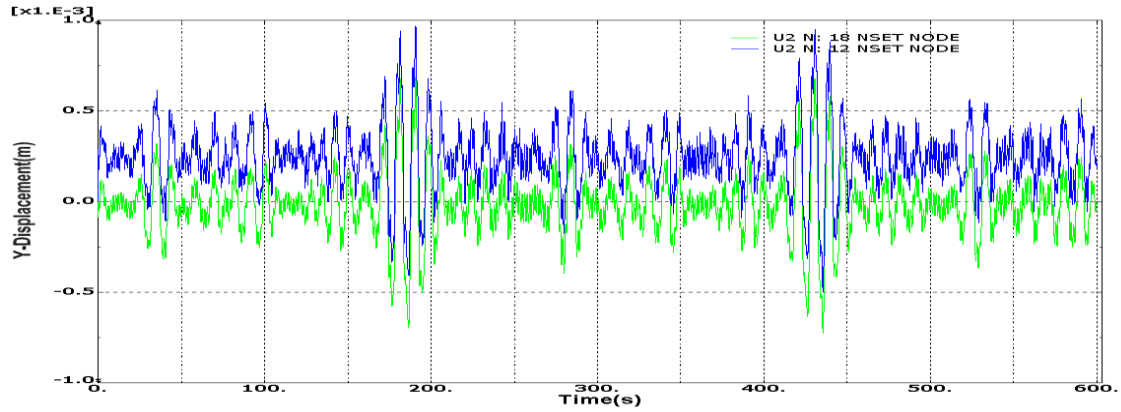


Figure 5.34 Transition Piece Stress Condition at Time Point of Max. under Aero & Hydro Load from Identical Direction

Structural stress condition under this case is almost the same with previous analysis without the hydro load (Figure 5.14). Maximum stress reaches almost the same value and occurs at the same location (Figure 5.34). Displacement under the combined load at the transition piece base and top in X and Y directions is shown in Figure 5.35. Due to the removal of spring system as the boundary, transition piece response is generally following the lattice top response under the hydro load while the rotor thrust does not present severe problem on the transition piece vibration any more.



(a)X-displacement at TP Top(blue) and Base(green)



(b)Y-displacement at TP Top(blue) and Base(green)
 Figure 5.35 Displacement in X & Y Direction of Transition Piece under Combined Aero & Hydro Load at Identical Wind-Wave Direction

With this result, yaw moment load is further applied on transition piece in addition to the hydro acceleration at the TP base and rotor thrust, rotor torque at TP top. Maximum stress situation still occurs at time point 271.1s when the yaw moment load reaches its peak value. Compared with analysis result without the hydro load in Figure 5.26, a vibrating transition piece base due to the hydro load appears to have an effect of easing the structural stress condition with maximum stress reduction by over 30%. In addition, critical stress condition has shifted from the transition piece base connection joints to the upper part accounted by the motion behaviour at the base area. Maximum stress occurs at the upper edge which shows also the influential effect from the torque.

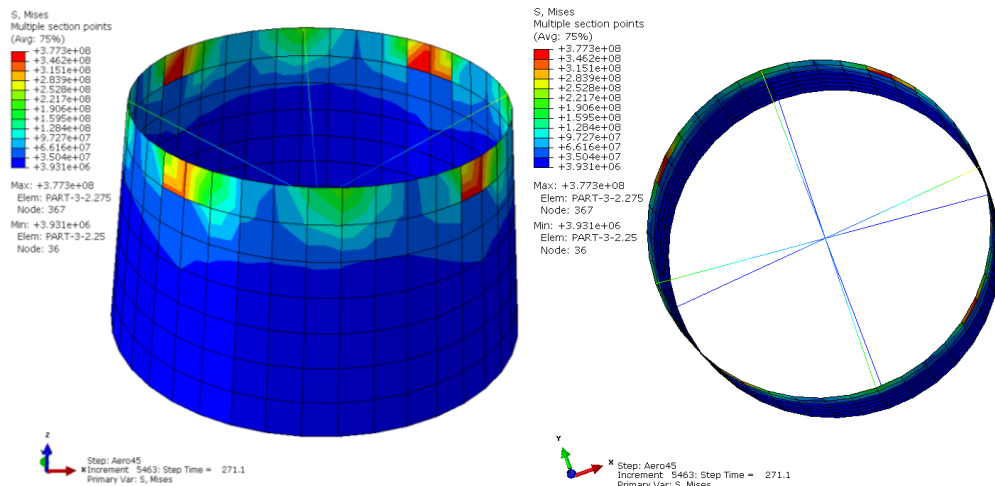


Figure 5.36 Transition Piece Stress Condition at Time Point of Max. under Aero-Hydro Load & Yaw Moment at Identical Wind-Wave Direction

Time series of stress at the critical location under this load case is shown below (blue line) in comparison with the stress at the base connection joint which is found to be the most critical stress location in previous analysis without the hydro influence (green line). The lower part of transition piece has a sharply reduced contribution to the transition piece structural strength and the upper part which is subjected to rotor torque and yaw moment load directly is much more mobilized. Torsional motion along the yaw axis at critical node is shown in Figure 5.38. Magnitude of the rotational motions has also been reduced to range from only -0.4° to 0.8° .

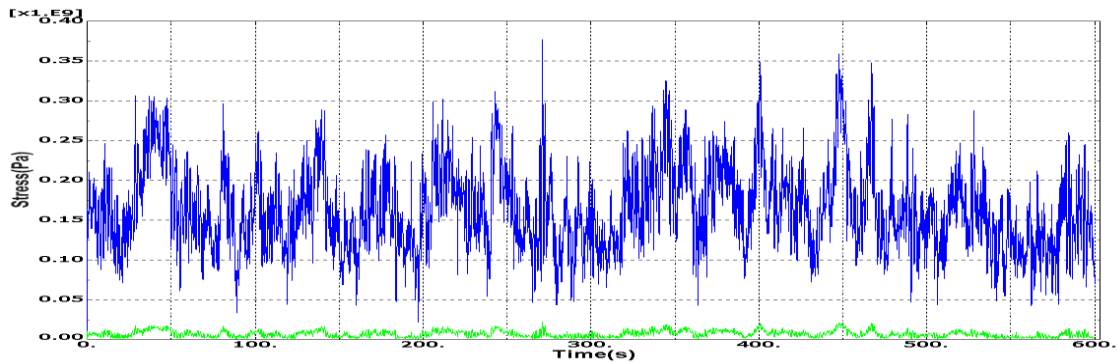


Figure 5.37 Time Series of Stress at Critical Top Edge and Base Joint under Aero-Hydro Load with Yaw Moment at Identical Wind-Wave Direction

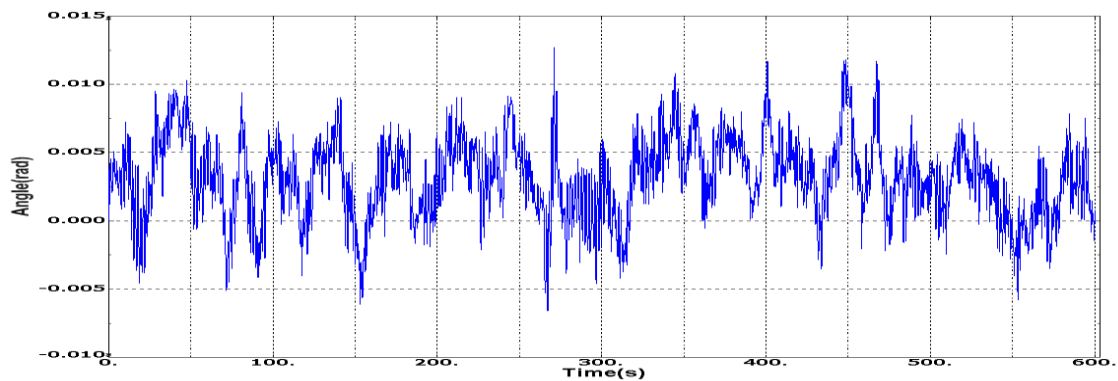


Figure 5.38 Torsional Vibration along Yaw Axis at Critical Node under Aero-Hydro Load with Yaw Moment at Identical Wind-Wave Direction

5.5.5 Operation under aero & hydro load with unidentical wind wave direction

Previous section explores transition piece performance under combined hydro & aero loads with identical incoming wind and wave direction. In reality, the incoming wind and wave directions should have a certain degree of misalignment. The misaligned angle between the wind and wave direction is instantaneously changing in the real offshore environment. In this section, an unrealistic situation with perpendicular incoming wind and wave directions (Figure 5.39) is assumed to investigate transition piece performance under this extreme event.

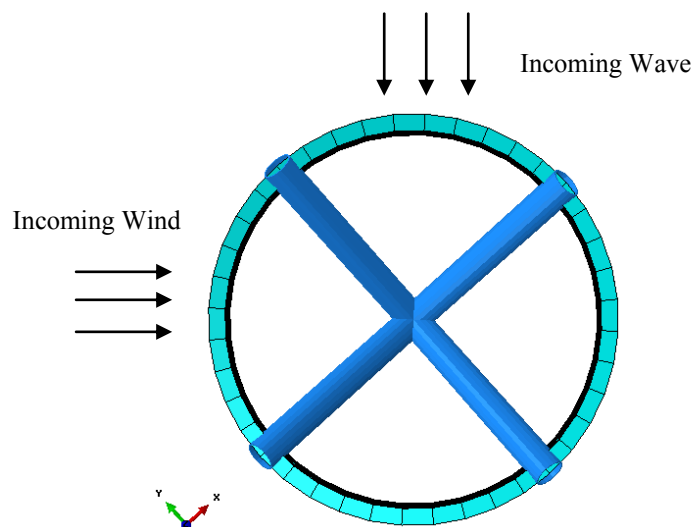


Figure 5.39 Illustration of Perpendicular Incoming Wind & Wave Directions

Final Design of Transition Piece *Lattice Tower Design of Offshore Wind Turbine Support Structures*

In the first analysis case, aero loads include rotor thrust and rotor torque from the incoming wind direction while yaw moment is excluded. As for the hydro load, acceleration response of lattice top under the previously applied 10.0m wave is acting on the transition piece base to simulate the hydro effect on transition piece. Maximum stress condition occurs at time point 276.5s when the rotor torque load reaches the peak value, which agrees with previous analysis without the hydro influence (Figure 5.14).

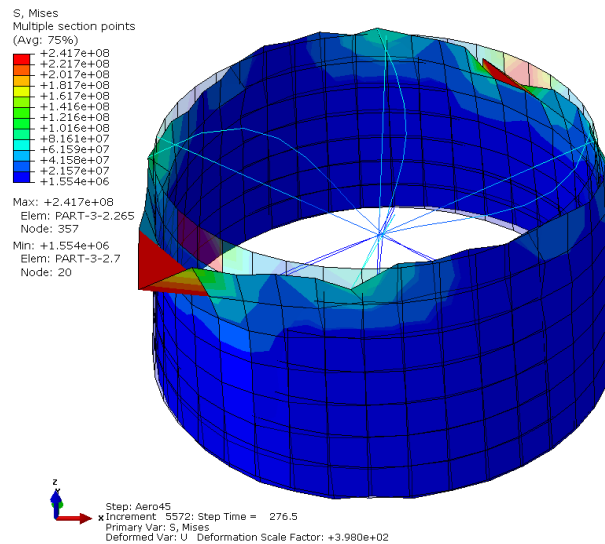


Figure 5.40 Transition Piece Stress Condition at Time Point of Max. under Aero & Hydro Load with Perpendicular Wind-Wave Direction (Transparent Model is the Initial Undeformed Structural Model)

Location of critical stress condition is also at the two sides on the upper edge perpendicular to the incoming wind direction. The dominating effect of rotor torque load is obviously seen and the structure shows obvious tilting deformation under the torque load (Figure 5.40). Time series of stress at critical location is shown in Figure 5.41. As for structural response, transition piece is basically vibrating under the hydro influence while the effect of the rotor thrust is not representing any more.

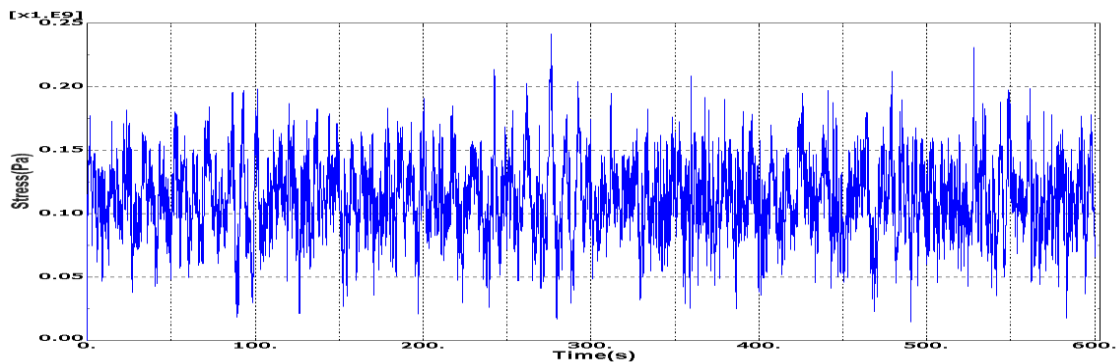


Figure 5.41 Time Series of Stress at Critical Location under Aero & Hydro Load with Perpendicular Wind-Wave Direction

For the second analysis case, yaw moment load is applied on transition piece in addition to the above loads. Maximum stress condition is found to occur at time point 271.1s when the yaw moment reaches its peak value, which agrees well with all the previous load cases that contain the yaw moment load. Maximum stress of 377.3MPa in this case is the same compared with previous case of identical incoming wind and wave direction (Figure 5.36) and reduced by 32% if it's compared with the case without including the

hydro effect (Figure 5.26). Maximum stress occurs on the upper edge of transition piece where all the aero loads are directly acting on.

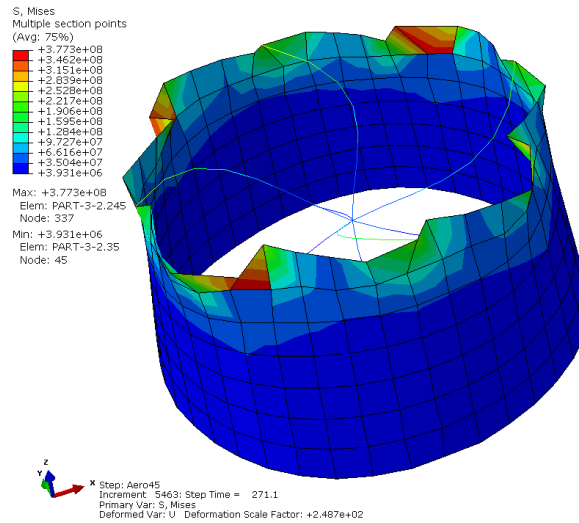


Figure 5.42 Transition Piece Stress Condition at Time Point of Max. under Aero & Hydro Load with Yaw Moment with Perpendicular Wind-Wave Direction (Transparent Model is the Undeformed Model)

Due to the imposed vibrating motion at transition piece base based on hydro load analysis, critical stress location are mostly shifted to the upper part of the transition piece structure while the lower part is not as much as mobilized as in the case of a non-vibrating base without the hydro influence (Figure 5.26), which also agrees with previous case analysis with identical incoming wind-wave direction (Figure 5.36). Comparing this analysis case with the previous one without including the yaw moment load (Figure 5.40), it can be seen that location of maximum stress has changed, which can only be explained by the additional effect from the yaw moment load. Time series of stress at critical location is shown in figure below. The stress time series is in general following the yaw moment load (Figure 4.39) with influence from the thrust, torque and hydro loads.

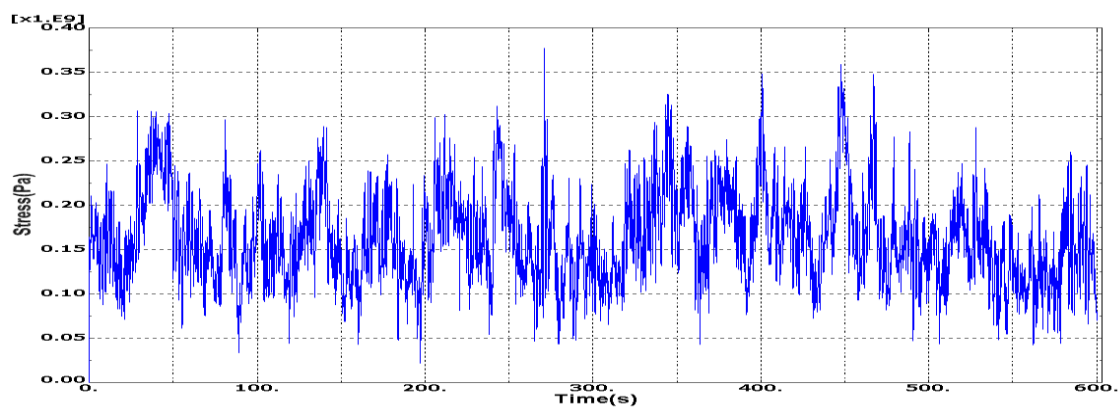


Figure 5.43 Time Series of Stress at Critical Location under Aero & Hydro Load with Yaw Moment with Perpendicular Wind-Wave Direction

As for structural response under this load case, transition piece vibration includes the hydrodynamic related vibration in the incoming wave direction, the torsional motion around the yaw axis due to the yaw moment and the tilting deformation under the rotor torque while the rotor thrust effect is insignificant. Torsional vibration at critical node under this load case is shown in Figure 5.45. The magnitude of vibration along the yaw

axis is very close to the result under identical wind-wave direction analysis (Figure 5.38).

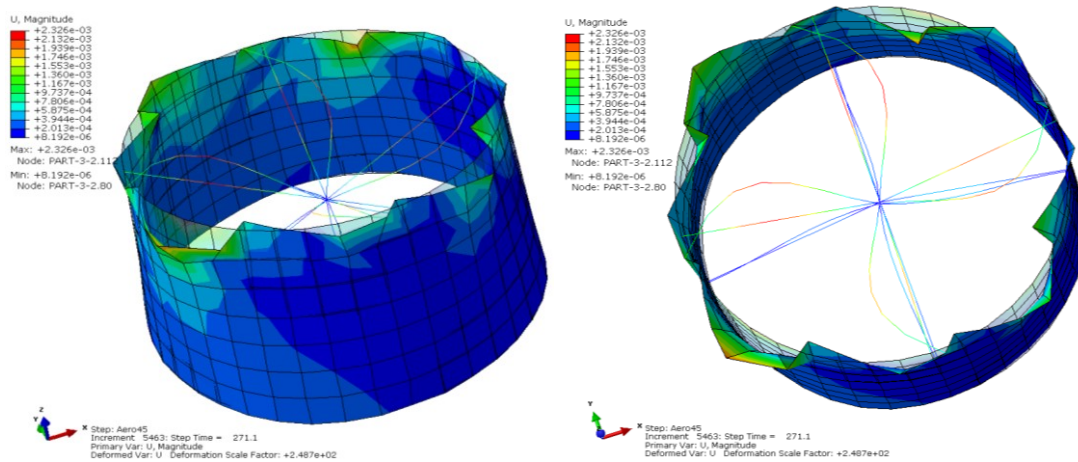


Figure 5.44 Transition Piece Response under Aero & Hydro Load with Yaw Moment with Perpendicular Wind-Wave Direction (Transparent Model is the Undeformed Model)

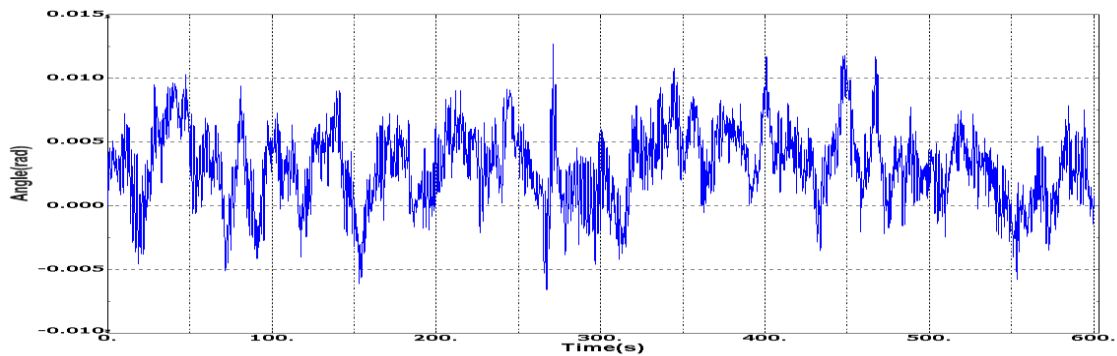


Figure 5.45 Torsional Vibration along Yaw Axis at Critical Node under Aero-Hydro Load with Yaw Moment with Perpendicular Wind-Wave Direction

As a summary, Para. 5.5.4 & 5.5.5 try to explore transition piece structural model response under the combined hydro and aero loads. Maximum stress conditions have shown reduction by the induced motion at transition piece base due to the hydrodynamic load under the yaw moment load. With yaw moment load, simulation results indicate that vibrating transition piece base due to the hydrodynamic effect has an effect of shifting the load bearing zone from the lower part of transition piece to the upper edge where the aero dynamic loads are applied. However, contributing effect from the inner truss system is clearly seen under yaw moment load. The inner truss system can be further enhanced to achieve a better structural robustness to resist the yaw moment load.

Comparing analysis results of Para. 5.5.4 & 5.5.5, it can be concluded that varying wind-wave misalignment does not lead to severe difference on transition piece structural behaviour. Maximum stress condition is nearly the same when the incoming wind and wave direction is identical or perpendicular. Structural deformation pattern is changed by the change of wind and wave directions but in no case the structural deformation appears too severe calling for special attention. Transition piece performance under all the previous load cases is summarized in Table 5.7.

Final Design of Transition Piece
Lattice Tower Design of Offshore Wind Turbine Support Structures

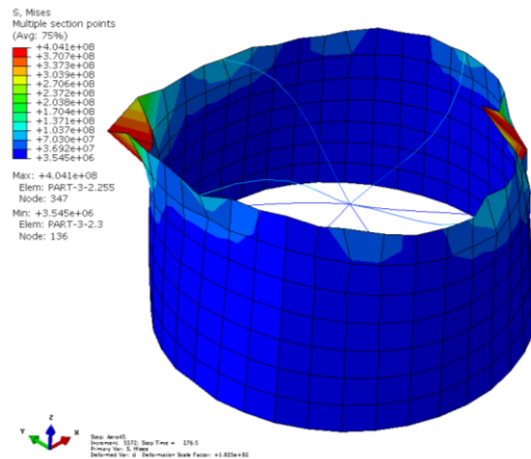
Table 5.7 Transition Piece Response under Various Load Cases

Load Case	Transition Piece Performance		Comment
RNA Weight	Max. Stress	9.34MPa	
	Max. Stress Location	Base connection joints	
RNA Weight & Moment	Max. Stress	20.24MPa	Stress increase due to RNA weight induced moment. The moment is applied on cone top edge.
	Max. Stress Location	Cone top edge	
Aero Load (Thrust & Torque)	Max. Stress	201.8MPa	Vibration induced by thrust load reaches $\pm 0.5m$ magnitude, based on applied lattice support structure stiffness. This value is validated by means of thrust load analysis on lattice support structure model.
	Max. Stress Location	Cone top edge ends without truss supports	
	Structural Deflection	$\pm 0.5m$ at TP base, negligible within TP	
Angled Aero Load (Thrust & Torque)	Max. Stress	239.4MPa	Stress increase due to change of aero load direction. Decreased magnitude of vibration under thrust load due to stiffness increase in the wind direction.
	Max. Stress Location	Cone top edge ends perpendicular to incoming wind dir.	
	Structural Deflection	$\pm 0.4m$ at TP base, negligible within TP	
Aero Load with Yaw Motion	Max. Stress	565.3MPa	Inner truss system found to contribute much to load bearing function under yaw moment load. Torsional vibration magnitude is reduced compared to preliminary designs.
	Max. Stress Location	Base connection joints of truss	
	Structural Deflection	Translational vibration under thrust & $-1.4^\circ \sim +2.7^\circ$ torsional vibration under yaw	
Angled Aero Load with Yaw Motion	Max. Stress	554.5MPa	Stress condition is slightly reduced due to change of load direction.
	Max. Stress Location	Base connection joints of truss	
	Structural Deflection	Similar as above case	
Combined Aero-Hydro Load with Identical Wind-Wave Dir.	Max. Stress	241.7MPa	Vibration mainly under hydro load. Rotor torque shows dominating effect.
	Max. Stress Location	Cone top edge ends perpendicular to incoming wind dir.	
Combined Aero-Hydro Load with Perpendicular Wind-Wave Dir.	Max. Stress	241.7MPa	Unchanged stress due to wind-wave misalignment.
	Max. Stress Location	Cone top edge ends perpendicular to incoming wind dir.	
Combined Aero-Hydro Load with Yaw Motion with Identical Wind-Wave Dir.	Max. Stress	377.3MPa	Vibrational TP base due to hydro load is found to significantly ease structural stress condition under the yaw load. Critical stress zone is shifted from the lower part truss to the upper part of the transition piece.
	Max. Stress Location	Cone top edge	
	Structural Deflection	$-0.4^\circ \sim +0.8^\circ$ torsional vibration under yaw	
Combined Aero-Hydro Load with Yaw Motion with Perpendicular Wind-Wave Dir.	Max. Stress	377.3MPa	Unchanged stress due to wind-wave misalignment.
	Max. Stress Location	Cone top edge	
	Structural Deflection	Close to above case	

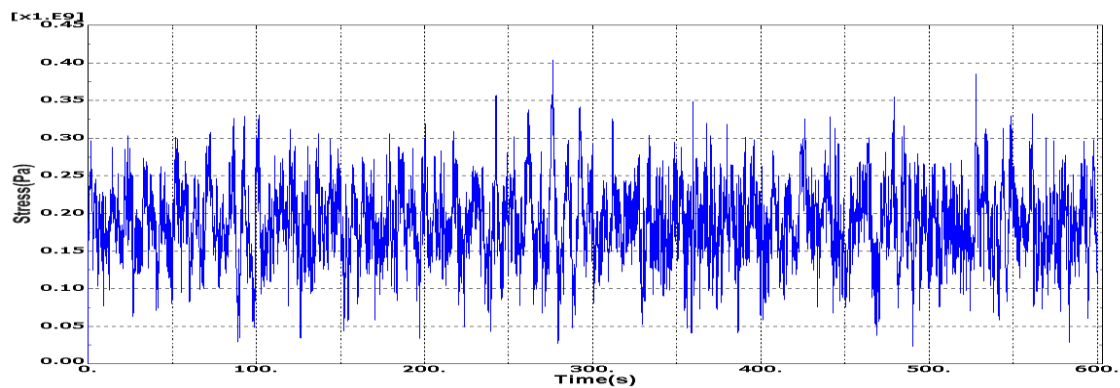
5.6 Investigation on more compact design

Based on conclusion drawn in Para. 5.5.4 & 5.5.5, since a vibrating transition piece under hydrodynamic load transferred by lattice support structure appears to have an effect of changing the transition piece stress condition under the aerodynamic loads, a more compact design is possible to be proposed for purpose of cost reduction as well as ease of manufacturing. Model 3-15 (3m high, 0.15m thick cone) in Table 5.1 is selected to investigate this possibility. Previous loads are applied on the transition piece structural model in the same manner as previous analysis. For simplicity, here only load condition with identical incoming wind-wave direction is considered (Figure 5.33). Transition piece stress condition at time point of maximum stress under two load cases is shown below in Figure 5.46 & 5.47.

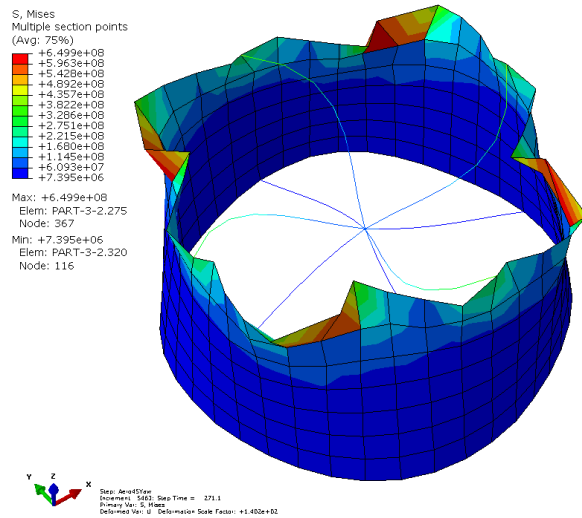
Comparing behaviour of this compact design model with the previously analyzed one, stress condition pattern remains the same under the combined aerodynamic and hydrodynamic load conditions. Maximum stress increases by around 70% in both of the two load cases whereas material is saved by 24%. Apparent benefit of the compact design model does not show up but it is still very possible to achieve the cost reduction purpose by means of regional enhancement of critical stress zone in the transition piece structure while the other less critical zone applies characteristics of the above compact design.



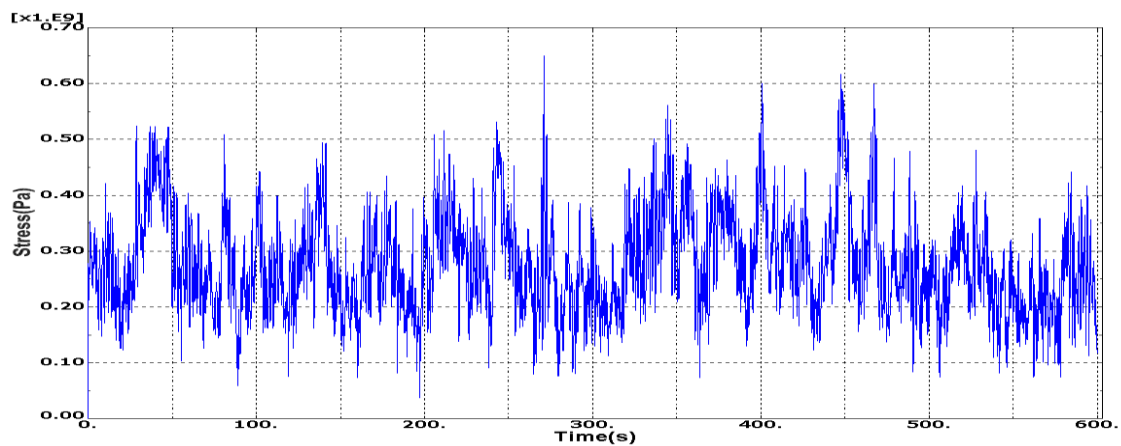
(a) Stress Condition of Compact Transition Piece under Combined Aero & Hydro Loads at Time Point of Max. Stress



(b) Time Series of Stress at Critical Location of Compact Transition Piece under Aero & Hydro Loads
 Figure 5.46 Response of Compact Transition Piece Design under Combined Aero & Hydro Loads



(a) Stress Condition of Compact Transition Piece under Combined Aero & Hydro Loads with Yaw Motion at Time Point of Max. Stress

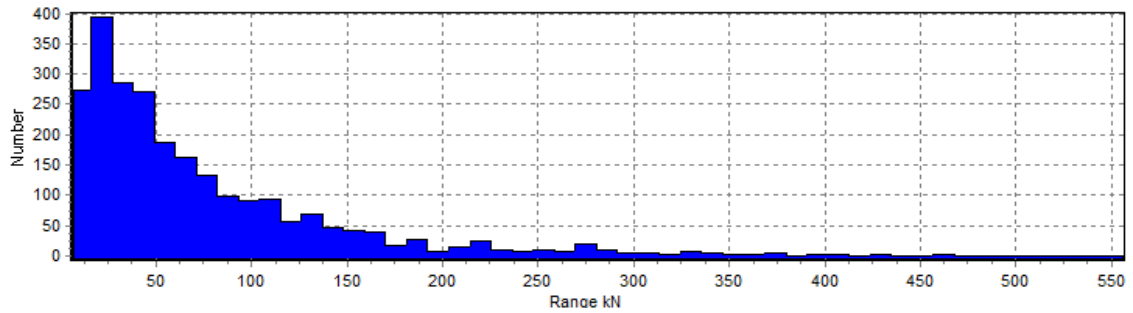


(b) Time Series of Stress at Critical Location of Compact Transition Piece under Aero & Hydro Load with Yaw Motion

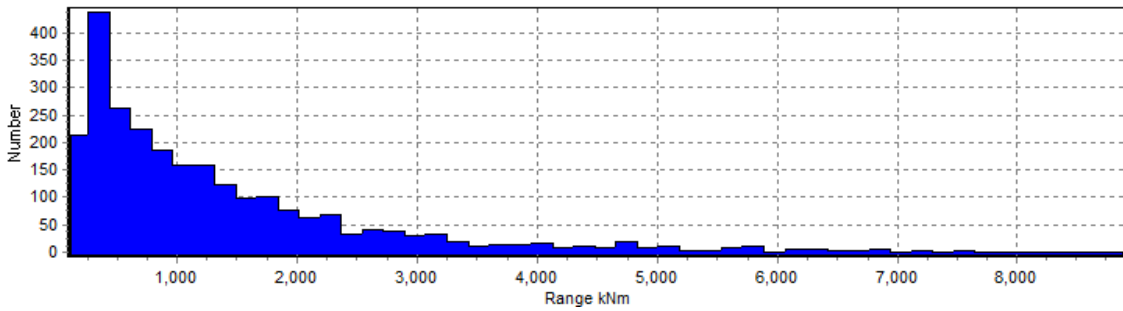
Figure 5.47 Response of Compact Transition Piece Design under Combined Aero & Hydro Loads with Yaw Motion

5.7 Fatigue

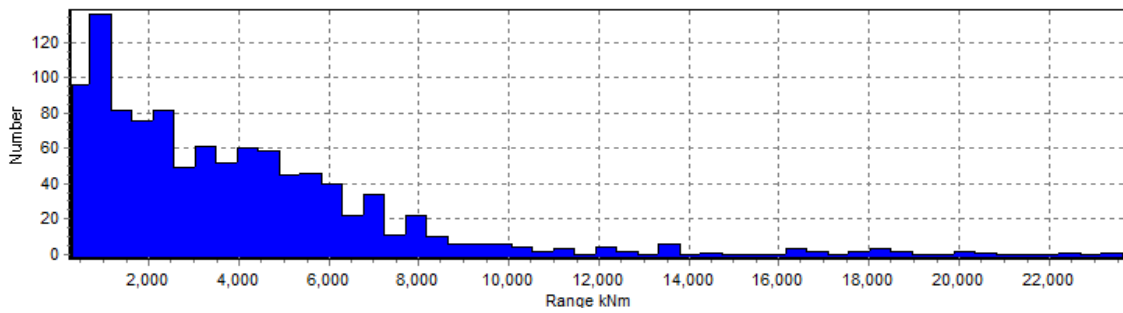
Fatigue analysis of transition piece structural model is among the most important aspects, especially for the joint of the supporting truss components and the connections between the truss components and the cone. Both aerodynamic and hydrodynamic loads possess instantaneously changing characteristics both in magnitude and direction which brings the major source for fatigue load, not to mention the vibration of mechanical components within the nacelle. Rainflow counting of the dynamic rotor thrust, rotor torque, yaw moment loads within the simulation time period of 600s is illustrated below in Figure 5.48. The first two loads are in general lower in load range but higher in number of cycles while the yaw moment is higher in load range but relatively lower in number of cycles. Rotor thrust and torque have close number of cycles in respective load range bins because their characteristics are basically linked with the performance of the rotating rotor. As for the yaw moment load, cross-wind condition is playing a more important role. S-N curve (load versus number of cycles to failure) [39] for the material of the structure is calculated as in Figure 5.49.



(a) Cycle Number-Load Range for Rotor Thrust



(b) Cycle Number-Load Range for Rotor Torque



(c) Cycle Number-Load Range for Yaw Moment

Figure 5.48 Rainflow Counting of Cycle Number against Load Range for Aerodynamic Loads within Simulation Period of 600s

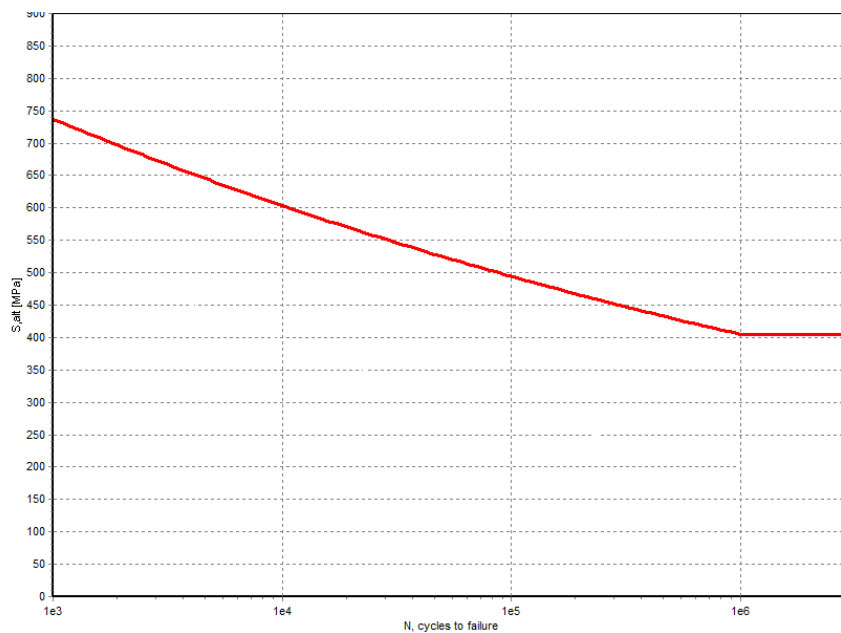


Figure 5.49 Material S-N Curve

Previous analysis results show that under different load cases, time series of stress condition at critical stress regions behave in different patterns. Stress condition is in general in phase with the external load trend but magnitude and frequency of stress condition under each load case at critical stress zone is specific. According to the above S-N curve, stress range below 400MPa does not trigger challenge for fatigue protection. Fatigue damage and life time prediction under various load cases is summarized in below Table 5.8.

Table 5.8 Fatigue Life Prediction under Various Load Cases at Critical Structural Stress Region

Load Case	Stress Range at Critical Structural Region (MPa)	Predicted Life Time (Cycles)	Damage per Cycle
Aero Loads	20-250	1.00E+30	0
Aero Loads with Yaw	0-550	1.25 E+04	7.99E-05
Aero & Hydro Loads	20-250	1.00E+30	0
Aero, Hydro with Yaw	20-400	1.00E+30	0

5.8 Manufacturing

As for manufacturing of the transition piece, a major challenge could be casting of the truncated cone component. In the original design, 200mm wall thickness appears to be relatively significant, which makes it not convenient for easy manufacturing process such as rolling. Truss components could be manufactured by means of standard steel pipe process whereas welding of the supporting truss components and their connection with the cone component as well as the lower lattice support structure is another critical issue during the manufacturing process. Casting process might appear expensive in the early phase of development but cost reduction could be achieved when future market is welcoming mass production.

5.9 Conclusion

In this chapter an optimized transition piece design model is proposed with sufficient analysis under various load conditions as well as fatigue aspect. This new design is of less weight and thus lower material cost than the previous analysis models in Chapter 4 but its structural performance under all load cases surpass that of the preliminary analysis models. Behavior of this optimized design under various load cases is summarized in Table 5.7. Torque and yaw moment are among the most important loads and hydrodynamic influence from the support structure affects the load bearing pattern of the transition piece to a significant degree.

Cone thickness of this optimized design is found to be critical for structural load bearing capacity, especially under the yaw moment load. This parameter comes out as a compromise between the structural strength and the cost of production. A more compact design applying a smaller thickness is discussed in Para. 5.6. Structural behavior of the compact design is less sound than the original one but cost reduction could be possibly achieved by combination of both design characteristics. Fatigue failure is a challenge under the aerodynamic and hydrodynamic loads. Structural material properties and the characteristics of external loads have dominating effects of structural fatigue life. When utilization of an advanced material type is not possible, regular maintenance could be able to help to an extent.

6 CONCLUSION AND RECOMMENDATION

6.1 Conclusion

In context of global environment change and increasing deficiency of conventional energy sources, offshore wind industry is progressively developing with a promising future even seen from now. Under this background, prevention of failure and optimization of input cost remain challenges for further mass production of offshore wind turbines in future. Support structure of offshore wind turbine contributes to a significant proportion among the total input and also relates closely to the safety of the turbine's operation and thus is the main interest of this thesis.

Conventional support structures like monopile, tripod and concrete block for foundation and monotower for turbine support have been seen in industrial practice in relatively shallow water up to present with certain amount of experience and knowledge. However, as future industry challenges deeper sea, lattice structure could become a sound solution as wind turbine support structure because of its robustness in structural strength and efficiency in cost reduction. Existing projects employing lattice structure as wind turbine foundation in water depth of 30m to 50m can be regarded as a prediction for future trend.

This thesis work is based on experience learnt from existing hybrid offshore wind turbine support structures and further proposes a full lattice concept used as both foundation and tower for future industrial application. Under this concept, transition piece which connects a full lattice support structure and the turbine rotor nacelle assembly becomes an important aspect which deserves detailed consideration and analysis second to none. Existing research and practice sees a lack of study of this transition piece concept and in this thesis the critical subject is investigated with much effort.

After introduction of existing hybrid support structure consisting of the lattice structure and transition piece components, a conceptual model of transition piece is built which takes into consideration of various aspects including its geometrical requirement, function requirement (power cable and yaw) as well as mechanical connection requirement. A mechanical model of the transition piece concept is established depicting its boundary relation with the lattice support structure and various aerodynamic and hydrodynamic loads it is subjected to. Preliminary design process analyzes two different transition piece concepts, namely, frame-cylinder and cone-strut, mostly based on existing hybrid support structure experience in a comparative manner. Comparative load analysis of the two concepts by means of finite element analysis technique shows similar structural performance of these two concepts which are at close dimension and weight but different structural forms.

A new design by experience of numerical analysis learnt from the preliminary design models which considers more practical conditions including suitability of connection with a lattice support structure is finalized in the final design process. This new design is slightly reduced in weight compared with preliminary concepts but has much better optimized structural behavior under load analysis scenarios. Response of this new transition piece design under various load cases is carefully investigated in addition to briefly considered fatigue and manufacturing aspects. A relatively more compact

Conclusion and Recommendation
Lattice Tower Design of Offshore Wind Turbine Support Structures

version of this new design is also discussed which provides information for further optimization and cost reduction strategy. General comparison of the two preliminary and two final concepts is given in table below.

Table 6.1 Comparison of Various Transition Piece Concepts

Transition Piece Concept	Preliminary Concept		Final Concept	
	Frame-cylinder	Cone-strut	0.2m thickness	0.15m thickness
Dimension	6m height 6m×6m base refer to Table 4.2	6m height 6m×6m base refer to Table 4.3	3m height 4m×4m base refer to Table 5.2	3m height 4m×4m base refer to Table 5.1
Weight (tons)	118	140	95	75
Maximum stress under yaw load ⁽¹⁾	1.26	1.32	1	1.47
	refer to Table 4.10		refer to Table 5.7	
Maximum stress under combined hydro-aero load with yaw motion ⁽²⁾			1	1.72
			refer to Table 5.7	

(1), (2) Normalized by stress condition of 0.2m thickness final concept model.

6.2 Recommendation

In this thesis, analysis of lattice support structure is provided to an extent and the more extensive attention is placed on design and analysis of the transition piece. Structural analysis result of varying lattice designs can be used as reference for relevant application. Conceptual model of transition piece which takes into consideration of multiple requirements and mechanical model including boundary condition and load condition have covered the principal and critical aspects for transition piece modeling, which can be referred to with reasonable amount of adequacy. Nevertheless, not all miscellaneous aspects are included and in fact for practical model computation purpose, they should rather not be.

Preliminary design models are from experience of hybrid support structure and the transition piece concepts are more suitable for this type of support structure. On the other hand, final design model is tailored for a full lattice support structure concept which however remains as a conceptual proposal so far without practical experience. Analysis of the final design transition piece model is majorly focusing on the less compact design. Cost reduction can be further achieved through regional redesign according to more compact design parameters but this should be dealt with carefully.

The applied boundary condition and load cases in combination of various aerodynamic load and hydrodynamic load conditions are for the proposed models in this thesis and not designed for any specific project. Design of an offshore wind turbine or a wind farm should always investigate its site-specific topographical, meteorological and sea state conditions to determine the relevant aerodynamic and hydrodynamic loads for support structure's ultimate and fatigue analysis.

Finally, this thesis work endeavors to provide solution and reference for future relevant research or practical purpose at the maximum capacity within its scope. Due to physical and temporal limitations, further verification and correction will be very much appreciated from interested readers.

REFERENCE

- [1]Jespersen, KD, 1991, “Vindeby-The First Offshore Wind Farm in the Danish Wind Power Programme”, Proceedings Windpower.
- [2]Alexandra Bech Gjørvi Oil & Energy, 2006-05-24, “Hywind Floating Wind Power Production”.
- [3]Hau, E., 2006, *Wind Turbines: Fundamentals, Technologies, Application, Economics*. Springer-Verlag, Berlin Heidelberg.
- [4]Sinning, F., 2001, “Fachwerktürme für Windkraftanlagen die bessere Wahl”, im Auftrag von Seeba-Energiesysteme GmbH, Stenwede.
- [5]<http://www.owectower.no>.
- [6]Talisman Energy, “Beatrice Wind Farm Demonstrator Project Scoping Report”, <http://www.beatricewind.co.uk>.
- [7]Deutsche Offshore-Testfeld und Infrastruktur GmbH & Co.KG, 2011, “Alpha Ventus Fact Sheet”, <http://www.alpha-ventus.de>.
- [8]Seidel, M., 2007, “Jacket substructures for the REpower 5M wind turbine”, Conference Proceedings European Offshore Wind 2007, Berlin.
- [9]Naveen Kumar Vemula, et al, 2010, “UpWind_WP4_D4.2.5_Design solution for the Upwind reference offshore support structure”, Rambøll, Esbjerg, Denmark.
- [10]Vorpahl, F., Kaufer, D., 2010, “Description of a basic model of the ‘Upwind reference jacket’ for code comparison in the OC4 project under IEA Wind Annex XXX”, Fraunhofer Institute for Wind Energy and Energy System Technology (IWES), Bremerhaven, Germany.
- [11]WeserWind Offshore Construction Georgsmarienhütte, <http://www.weserwind.de>.
- [12]<http://www.vestas.com>.
- [13]European Wind Energy Association (EWEA), “Offshore Support Structure”, <http://www.wind-energy-the-facts.org>.
- [14]<http://www.abb.no>.
- [15]ABB, 2011, “Submarine Power Cables: Cables for offshore wind farms and platforms”, <http://www.abb.no>.
- [16]ABB, 2006, “HVDC Light[®] Cables”, <http://www.abb.com/cables>.
- [17]ABB, 2010, “XLPE Submarine Cable Systems”, <http://www.abb.com/cables>.
- [18]Bilfinger Berger, Ingenieurbau GmbH, “Offshore Wind Farm Alpha Ventus Transformer Station”.
- [19]<http://en.wikipedia.org>.
- [20]Corrigan, R.D., Viterna, L.A., 1981, Free Yaw Performance of the MOD-0 Large Horizontal Axis 100 kW Wind Turbine, Cleveland: Lewis Research Center, 44135, Ohio.
- [21]Huß, G., 1993, Anlagentechnisches Meßprogramm an der Windkraftanlage WKA-60 auf Helgoland, BMFT report 0328508D.
- [22]Astron Overseas Enterprise, “Slewing Bearing for Wind Turbine”.
- [23]Jonkman, J., Butterfield, S., Musial, W., Scott, G., 2009, “Definition of a 5-MW Reference Wind Turbine for Offshore System Development”, Technical Report NREL/TP-500-38060.
- [24]Johnson, W., 1994, *Helicopter Theory*, Princeton University Press, Princeton, USA.
- [25]Morison, J. R., O'Brien, M. P., Johnson, J. W., Schaaf, S. A., 1950, “The Force Exerted by Surface Waves on Piles”, Petroleum Transactions (American Institute of Mining Engineers), 189, pp. 149–154.

- [26]Peeters, J., Vandepitte, D., Sas, P., 2006, “Structural analysis of a wind turbine and its drive train using the flexible multibody simulation technique”, Proceedings of ISMA.
- [27]RPP Rijs., 1990, “Blade Element Theory for Performance Analysis of Slow Running Wind Turbines”, Wind Engineering.
- [28]http://www.simulia.com/products/abaqus_fea.
- [29]<http://www.risoe.dtu.dk>.
- [30]BVG Associates, The Crown Estate, “A Guide to an Offshore Wind Farm”.
- [31]Abaqus/CAE User's Manual, <http://www.engin.brown.edu:2080/v6.10/index>.
- [32]von Mises, R., 1913, *Mechanik der festen Körper im plastisch deformablen Zustand*, Göttin. Nachr. Math. Phys., vol. 1, pp. 582–592.
- [33]Frohboese, P., Schmuck, C., 2010, “Thrust Coefficients used for Estimation of Wake Effects for Fatigue Load Calculation”, European Wind Energy Conference 2010, Warsaw, Poland.
- [34]International Electrotechnical Commission, 2007, “Wind turbines Part 1: Design requirements”, IEC 61400-1, Edition 3.0, 2005-08.
- [35]Gumbel, E.J., 1958, *Statistics of Extremes*, Columbia Uni. Press, p. 73.
- [36]Cramer, H., 1966, *On the Intersections Between Trajectories of a Normal Stationary Stochastic Process and a High Level*, Arkiv for Matematik, V.6, pp. 337-349.
- [37]Airy, G. B., “Tides and Waves,” In Rose, H. J. et al., *Encyclopaedia Metropolitana Mixed Sciences 3 1817–1845*.
- [38]Hasselmann K. et al., 1973, Measurements of wind-wave growth and swell decay during the Joint North Sea Wave Project (JONSWAP), 'Ergänzungsheft zur Deutschen Hydrographischen Zeitschrift Reihe, A(8) (Nr. 12), p.95.
- [39]W. Schutz, 1996, A history of fatigue. *Engineering Fracture Mechanics* 54: 263-300. DOI.

APPENDIX I

Application of HVDC and XLPE Power Transmission Cable on Offshore Wind Farm Projects [15]

I.1 DC cable offshore applications

— DoIWin1 Offshore Wind Project, Germany

2x74 km, 800 MW, +/- 320 kV HVDC Light submarine power cables with Cu conductor and 2x90 km, 800 MW, +/- 320 kV HVDC Light underground cables with Al conductor. 7,5 km, 200 MW, 155 kV AC submarine cable with Cu conductors and integrated optical fiber cable.

— BorWin1 Offshore Wind Project, Germany

2x125 km, 400 MW, +/-150 kV HVDC Light submarine power cables with Cu conductor and 2x75 km, 400 MW, +/-150 kV HVDC Light underground cables with Al conductor.

I.2 AC cable offshore applications

— Thornton Bank Offshore Wind Farm Phase 2 & 3, Belgium

38 km, 150 MW, 150 kV shore connection power cable with Al conductors and integrated optical fiber cable and 26 + 34 km, 33 kV inter-turbine cables with Al and Cu conductors and integrated optical fiber cable.

— Nordsee Ost Offshore Wind Farm, Germany

63 km, 33 kV inter-turbine cables with Cu conductor and integrated optical fiber cable.

— Thornton Bank Offshore Wind Farm, Belgium

38 km, 150 MW, 150 kV shore connection power cable with Al conductors and integrated optical fiber cable and 4 km, 33 kV inter-turbine cables with Al conductors and integrated optical fiber cable.

— Prinses Amaliawindpark (Q7), the Netherlands

28 km, 120 MW, 170 kV shore connection power cable with Cu conductors and integrated optical fiber cables and 40 km, 24 kV inter-turbine cables with Al and Cu conductors and integrated optical fiber cable.

— Lillgrund Offshore Wind Farm, Sweden

33 km, 110 MW, 145 kV shore connection power cable and 36 kV inter-turbine cables with Cu conductors and integrated optical fibers.

- Burbo Banks Offshore Wind Farm, UK
40 km, 90 MW, 36 kV inter-turbine and shore connection power cables with Cu conductors.

- Yttre Stengrund Offshore Wind Farm, Sweden
22 km, 10 MW, 24 kV inter-turbine and shore connection power cables with Al conductors and integrated optical fibers.

- Utgrunden Offshore Wind Farm, Sweden
11 km, 10 MW, 24 kV inter-turbine and shore connection power cables with Al conductors and integrated optical fiber cable.

- Samsö Offshore Wind Farm, Denmark
7.5 km, 20 MW, 36 kV inter-turbine and shore connection power cable with Cu conductors integrated optical fiber cable.

- Nysted Offshore Wind Farm, Denmark
55 km, 165 MW, 36 kV inter-turbine power cables with Al- and Cu conductors and integrated optical fiber cable.

APPENDIX II

Eigen modes of a full lattice support structure for a 5 MW reference offshore wind turbine with 12m×12m base area and light weight design (Table 3.4) are shown below:



1st fore-aft bending



1st side-side bending



2nd fore-aft bending



2nd side-side bending

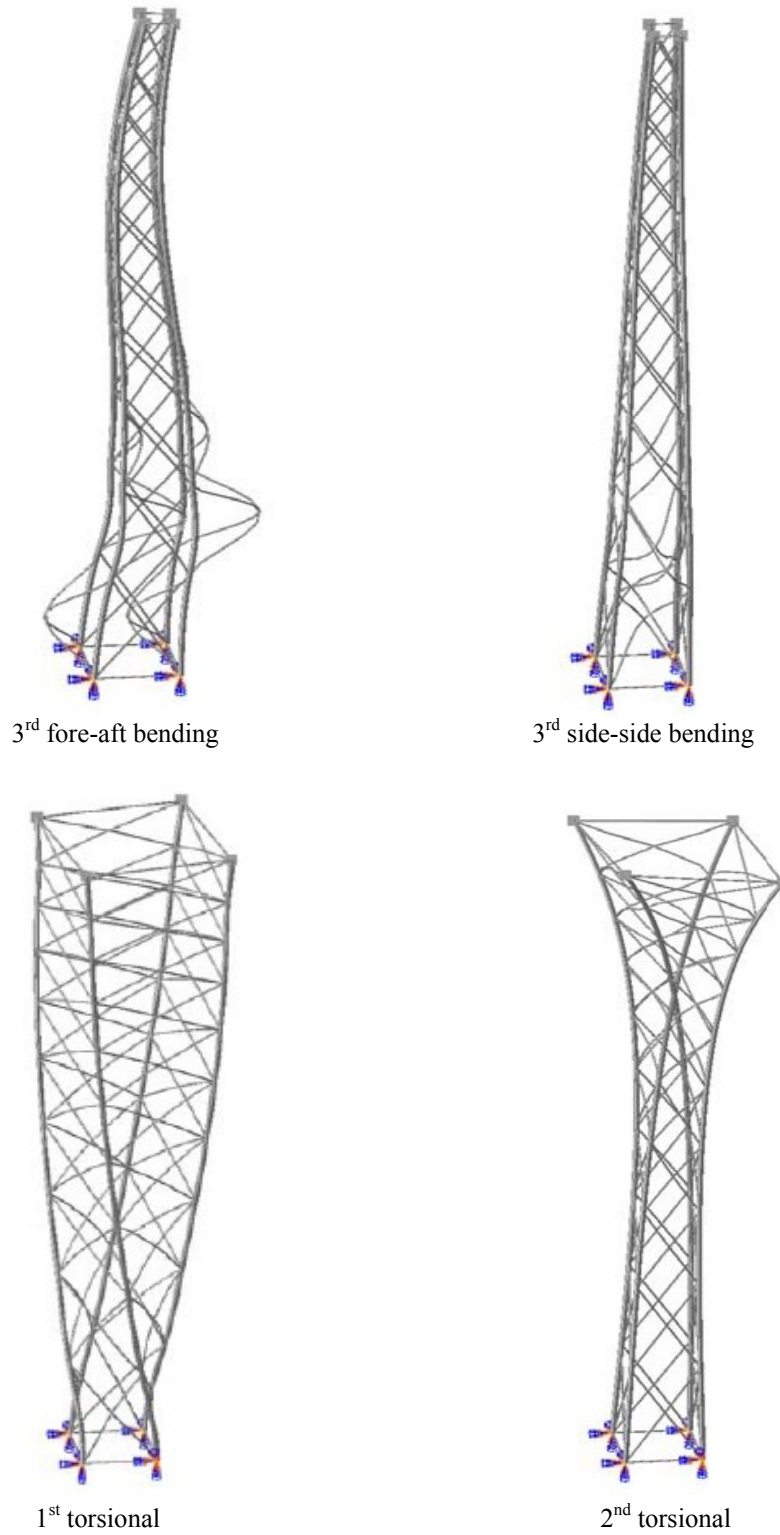


Figure II.1 Modal Shapes of Numerical Lattice Model 12L (Base Width 12m, Light Weight Design)

APPENDIX III

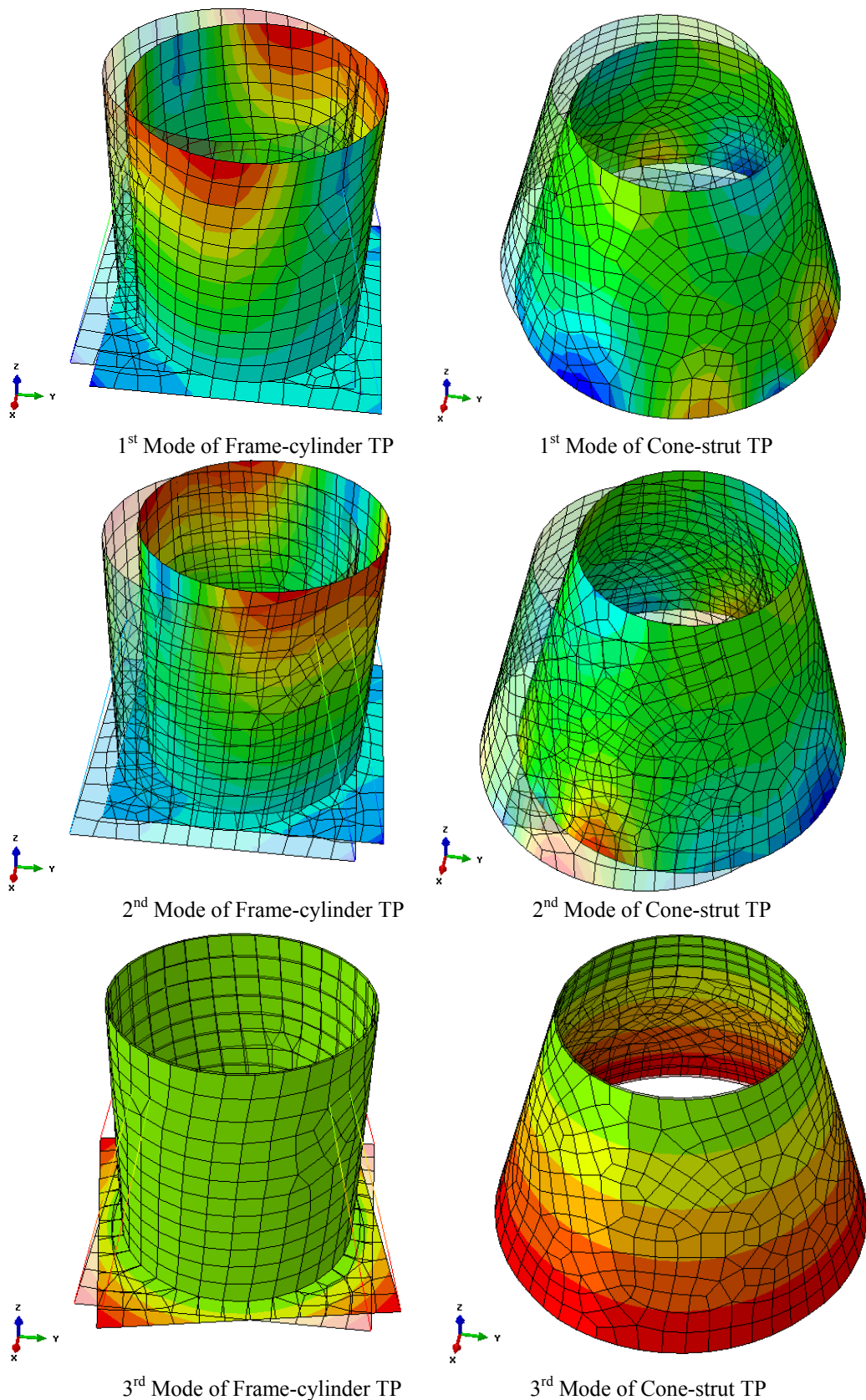


Figure III.1 Eigen Models of Transition Piece (Transparent Model Indicates the Original Undeformed Model and Colour Contour Indicates the Magnitude of Structural Deflection)

APPENDIX IV

If structural stress is assumed to be related to the load, the stress will thus progressively increase with the increasing load. The strength of a structure can therefore be defined in terms of an ultimate load that leads to failure.

For the aerodynamic loads on wind turbines, the loads depend on the instantaneously changing wind condition including the mean wind speed, wind direction, the turbulence intensity, etc. In order to determine a suitable characteristic load for structural strength assessment, it is necessary to analyze the extreme values of the aerodynamic load on a statistical basis.

IEC 61400 [34] provides method of statistical extrapolation of aerodynamic loads for ultimate strength analysis for wind turbines based on probabilistic methods by Gumbel & Cramer [35, 36]. Using this method, wind speeds around the rated and cut-out points should be paid attention, along with the adequacy and resolution of the number of wind speed bins.

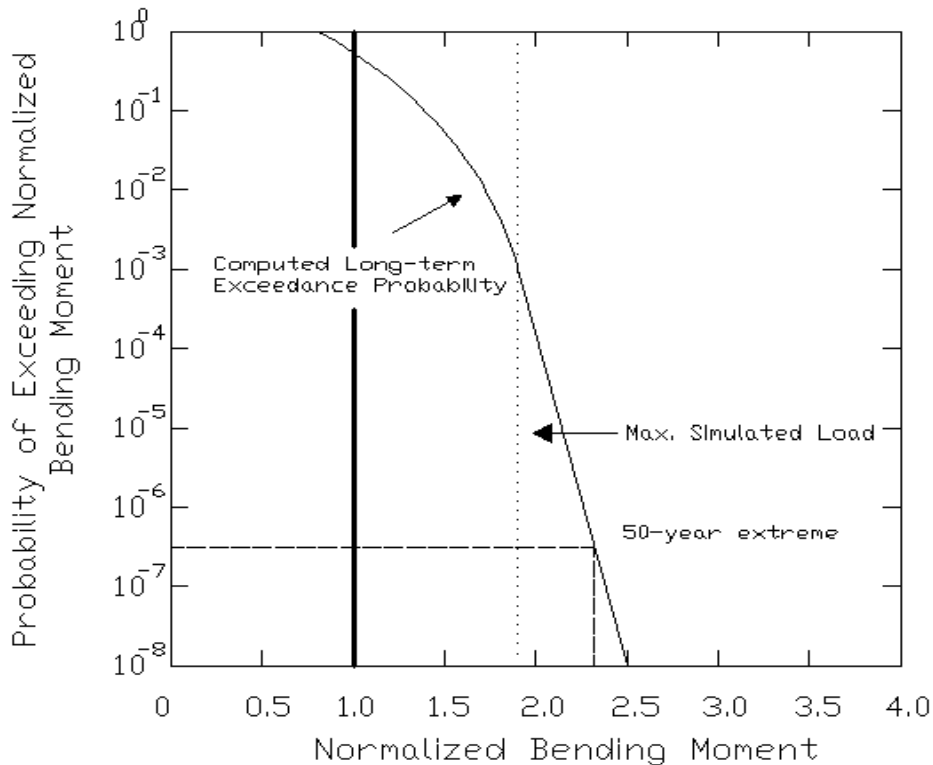
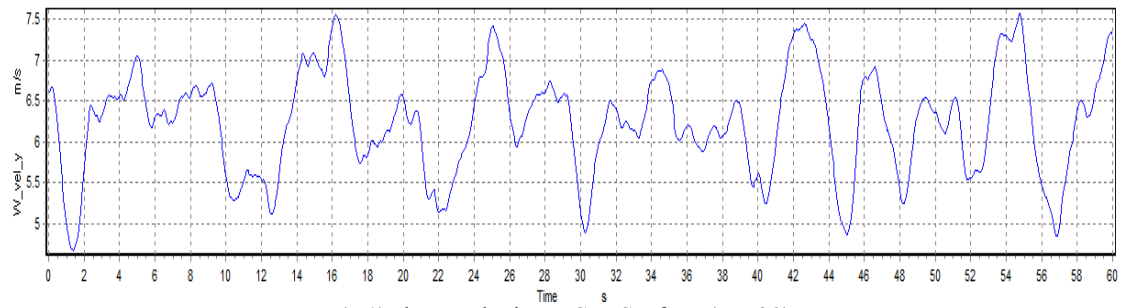


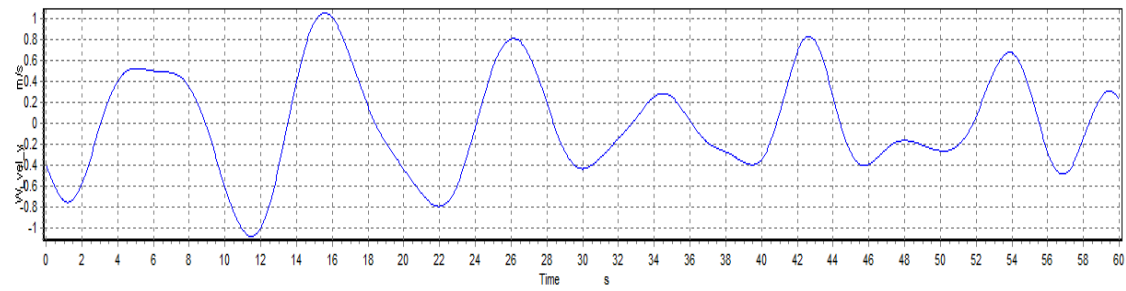
Figure IV.1 Exceedance Probability for Largest Out-of-plane Blade Bending Load in 10-minute (Normalized by Mean Bending Load at Rated Wind Speed) (Source: IEC 1257/05)

Applying the method, the figure above shows the computed long-term exceedance probability of a blade bending load normalized by the mean blade bending load at rated wind speed (bold line). The dash line refers to the largest computed blade bending load for all the simulations at the different mean wind speeds between cut-in and cut-out. The 50-year extreme bending load thus exceeds the maximum simulated load. Based on this thought, the aerodynamic loads used in this thesis based on normal turbulent wind model at mean wind speed of 24m/s, close to the cut-out speed, are assumed to approximate a relatively extreme load case. A specific analysis of the long-term load exceedance probability should be performed in the realistic project.

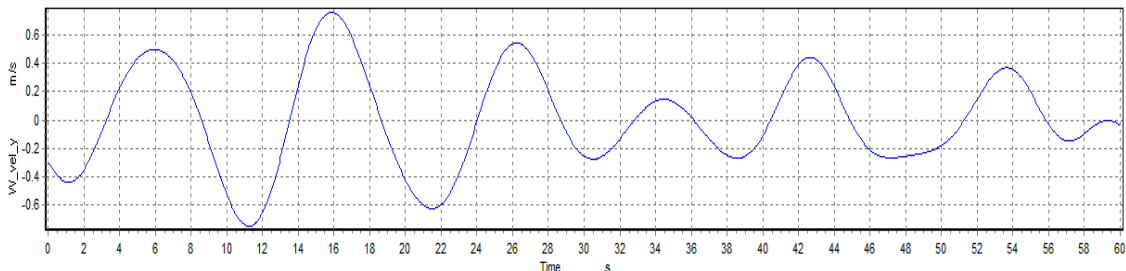
APPENDIX V



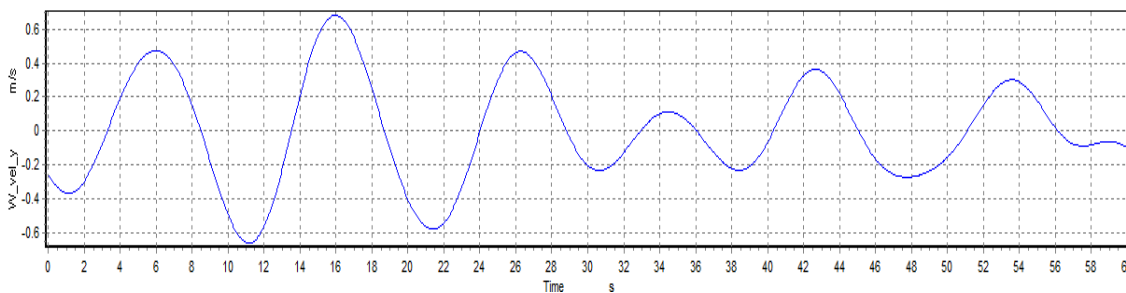
(a.1) Flow Velocity at Sea Surface (Z=-30)



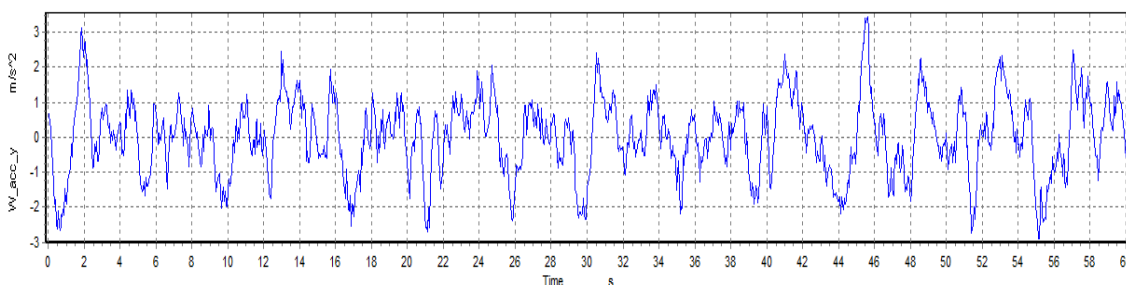
(a.2) Flow Velocity at 10m Water Depth (Z=-20)



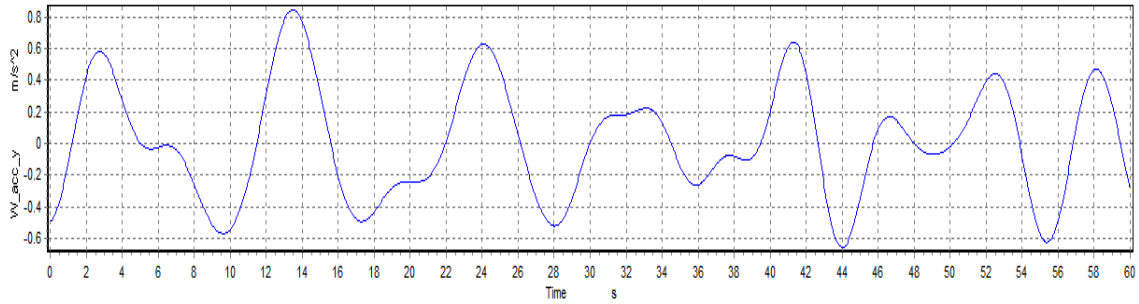
(a.3) Flow Velocity at 20m Water Depth (Z=-10)



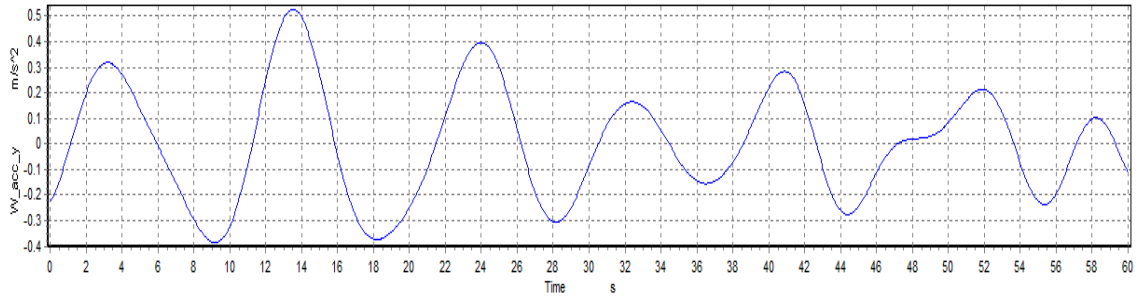
(a.4) Flow Velocity at 29m Water Depth (Seabed Z=-1)



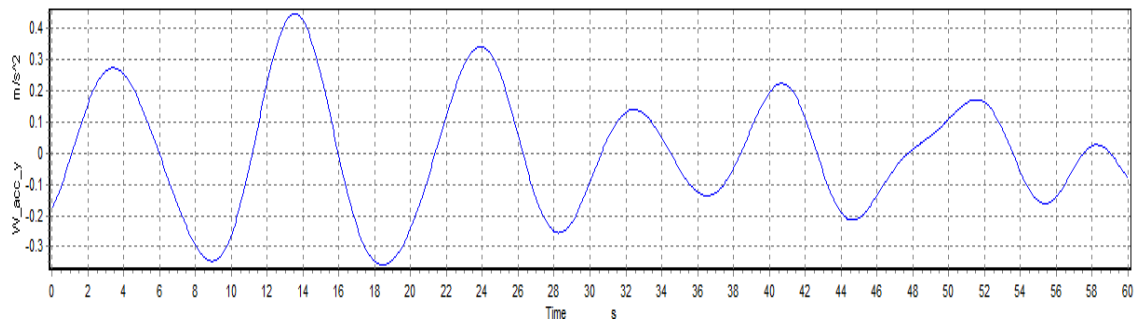
(b.1) Flow Acceleration at Sea Surface (Z=-30)



(b.2) Flow Acceleration at 10m Water Depth (Z=-20)

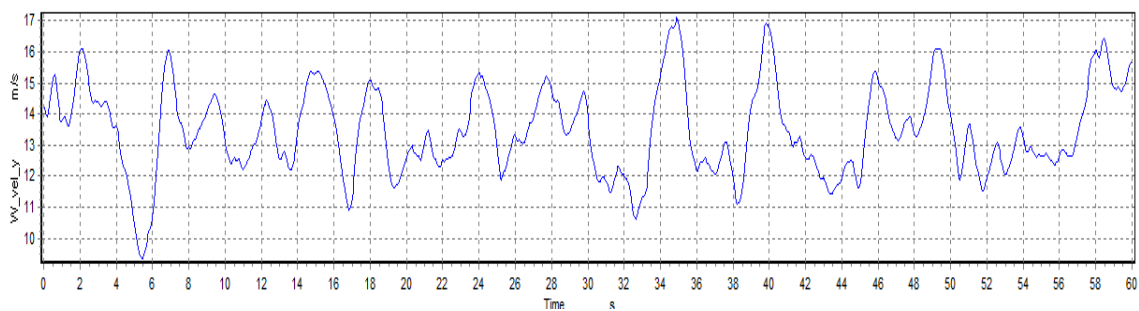


(b.3) Flow Acceleration at 20m Water Depth (Z=-10)

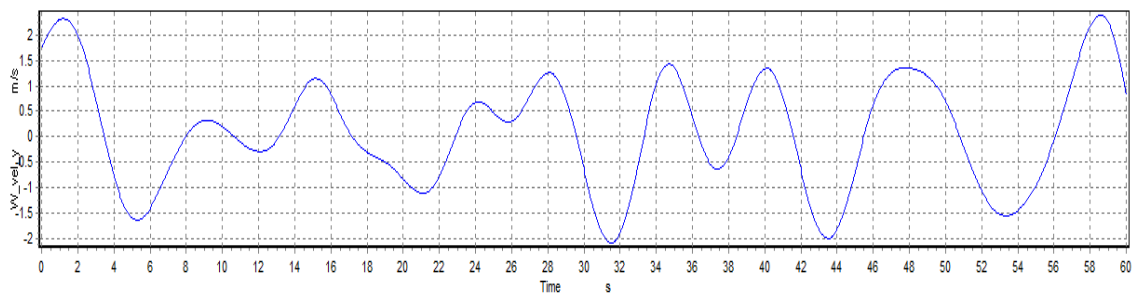


(b.4) Flow Acceleration at 29m Water Depth (Seabed Z=-1)

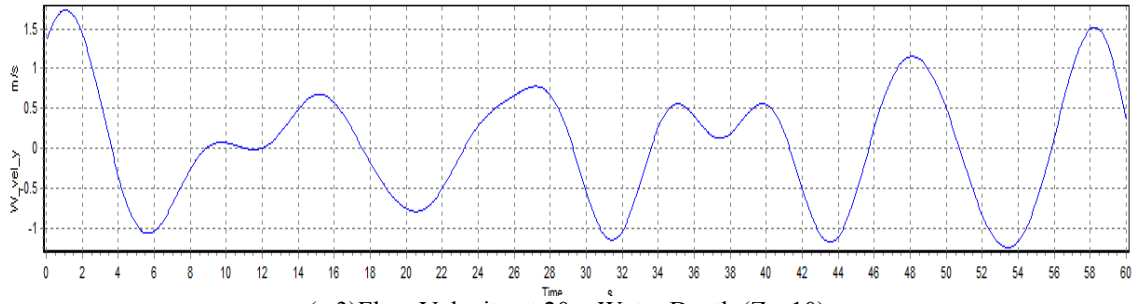
Figure V.1 Flow Velocities and Accelerations at Varying Water Depths for a 4.0m Wave Condition



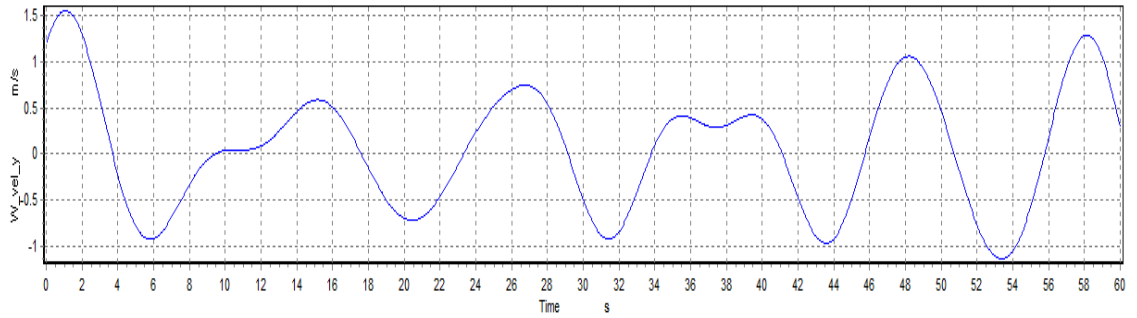
(a.1) Flow Velocity at Sea Surface (Z=-30)



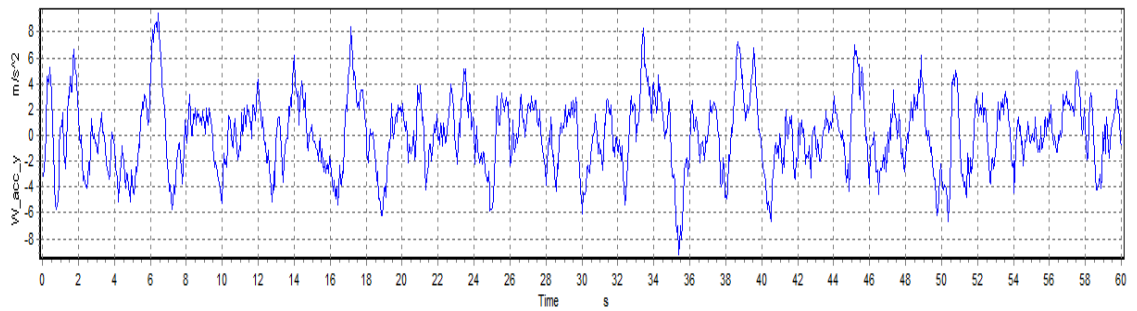
(a.2) Flow Velocity at 10m Water Depth (Z=-20)



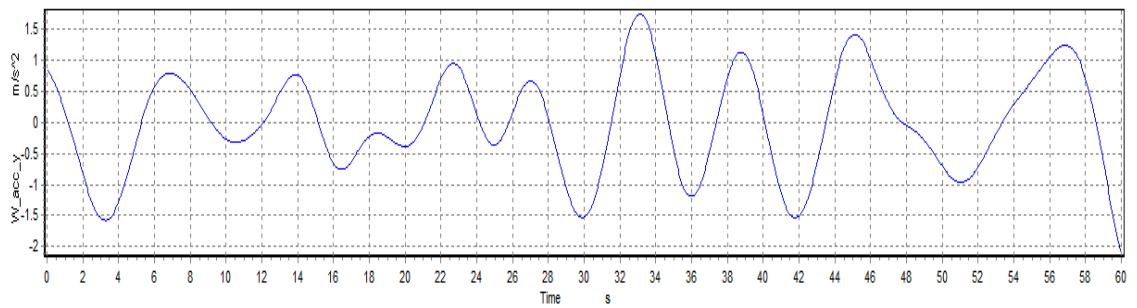
(a.3) Flow Velocity at 20m Water Depth (Z=-10)



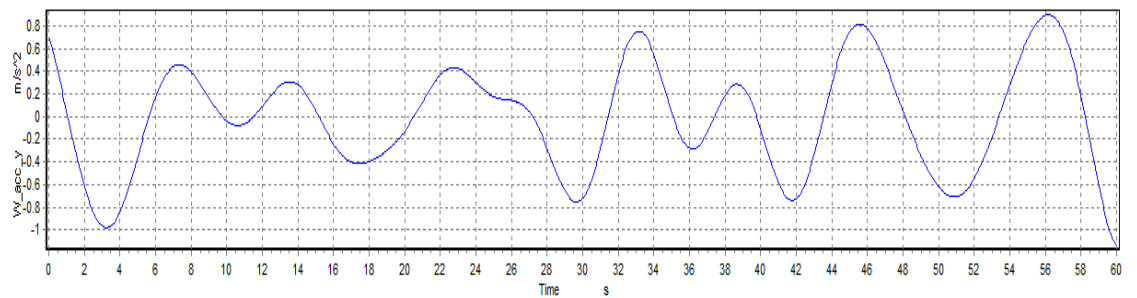
(a.4) Flow Velocity at 29m Water Depth (Seabed Z=-1)



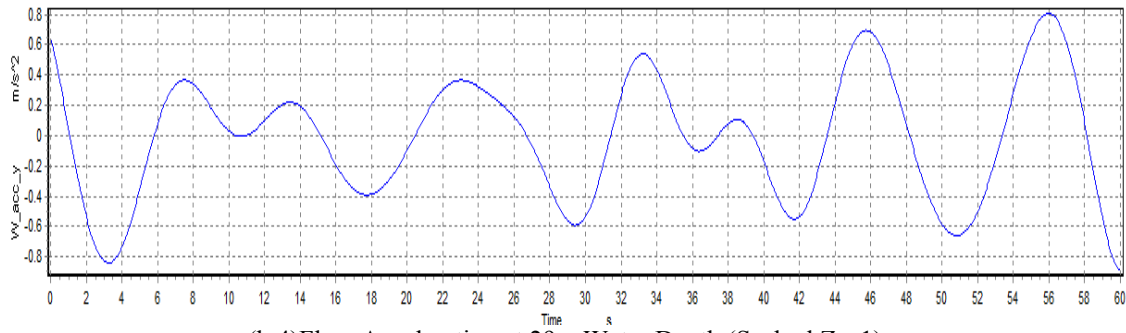
(b.1) Flow Acceleration at Sea Surface (Z=-30)



(b.2) Flow Acceleration at 10m Water Depth (Z=-20)



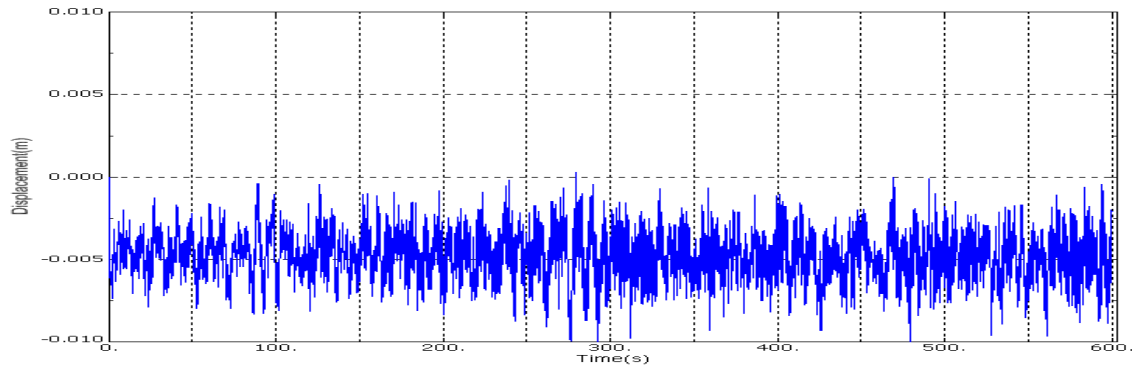
(b.3) Flow Acceleration at 20m Water Depth (Z=-10)



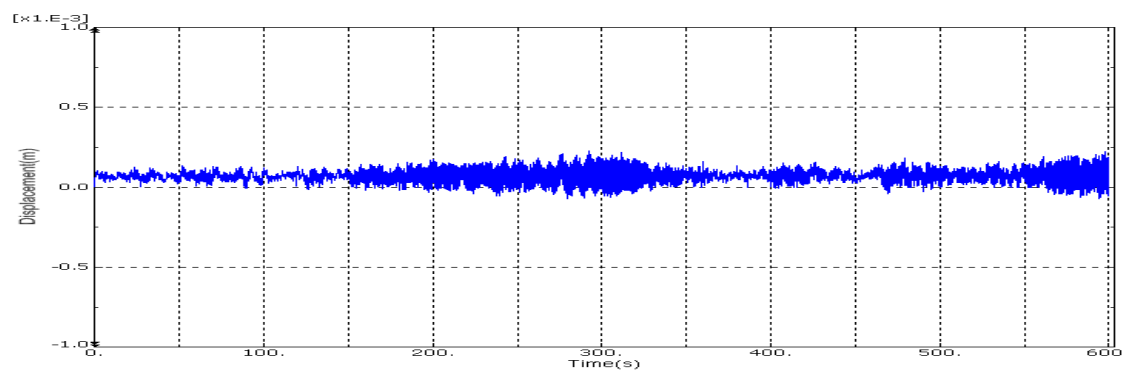
(b.4) Flow Acceleration at 29m Water Depth (Seabed Z=-1)

Figure V.2 Flow Velocities and Accelerations at Varying Water Depths for a 10m Wave Condition

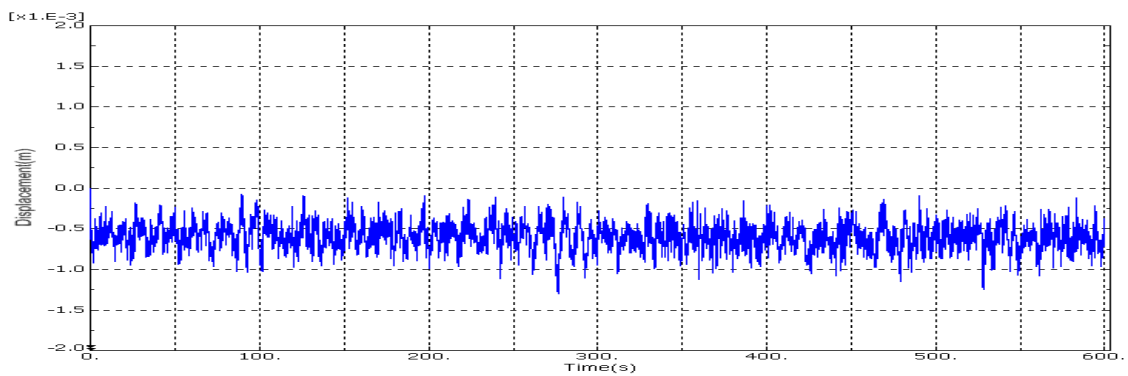
APPENDIX VI



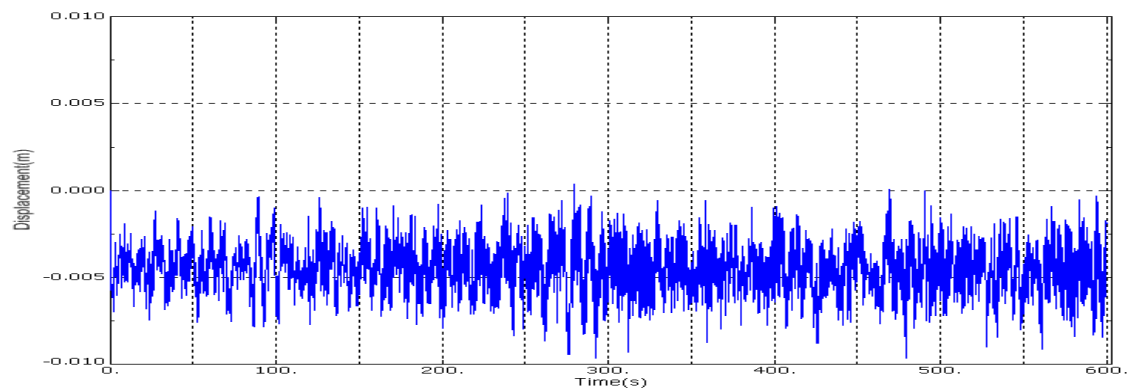
(a) X-displacement of Left-side (-X region) Node on Cylinder Top Edge



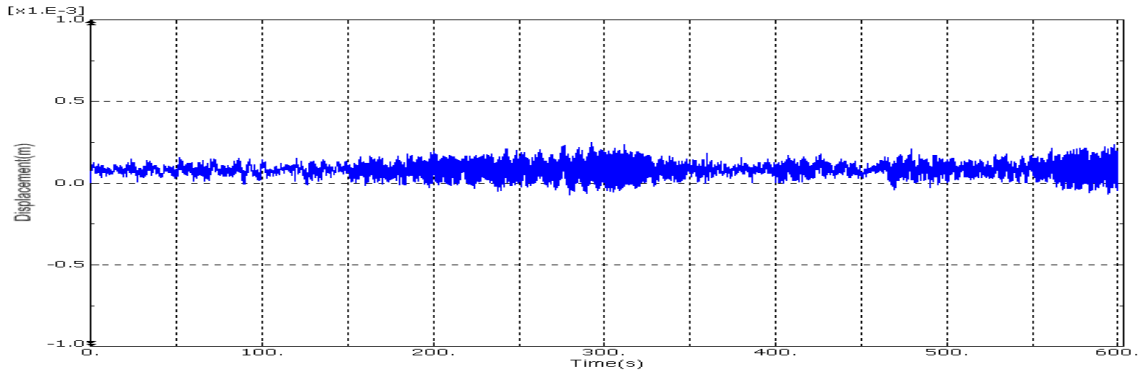
(b) Y-displacement of Left-side (-X region) Node on Cylinder Top Edge



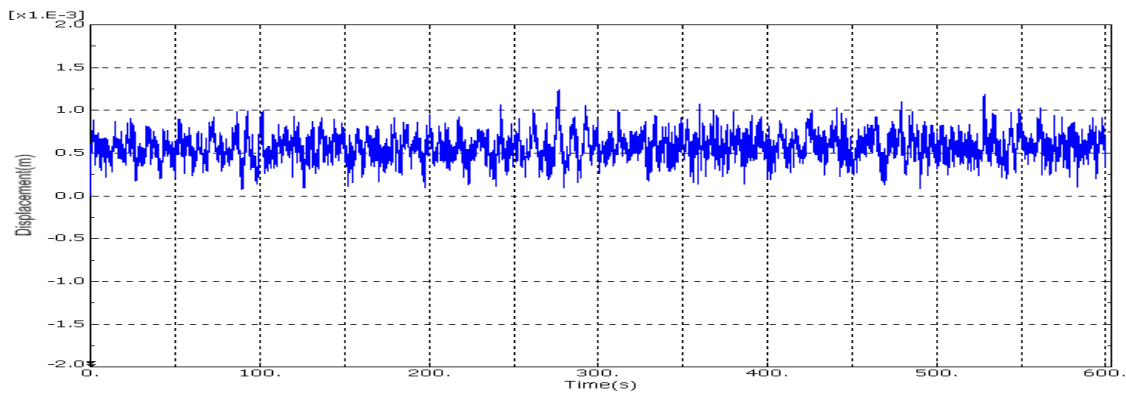
(c) Z-displacement of Left-side (-X region) Node on Cylinder Top Edge



(d) X-displacement of Right-side (+X region) Node on Cylinder Top Edge

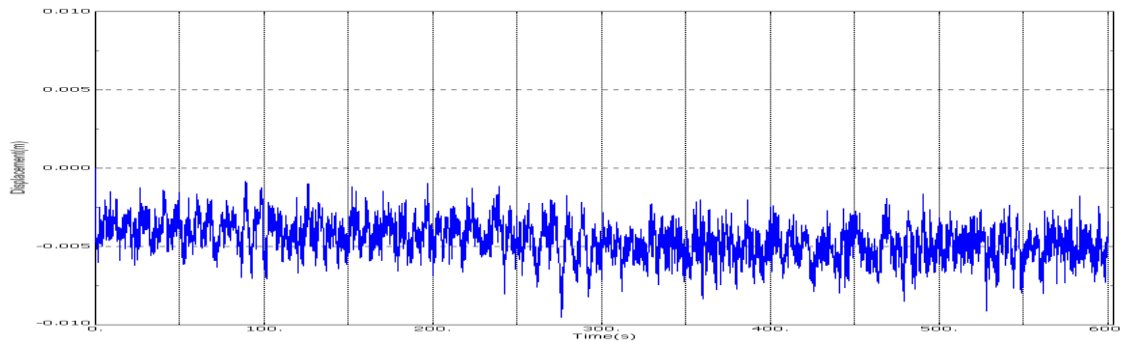


(e) Y-displacement of Right-side (+X region) Node on Cylinder Top Edge

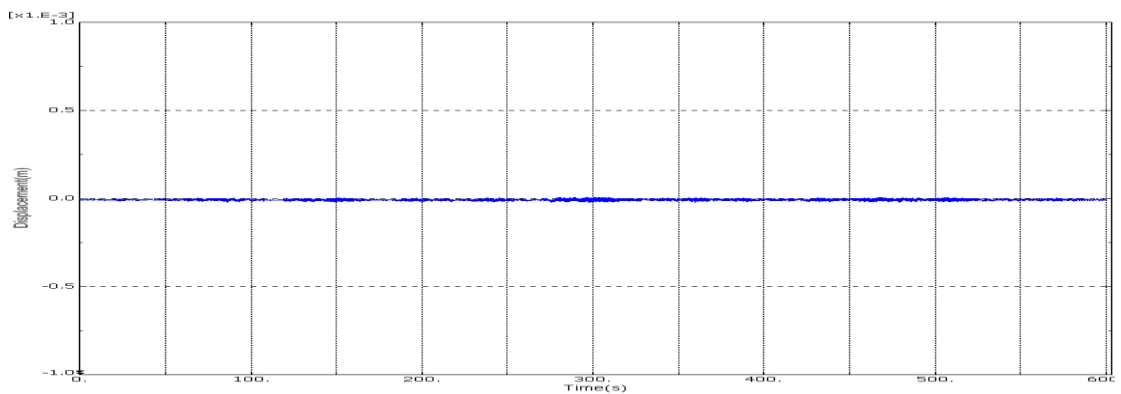


(f) Z-displacement of Right-side (+X region) Node on Cylinder Top Edge

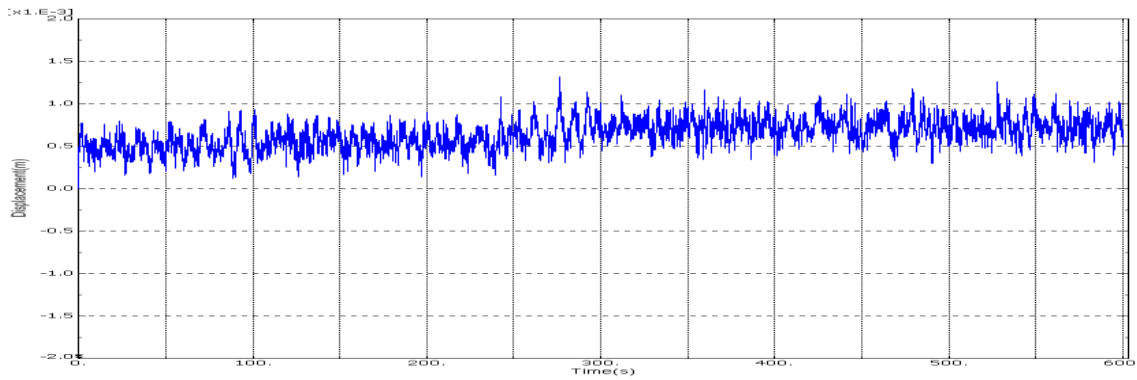
Figure VI.1 Deflection of Cylinder Top Edge Points of the Frame-cylinder TP under Rotor Torque



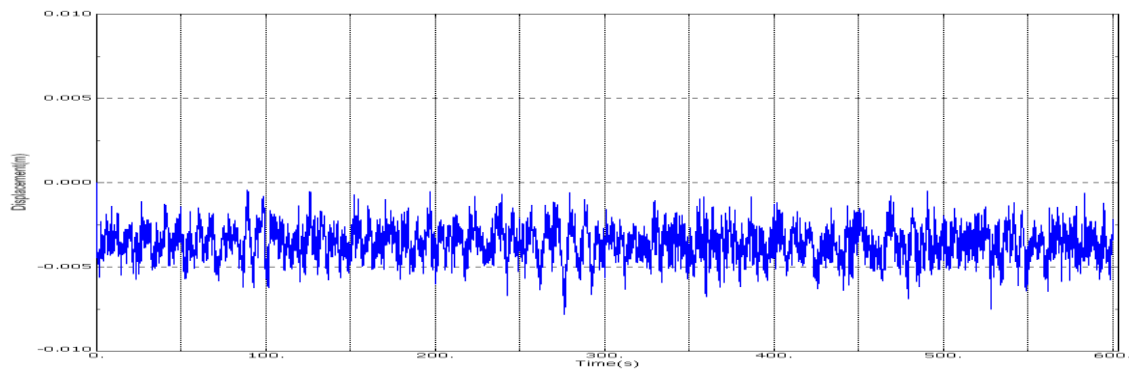
(a) X-displacement of Left-side (-X region) Node on Cone Edge



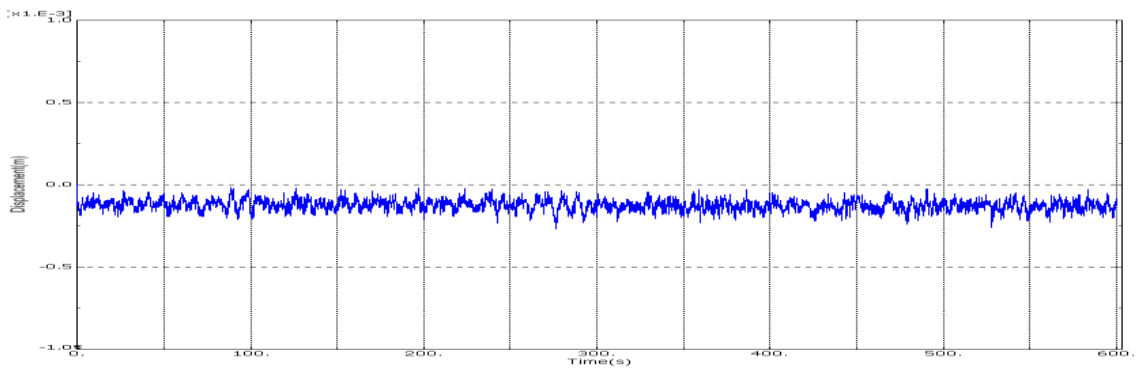
(b) Y-displacement of Left-side (-X region) Node on Cone Edge



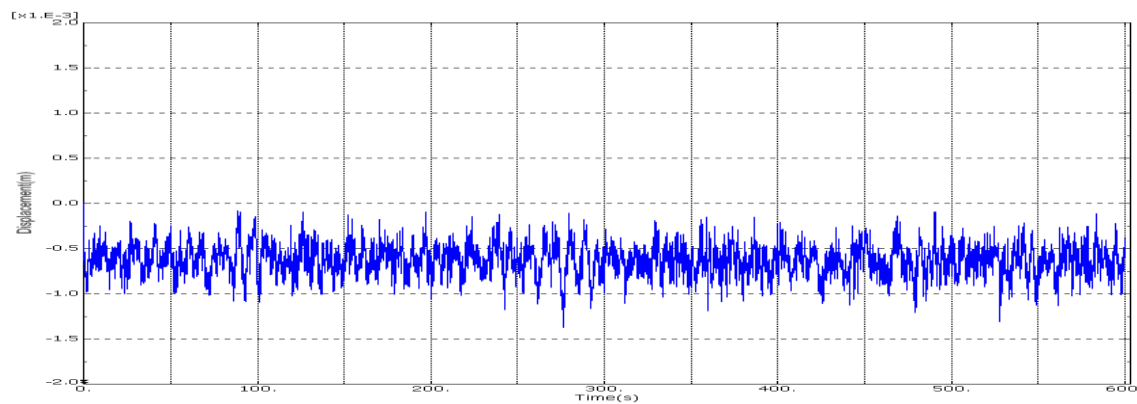
(c)Z-displacement of Left-side (-X region) Node on Cone Edge



(d)X-displacement of Right-side (+X region) Node on Cone Edge



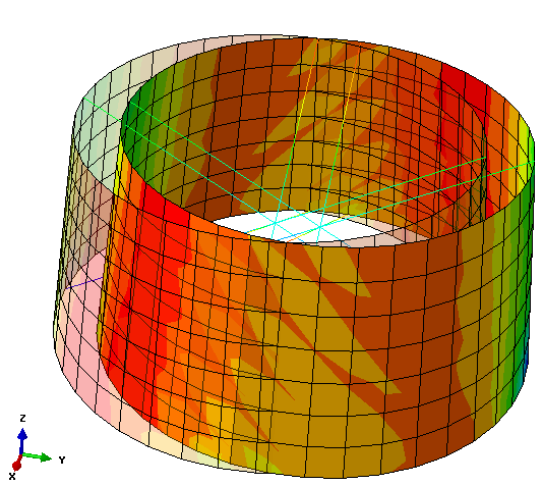
(e)Y-displacement of Right-side (+X region) Node on Cone Edge



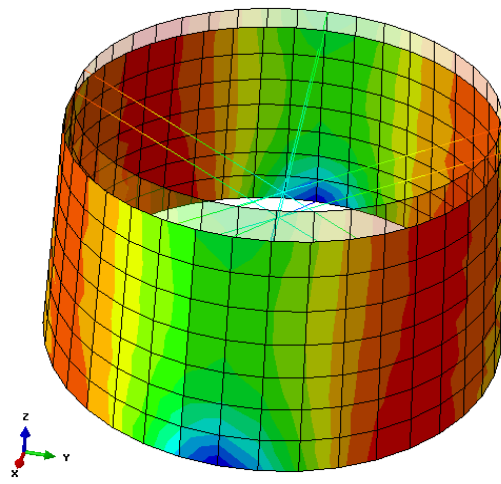
(f)Z-displacement of Right-side (+X region) Node on Cone Edge

Figure VI.2 Deflection of Cone Top Edge Points in the Cone-strut TP under Rotor Torque

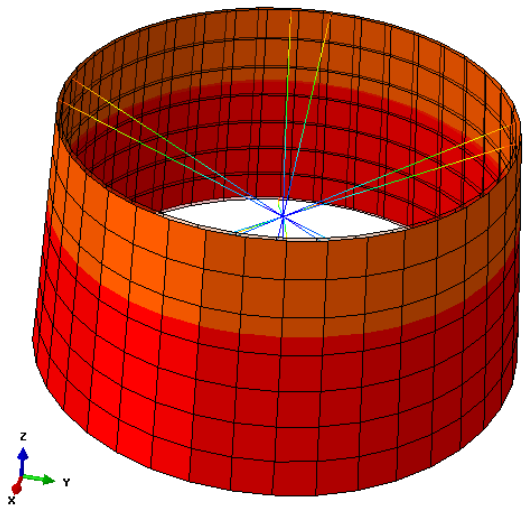
APPENDIX VII



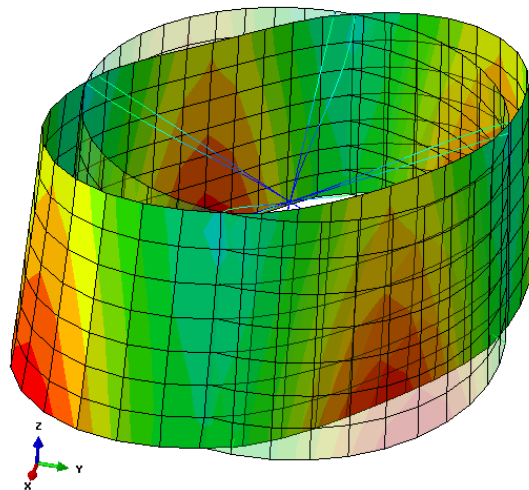
1st Eigen Mode



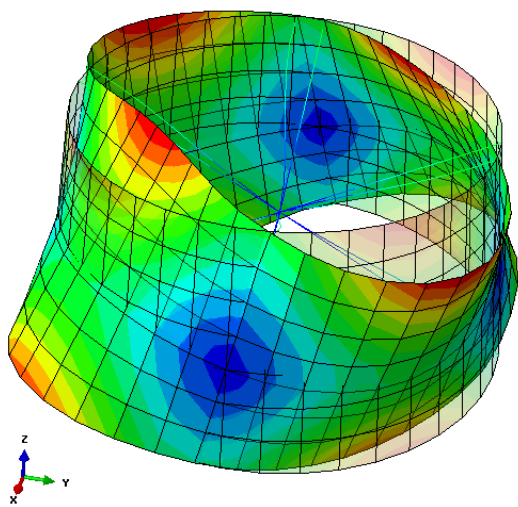
2nd Eigen Mode



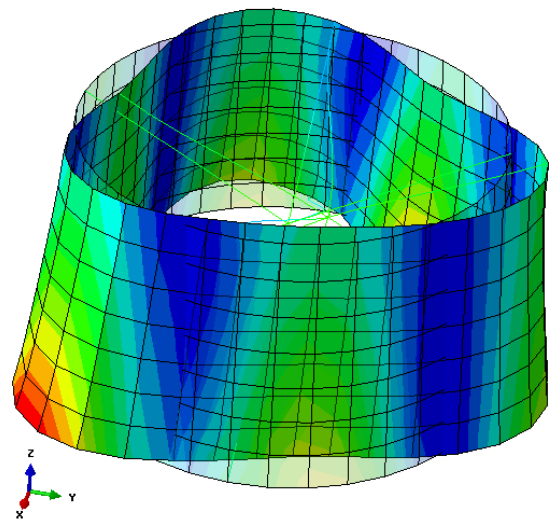
3rd Eigen Mode



4th Eigen Mode



5th Eigen Mode



6th Eigen Mode

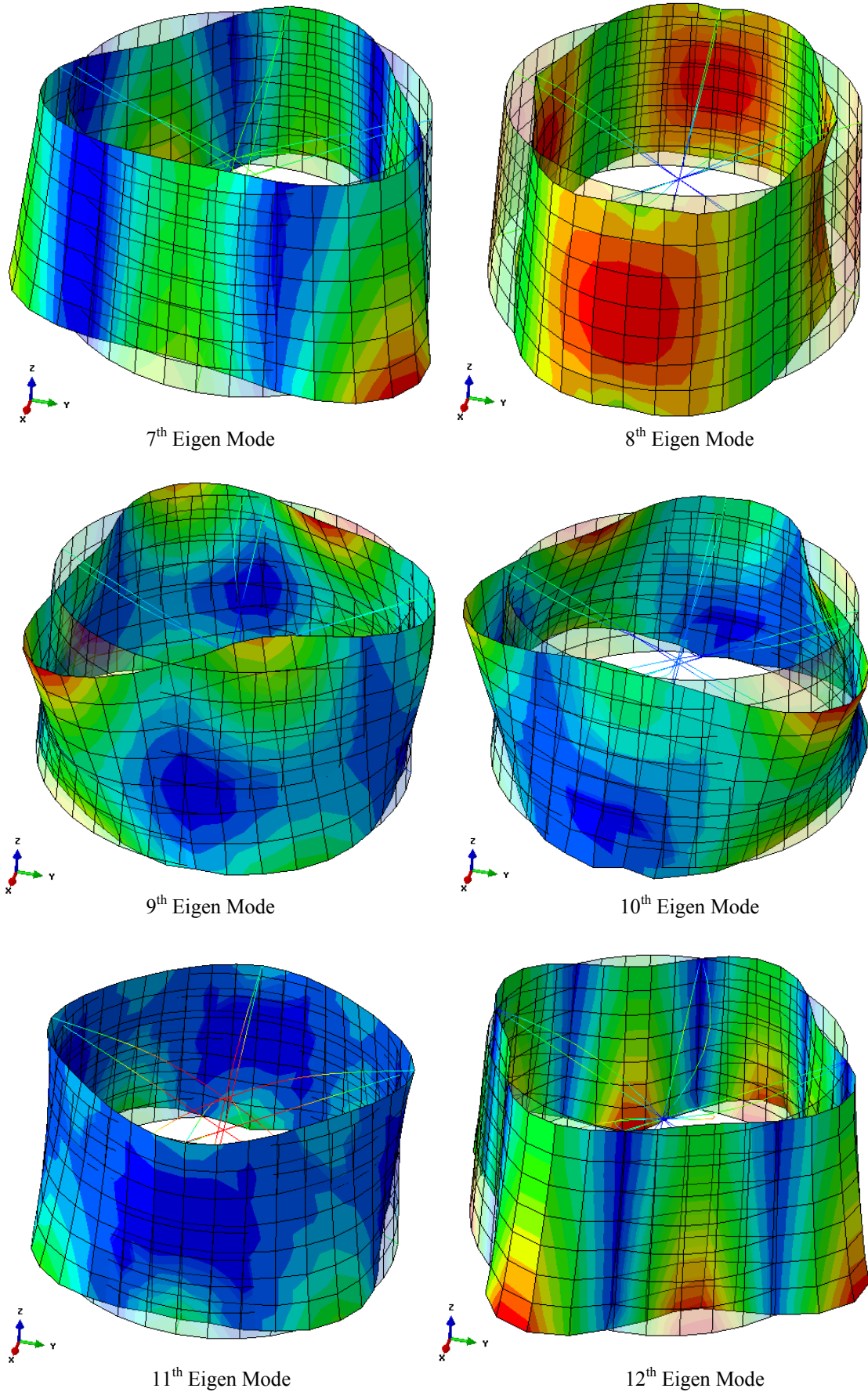


Figure VII.1 First 12 Eigen Modes of Transition Piece of 3m-high and 0.2m-thick (Transparent Model is the Original Undeformed One and Colour Contours Indicate Degree of Deformation)

